INTERACTIVE EFFECTS OF OCEAN ACIDIFICATION AND WARMING ON SEDIMENT-DWELLING MARINE CALCIFIERS

SUTINEE SINUTOK

B.SC. (FIRST CLASS HONOURS) & M.SC. (ECOLOGY)

JANUARY 2013

A THESIS SUBMITTED IN FULFILMENT OF THE REQUIREMENTS FOR THE DEGREE OF DOCTOR OF PHILOSOPHY IN SCIENCE

SCHOOL OF THE ENVIRONMENT
PLANT FUNCTIONAL BIOLOGY AND CLIMATE CHANGE CLUSTER
UNIVERSITY OF TECHNOLOGY, SYDNEY

CERTIFICATE OF AUTHORSHIP / ORIGINALITY

I certify that the work presented in this thesis has not previously been submitted for a degree nor has it been submitted as part of requirements for a degree except as fully acknowledged within the text.

I also certify that the thesis has been written by me. Any help that I have received in my research work and the preparation of the thesis itself has been acknowledged. In addition, I certify that all information sources and literature used are indicated in the thesis.

Sutinee Sinutok

ACKNOWLEDGEMENTS

First, I would like to thank to my supervisors Professor Peter Ralph, Dr Ross Hill and Dr Martina Doblin for their guidance, advice and support and all the opportunities they have provided during my candidature. I would like to thank Dr Ross Hill for inspiring me and assisting me throughout my PhD.

I would like to thank Professor Michael Kühl for teaching me the microsensor technique. Professor Anthony Larkum, Dr Justin Seymour, Dr Lucy Buxton, Dr Isabel Jimenez, Dr Nikolaus Császár, Dr Milan Szabo, Dr Katharina Petrou, Dr Daniel Neilson and Dr Raymond Ritchie are also thanked for their guidance during the completion of this research.

Thanks are also extended to Professor Louise Evans and Linda Xiao, Mark Berkahn, Dr Richard Wuhrer, David Bishop and Dr Michael Johnson for assistance with autotitration, X-ray diffraction, environmental scanning electron microscopy, ICP-MS, and Confocal microscopy, respectively. Thank you Professor Robert DeWreede, Dr. Joshua Madin and Dr. Yusuke Onoda for your assistance on the biomechanical work. Thank you Dr. Klairung Samart for her guidance on statistical analyses.

Thank you to all laboratory, technical and administrative staff at UTS and Heron Island Research Station. Special thanks to Dr Vinod Kumar, Marlene Fretz (Zbinden) and John Moore for their assistance.

Thank you to all members of the Aquatic Processes Group (APG) and special thanks to Verena Schrameyer, Ying Hong and Olivia Sackett, for their support and friendship. I have thoroughly enjoyed working with you all.

I would like to thank my lovely husband Ponlachart Chotikarn for his support and inspiration. I would like to also thank my family and friends for their support.

Thank you to Professor Tony Moon for his kind support and special thanks to Dr Auppatham Nakaruk, Bhanupong Dhechanunt, Pojwaree Lertsutthichawan, Weenaththa

Likitkom, Supitcha Supansomboon and Sirinut Sawatdeenarunat for their friendship and support.

I have received financial support from a number of sources. These include the Faculty of Science, School of the Environment, Plant Functional Biology and Climate Change Cluster at UTS, the Australian Government, the Australian Coral Reef Society, and the Phycological Society of America. Without these financial contributions, this research would not have been possible. In addition, I would like to thanks the Australian Coral Reef Society and the Australasian Society for Phycology and Aquatic Botany for travel funding to attend international and domestic conferences.

I would also like to acknowledge the Great Barrier Reef Marine Park Authority for approving the research permit (G09/30853.1 and G11/34063.1).

PUBLICATIONS

Peer reviewed journal articles arising directly from this thesis:

Chapter 2:

Sinutok S, Hill R, Doblin MA, Ralph PJ. The effect of irradiance on photosynthetic efficiency and calcification in three *Halimeda* species

Chapter 3:

Sinutok S, Hill R, Doblin MA, Ralph PJ. Diurnal photosynthetic response of the symbiotic benthic foraminiferan *Marginopora vertebralis*. *Marine Ecology Progress Series.* In press.

Chapter 4:

Sinutok S, Hill R, Doblin MA, Wuhrer R, Ralph PJ (2011) Warmer more acidic conditions cause decreased productivity and calcification in subtropical coral reef sediment-dwelling calcifiers. *Limnology and Oceanography* 56(4): 1200-1212.

See Appendix 1

Chapter 5:

Sinutok S, Hill R, Doblin MA, Kühl M, Ralph PJ (2012) Microenvironmental changes support evidence of photosynthesis and calcification inhibition in *Halimeda* under ocean acidification and warming. *Coral Reefs* 31:1201-1213.

See Appendix 2

Chapter 6:

Sinutok S, Hill R, Doblin MA, Kühl M, Ralph PJ. Ocean acidification and warming alter microscale photosynthesis and calcification of the symbiont-bearing foraminifera *Marginopora vertebralis*. Submitted to *Marine Biology*.

Chapter 7:

Sinutok S, Hill R, Doblin MA, Madin J, Berkahn M, Bishop D, Ralph PJ. Ocean acidification and warming will increase vulnerability of *Halimeda* sp. to breakage and removal. Submitted to *Global Change Biology*.

TABLE OF CONTENTS

LIST OF FIGURES

Figure 3.1: A) Irradiance (μmol photon m^{-2} s^{-1}) (closed circles) and seawater temperature (ºC) (open circles) on Heron Island reef flat from 0430 to 1900 h. Data represent mean from three consecutive days ± SE (n = 3) and B) Density (cm^{-2}) of exposed (open circles) and sheltered (closed circles) foraminifera on Heron Island reef flat from 0430 to 1900 h. Data represent mean ± SE (n = 10). * indicates significant differences between sheltered and exposed.

Figure 3.2: A) Effective quantum yield of PSII ($\Delta F/F_M'$), B) maximum relative electron transport rate ($rETR_{max}$; μmol electrons m^{-2} s^{-1}) and C) minimum saturating irradiance (I_k; μmol photons m^{-2} s^{-1}) of exposed (open circles) and sheltered (closed circles) foraminifera on Heron Island reef flat from 0430 to 1900 h. Data represent mean ± SE (n = 5). * indicates significant differences between sheltered and exposed.

Figure 3.3: Rapid light curves (relative electron transport rate (rETR vs. irradiance) from exposed (open circles) and sheltered (closed circles) foraminifera at 10 irradiance steps (0 to 950 μmol photons m^{-2} s^{-1}) on Heron Island reef flat from 0430 (A), 0900 (B), 1200 (C), 1500 (D) and 2000 h (E). Data represent mean ± SE (n = 5).

Figure 3.4: A) Irradiance (μmol photon m^{-2} s^{-1}) (closed circles) and seawater temperature (ºC) (open circles) from 0430 to 1900 h. Data represent mean from three consecutive days ± SE (n = 3). B) Number of foraminifera exposed to the sun in sun-exposed (open circles), sheltered (closed circles), sun-exposed with DCMU (open triangles) and sheltered with DCMU (closed triangles) treatments from 0430 to 1900 h. Data represent mean ± SE (n = 4). * indicates significant differences between sheltered and exposed.

Figure 3.5: A) Maximum quantum yield of PSII (F_V/F_M), B) effective quantum yield of PSII (Y(II)), C) non-photochemical quenching yield (Y(NPQ)), and D) non-regulated heat dissipation yield (Y(NO)) from foraminifera in sun-exposed (open circles), sheltered (closed circles), sun-exposed with DCMU (open triangles) and sheltered with

LIST OF TABLES

and temperature (28ºC, 32ºC) treatment used in experiments. Data represent mean ± S.E. (n = 3)

ABSTRACT

The increase in human activities, such as the burning of fossil fuels, has elevated the concentration of atmospheric carbon dioxide and warmed the planet through the greenhouse effect. In addition, approximately 30% of the CO_2 produced by human activities has dissolved into the oceans, lowering pH and reducing the abundance, and hence the availability, of carbonate ions (CO_3^{2-}), which are essential for calcium carbonate deposition. Of great concern is the impact to photosynthetic marine calcifiers, elevated CO_2 and temperature is expected to have a negative impact on the health and survivorship of calcifying marine organisms.

This thesis explores the effects of elevated CO_2 and temperature on the microenvironment, photosynthetic efficiency, calcification and biomechanical properties in important sediment producers on coral reefs. The reef-building and sediment-dwelling organisms, *Halimeda* and symbiont-bearing foraminifera are prominent, co-existing taxa in shallow coral reefs and play a vital role in tropical and subtropical ecosystems as producers of sediment and habitats and food sources for other marine organisms. However, there is limited evidence of the effects of ocean warming and acidification in these two keystone species. Irradiance alone was not found to influence photosynthetic efficiency, photoprotective mechanisms and calcification in *Halimeda macroloba*, *Halimeda cylindracea* and *Halimeda opuntia* **(Chapter 2)**. There is also limited knowledge of foraminiferal biology on coral reefs, especially the symbiotic relationship between the protest host and algal symbionts. *Marginopora vertebralis*, the dominant tropical foraminifera, shows phototactic behavior, which is a unique mechanism for ensuring symbionts experience an ideal light environment. The diurnal photosynthetic responses of *in hospite* symbiont photosynthesis was linked to host movement and aided in preventing photoinhibition and bleaching by moving away from over-saturating irradiance, to more optimal light fields **(Chapter 3)**.

With this greater understanding of *Halimeda* and foraminiferan biology and

photosynthesis, the impacts of ocean warming and acidification on photosynthesis and calcification were then tested **(Chapter 4, 5 and 6)**. Impacts of ocean acidification and warming were investigated through exposure to a combination of four temperature (28, 30, 32, 34°C) and four pCO_2 levels (380, 600, 1000, 2000 µatm; equivalent to future climate change scenarios for the current and the years 2065, 2100 and 2200 and simulating the IPCC A1F1 predictions) **(Chapter 4)**. Elevated CO_2 and temperature caused a decline in photosynthetic efficiency (F_V/F_M), calcification and growth in all species. After five weeks at 34°C under all CO_2 levels, all species died. The elevated CO_2 and temperature greatly affect the $CaCO_3$ crystal formation with reductions in density and width. *M. vertebralis* experienced the greatest inhibition to crystal formation, suggesting that this high Mg-calcite depositing species is more sensitive to lower pH and higher temperature than aragonite-forming *Halimeda* species. Exposure to elevated temperature alone or reduced pH alone decreased photosynthesis and calcification in these species. However, there was a strong synergistic effect of elevated temperature and reduced pH, with dramatic reductions in photosynthesis and calcification in all three species. This study suggested that the elevated temperature of 32°C and the pCO_2 concentration of 1000 µatm are the upper limit for survival of these species art our site of collection (Heron Island on the Great Barrier Reef, Australia).

Microsensors enabled the detection of O_2 surrounding specimens at high spatial and temporal resolutions and revealed a 70-80% in decrease in O_2 production under elevated CO_2 and temperature (1200 µatm 32°C) in *Halimeda* **(Chapter 5)** and foraminifera **(Chapter 6)**. The results from O_2 microprofiles support the photosynthetic pigment and chlorophyll fluorescence data, showing decreasing O_2 production with declining chlorophyll *a* and *b* concentrations and a decrease in photosynthetic efficiency under ocean acidification and/or temperature stress. This revealed that photosynthesis and calcification are closely coupled with reductions in photosynthetic efficiency leading to reductions in calcification.

Reductions in carbonate availability reduced calcification and that can lead to weakened calcified structures. Elevations in water temperature is expected to augment this

weakening, resulting in decreased mechanical integrity and increased susceptibility to storm- and herbivory-induced mortality in *Halimeda* sp. The morphological and biomechanical properties in *H. macroloba* and *H. cylindracea* at different wave exposures were then investigated in their natural reef habitats **(Chapter 7)**. The results showed that both species have morphological (e.g. blade surface area, holdfast volume) and biomechanical (e.g. force required to uproot, force required to break thalli) adaptations to different levels of hydrodynamic exposure. The mechanical integrity and skeletal mineralogy of *Halimeda* was then investigated in response to future climate change scenarios **(Chapter 7)**. The biomechanical properties (shear strength and punch strength) significantly declined in the more heavily calcified *H. cylindracea* at 32ºC and 1000 µatm, whereas were variable in less heavily calcified *H. macroloba*, indicating different responses between *Halimeda* species. An increase in less-soluble low Mg-calcite was observed under elevated CO_2 conditions. Significant changes in Mg:Ca and Sr:Ca ratios under elevated CO_2 and temperature conditions suggested that calcification was affected at the ionic level. It is concluded that *Halimeda* is biomechanically sensitive to elevated temperature and more acidic oceans and may lead to increasing susceptibility to herbivory and higher risk of thallus breakage or removal from the substrate.

Experimental results throughout the thesis revealed that ocean acidification and warming have negative impacts on photosynthetic efficiency, productivity, calcification and mechanical integrity, which is likely to lead to increased mortality in these species under a changing climate. A loss of these calcifying keystone species will have a dramatic impact on carbonate accumulation, sediment turnover, and coral reef community and habitat structure.

CHAPTER 1:

GENERAL INTRODUCTION

1.0 GENERAL INTRODUCTION

1.1 CORAL REEFS: ECOSYSTEM AND PROBLEMS

Coral reefs are dynamic ecosystems because of their ecological complexity (Harrison and Booth, 2007). The foundation of coral reef ecosystems is constructed by reef-building scleractinian corals (Buddemeier et al. 2004), coralline algae, as well as *Halimeda*, a green alga (Smith et al. 2004), and other calcifying organisms such as foraminifera (Hallock et al. 2003). Coral reefs are the most diverse and productive habitats in the world containing 32 out of the 34 recognised animal phyla (in comparison to tropical rainforests which only contain 9; Wilkinson 2002) providing important habitat for many marine organisms, such as protists, microalgae, macroalgae, invertebrates, molluscs, crustaceans, and vertebrates, including fish and mammals (Lesser 2004; Harrison and Booth 2007). In addition to their ecological importance, coral reefs support the livelihood of 500 million people worldwide (Wilkinson 2002) and provide ecosystem services to the value of US$375 billion per year in the form of coastal protection, food production and tourism (Costanza et al. 1997).

1.1.1 Reef-building organisms

Two important reef-building and sediment-dwelling organisms on coral reefs are the calcareous green alga *Halimeda* and benthic foraminifera. They play a vital role in tropical and sub-tropical ecosystems as producers of sediment (Hallock 1981a; Drew 1983), primary producers (Bach 1979) and food sources for grazers (Walter et al. 2002; Smith et al. 2004). Below are the classifications of the alga *Halimeda* and the benthic foraminifera *Marginopora vertebralis* (Loeblich and Tappan 1984; Kooistra et al. 2002; Pröschold and Leliaert 2007):

Halimeda:

Kingdom: Plantae
Division: Chlorophyta
Class: Bryopsidophyceae
Order: Bryopsidales
Family: Halimedaceae
Genus: *Halimeda*

(Kooistra et al. 2002; Pröschold and Leliaert 2007)

***Marginopora vertebralis*:**

Kingdom: Protista
Phylum: Foraminifera
Class: Foraminiferida
Order: Foraminiferida
Family: Soritidae
Genus: *Marginopora*
Species: *Marginopora vertebralis*

(Loeblich and Tappan 1984)

1.1.1.1 The calcareous green alga *Halimeda*

Calcareous green algae from the genus *Halimeda* are widely distributed in tropical and subtropical marine environments (Hillis-Colinvaux 1980) such as Florida (Bach 1979; Beach et al. 2003), Panama (Anderson et al. 2006), the Mediterranean Sea (Ballestoros 1991), the Red Sea (El-Manawy and Shafik 2008), the Andaman Sea (Sinutok et al. 2008), the Caribbean Sea (Clifton and Clifton 1999) and the Great Barrier Reef (Drew 1983). *Halimeda* is important as a carbonate sediment producer (Drew 1983), as a source of food for herbivores (Smith et al. 2004; Walter et al. 2002), as a phototroph (Bach 1979), and as a provider of shelter and nursery ground for invertebrates (Hillis-Colinvaux 1980) on coral reefs. Reefs containing meadows of *Halimeda* (up to 500 g m^{-}

^{2}) are major contributors to calcium carbonate ($CaCO_3$) production and have high sediment production rates (Drew 1983). For example, on Pandora, Rib, Broadhurst, Davies, Myrmidon and Flinders reefs on the Central Great Barrier Reef, *Halimeda* produces 2.2 kg of $CaCO_3$ m^{-2} y^{-1} (Drew 1983).

Halimeda consists of plate-like, calcified segments, which are joined together by uncalcified nodes. These form branching chains to produce a bushy thallus (Figure 1.1). Growth of *Halimeda* involves the development of new segments, which begin as white, conical lobes from the apex of the most recent segment (Hillis-Colinvaux 1980). Within 24 h, this white lobe has grown into a complete and green segment. Calcification of the new segment begins after approximately 36 h (Hillis-Colinvaux 1980). Length and width of the segment is fixed within the first few days through the precipitation of $CaCO_3$ in the form of aragonite (orthorhombic crystal structure) (Borowitzka and Larkum 1977; Hillis-Colinvaux 1980) (Figure 1.2). Calcification results in changes in segment thickness depending on the species and the segment's location within the thallus. For example, *Halimeda macroloba* Decaisne is moderately to lightly calcified compared to *Halimeda opuntia* (Linnaeus) Lamouroux which is more heavily calcified. Younger apical segments found on the apical branches have a lower amount of calcium carbonate than older, basal segments (Hillis-Colinvaux 1980).

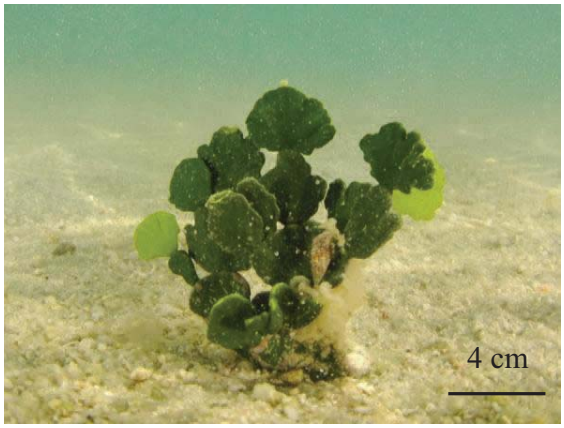

Figure 1.1*: Halimeda macroloba* from 1 m depth at Hat *Khanom* Mu Ko Thale Tai Marine *National Park, Gulf of Thailand* (Photo by Nat Sumanatemeya, 2008). Scale bar = 2 cm.

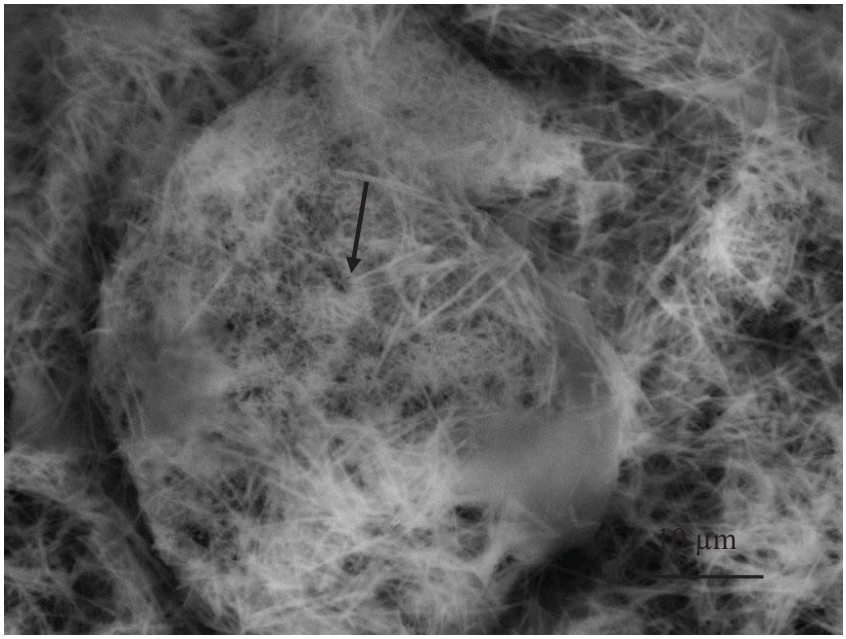

Figure 1.2: SEM photograph of *Halimeda macroloba* Decaisne showing aragonite crystals (arrow). Scale bar = 10 μm.

Each species of *Halimeda* has different habitats and growth forms. The rock growers (e.g., *H. opuntia*) are attached by a single, small holdfast and grow on rock surfaces or hang as drapes from rocks. The second group of species sprawls across rock, sand or coarse algal and coral debris via rhizoids and is known as a sprawler (e.g., *Halimeda gracilis* Harvey *ex* J. Agardh). The third group grows in sandy substrate and forms a large holdfast attached to sand and is known as a sand grower (e.g., *H. macroloba*) (Figure 1.3) and has the ability to obtain nutrients directly from the sediment (Williams 1984; Fong et al. 2003; Littler et al. 2004; Verbruggen 2005) which may help explain its wide distribution and rapid growth (Multer and Clavijo, 1989).

Many biological and physical factors influence *Halimeda* growth and calcification. The studies of *H. tuna* in the Florida Keys (Vroom et al. 2003) and *H. macroloba* at Phuket, Thailand (Sinutok et al. 2008) have revealed that the growth rate of *Halimeda* fluctuates because of seasonal changes in light intensity (Vroom et al. 2003; Sinutok et al. 2008), the photoperiod (Vroom et al. 2003) and temperature (Vroom et al. 2003).

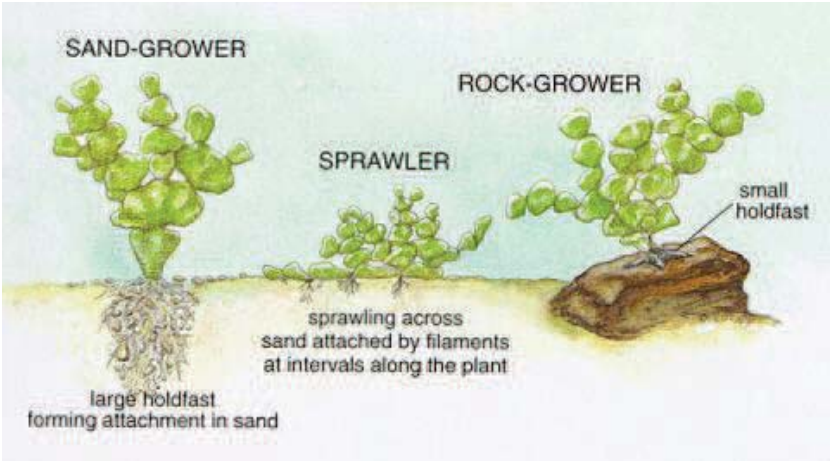

Figure 1.3: *Halimeda* growth forms and holdfast systems (photo from Australian Institute of Marine Science; modified after Hillis-Colinvaux 1980)

Beach at al. (2003) also found that the photosynthetic performance of *Halimeda* varied temporally depending on light and nutrient availability. *Halimeda* segments were observed to become paler in colour in the late afternoon and at night (Drew and Abel 1990; Sinutok 2008). The chloroplasts migrate from the surface utricle (the branch of cortex filament) through the secondary utricles into the internal medullary filaments without any loss of chlorophyll (Figure 1.4). This process minimises damage from surface grazers (Drew and Abel 1990) and reduces photoinhibition (by protecting from exposure to high irradiance) (Drew 1979). Many studies have shown that the calcification process in *Halimeda* is decreased by thallus age (Borowitzka and Larkum 1976a; Hillis-Colinvaux 1980), higher respiration rate (Stark et al. 1969), higher CO_2 concentration (Stark et al. 1969; Borowitzka 1977), and higher phosphate concentration (Simkiss 1964; Demes et al. 2009) and is increased with higher growth rate, higher photosynthetic rate (Borowitzka and Larkum 1976b), higher light intensity (Borowitzka and Larkum 1976b, c), higher concentration of Ca^{2+} and CO_3^{2-} ions (Simkiss 1964), and higher herbivory (Paul and Van Alstyne 1988).

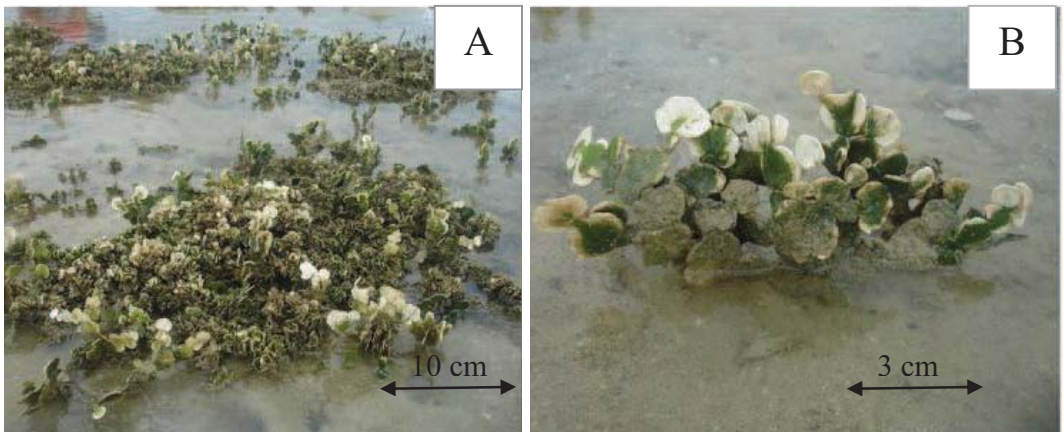

Figure 1.4: *Halimeda macroloba* with white band at the tip of their segments at Tangkhen Bay, Phuket, Thailand. A: Natural habitat, scale bar = 10 cm, B: Close up, scale bar = 3 cm.

1.1.1.2 Benthic foraminifera

Foraminifera are single-celled organisms. They are a group of amoeboid protists with reticulating pseudopodia: fine strands that branch and merge to form a dynamic net used for motility, attachment, shell construction, protection and food trapping (Goldstein 1999). They are important as producers of sediment on coral reefs, contributing 2.8 kg $CaCO_3$ m^{-2} y^{-1} in Western Coroline Islands (Hallock 1981a; Nobes and Uthicke 2008). Foraminifera are often used as index fossils for paleoecological research (Loeblich and Tappan 1984), and can be used as environmental indicators for changes in water quality (Nobes and Uthicke 2008).

The foraminifera (Figure 1.5, 1.6) consist of protoplasm enclosed by a calcium carbonate shell in a form of magnesium calcite (Goldstein 1999) (Figure 1.7). The foraminifer consists of one (unilocular) or several (multilocular) chambers depending on age and species (Figure 1.8) (Patterson and Richardson 1987; Goldstein 1999). Growth of foraminifera is defined by an increase in size of a single chamber or addition of new chambers (Goldstein 1999).

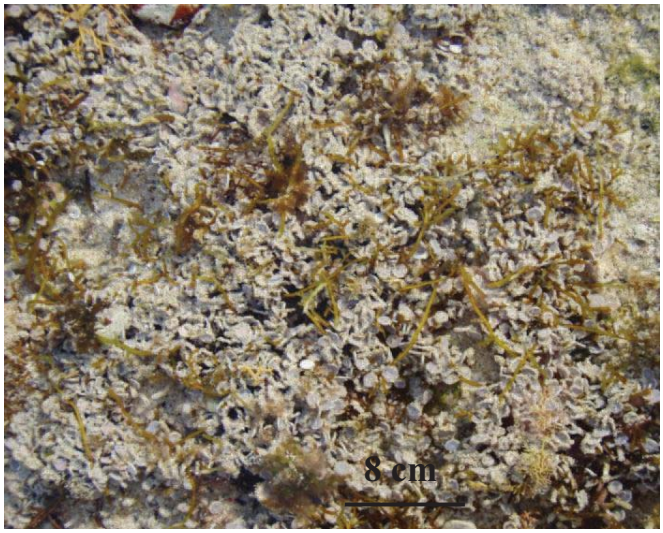

Figure 1.5: Foraminifera at Lord Howe Island (Photo by Dr. Ross Hill). Scale bar = 8 cm.

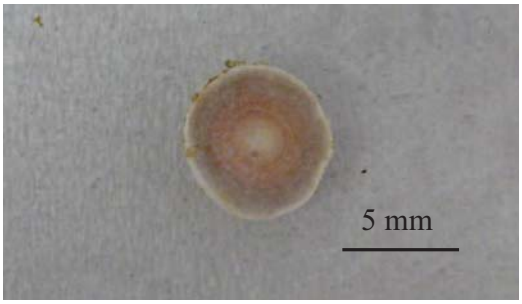

Figure 1.6: Foraminifera, *Marginopora vertebralis* Quoy & Gaimard, from Heron Island, Great Barrier Reef. Scale bar = 5 mm.

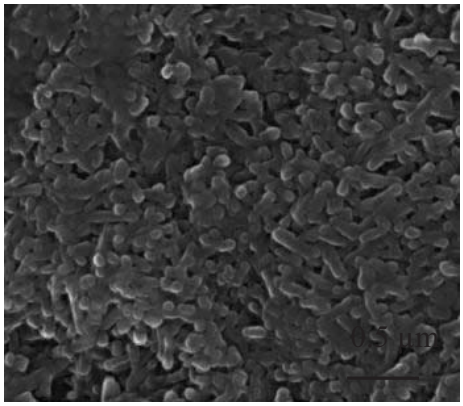

Figure 1.7: SEM photograph of *M. vertebralis* Mg-calcite crystals. Scale bar = 0.5 μm (Sinutok et al. 2011).

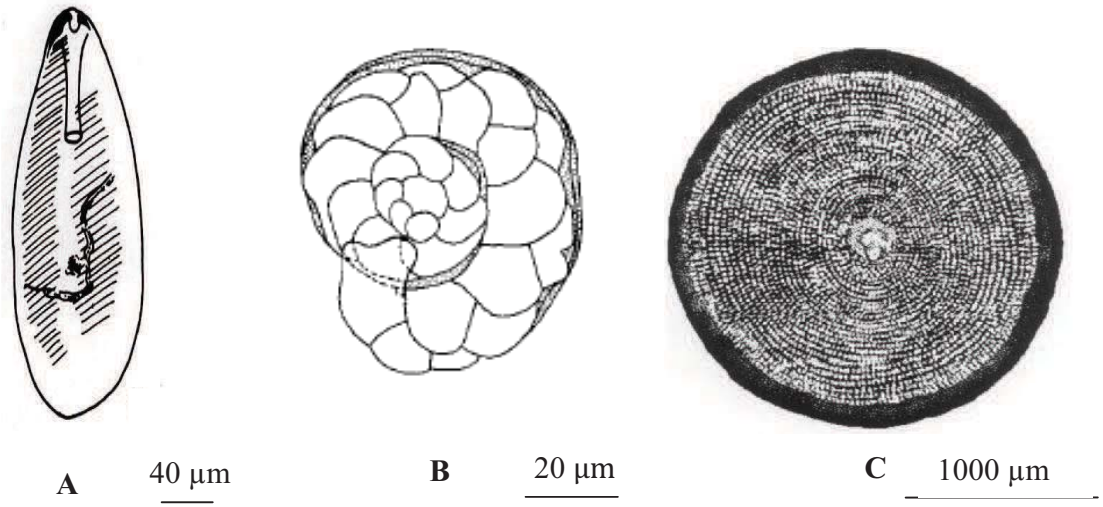

Figure 1.8: Diagram of A) one (unilocular) chamber of *Duplella* sp. (photo from Patterson and Richardson 1987). Scale bar = 40 µm, B) several (multilocular) chambers of *Heterostegina depressa* d'Orbigny (image from Röttger 1974). Scale bar = 20 µm, and C) several (multilocular) chambers of *Marginopora vertebralis* Quoy & Gaimard (image from Gudmundsson 1994) Scale bar = 1000 µm.

In the benthic foraminiferal species, *Marginopora vertebralis* Quoy & Gaimard, there are three growth stages: i) an embryonic or nucleoconch stage, ii) a cyclical chamberletted stage, and iii) a chambered reproductive stage (Figure 1.9) (Ross 1972). The embryonic stage involves the formation of a proloculus, an initial chamber, within the reproductive chambers of the parent and then the release of the embryons from the parent after they are fully formed. The initial chamber receives the symbiotic algae from the parent protoplasm (Röttger 1974). At the second stage, a series of small chamberlets (subdivided chamber) is added along the embryonic apparatus. The chamberlets commonly vary in size from 0.04-0.28 mm (Ross 1972). The newly formed chamberlets are partially calcified, thin and easily dislodged, with complete calcification taking seven to ten days (Ross 1972). Magnesium calcite crystals are precipitated in the calcification process and are generally deposited perpendicular to the shell surface in the outermost layer (Hansen 1999). The cycle of adding chamberlets occurs every four or

five days. At the third stage of growth, 4-58 days after formation of last chambers (Röttger 1974), reproduction chambers are formed (Ross 1972).

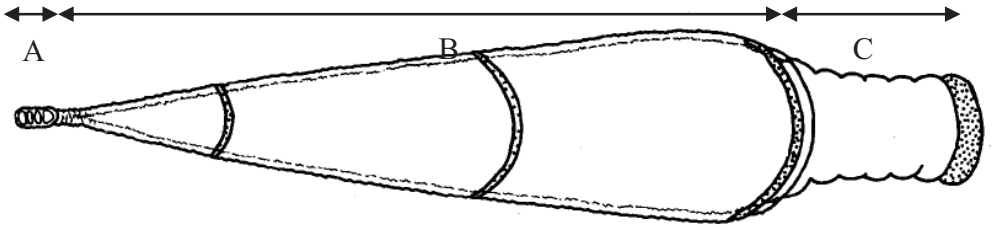

Figure 1.9: Growth stage of *Marginopora vertebralis* Quoy and Gaimard. A: an embryonic or nucleoconch stage, B: a cyclical chamberletted stage and C: a chambered reproductive stage (Modified from Ross 1972).

1.1.1.2.1 Symbiotic partners of benthic foraminifera

In shallow water, many benthic foraminiferal species have algal symbionts, also known as zooxanthellae, which come from a variety of algal groups such as diatoms, dinoflagellates. Other groups host unicellular chlorophytes, unicellular rhodophytes, and/or cyanobacteria. In addition, they can harbour chloroplasts obtained by feeding on algae (e.g., diatoms) (Goldstein 1999; Lee et. al. 2004; Lee 2006). Symbionts are contained below the shell walls within the chamber cytoplasm (Leutenegger 1984). Fay et al (2009) found a distinct pattern in distribution of the zooxanthellae symbiont in *Amphisorus hemprichii* Ehrenberg living in Papua New Guinea. The symbionts were mostly found in the 'intermediate' zone of the foraminifera, with fewer in the 'inner' or 'outer' zones (Figure 1.10) (Fay et al. 2009). A single species of foraminifera may host different species of symbionts, as well as multiple clades (a taxonomic group of organisms classified on the basis of homologous features traced to a common ancestor) of symbionts. In addition, an individual foraminifera may harbour multiple species of algae simultaneously (Fay et al. 2009). For example, *Marginopora vertebralis* Quoy & Gaimard hosts several species of dinoflagellates, i.e., *Gymnodinium obesum* Schiller, *Gymnodinium Rotundatum* Klebs and *Symbiodinium microadriaticum* Freudenthal

(Ross 1972; Pawlowski el al. 2001; Lee et al. 2009). Of the *Symbiodinium* symbionts, clade F was found to be enriched in the inner chamber while clade C was dominant in the outer zone of *A. hemprichii*, suggesting spatial variation in algal symbiont distribution (Figure 1.10) (Fay et al. 2009).

1.1.1.2.2 The symbiotic relationship

Symbiotic relationships between foraminifera and algal symbionts are varied and complex (Goldstein 1999). The host foraminifera benefit from maintaining an algal symbiosis by obtaining the energy from photosynthesis (mostly sugar and glycerol) which is translocated from the symbiont to the host (Murray 2006). This is highly beneficial to the foraminifera, allowing them to flourish in the oligotrophic water of coral reefs. An additional benefit provided by these photosynthetic symbionts is that they enhance the rate of calcification in the foraminifera. Removal of CO_2 increases the surrounding pH which favours $CaCO_3$ precipitation (Hallock 1999). In other words, the algal partner in this symbiosis allows the foraminifera to function as a primary producer (autotrophic nutrition). However, foraminifera can also gain nutrition through heterotrophic feeding by consuming small bacteria, algae, protists, invertebrates and/or organic particles via the pseudopodia (Hallock 1999). In return, the foraminifera provide the symbionts with a stable microenvironment and a nutrient supply in the form of dissolved nitrogen and phosphorus (Goldstein 1999).

Growth of the foraminifera is influenced by the energy obtained from autotrophy and heterotrophic feeding. Hallock (1981a) developed three models based on growth in an autotroph (algal cell), a heterotroph (foraminifera), and a symbiotic system (foraminifera-algal symbiosis). This study found that energy available for growth and respiration was greatest in the symbiotic system and lowest in the heterotrophy system (Hallock 1981a). Thus, an algal symbiosis is advantageous for foraminifera inhabiting an oligotrophic environment where light energy is abundant because they can gain energy from their symbiotic partners (Hallock 1981a).

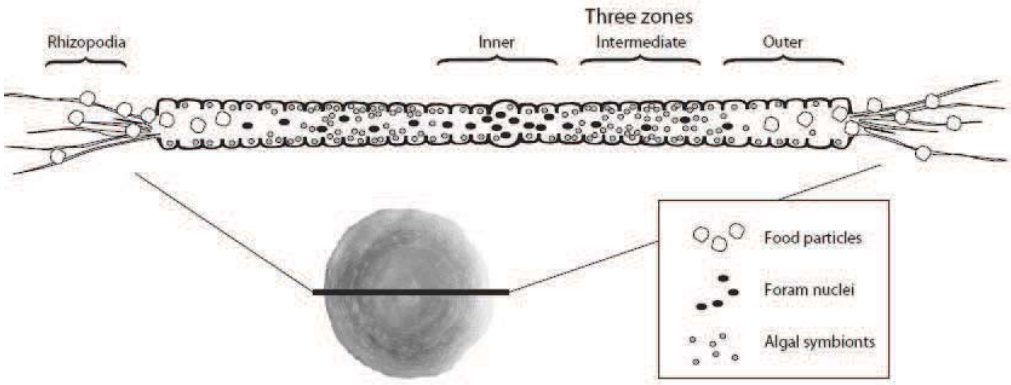

Figure 1.10: A cross section diagram of *Amphisorus hemprichii*. The shell is divided into three zones: 1) inner zone, 2) intermediate zone, and 3) outer zone (image from Fay et al. 2009).

The study of Hallock (1981b) indicated that the benthic symbiont-bearing foraminifera *Amphistegina lessonii* d'Orbigny and *Amphistegina lobifera* Larsen had faster growth when grown in high light (although photoinhibition, a light-dependent downregulation of the quantum yield of photosynthesis, did occur in full sunlight), likely due to their adaptation to shallow water habitats. In contrast, the study of Nobes et al. (2008) showed no difference in growth rate between different light regimes in *Amphistegina* spp. and *Calcarina* spp. and highest growth rate under low light conditions (60 µmol photons m^{-2} s^{-1}) in *Heterostegina depressa* d'Orbigny. The different results in the studies of Hallock (1981b) and Nobe et al. (2008) are likely to be a result of the light intensities used to determine high, medium and low light intensity (1200, 375, and 60 µmol photons m^{-2} s^{-1} in Nobes et al. (2008) and 240, 64, and 28 µmol photons m^{-2} s^{-1} in Hallock (1981b), respectively). Nobes et al (2008) also found that *Amphistegina* spp., *Calcarina* spp and *Heterostegina depressa* d'Orbigny can rapidly acclimate to changes in light conditions in the field and laboratory, suggesting light may not be the main limiting factor which controls distribution.

1.1.1.2.3 The response of algal symbionts in benthic foraminifera to light

Compared to corals and macroalgae, foraminifera are not sessile. They have the ability to move with their pseudopodia or rhizopodia, at speeds up to 0.139 mm min^{-1} in *Elphidium* sp. (Khare and Nigam 2000) (Figure 1.10). This provides foraminifera with the capacity to optimise their light environment and actively seek heterotrophic food. Evidence of phototaxis has been found in foraminifera, where individuals control their orientation in response to light availability (Lee et al. 1980). *Amphistegina lobifera* Larsen was positively phototaxic, moving toward the light source, at low light (1.35-13.5 μmol photons m^{-2} s^{-1}) and negatively phototaxic, moving to dimly lit areas of the flask, at higher light levels (> 135 μmol photons m^{-2} s^{-1}) which cause photoinhibition (Lee et al. 1980), indicating the role of light on the distribution of symbiont bearing foraminifera.

1.1.2 Climate change

Human activities such as the burning of fossil fuels, industrialization, deforestation and intensive agricultural activities have raised atmospheric concentrations of various greenhouse gases including methane and CO_2 since the beginning of the industrial revolution (Kleypas et al. 2006). This has lead to an increase in global temperatures through the trapping of heat through the Greenhouse Effect. As a consequence, surface seawater temperature has increased since the last century by an average of 0.6°C (Solomon et al. 2007). Increases in temperature elevate sea level by changing the density and volume of water, as well as the melting of polar ice caps, and increase precipitation and evaporation, which leads to more frequent and intense storms (Emanuel 2005; Schubert et al. 2006).

Furthermore, the rising atmospheric CO_2 concentration leads to ocean acidification by increasing the dissolved CO_2 concentration in the ocean surface layers which lowers pH. It is estimated that 2 Gt of CO_2 in the atmosphere each year dissolves into the oceans (Houghton 2009). This is approximately 30% of the anthropogenically released CO_2

(Anthony et al. 2011). Atmospheric CO_2 has increased from pre-industrial levels of 280 ppm to approximately 384 ppm today (Solomon et al. 2007). The rate of change is 100-1,000 times faster than the most rapid changes in temperature and CO_2 in at least the last 420,000 years (Hoegh-Guldberg et al. 2007). Models parameterized with CO_2-emission trends for 1990-1999 (so-called "SRES scenarios"; IPCC 2007) predict that CO_2 concentrations will rise 150-250% (to ≤ 1000 ppm) by the year 2100 (Friedlingstein et al. 2006). The surface ocean pH is already 0.1 units lower than pre-industrial values (Haugan and Drange 1996; Orr et al. 2005) (which is equivalent to a 30% increase in H^+ ions; Raven et al. 2005) and is predicted to decrease by a further 0.4 to 0.5 units by 2100 and by 0.7 units by 2200 (Raven et al. 2005; Lough 2007; Hofmann and Schellnhuber 2009).

Dissolved inorganic carbon (DIC) in the ocean occurs in forms of CO_2 (carbon dioxide), HCO_3^- (bicarbonate ion), and CO_3^{2-} (carbonate ion). The abundance of each form of DIC reaches an equilibrium based on the input of CO_2 into the system. Equation 1 shows the process of DIC equilibrium in seawater.

$$CO_{2\,(gas)} + CO_{2\,(aq)} + H_2O \rightleftharpoons H_2CO_3 \rightleftharpoons H^+ + HCO_3^- \rightleftharpoons 2H^+ + CO_3^{2-} \qquad (1)$$

CO_2 in the atmosphere dissolves in seawater and forms carbonic acid (H_2CO_3), which quickly dissociates to hydrogen ions and bicarbonate (HCO_3^-) and carbonate (CO_3^{2-}) ions. At the present day seawater pH of 8.1, the proportion of HCO_3^- ions to CO_3^{2-} ions and to the dissolved CO_2 concentration is approximately 90: 9: 1 (Figure 1.11, Table 1.1) (Leclercq et al 2000; Doney et al. 2009). When pH drops to pH 7.7 (as predicted in 2100), the concentration of CO_2 and HCO_3^- increase, but the concentration of CO_3^{2-} decreases (Leclercq et al 2000; Doney et al. 2009).

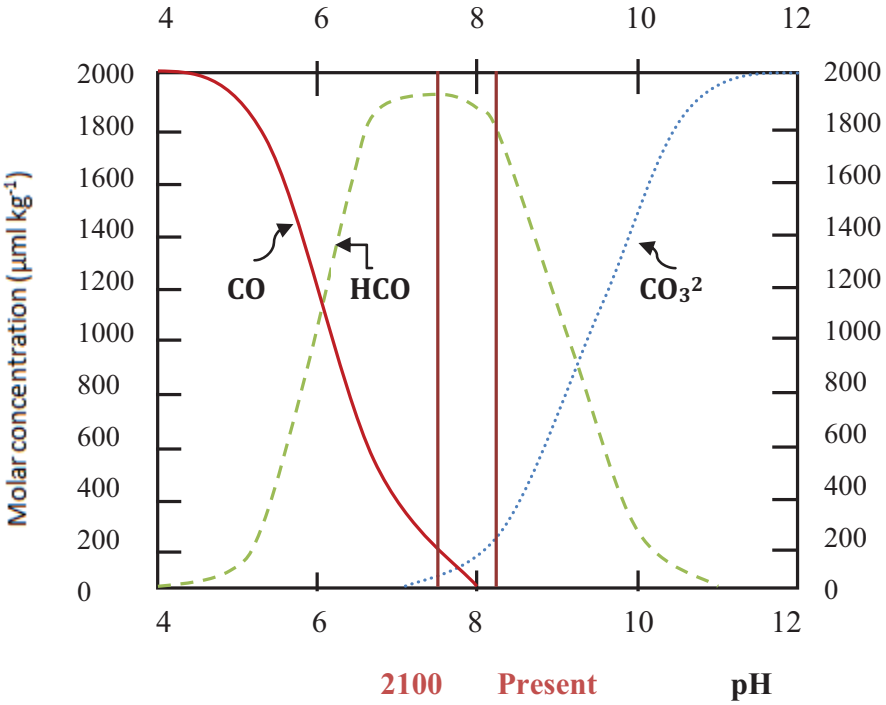

Figure 1.11: Relative proportions of the three inorganic forms of CO_2 dissolved in seawater; CO_2, HCO_3^-, and CO_3^{2-}. The present day pH of 8.1 and the expected 2100 pH of 7.7 are indicated by the vertical lines (Raven et al. 2005; Doney et al. 2009).

The increase in CO_2 concentration produces H^+ ions which increases seawater acidity. As the pH drops, the concentration of CO_3^{2-} ions decreases, while the concentration of HCO_3^- ions increases (see Figure 1.11). The decrease in the availability of the essential CO_3^{2-} ion for calcification ($CaCO_3$ deposition) will affect a range of marine organisms, such as calcifying algae, foraminifera, corals, plankton, molluscs, echinoderms and crustaceans. Reduced rates of calcification under severe acidification conditions; where dissolution of $CaCO_3$ have been found (Feely et al. 2004; Yates and Halley 2006a,b).

Table 1.1: Carbonate chemistry of tropical surface seawater in pre-industrial, present day conditions and prediction for the years 2065 and 2100 (Solomon et al. 2009).

Parameters	Unit	Pre-industrial	Present	2065 2 x CO_2	2100 3 x CO_2
CO_2	µmol kg^{-1}	280	384	560	840
HCO_3^-	µmol kg^{-1}	1739	1827	1925	2004
CO_3^{2-}	µmol kg^{-1}	222	186	146	115
pH		8.16	8.05	7.91	7.76

Calcification will slow and the risk of dissolution increase as the saturation state of calcium carbonate (Ω) declines (Feely et al. 2004; Raven et al. 2005; Anthony et al. 2008; Doney et al. 2009). The process of calcification occurs by the reaction shown in equation 2 and the calcium carbonate saturation state is shown in equation 3.

$$Ca^{2+} + CO_3^{2-} \rightleftharpoons CaCO_3 \qquad (2)$$

$$\Omega = [Ca^{2+}]\,[CO_3^{2-}]/\,K'sp \qquad (3)$$

Where $[Ca^{2+}]$ is the calcium concentration, $[CO_3^{2-}]$ is the carbonate concentration (in mmol kg^{-1}); K'sp is the stoichiometric solubility product for $CaCO_3$ which depends on temperature, salinity and pressure (Lough 2007; Doney et al. 2009). Seawater is supersaturated with calcium carbonate when the saturation degree (Ω) is greater than 1 and undersaturated when the saturation degree (Ω) is lower than 1 (Feely et al. 2004).

Calcite (trigonal-rhombohedral) and aragonite (orthorhombic) are two major polymorphs (or crystal structures) of calcium carbonate (Figure 1.12, 1.13). The current saturation state of calcite (Ω-calcite = 5-6) is higher than aragonite (Ω-aragonite = 3-4), which is higher than high-magnesium calcite (Ω-high-magnesian calcite = 2-3) (Kleypas et al. 1999; ISRS 2008). Thus, calcium carbonate precipitated as high-magnesium

calcite will be more sensitive to the increase of anthropogenic CO_2, than calcium carbonate precipitated as aragonite, which will be more sensitive than calcium carbonate precipitated as calcite (Kleypas et al. 1999).

As aragonite is more soluble than calcite; the saturation depth (the level of thermodynamic equilibrium) for aragonite is shallower than for calcite (Feely et al. 2004). Kleypas et al. (1999) predicts that the seawater saturation state for aragonite will drop to 3.1±0.2 by the year 2065 and to 2.8±0.2 by 2100, while high-magnesium calcite will drop 17-35% by 2100. In addition, the global biogeochemical ocean model predicts that the calcite saturation state will decline when the atmospheric CO_2 concentration reaches 800 ppm in approximately 2100 (Ilyina et al. 2009). Thus, it is likely that there will be an even higher risk of calcium carbonate dissolution in the future.

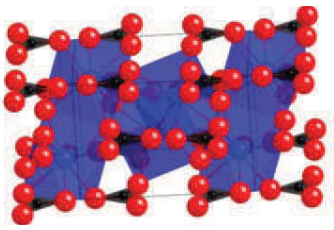

Figure 1.12: Aragonite crystal structure (orthorhombic). Calcium atoms are blue, oxygen atoms red, and carbon atoms black. Carbonate groups are flat triangles (image by Judge Nutmeg).

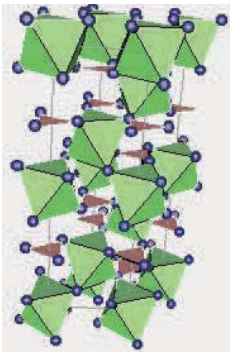

Figure 1.13: Calcite crystal structure (trigonal-rhombohedral). Calcium atoms are green, oxygen atoms blue, and carbon atoms brown (image by Crystal Structure Design AS).

1.1.3 Impact of ocean acidification and ocean warming on marine organisms

Many studies have shown that an increase in sea temperature and atmospheric CO_2 influence the health and survivorship of marine organisms, especially calcifying species, such as molluscs, crustaceans, echinoderms (Dupont and Thorndyke 2009), corals (Reynaud et al. 2003; Jokiel et al. 2008), calcareous algae (Smith and Roth 1979; Jokiel et al. 2008), foraminifera (Hallock 2000) and some phytoplankton (Rost and Riebesell 2004; Raven et al. 2005; Iglesias-Rodriguez et al. 2008). Each species responds differently in terms of growth, photosynthesis, calcification, reproduction, and survivorship to ocean acidification and global warming (Anthony et al. 2008; Dupont and Thorndyke 2009; Illyina et al. 2009; Johnson and Marshall 2007). Temperature influences the physiological process including photosynthesis, respiration and calcification (Howe and Marshall 2002; Necchi Jnr 2004; Hancke et al. 2008). Thermal stress leads to mortality and changes in reproduction, such as spawning time, flowering, and seed germination in seagrass, which may result in the shift in distribution and abundance (McQuaid and Branch 1984; Short and Neckles 1999; Fraile et al. 2009). Necchi Jnr (2004) found variation in electron transport rate (ETR), non-photochemical quenching (NPQ), respiration, and the photosynthesis: respiration ratio (P:R ratio) with temperature in tropical lotic macroalgae, such as *Terpsinoe musica* Ehrenberg (Bacillariophyta), *Cladophora glomerata* (Linnaeus) Kutzing (Chlorophyta) and *Compsopogon coeruleus* (Balbis ex C. Agardh) Montagne (Rhodophyta), indicating the difference in optimum temperature and adaptation mechanisms of the photosynthetic apparatus to temperature changes among species. In *Halimeda*, the photosynthetic and respiratory responses to temperature are known to be varied among species (Abel and Drew 1985). The temperature tolerant species, *Halimeda tuna* (Ellis & Solander) Lamouroux, is dominant in the Great Barrier Reef, Pacific and Caribbean shallow water coral reef habitats, where temperatures can exceed 30°C (Abel and Drew 1985). Temperature may also play a role in sexual reproduction in *Halimeda* by triggering mass gamete release at approximately 28-30°C (Clifton and Clifton 1999). Elevated seawater temperatures of 30 to 35°C retarded the growth rate in the benthic foraminifera,

Rosalina leei Hedley & Wakefield (Nigam et al. 2008) and is known to induce symbiont lost in *Amphistegina gibbosa* d'Orbigny when temperatures reach 32°C (Talge and Hallock 2003). In reef-forming (scleractinian) corals, warmer temperatures increase the rate of calcification (Lough and Barnes 1997; Lough and Barnes 2000), although increases as small as 1-2°C above summer averages can lead to mass coral bleaching events (large areas of coral colonies expelling symbiotic algae) and sometimes death (Hoegh-Guldberg 1999). It is expected that those species most vulnerable to bleaching will become less abundant as the oceans become warmer (e.g., acroporids and pocilloporids) (Strychar et al. 2004), resulting in a shift in species composition on a reef, to domination by tolerant species (e.g., *Porites* spp.) (Hoegh-Guldberg 1999).

Ocean acidification has been suggested to have a positive effect on organisms such as seagrass and non-calcifying macroalgae, which utilise CO_2 as the building-block for carbon fixation in photosynthesis (Gao et al. 1993a; Short and Neckles 1999; Invers et al. 2002; Hobday et al. 2006). In elevated CO_2 conditions, the seagrass *Posidonia oceanica* (L.) Delile and the red algae, *Gracilaria* sp. and *Gracilaria chilensis* Bird, McLachlan & Oliveira showed an increase in productivity (net oxygen release) (Invers et al. 2002) and growth (Gao et al. 1993a), respectively. However, ocean acidification is likely to have a negative impact on calcified organisms, such as molluscs, corals, some microalgae, foraminifera and calcifying algae, by decreasing the availability of CO_3^{2-} ions and hence the organisms' ability to produce their calcium carbonate skeleton. This can lead to an increase in calcium carbonate dissolution as the saturation state of calcium carbonate (Ω) declines. Photosynthesis can influence the carbonate chemistry and offset ocean acidification by increasing local pH around the phototrophs and thereby indirectly favour calcification (Anthony et al. 2011). Reduced calcification, recruitment, growth and productivity were found in the articulated coralline alga, *Corallina pilulifera* Postels & Ruprecht, and crustose coralline algae (CCA) in elevated pCO_2 (partial pressure of CO_2) seawater (Smith and Roth 1979; Gao et al. 1993b; Kuffner et al. 2007; Anthony et al. 2008). In the Pacific coral, *Montipora capitata* Dana, Jokiel et al. (2008) found a decrease of 15-20% in calcification for acidified conditions. The study of

Leclercq et al. (2000) predicted that the rate of calcification in scleractinian corals may decrease by 21% from 1880 to 2065. Two recent studies on the effect of ocean acidification on coccolithophorids (marine calcifying phytoplankton) have found conflicting results. Riebesell et al. (2000) showed reduced calcification and malformations in calcium carbonate plates (coccoliths) with *Emiliania huxleyi* (Lohm.) Hay & Mohler and *Gephyrocapsa oceanica* Kamptner, while Iglesias-Rodriguez et al. (2008) found an increase in calcification and net primary production rate in *E. huxleyi*. The reasons for these differences include the difference in modifying carbonate system using acid/base and bubbling CO_2 to control pH which lead to the difference in calcium carbonate saturation state and dissolved inorganic carbon concentration (DIC). The use of the CO_2 bubbling method has become the most accepted and widespread method for simulating future CO_2 conditions as it influences the carbonate chemistry (Iglesias-Rodriguez et al. (2008; Hurd et al., 2009). CO_2 bubbling has advantages over other methods due to its ability to mimic carbonate chemistry in the future climate change scenarios as an increase in pCO_2 and DIC (decrease in pH) without alteration of total alkalinity (Gattuso et al. 2010).

The synergistic effects of ocean warming and acidification have also been identified in some studies. Combined elevated temperature and pCO_2 decreased the rate of calcification in the scleractinian coral *Stylophora pistillata* Esper (Reynaud et al 2003). In the corals *Acropora intermedia* Brook and *Porites lobata* Dana, Anthony et al. (2008) found that simulated ocean acidification and warming scenarios together (rather than ocean acidification conditions in isolation) resulted in bleaching, reduced productivity, as well as calcium carbonate dissolution and erosion in *A. intermedia* and *P. lobata* and in crustose coralline algae (CCA).

The quantity of research into the impacts of ocean acidification on *Halimeda* and foraminifera is modest in comparison to other reef-dwelling calcifiers. Borowitzka and Larkum (1976b) showed a negative response in calcification in *Halimeda tuna* (Ellis & Solander) Lamouroux from the Great Barrier Reef when seawater pH was dropped from 8.0 to 7.5. A more recent study found thinner aragonite crystals and higher crystal

density (count of crystals per unit area) in *H. tuna* and *H. opuntia* grown in pH 7.5 when compared to those grown at a pH of 8.1 (Robbins et al. 2009). Research on symbiotic and non-symbiotic planktonic foraminifera (*Orbulina universa* d'Orbigny and *Globigerina sacculifers* Brady, respectively) showed a decrease in shell weight with decreasing availability of the carbonate ion in seawater (Bijma et al. 2002). These results indicate that a decrease in calcification is likely in these organisms under the acidified conditions expected to occur in the future.

In conclusion, increasing atmospheric CO_2 and water temperatures will have many negative impacts on calcifying marine organisms by altering calcification, productivity, survival and reproduction and may lead to mortality. The loss of these calcifying organisms will affect other associated species such as the fish community and invertebrates. Other marine organisms, which may benefit from the future climate change scenarios, may become dominant. These effects will traverse all trophic levels, leading to community and ecosystem scale impacts, as coral reef ecosystems change in structure, composition and function.

1.2 PHOTOSYNTHESIS

Photosynthesis converts light energy into chemical energy in the form of sugars, starches, or other organic compounds through chemical reactions that occur in the chloroplasts of phototrophs. Light energy is absorbed by chlorophyll pigments in the chloroplast which initiates the photochemical reactions in the thylakoid membranes (light reactions). The products from the light reactions are then used to fix carbon in the stroma (dark reactions). The end result is the formation of carbohydrates. This energy can then be used for survival, growth and reproduction (Atwell et al. 1999).

1.2.1 Light reactions of photosynthesis

Light reactions occur in the thylakoid membranes of chloroplasts (Jeffery and Ross 2007). These membranes are made of a phospholipid bilayer and contain chlorophyll-protein complexes, which are also known as photosystems (Jeffery and Ross 2007).

Photons are absorbed by chlorophyll pigments (as well as carotenoids and phycobilins in some cases) and the energy is transferred to the photosystem reaction centre (Taiz and Zeiger 2006). Photosystem II (PSII), which is also known as P680, absorbs light maximally at 680 nm (Falkowski and Raven 2007). When a photon is captured by PSII, the reaction centre is excited, sending an electron from PSII to a higher energy state and on to the primary electron acceptor, Q_A, which is a quinone bound to the D2 protein (Falkowski and Raven 2007). The oxygen evolving complex (OEC) splits a water molecule to replace the lost electron and as a byproduct, molecular oxygen (O_2) is produced (Hall and Rao 1994). The electron is passed to Q_A and is then transferred to Q_B on the D1 protein. Once Q_B receives two electrons, the electrons are transferred in the thylakoid membrane to the cytochrome b_6f complex (Falkowski and Raven 2007). When electrons arrive at Photosystem I (PSI or P700, absorbs light maximally at 700 nm), the acceptors, A_0, A_1, F_X, F_B, F_A, F_d, pass an electron to $NADP^+$ which is reduced to NADPH using NADP reductase (Atwell et al. 1999). Electrons lost from this process are replaced by electrons from PSII (Figure 1.14) (Taiz and Zeiger 2006). The concentration of H^+ ions inside the thylakoid membrane (from water splitting and protons pumped across the thylakoid membrane) is used to synthesize ATP from ADP and P_i using ATP synthase. This process is called photophosphorylation (Hall and Rao 1994).

1.2.2 Dark reactions

The dark reactions (also known as the Calvin cycle) occur in the stroma of the chloroplast and use the products from the light reactions (i.e., ATP and NADPH) to fix inorganic carbon (CO_2) to produce organic compounds such as glucose. This reaction is catalysed by the enzyme ribulose-1, 5-biphosphate carboxylase/oxygenase (Rubisco). The 6-carbon sugar formed by this process can break down to two 3-carbon molecules or phosphoglycelic acid (PGA). The PGA molecules are phosphorylated by ATP and reduced by NADPH to form phosphoglyceraldehyde (PGAL) which is the starting material for glucose or 6-carbon sugar (Falkowski and Raven 2007; Jeffery and Ross 2007) (Figure 1.15).

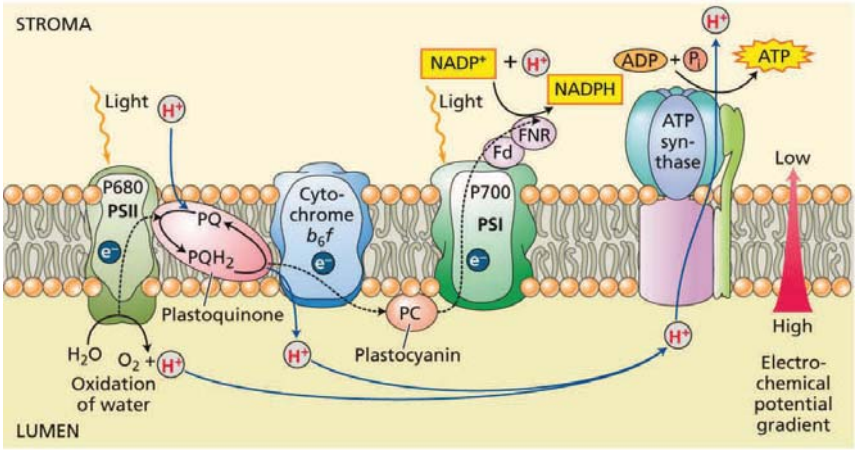

Figure 1.14: Photosystem II (P680), photosystem I (P700) and electron carriers in the thylakoid membrane. Photons are absorbed by pigments and transferred to the photosystem reaction centres. Electrons are transported through the electron acceptors to produce NAHPH and the pH gradient leads to the production of ATP (image from Taiz and Zeiger 2006).

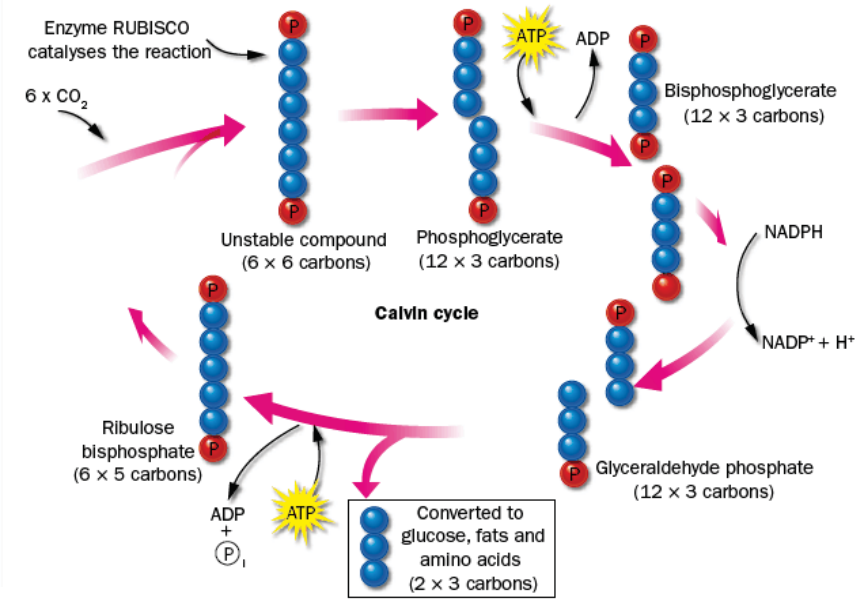

Figure 1.15: The Calvin cycle. ATP and NADPH are used in this reaction to drive CO_2 fixation by the Rubisco enzyme and form the glucose or 6-carbon sugar (image from Jeffery and Ross 2007).

The process of photosynthesis is summarised in Equation 4 and Figure 1.16. In the light reactions (Photosystem II and I), light is absorbed and the reaction centre is excited. Electrons are transported through the electron transport chain. The substrates for light reaction are CO_2 and H_2O and the products from the light reactions are O_2, ATP and NADPH. ATP and NADPH from the light reactions are used to fix carbon dioxide (CO_2), the substrate for the dark reactions, to produce organic compounds such as glucose in the Calvin cycle (Jeffery and Ross 2007).

$$6CO_2 + 12H_2O \longrightarrow C_6H_{12}O_6 + 6H_2O + 6O_2 \qquad (4)$$

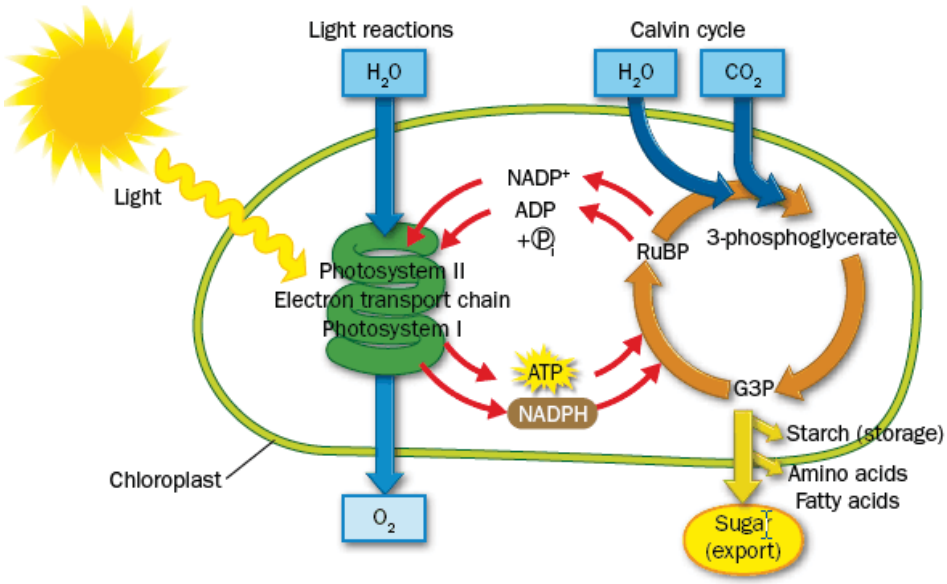

Figure 1.16: An overview of photosynthesis; The link between light reactions (photosystem II and I) and dark reactions (Calvin cycle) in the chloroplast (image from Jeffery and Ross 2007).

1.2.3 Chlorophyll *a* fluorescence

There are many parameters used to measure the photosynthetic condition of photosynthetic organisms, such as biomass (Merrett and Armitage 1982), inorganic carbon uptake (Gao et al. 1993b; Zondervan et al. 2002; Haikali et al. 2004), and

evolution of oxygen (Borowitzka 1981; De Beer and Larkum 2001). One of the most powerful and widely used techniques for plant physiologists and ecophysiologists is chlorophyll *a* fluorescence analysis (Maxwell and Johnson 2000) which measures photosynthetic efficiency of photosystem II at ambient temperature (e.g., Ralph and Gademann 2005; Ralph et al. 2005a; Ralph et al. 2005b; Cruz and Serodio 2008). Pulse Amplitude Modulated (PAM) fluorometry (Walz GmbH, Effeltrich, Germany), is a non-destructive, non-invasive, rapid and easy to use technique both in the field and in the laboratory (Maxwell and Johnson 2000; Roger 2001; Baker 2008). There is a wide variety of PAM fluorometers designed for different applications, environments, and experimental conditions, such as the Diving-PAM for underwater measurements, Water-PAM for measurements on low concentration phytoplankton in water sample, Microscopy-PAM for assessing the condition of single cells, Imaging-PAM for measuring images of photosynthetic activity on a two-dimensional surface, and Mini-PAM for field or laboratory studies.

The light energy which is absorbed by light harvesting complexes (LHCs) of PSII has three potential fates (Maxwell and Johnson 2000; Roger 2001; Schreiber 2004):

1) Light energy is transferred to the PSII reaction centre (P680) and used to drive photosynthesis (photochemical quenching)
2) Excess light energy is dissipated as heat in the form of non-photochemical quenching (NPQ)
3) Light is re-emitted at a longer wavelength, as chlorophyll fluorescence; (Figure 1.17).

At ambient temperature, most fluorescence (90%) comes from the chlorophyll *a* molecules which are associated with photosystem II (Govindjee 1995; Roger 2001). The total amount of chlorophyll fluorescence is only 1 to 2% of total light absorbed (Maxwell and Johnson 2000; Roger 2001; Schreiber 2004).

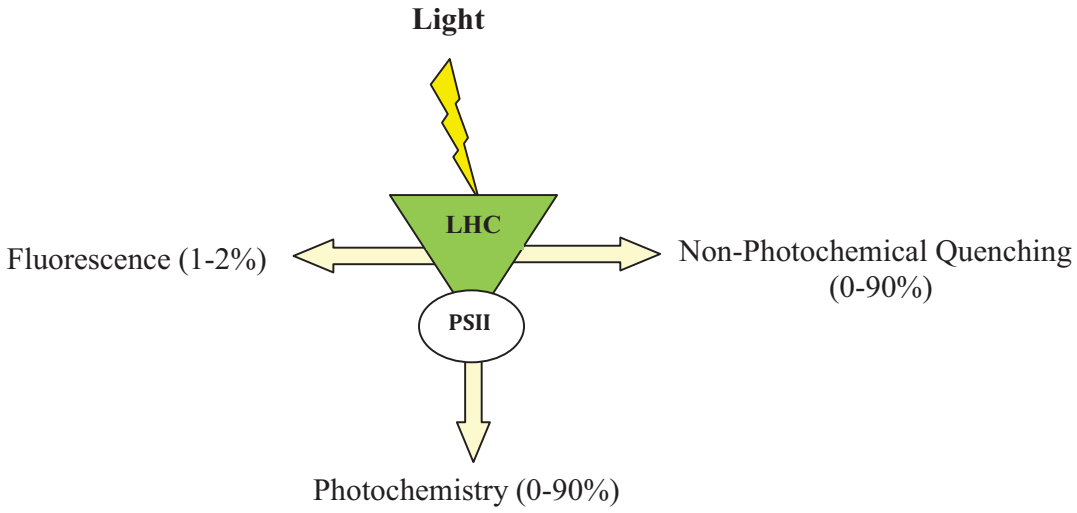

Figure 1.17: The three potential fates of absorbed light energy by the LHCs of PSII

Pulse Amplitude Modulated (PAM) fluorometry can measure the fluorescence parameters such as effective quantum yield of PSII (Φ_{PSII}), maximum quantum yield of PSII (F_v/F_m), non-photochemical quenching (NPQ), and Relative Electron Transport Rate (rETR) (Maxwell and Johnson 2000):

Φ_{PSII}	Effective quantum yield of PSII	$(F_m' - F_t)/F_m'$	(5)
F_v/F_m	Maximum quantum yield of PSII	$(F_m - F_o)/F_m$	(6)
NPQ	Non-photochemical quenching	$(F_m - F_m')/F_m'$	(7)
rETR	Relative electron transport rate	Φ_{PSII} x PAR	(8)

where, F_m' is the maximum fluorescence in the light upon application of a saturating pulse, F_t is the minimum fluorescence in the light upon application of a saturating pulse, F_m is the maximum fluorescence in darkness upon application of a saturating pulse, F_o is the minimum fluorescence in darkness upon application of a saturating pulse, and PAR is the intensity of photosynthetic active radiation.

1.2.3.1 Effective quantum yield of PSII (Φ_{PSII})

Under ambient light conditions, fluorescence is measured during the application of measuring light (a low light intensity of < 0.15 μmol photons m^{-2} s^{-1} for detecting

fluorescence without inducing photosynthesis) on the sample, giving a measure of light-adapted minimum fluorescence (F_t) (Ralph and Gademann 2005). A saturation pulse (>10,000 μmol photons m^{-2} s^{-1} for assessing photosynthetic activity) is then applied for <1 s giving a measurement of light-adapted maximum fluorescence (F_m'). The effective quantum yield of PSII (Φ_{PSII}) can then be calculated using Equation 5 (Figure 1.18). Effective quantum yield of PSII (Φ_{PSII}) is the indicator of efficiency of photochemical processes in PSII when under the experimental light conditions (Maxwell and Johnson 2000; Schreiber 2004; Baker 2008).

1.2.3.2 Maximum quantum yield of PSII (F_V/F_M)

Following a period of dark adaptation (this varies between 5 and 60 minutes (Schreiber 2004)), minimum fluorescence (F_o) can be detected during the application of the low intensity measuring light. At this stage, the PSII centres are open (Q_A oxidized). When a saturating pulse of light is applied, dark-adapted maximum fluorescence (F_m) can be measured (PSII centres are closed by this flash (Q_A reduced)). Variable fluorescence ($F_v = F_m - F_o$) and maximum quantum yield of PSII (F_V/F_M) can be provided using Equation 6 (Figure 1.18). The maximum quantum yield of PSII (F_V/F_M) provides the maximum efficiency at which light absorbed by PSII is used for photochemistry. This parameter indicates stress or damage in PSII (Maxwell and Johnson 2000; Schreiber 2004; Baker 2008).

1.2.3.3 Steady state light curves (SSLCs)

After a period of dark adaptation and the application of a saturating pulse as explained above, an actinic light (the light to drive photosynthesis; can range up to 2,000 μmol photons m^{-2} s^{-1}) is turned on and kept constant for 5-10 mins each, with saturating pulses applied every 20-60 seconds, allowing for measurement of F_m' and F_t (Maxwell and Johnson 2000; Ulstrup et al. 2005; Baker 2008; Hill and Ralph 2008). The steady state light curve (fluorescence trace plotted over time) can be used to provide the photoacclimation status of the photosynthetic apparatus (Cruz and Serodio 2008).

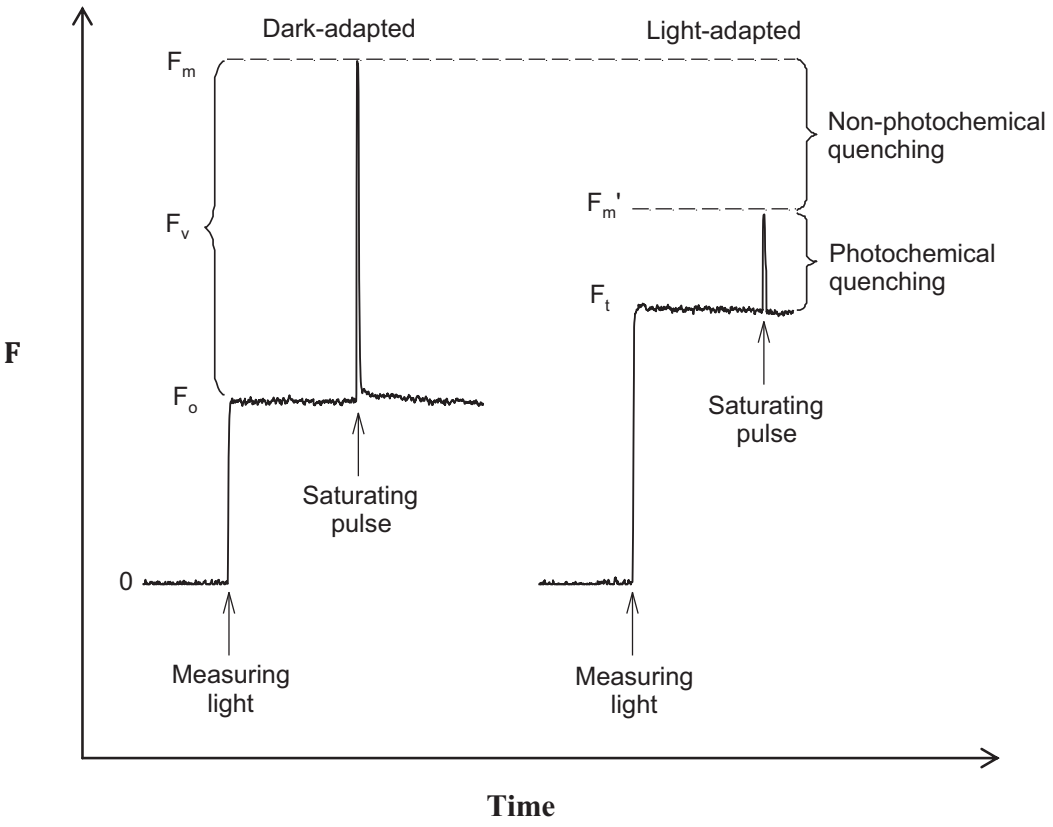

Figure 1.18: Fluorescence traces showing the fundamental measures used to calculate dark-adapted maximum quantum yield, light-adapted effective quantum yield and non-photochemical quenching (image from Hill 2008).

1.2.3.4 Rapid light curves (RLCs)

Rapid light curves (RLCs) are shortened SSLCs providing a measure of the photosynthetic performance as a function of irradiance. However, in RLCs photosynthesis does not reach steady state conditions during each light step (Ralph and Gademann 2005). Without dark adaptation, an actinic light is turned on and saturating flashes at different irradiance levels are applied every 10 seconds for nine light steps. The rapid light curve can be completed in 90 seconds (Ralph and Gademann 2005) and

is useful in situations where a large number of samples are to be measured in short period of time (e.g., during SCUBA diving).

1.2.3.5 Non-photochemical quenching (NPQ)

Non-photochemical quenching (NPQ) can be calculated (equation 7) by performing dark-adapted measurement, steady state light curves, and rapid light curves (Figure 1.18). Non-photochemical quenching (NPQ) indicates the operation of heat dissipation processes, such as the photoprotective mechanisms of the xanthophyll cycle (Maxwell and Johnson 2000; Ralph and Gademann 2005; Baker 2008; Cruz and Serodio 2008). Exposure to high light intensity leads to photoinhibition (high NPQ) and low photosynthetic efficiency (Winters et al. 2003).

1.2.3.6 Relative electron transport rate (rETR)

Relative electron transport rate (rETR) can be calculated (equation 8) when running steady state light curves and rapid light curves (Figure 1.18). Relative electron transport rate (rETR) indicates the rate of electron flow from PSII onwards during the application of a known light intensity (Maxwell and Johnson 2000; Ralph and Gademann 2005; Baker 2008; Cruz and Serodio 2008).

1.3 CALCIFICATION

Calcification is the process of calcium carbonate ($CaCO_3$) deposition around or within a cell (McConnaughey and Whelan 1997; McNiel et al 2004). H_2O is generated in the calcification process as well as $CaCO_3$ and CO_2 (Equation 9) (McConnaughey and Whelan 1997).

$$Ca^{2+} + 2HCO_3^- \longrightarrow CaCO_3 + H_2O + CO_2 \qquad (9)$$

The calcification process starts with the nucleation process which involves the formation of a solid phase from a liquid phase (when the Ca^{2+} and CO_3^{2-} ions are supersaturated

and there is sufficient time and energy (in the form of ATP) for the process to be completed) (Barnes and Chalker 1990). Once nucleation is complete, diffusion of solutes to the crystal-solution interface occurs and the solutes absorb to the $CaCO_3$ crystal surface (Borowitzka 1984 after Nancollas and Purdie 1964).

1.3.1 *Halimeda* calcification and photosynthesis

The calcification process in *Halimeda* is related to the rate of photosynthesis and is stimulated by light (Borowitzka and Larkum 1976b,c; Jensen et al. 1985). Photosynthesis stimulates calcification by removing CO_2 from the intercellular space resulting in increased pH and as a result, CO_3^{2-} availability. In contrast, respiration-derived CO_2 and the consequential decrease in pH and CO_3^{2-} results in an inhibition of calcification (Borowitzka and Larkum 1976b). Ca^{2+} and Ca^{2+} binding polysaccharides play a role in *Halimeda* calcification (Bohm and Goreau 1973). Ca^{2+} influx and outflux is almost the same in *H. opuntia* and is approximately 300 µg Ca^{2+} g $alga^{-1}$ min^{-1} while the Ca^{2+} net accretion is 3.6 µg Ca^{2+} g $alga^{-1}$ min^{-1} (Bohm and Goreau 1973). Borowitzka and Larkum (1976c) also found that *Halimeda* can use HCO_3^- as a carbon source for photosynthesis because when photosynthetic rate is high, pH can reach 9.0 where only 0.06% of the inorganic carbon exists as CO_2. In acidified conditions where HCO_3^- in seawater is higher (see Figure 1.11), *Halimeda* may be able to take up more HCO_3^- and increases its photosynthetic rate.

1.3.2 Foraminiferal calcification

Foraminifera precipitate $CaCO_3$ in a form of magnesium-calcite within intracellular vacuoles formed during chamber construction (Hansen 1999). Similarly to *Halimeda*, the removal of CO_2 by photosynthesis has been suggested to increase the calcification of symbiont-bearing foraminifera (Erez 2003). Calcification in foraminifera, with algal symbionts is stimulated by light (Smith and Weibe 1977; Duguay and Taylor 1978; Duguay 1983), with calcification rates 2-3 times faster in light than in the dark (Duguay 1983). Ter Kuile et al. (1989a) observed that foraminiferal calcification was increased

with artificially elevated C_i (inorganic carbon), CO_3^{2-}, and Ca^{2+} concentrations in the symbiont-bearing foraminifera, *Amphistegina lobifera* Larsen and *Amphisorus hemprichii* Ehrenberg. In the presence of DCMU (3(3,4-dichlorophenyl)-l,l-dimethylurea), an inhibitor of the light reactions of photosynthesis (DCMU binds to the Q_B site on the D1 protein of PSII), the rate of calcification was not affected, indicating that there was no direct linkage between photoassimilation of CO_2 and calcification (ter Kuile et al. 1989a). Ter Kuile et al. (1989b) also found evidence of competition for C_i (CO_2, HCO_3^- or CO_3^{2-}) between photosynthesis and calcification in the symbiont-bearing foraminifera *A. lobifera*, with photosynthesis taking priority on the consumption of the incoming C_i (CO_2, HCO_3^- or CO_3^{2-}).

Calcite precipitation in foraminifera is inhibited by Mg (Toler et al. 2001). Zhang and Dawn (2000) found lower rates of $CaCO_3$ precipitation in solutions with higher Mg/Ca ratios. The inhibition of calcite growth is caused by the incorporation of Mg into the calcite crystal at calcium ion sites (Zhang and Dawn 2000). The Mg content varied between 0 to 14% depending on the availability of the elements in artificial seawater and temperature (Katz 1973; Zhang and Dawn 2000).

1.4 RESEARCH OBJECTIVES AND THESIS OUTLINE

The major objectives of this research are to provide insight into the effects of elevated CO_2 and temperature on calcification and photosynthesis of the calcifying algae *Halimeda* spp. and symbiont-bearing benthic foraminifera. This project will provide a better understanding of potential impacts of climate change on coral reef ecosystems and improve our predictive capacity of potential changes into the next century.

Chapter 1 provides a detailed review of the literature, significance of the thesis and outlines the research objectives.

Chapter 2 presents data on the effects of irradiance on photosynthetic efficiency, photoprotective mechanisms and calcification in *Halimeda macroloba*, *Halimeda cylindracea*, and *Halimeda opuntia*.

Chapter 3 provides data on the movement and photosynthetic response of the symbiotic benthic foraminifera, *Marginopora vertebralis*, during diurnal changes in light intensity and answer the question if foraminiferal movement is controlled by symbiont photosynthesis. This chapter intends to link the behavioural movement of foraminiferans with their photosynthetic condition and evaluated the degree of communication between the host and symbionts to ensure an optimal light environment is achieved.

Chapter 4 evaluates the effects of elevated CO_2 and temperature conditions on calcification and photosynthesis in the calcifying algae *H. cylindracea*, *H. macroloba* and symbiont-bearing benthic foraminifera, *Marginopora vertebralis*. The hypothesis tested was that the calcifying macroalga, *Halimeda* would perform better than benthic foraminifera under high CO_2 conditions and that all organisms would show greater effects under the combined effect of elevated CO_2 and temperature.

Chapter 5 and **Chapter 6** present data on how the microenvironment, photosynthesis and respiration of *Halimeda* and foraminifera is affected by changing pCO_2 and temperature conditions.

Chapter 7 provides an insight into the biomechanical (e.g., force required to detach or break, break location, strength) and morphological (e.g., blade surface area and holdfast volume) properties of *Halimeda* under different degree of exposure. This chapter presents data on the impact of ocean acidification and ocean warming on skeletal mineralogy and mechanical integrity of *Halimeda* spp. The impact of ocean acidification on *Halimeda* is hypothesised to weaken calcified structures, thus altering particular biomechanical properties and subsequently reducing the ability of *Halimeda* to cope with wave action under the predicted increase in storm intensity.

Chapter 8 summarizes the key findings of this thesis, discusses the impact of ocean acidification and warming on the microenvironment, photosynthesis, calcification, skeletal mineralogy and biomechanical properties and implications for community and coral reef ecosystem, and suggests avenues for future research.

CHAPTER 2:

THE EFFECT OF IRRADIANCE ON PHOTOSYNTHETIC EFFICIENCY AND CALCIFICATION IN THREE *HALIMEDA* SPECIES

2.0 THE EFFECT OF IRRADIANCE ON PHOTOSYNTHETIC EFFICIENCY AND CALCIFICATION IN THREE *HALIMEDA* SPECIES

Laboratory work, data collection and data analyses were undertaken by Ross Hill and me. I was mostly responsible for the write up of the manuscript.

2.1 INTRODUCTION

The sediment-producing macroalgae, *Halimeda* (Chlorophyta), is pre-dominantly distributed in tropical to sub-tropical marine ecosystems. *Halimeda* plays a vital role on coral reefs as a producer of carbonate sediment providing as much as 2.2 kg of $CaCO_3$ m^{-2} yr^{-1} (Drew 1983), an ecosystem engineer (Kleypas and Yates 2009), a food source for herbivores (Smith et al. 2004) and provider of shelter and a nursery for invertebrates (Hillis-Colinvaux et al. 1980). *Halimeda* may grow in depths up to 100-150 meters, where light levels may be as low was 0.05-0.08 percent of the surface intensity (Hillis-Colinvaux et al. 1980). *Halimeda* from shallow water habitat experiences a large variation in irradiance during the day.

On coral reefs, light is a major environmental factor influencing photosynthetic marine organisms such as seagrass, microalgae and macroalgae, coral and foraminifera (Hallock 1981; Häder et al. 1996; Winters et al. 2003). However, exposure to high levels of photosynthetic active radiation (PAR) at shallow depths can lead to a loss of photosynthetic activity through light-dependent down-regulation of photosynthesis or a rise in photoinhibition (Hanelt et al. 1993). Down-regulation of photosynthesis can be defined as a loss of photosynthetic efficiency (quantum yield) of PSII (e.g., maximum quantum yield (F_V/F_M) and effective quantum yield ($\Delta F/F_M'$)) and a decrease in electron transport rate and involves photoprotection processes (Larkum et al. 2006). Photoprotection can occur as non-photochemical quenching in a form of thermal dissipation via the xanthophyll cycle, which can reduce the possibility for photodamage (Demmig-Adams and Adams 1992). The de-epoxidation of xanthophyll pigments from

violaxanthin to zeaxanthin via the intermediate antheraxanthin is involved in the photoprotective mechanism (Demmig-Adams and Adams 1992). Once saturating irradiances ease, this photoinhibition will relax and allow for the recovery of PSII photosynthetic efficiency and the conversion of zeaxanthin back to violaxanthin. However, the long-term exposure to saturating irradiance can lead to long-term photoinhibition due to structural change and damage to sensitive proteins, such as D1 in the reaction centre of PSII (Häder 2008), resulting in a long-term reduction in F_V/F_M and requiring the resynthesis of damaged D1 protein (Häder 2008). When the rate of damage in D1 protein exceeds the rate of repair, photodamage occurs (Häder and Figueroa 1997).

A number of studies using measurements of chlorophyll fluorescence using Pulse Amplitude Modulated (PAM) fluorometry in macroalgae have been used to investigate the photosynthetic response to irradiance (Häder et al. 1996; Häder et al. 2002; Beach et al. 2003). Franklin et al. (1996) found a decrease in photosynthetic efficiency (F_V/F_M) during high light exposure in the middle of the day in the coral reef macroalgae *Lobophora variegata*, *Chlorodesmis fastigiata* and *Halimeda tuna*, which indicates a down-regulation of PSII or photoinhibition.

The violaxanthin de-epoxidase inhibitor, dithiothreitol (DTT) has been used to investigate the function of the xanthophyll cycle (Häder et al. 2008). Häder et al. (2002) observed that DTT strongly inhibited photoinhibition and recovery in the green alga *Ulva* and the brown alga *Dictyota.* The chloroplast protein synthesis inhibitor, lincomycin, has been used to study the D1 protein repair mechanism necessary to maintain PSII function in the green alga *Chlorodesmis fastigiata* (Franklin and Larkum 1997; Campbell et al. 2003; Six et al. 2009). Six et al. (2009) observed that by blocking PSII repair in the green alga *Ostreococcus* sp., there was a sharp drop in PSII function and higher susceptibility to photoinactivation (Six et al. 2009).

The light-harvesting complexes (LHCs) in photosynthetic organisms capture photons and channel the light energy towards the reactions centrers (Koziol et al. 2007; Hill et al.

2012). LHCs in green algae are lutein-Chl *a*/b-protein complexes (Chen et al. 2002; Koziol et al. 2007). However, for siphonous green alga, e.g., *Halimeda* and *Codium*, the main LHCs are siphonaxanthin-Chl *a/b*-protein complexes (Chen et al. 2002). The LHCs are distributed between PSI and PSII and the distribution is dependent on environmental condition e.g. light quality and quantity and temperature (Mullineaux and Emlyn-Jones 2004; Rochaix 2011). At 77K, the absorption spectra of the antenna protein in PSI and PSII are different as PSI absorbs light in the far-red region (700 nm) whereas PSII absorbs shorter wavelengths around 650 nm (Wollman 2001). Green algae are able to balance excitation energy between the two photosystems to optimize photosynthetic performance and avoid over-excitation and photodamage (Wollman 2001; Jia and Li 2003). Under light conditions where PSII is favoured, the light harvesting complex II (LHC II) may move from PSII to PSI (state 1 to state 2 transition). Alternatively, under light conditions that favour PSI, the LHC I may redistribute from PSI to PSII (state 2 to state 1 transition) (Allen 2003; Jia and Li 2003). State transitions can play vital roles as a form of photoprotection against photoinhibition (Jia and Li 2003). *Halimeda* experienced a large variation in light intensity during the day. *Halimeda* are sessile and unable to adjust their light environment, therefore they must deal with prevailing light conditions. To avoid photodamage and maintain photosynthesis, *Halimeda* may employ several photoprotective mechanisms. LHC detachment and/or redistribution may be a pathway used by *Halimeda*. The capacity of state transition in *Halimeda* has not been studied.

Halimeda photosynthesis has been shown to be strongly influenced by the temperature and pH of the surrounding environment (Borowitzka and Larkum 1976b; Sinutok et al. 2011). Although *Halimeda* can use bicarbonate (HCO_3^-) for photosynthesis (Borowitzka and Larkum 1976b), a decline in pH (or an increase in CO_2 and HCO_3^-) can lead to a down-regulation of PSII (Sinutok et al. 2011). The investigation of *H. tuna* and *H. opuntia* photophysiology from 7 and 21 m deep in the Florida Keys revealed that deeper individuals were more susceptible to photoinhibition when exposed to surface irradiance due to their shaded-type acclimation (Beach et al. 2003). Häder et al. (1996) showed that

both shallow (1 m depth) and deep (5 m depth) thalli experience down-regulation of PSII under high irradiance as indicated by a decrease in the photochemical quenching and an increase in non-photochemical quenching (an indicator for photoprotection; NPQ). A partially recovery from oversaturating irradiance occurred within a few hours, evidenced by an increase in the photochemical quenching while photodamage was observed through an absence of oxygen production after 2 h recovery. The deeper thalli experienced more photodamage and recovered more slowly than the shallower thalli (Häder et al. 1996). Little is known about photoinhibition, recovery and photodamage mechanism in these algae (Häder et al. 1996). This study aimed to investigate the physiological responses in *Halimeda macroloba*, *H. cylindracea* and *H. opuntia* to changes in irradiance.

2.2 MATERIALS AND METHODS

Halimeda macroloba, *H. cylindracea*, and *H. opuntia* were collected from Heron Island reef flat (<2 m deep) in the southern Great Barrier Reef of Australia (151º55'E, 23º27'S). *H. macroloba* and *H. cylindracea* are commonly located in shallow water from above low-tide line to 12 m and 58 m deep, respectively (Hillis-Collinvaux 1980). *H. opuntia* sprawls over rock or dead coral surfaces, or grows as clumps on *Acropora* sp., from above low-tide line to 90 meters deep (Hillis-Collinvaux 1980). The irradiance at the surface of *Halimeda* spp. on Heron reef flat at low tide on a cloudless day was 1117±46 µmol photons m^{-2} s^{-1} (Mean ± SE). For 12 days, samples were maintained in flow-through seawater aquaria under three different light intensities adjusted by a neutral density filter, with peak midday irradiances of 50, 400, and 900 µmol photons m^{-2} s^{-1} (n = 4). These light intensities represented low, medium and high light conditions as indicated from natural light experienced *in situ.* The photosynthetic efficiency of thalli tips were determined through measures of chlorophyll *a* fluorescence using a Diving-PAM (Pulse Amplitude Modulated) fluorometer, once at the start of the experiment (1200 h) and three times at the end of the experiment (12 days later at 0600, 1200 and 1800 h) (n = 4). Steady state light curves (SSLCs; Kramer et al. 2004) with one irradiance step (372 μmol photons m^{-2} s^{-1} applied for 300 s) were performed after 10

min of dark adaptation. The maximum quantum yield (F_V/F_M), the effective quantum yield (Y(II)), the capacity for photoprotection (non-photochemical quenching yield (Y(NPQ)) and level of photoinhibition (non-regulated heat dissipation yield (Y(NO)) were determined, where Y(II) + Y(NPQ) + Y(NO) = 1 (Kramer et al. 2004). The F_V/F_M was calculated through the measurement of the dark-adapted minimum fluorescence (F_O; under measuring light of < 0.15 μmol photons m^{-2} s^{-1}) and the dark-adapted maximum fluorescence (F_M; under saturating pulse of 0.8 s and > 4500 μmol photons m^{-2} s^{-1}, saturating width = 0.8 s, gain = 2).

Photosynthetic pigment concentration (chlorophyll (chl) *a* and *b*) was determined using the standard spectrophotometric method of Ritchie (2006) at the end of the experiment. Chlorophyll *a* and *b* (μg mm^{-2}) were extracted by homogenising samples in 4 ml of 90% acetone at 4°C for 24 h. Samples were centrifuged at 1500 *g* for 10 min and the supernatant placed into a quartz cuvette in a spectrophotometer (Varian, Australia), with absorbance measured at 630 and 647 nm (*n* = 4).

Growth rate and calcification rate were determined by staining the thalli with 1% Alizarin Red-S solution in a 10 L aquarium tank for 12 h immediately prior to the start of experiment (Vroom et al. 2003) (*n* = 4). After 12 h of staining, the thalli were washed with seawater and placed into the treatment tanks. At the end of the experiment, the thallus natural pigment colour was removed by placing in a 5-10% bleach solution for 10 min. The dry weight (dw) of stained segments (old growth) and unstained segments (new growth) was then measured using an electronic balance (AB204-S, Mettler Toledo, USA). The growth rate was calculated as the amount of biomass (mg dw) per day. The dry weight of $CaCO_3$ was determined by a dry weight comparison between new growth before and after decalcifying in a 5% HCl (Vroom et al. 2003). The calcification rate was calculated as the $CaCO_3$ accumulation (mg dw) per day.

To investigate photoprotection mechanisms and the function of PSII, segments of *H. macroloba*, *H. cylindracea* and *H. opuntia* were placed into individual 100 mL clear containers, with 70 mL of seawater (control), 3 mM lincomycin (Franklin and Larkum

1997) and 1 mM 1,4-dithiothreitol (DTT) (Häder et al. 2002) (n = 4) for two days from 0600 to 2000 h. DTT and lincomycin were applied to the samples in the dark 1 h prior to the start of experiment. Lincomycin inhibits chloroplast protein synthesis which is necessary for maintaining PSII function (Aro et al. 1993; Franklin and Larkum 1997). DTT inhibits the violaxanthin de-epoxidase, which is involved in the de-epoxidation of violaxanthin to antheraxanthin and zeaxanthin in xanthophylls cycle (Rockholm and Yamamoto 1996).

The photosynthetic efficiency (F_V/F_M) was investigated after 10 min dark adaptation using at 0600 (pre-dawn), 1200 (high irradiance) and 2000 (recovery period) h (n = 4) for two consecutive days. Light intensities at the experimental depth were recorded every 5 mins for two consecutive days using submersible data recorders (Odyssey, New Zealand).

Chlorophyll fluorescence emission spectra were determined using a spectrally calibrated fibre optic spectrometer (USB2000+ UV-VIS, Ocean Optics, Florida, USA) at 0700 (low irradiance) and 1100 h (high irradiance) (Hill et al. 2012). *Halimeda* samples were ground and filtered onto a 25 mm diameter Whatman GF/F filter (n = 4). An 8 mm long, 3 mm wide oval disc was removed from the centre of the filter using a custom-built hole-punch, placed into a groove at the end of a metal shaft and then immersed in a liquid nitrogen glass dewar surrounded by a portable, light-weight, custom-built fluorescence spectrophotometer. The orientation of the sample in the dewar to the direct beam of a blue LED excitation light (peak λ 470 nm) was 45º. The fluorescence emission from the sample was detected at the orientation of 90º to the excitation light source and 45º to the sample (Hill et al. 2012). The fluorescence intensity (photon counts; relative units) was detected every 0.3 nm using a 650 nm long-pass filter. The fluorescence emission spectrum from 650 to 750 nm was deconvoluted into component bands (peak λ 682, 691, 702, 715 and 729) using PeakFit (SeaSolve Software Inc, Framingham, Massachusetts, USA). The percentage area under each component band was calculated.

To determine any significant differences among treatments and time on the independent samples, one-way analysis of variance (ANOVA) and Tukey's post hoc multiple comparison tests ($\alpha = 0.05$) were performed (SPSS version 17). To determine any significant differences over time in chlorophyll fluorescence parameters, repeated-measures analysis of variance (rmANOVA) tests were performed. If data did not meet the assumptions of normality (Kolmogorov-Smirnov test) and equal variance (Levene's test), the data were transformed using $\log_{10}$ or square root.

2.3 RESULTS

After 12 days of exposure to the treatment light intensities, all species showed no significant differences between light treatments in growth rate ($P > 0.05$; Fig. 2.1a), $CaCO_3$ accumulation rate ($P > 0.05$; Fig. 2.1b), chlorophyll *a* and *b* concentration and chlorophyll *a*:*b* ratio ($P > 0.05$; Fig. 2.2a-c). Chlorophyll *a* fluorescent measurements revealed significant differences in photosynthetic efficiency (F_V/F_M) and the level of photoinhibition (Y(NO)) between light treatments (Fig. 2.3a-c, g-i). In *H. macroloba*, significantly higher maximum quantum yield (F_V/F_M) was observed in the samples treated at low light (50 μmol photons m^{-2} s^{-1}) at 0600, 1200 and 1800 h compared to other light treatments ($P < 0.001$; Fig. 2.3a), whereas there were no significant differences in effective quantum yield (Y(II)) between treatments at all time of sampling ($P > 0.05$; Fig. 2.3d). In *H. cylindracea*, F_V/F_M was higher at lower light treatment (50 and 400 μmol photons m^{-2} s^{-1}) at 0600, 1200 and 1800 h ($P = 0.001$; Fig. 2.3b), whereas there were no significant differences in effective quantum yield (Y(II)) between treatments at all sampling time points ($P > 0.05$; Fig. 2.3e). F_V/F_M in *H. opuntia* under high lights was significantly lower than other irradiance treatments at 1200 h and 1800 h ($P = 0.040$; Fig. 2.3c), whereas there were no significant differences in Y(II) between treatments at all time of sampling ($P > 0.05$; Fig. 2.3f). No significant differences in F_V/F_M and Y(II) were observed between times of sampling in all species from all light treatments ($P > 0.05$; Fig. 2.3a-f).

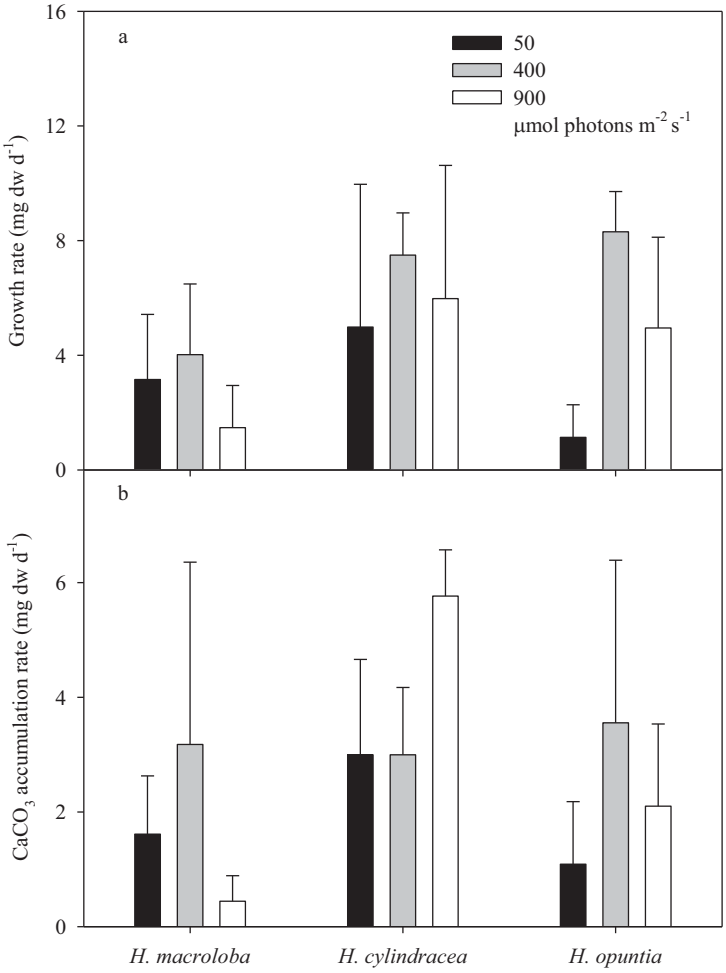

Figure 2.1: Growth rate (mg dw d^{-1}; a) and $CaCO_3$ accumulation rate (mg dw d^{-1}; b) of *H. macroloba*, *H. cylindracea* and *H. opuntia* from 50 (black boxes), 400 (light grey boxes) and 900 (dark grey boxes) µmol photons m^{-2} s^{-1} treatments. Averages + S.E. shown (*n* = 4).

In *H. macroloba*, *H. cylindracea* and *H. opuntia*, Y(NO) was significantly greater in the high light treatment at 0600, 1200 and 1800 h compared to other light treatments (P = 0.002, 0.001 and 0.039; Fig. 2.3g-i). However, no significant differences between times were observed in Y(NO) in all treatments and species (P > 0.05; Fig. 2.3g-i). Interestingly, there were no significant differences in the capacity for photoprotection (non-photochemical quenching yield (Y(NPQ)) between light treatments and times in all species (P > 0.05; Fig. 2.3j-l).

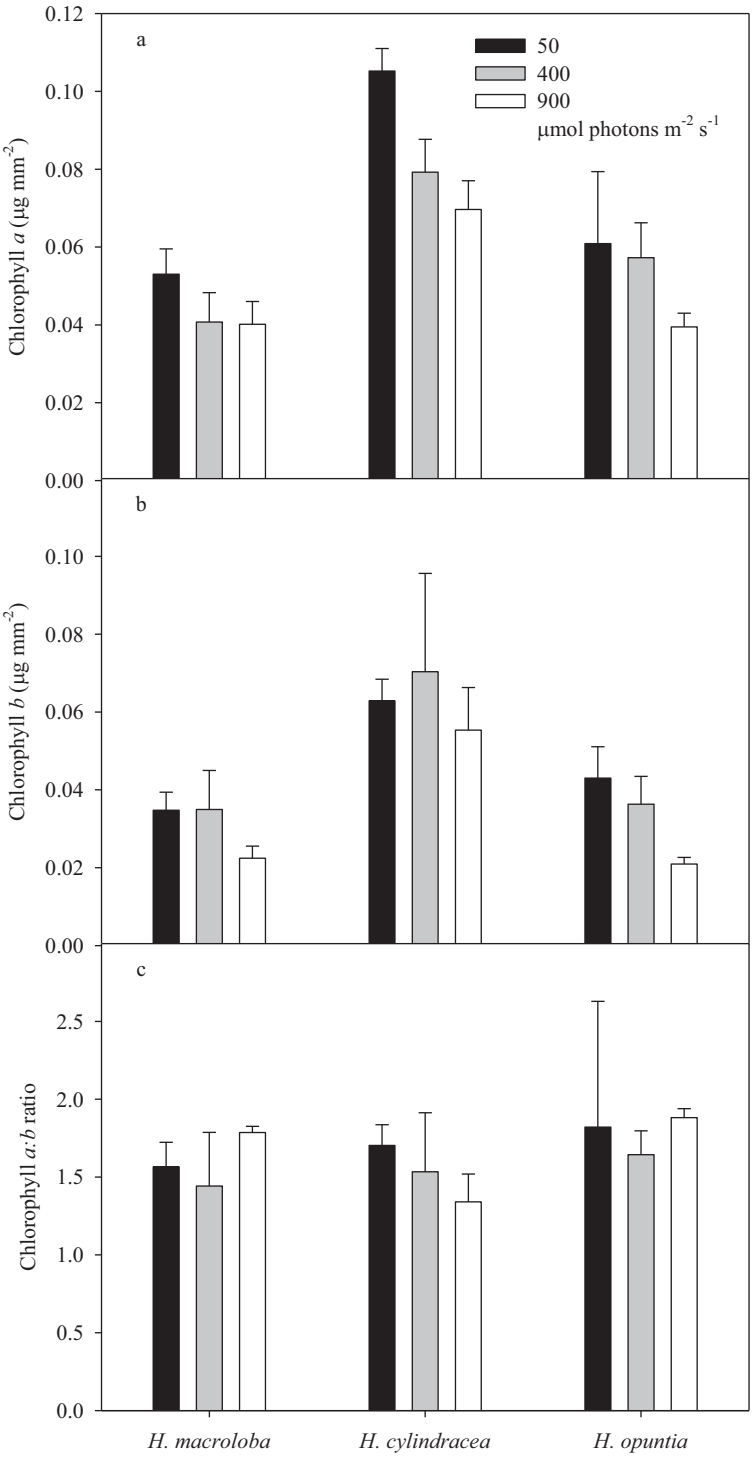

Figure 2.2: Chlorophyll *a* (a), *b* (b) and chlorophyll *a*:*b* ratio (c) of *H. macroloba*, *H. cylindracea* and *H. opuntia* from 50 (black boxes), 400 (light grey boxes) and 900 (dark grey boxes) µmol photons m^{-2} s^{-1} treatments. Averages + S.E. shown (*n* = 4).

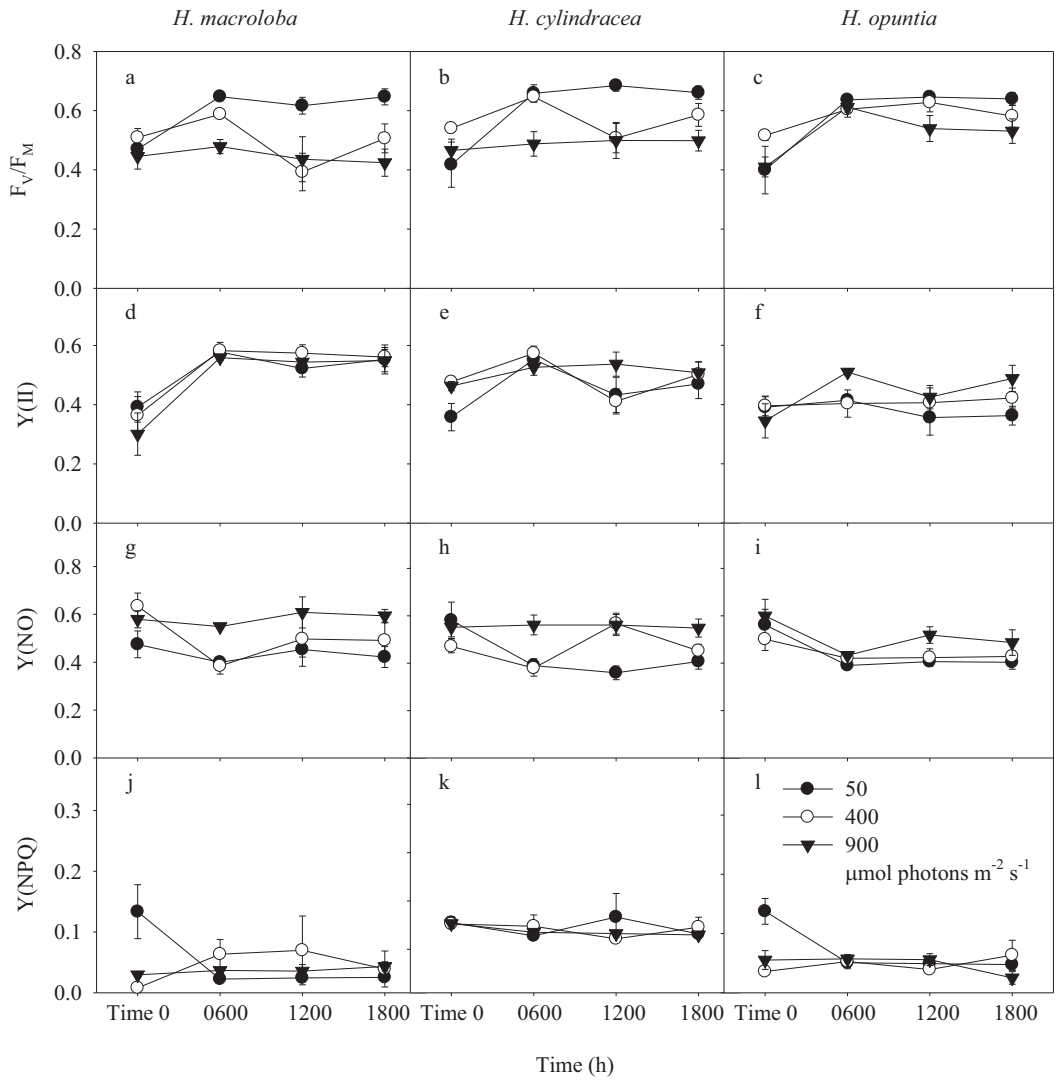

Figure 2.3: Maximum quantum yield (F_V/F_M; a-c), effective quantum yield (Y(II); d-f), non-regulated heat dissipation yield (Y(NO); g-i), and non photochemical quenching yield (Y(NPQ); j-l), and from *H. macroloba*, *H. cylindracea* and *H. opuntia* from 50 (closed circles), 400 (open circles) and 900 (closed downward triangles) µmol photons m^{-2} s^{-1} treatments. Averages ± S.E. shown (n = 4).

In an inhibitor experiment, measures of F_V/F_M showed the diel dynamic in photosynthetic efficiency (0600 to 2000 h) over the 2 experimental days in control treatment (Fig. 2.4). At each day in all species, F_V/F_M was highest at 0600 h,

significantly decreased at 1200 h ($P < 0.001$) where the highest light intensity was observed and then slightly recovered at 2000 h (Fig. 2.4a-f). In *H. opuntia*, the recovery of F_V/F_M from midday irradiance was low on both days. In *H. macroloba* at midday, F_V/F_M in control treatments was greater than lincomycin and DTT treatments (Fig. 2.4b). F_V/F_M in *H. cylindracea* and *H. opuntia* from lincomycin and DTT treatments were significantly lower than the control treatment at midday and 2000 h (Fig. 2.4a, c).

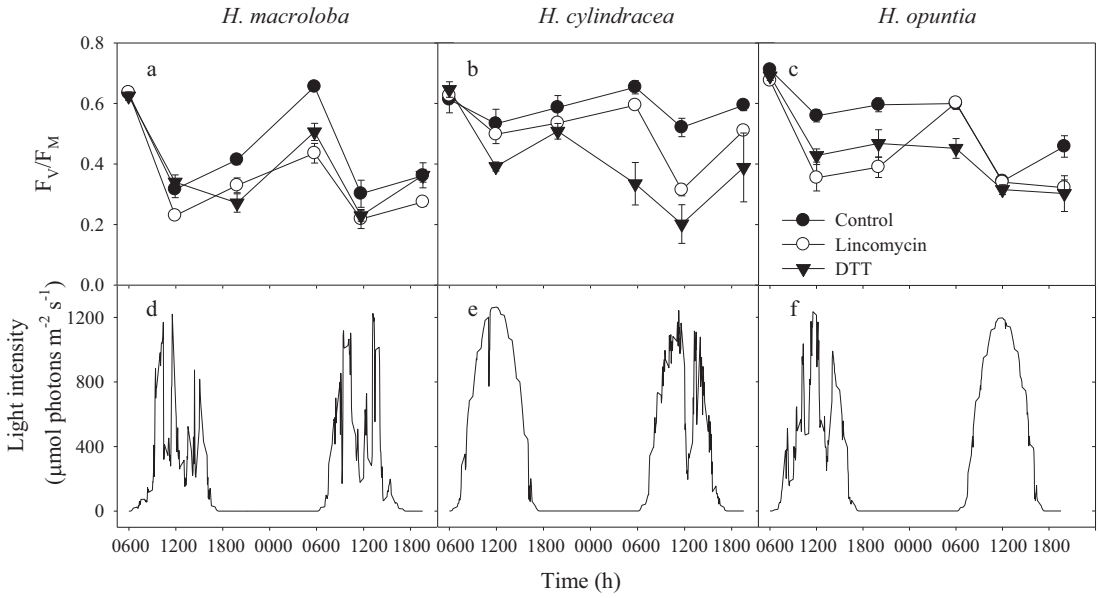

Figure 2.4: Maximum quantum yield (F_V/F_M) for *Halimeda cylindracea* (a), *Halimeda macroloba* (b) and *Halimeda opuntia* (c) over each two day period in the control (closed circles), lincomycin (closed upward triangles) and DTT (open downward triangles) treatments (averages ± S.E. shown; $n = 4$). Light intensity for each day (µmol photons m^{-2} s^{-1}; d-f) corresponds to each species.

The 77 K chlorophyll fluorescence emission spectra at 0700 and 1100 h indicate the attachment and location of LHCs on PSII and PSI and rearrangement between the two photosystems from low and high irradiance. In *H. macroloba*, the percentage area in all bands was not significantly different between treatments or time of sampling ($P > 0.05$; Fig. 2.5a,g,m) except at 691 and 715 nm (Fig. 2.5d,j).

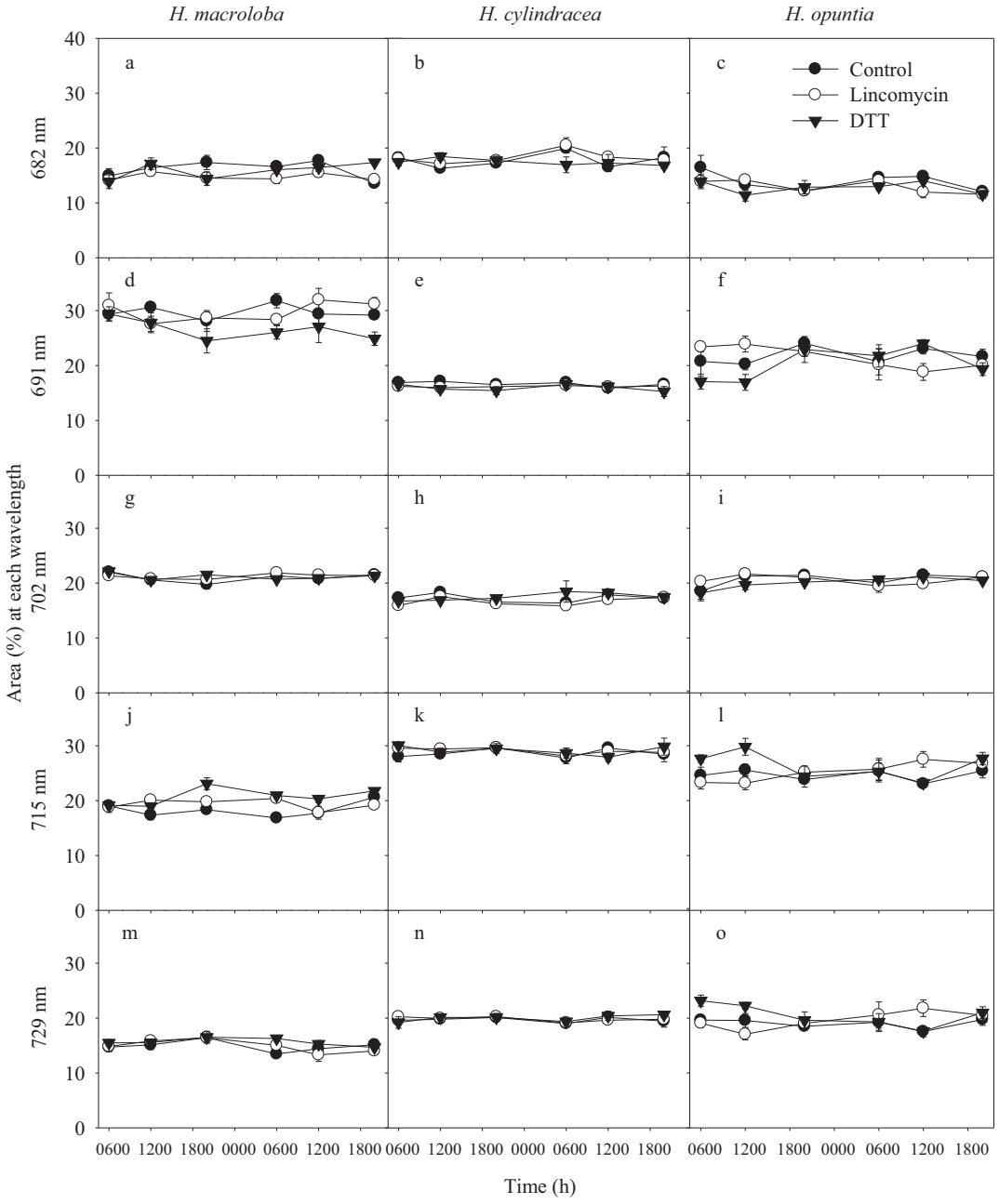

Figure 2.5: Area (%) of component bands in the fluorescence emission spectra at 77K (normalised to 686 nm) at 682 (a-c), 691 (d-f), 702 (g-i), 715 (j-l), and 729 nm (m-o) for *H. macroloba*, *H. cylindracea* and *H. opuntia* in control (closed circles), lincomycin (open circles) and DTT (closed downward triangles). Averages ± S.E. shown (n = 4).

The percentage area under the 691 nm band of the DTT treatment was significantly lower than in the control treatment at all time points on day 2 ($P = 0.002$; Fig. 2.5d). In comparison, the percentage area under the 715 nm band of DTT treated *H. macroloba* was significantly greater than in the control treatments at 2000 h on day 1 and 0600 h on day 2 ($P = 0.012$; Fig. 2.5j).

In *H. cylindracea*, the percentage area in all bands was not significantly different between treatments or time of sampling ($P > 0.05$; Fig. 2.5b,e,h,k,n). In *H. opuntia*, the percentage area in all bands was not significant different between treatments or time of sampling ($P > 0.05$; Fig. 2.5c,i,o) except at 691 and 715 nm (Fig. 5f,l). The percentage area under the 691 nm band in the DTT treatment was significantly lower than the control at 1200 h on day 1 and significantly greater than the lincomycin treatment at 1200 h on day 2 ($P = 0.031$; Fig. 2.5f). The percentage area under 715 nm band in the DTT treatment was significantly greater than control at 1200 h on day 1 and significantly lower than the lincomycin treatment at 1200 h on day 2 ($P = 0.022$; Fig. 2.5l).

2.4 DISCUSSION

This study revealed that the growth rate and $CaCO_3$ accumulation rate of *H. macroloba*, *H. cylindracea* and *H. opuntia* from Heron Island reef flat are independent of irradiance over 12 days. These results indicate that short-term exposure to different irradiances may not affect the growth rate and $CaCO_3$ accumulation rate in these species. However, changes in PSII photochemical efficiency and level of photoinhibition were found. This is the first study on the potential for LHC detachment and movement to provide photoprotection from high irradiance in *Halimeda* species.

In contrast to earlier observations (Beach et al. 2003), photosynthetic pigment (Chl *a* and *b*) concentrations and Chl *a*:*b* ratio in this study did not significantly change during exposure to different irradiance treatments. Other studies showed that light intensity influenced growth rate and photosynthetic concentration in *Halimeda* from 7 and 21 m

depth over 8 days (Beach et al. 2003; Vroom et al. 2003). Vroom et al. (2003) observed that *H. tuna* from a deep site (15-22 m; 115 μmol photon m^{-2} s^{-1}) in the Florida Keys had a higher growth rate than a shallower population (4-7 m; 405 μmol photon m^{-2} s^{-1}) probably due to photoinhibition observed by chlorophyll *a* fluorescence in shallower environments (Beach et al. 2003). In addition, the highest growth rate was found in the deeper population in summer during long photoperiods (13 h d^{-1}) and high temperature (30ºC). Beach et al. (2003) found variation in growth rates over depth and sampling times during four years observation due to other parameters such as nutrient availability. At Heron Island reef flat, *H. macroloba* and *H. cylindracea* experienced higher light intensity (1117 μmol photons m^{-2} s^{-1}) compared to Florida Keys (Beach et al. 2003; Vroom et al. 2003). The differences in light history may explain the irradiance dependence in growth, calcification and chlorophyll contents between locations in these species. Photosynthetic pigment contents were found to be higher in shaded-adapted plants to increase light capture efficiency (Broadman 1977). It is suggested that the decrease in irradiance lead to a rise in the Chl *a* concentration, while exposure to high irradiance resulted in decreasing Chl *a* concentration (Carnicas et al. 1999; Broadman 1977). When irradiance is higher, photosynthetic pigment contents decrease to reduce light capture efficiency to avoid photoinhibition (Broadman 1977). Pigment concentration can be rapidly changed in a daily pattern with a decrease in pigment concentration at noon and a recovery during afternoon (Figueroa et al. 1997). In *Halimeda*, however, Drew and Abel (1990) observed a daily pattern in chloroplast movements without change in pigment concentration. This mechanism is directly controlled by light and partly influenced by temperature and endogenous rhythm (Drew and Abel 1995). In the dark or at shade, chloroplasts move inwards in the radial outer filaments and the segments turn from a dark green colour to white. Before dawn or at light, the chloroplasts move outwards returning to the surface and the segments turn dark green (Drew and Abel 1990; Larkum et al. 2011). This mechanism may contribute to less susceptibility to grazing (Drew and Abel 1990) and provide advantages in dealing with variable light. This may explain why the photosynthetic pigment (Chl *a* and

b) concentrations and Chl *a*:*b* ratio in this study did not significantly change during exposure to different irradiance treatments.

Midday depressions in PSII photochemical efficiency, as well as a diurnal hysteresis in F_V/F_M and higher levels of Y(NO) in the high light treatments (900 µmol photons m^{-2} s^{-1}) in *H. macroloba* and *H. cylindracea* indicated photoinhibition (Maxwell and Johnson 2000; Kramer et al. 2004) and no recovery was observed by 1800 h. Franklin et al. (1996) observed that the photoinhibition (indicated by F_V/F_M) in *H. tuna* occurred after 30 min exposure to full sunlight (1400-1500 µmol photon m^{-2} s^{-1}) and a 30-50% and full recovery occurred after shading for 3 h and 19 h (Franklin et al. 1996). A diurnal pattern of photoinhibition (indicated by F_V/F_M) was observed in other macroalgae *Chlorodesmis fastigiata*, *Padina pymnospora* and *Laurencia intricata* with 50% decreased in PSII efficiency at 1300 h and complete recovery in the afternoon (1800 h). We suggested that a longer recovery period is required for recovery of *Halimeda*. Y(NPQ) was low in all treatments and in all three species which may indicate a low potential for photoprotection mechanisms in these algae.

To investigate photoprotection mechanisms and the function of PSII in *H. macrolob*a, *H. cylindracea* and *H. opuntia*, lincomycin and DTT were used to inhibit chloroplast protein synthesis and de-epoxidation of xanthophylls pigments, respectively (Rockholm and Yamamoto 1996; Franklin and Larkum 1997). The distinct diurnal pattern in PSII photochemical efficiency (F_V/F_M) was observed in *H. macroloba* and *H. cylindracea* from control treatment (Fig. 2.4a-b). F_V/F_M was highest in the morning and strongly reduced at noon due to photoinhibition and slightly recovered in the afternoon suggesting a short-term photoinhibition in these species (Häder et al. 1996). *H. opuntia*, however, had a smaller capacity to recover in the afternoon indicating a long-term photoinhibition and irreversible photodamage (Häder et al. 1997). This may be because *H. opuntia* is usually found in more shaded areas on coral reefs compared to other species of *Halimeda*. The diurnal pattern in photosynthetic efficiency was found in earlier studies in *H. tuna* and *Porphyra umbilicalis* (Häder et al. 1996; Häder et al. 1999) and the degree of photoinhibition and recovery (as shown by Y(II) and oxygen

production) was dependent on depth, where *H. tuna* from the greater depth recovered more slowly than the algae from the surface (Häder et al. 1996). This result may support my findings where differences in photoinhibitory effects and recovery were found between species which are from different light exposure in natural habitat. Moreover, the upper limit for survival and photoinhibition for these species at Heron Island is 32ºC (Sinutok et al. 2011). At below temperature threshold, the diurnal pattern of PSII photochemical efficiency indicates that *Halimeda* spp. from Heron Island are well-adapted to their shallow water habitat and is able to respond to high irradiance by up-regulating photoprotective mechanisms to avoid long-term photoinhibition.

A chlorophyll fluorescence spectrum at 77K was used to investigate the attachment and location of LHCs on PSII and PSI and rearrangement between the two photosystems (Murakami 1997; Yamasaki et al. 2006). LHCs in *Halimeda* are siphonaxanthin-Chl *a*/*b*-protein complexes (Chen et al. 2002). Here it is assumed the fluorescence emission at 682 and 691 are related to the PSII reaction centres (Murakami 1997; Yamasaki et al. 2006) and the fluorescence emission at 702, 715 and 729 are related to the PSI reaction centres (Murakami 1997; Yamasaki et al. 2006). Shifts in percentage area under each peak through time can demonstrate the dissociation and rearrangement of photosynthetic pigments at different light exposure (Hill et al. 2012). Lincomycin inhibits chloroplast protein synthesis, leading to the blockage of PSII repair and photodamage, which will result in a large increase in the fluorescence spectra related to PSI reaction centres. However, the shift in excitation distribution balance between PSII and PSI was not observed in lincomycin treatments at all times in all species suggesting that the state transition is not clearly seen in these species. Significantly greater F_V/F_M at midday and higher recovery in the afternoon in the control treatment compared to the lincomycin treated *Halimeda* were observed. The inhibition of chloroplast protein synthesis via lincomycin caused a greater reduction and less recovery in photosynthetic efficiency of PSII (F_V/F_M) due to the production of inactive PSII reaction centres via the degradation of the D1 protein and the blockage of PSII repair (Six et al. 2009). We suggest that the turnover of D1 protein is essential in preventing photodamage in *Halimeda* from

shallow habitat. *H. macroloba* in the control treatment showed a larger percentage area under 691 nm bands at all time points during day 2 compared to the 715 nm band which indicated the LHCs attached to PSII reaction centres and there was no over-excitation on PSII so this possible photoprotective strategy was not activated.

The DTT treated *Halimeda* showed lower F_V/F_M at midday and lower recovery in the afternoon compared to the control. Inhibition of the xanthophyll cycle via DTT resulted in greater loss in PSII photochemical efficiency and less recovery. The percentage area under 715 nm band of DTT treatment was significantly greater than those in control treatments at 2000 h on day 1 and 0600 h on day 2 indicating a redistribution of LHCs from PSII towards PSI (the transition from state 1 to 2). DTT is an inhibitor for de-epoxidation of xanthophyll pigments, therefore DTT-treated *Halimeda* exhibited greater reduction in PSII photochemical efficiency because they were unable to dissipate excess energy through xanthophylls cycle. The antenna detachment and/or movement between PSII and PSI in DTT-treated algae may be a mechanism intended to protect PSII from excessive irradiance in *H. macroloba.* Greater reduction in PSII photochemical efficiency in DTT treatment suggested that the xanthophyll cycle plays an important role in photoprotective mechanism against photodamage in these species.

The results on fluorescence emission data were not consistent between all species. In *H. opuntia*, inconsistency in the changes in fluorescence bands was observed. In *H. cylindracea*, no significant changes in fluorescence emission were found between times of sampling and treatments. Our results may indicate a lack of LHC disconnection and redistribution in these species. However, further investigation on this mechanism using other techniques (e.g., chlorophyll fluorescence) and other inhibitors (e.g., NaF, an inbibitor of a protein phosphatise involved in a state transition from PSII to PSI.) is needed.

In conclusion, these results showed that even though short-term exposure (12 days) at higher light intensities led to a decrease in PSII photochemical efficiency in these species, the growth rate and $CaCO_3$ accumulation rate may not be affected.

Photoprotective and recovery mechanisms are essential for *Halimeda* to prevent photodamage high light shallow water habitats. *H. opuntia* had a smaller capacity to recover in the afternoon indicating a long-term photoinhibition because *H. opuntia* is usually found in more shaded areas on coral reefs compared to other species of *Halimeda.*

CHAPTER 3:

DIURNAL PHOTOSYNTHETIC RESPONSE OF THE SYMBIOTIC BENTHIC FORAMINIFERAN *MARGINOPORA VERTEBRALIS*

3.0 DIURNAL PHOTOSYNTHETIC RESPONSE OF THE SYMBIOTIC BENTHIC FORAMINIFERAN *MARGINOPORA VERTEBRALIS*

All field and laboratory work, data collection, data analyses and write up were undertaken by me. Vinod Kumar and Marlene Zbinden assisted with the HPLC analyses.

3.1 INTRODUCTION

Benthic symbionts-bearing foraminifera are single-celled organisms that harbour a variety of groups of endosymbiotic microalgae in their test chamber, including dinoflagellates, diatoms, unicellular chlorophytes, unicellular rhodophytes, and cyanobacteria, and are also capable of chloroplast husbandry (Goldstein 1999; Lee 2006). The dominant tropical foraminiferan, *Marginopora vertibralis* Quoy & Gaimard predominantly hosts several species of dinoflagellates, i.e., *Gymnodinium obesum* Schiller*, Gymnodinium rotundatum* Klebs and *Symbiodinium microadriaticum* Freudenthal (Ross 1972; Pawlowski et al. 2001; Lee et al. 2009).

Relationships between foraminifera and algal symbionts are varied and complex (Goldstein 1999). The host foraminiferan has numerous benefits from its algal symbionts: photosynthetic energy, enhanced calcification and metabolite removal (Hallock 1999). In return, foraminifera provide the symbiont with a stable microenvironment and a nutrient supply in the form of dissolved nitrogen and phosphorus (Goldstein 1999). As a result of this symbiotic relationship, benthic foraminifera are found in well lit shallow waters of coral reefs (Nobes et al. 2008). The symbiont-bearing foraminiferan *M. vertebralis* is commonly found on sandy substrates and attached to the calcifying macroalga *Halimeda* (Severin 1987; Sinutok et al. 2011).

Foraminifera have a useful feature not shared by other algal-symbiont-bearing organisms, in that they are motile. Khare and Nigam (2000) showed that pseudopodially-mediated benthic foraminiferal movement on glass varied from 2.04 to 8.34 mm h^{1}. Despite algal symbionts being reliant on sunlight to obtain energy for

photosynthesis and calcification, exposure to high irradiances can lead to reduced photosynthetic efficiency and potentially photoinhibition, similar to algae and higher plants (Franklin et al. 1996; Winters et al. 2003). Nobes et al. (2008) showed no difference in growth rate during a wide range of irradiance (1200, 375, 60 μmol photons m^{-2} s^{-1}) for the high light requiring species, *Amphistegina* spp. and *Calcarina* spp., while in low light species, *Heterostegina depressa*, growth rate was highest under low light (60 μmol photons m^{-2} s^{-1}). Nobes et al (2008) found that in all three taxa, decreasing irradiance caused an increase in the initial slope (α) of electron transport and a decrease in minimum saturating irradiance (I_k), suggesting that these species can rapidly acclimate to changes in light conditions. In contrast, Hallock (1981) showed that the growth rates of the benthic foraminifera *Amphistegina lessonii* and *Amphistegina lobifera* were faster under higher irradiance (140 μmol photons m^{-2} s^{-1}), compared to low irradiance (32 and 14 μmol photons m^{-2} s^{-1}).

The capacity for movement in response to light (i.e., phototactic behaviour) has been observed in benthic symbiotic foraminifera under various light conditions (Zmiri et al. 1974; Lee et al. 1980; Murray 2006). *Amphistegina lobifera* showed positive phototaxis under low irradiance (1.35-13.5 μmol photon m^{-2} s^{-1}) and negative phototaxis under higher irradiances (>150 μmol photons m^{-2} s^{-1}), which may have had the potential to cause photoinhibition (Lee et al. 1980). Foraminifera may therefore be able to avoid photoinhibition by moving away from over-saturating light environments (e.g., uncovered substrate), to areas with more optimal light intensities (e.g., within seagrass and macroalgae foliage) (Lee and Bock 1976; Severin 1987; Murray 2006). Foraminifera are also known to move towards the top of habitat-forming macrophytes when requiring more light (positive phototaxis) and move downward or horizontally to a shaded area to avoid excess light (negative phototaxis). Sessile organisms such as corals, may respond to higher irradiances by decreasing symbiont density and/or chlorophyll content to maintain optimum photosynthetic rates (Fagoonee et al. 1999; Fitt et al. 2000; Rodolfo-Metalpa et al. 2008) and by inducing photoprotective mechanisms such as polyp retraction (Brown et al. 2002) and dissipation of excess energy through non-

photochemical quenching (NPQ) (Hill et al. 2004). Over-saturating irradiance can also lead to the expulsion of symbiotic algae from corals and/or a reduction in photosynthetic pigment concentration, resulting in coral bleaching (Hill et al. 2004; Hill et al. 2008). In foraminifera *Amphistegina*, damaged symbionts, which result in bleaching, are induced by light (Hallock et al. 2006). The phototactic behaviour of foraminifera provides a competitive advantage over their sessile counterparts by enhancing their ability to cope with high irradiance. Another factor that influences foraminiferal movement is heterotrophic feeding where the speed of movement is influenced by temperature and the need to search for food (Gross 2000; Murray 2006). The pseudopodia are used in both gathering food and digestion (Murray 2006). In symbiont-bearing foraminifera, heterotrophic feeding makes an important contribution to the protist's energy requirements, although Röttger et al. (1980) found that *A. lessonii* did not grow in the dark even when it was fed with algae, detritus, bacteria, protozoa and fungi. Along with the findings of Lee et al. (1991) this suggests that foraminiferal growth is dependent on light.

When a high level of photosynthetic active radiation (PAR) is applied, a down-regulation or photoinhibition to the photosynthetic apparatus of the symbiotic algae may occur (Hill and Ralph 2005). Down-regulation of photosynthesis involves photoprotective processes and can be defined as short-term photoinhibition and the reversible loss of photosynthetic efficiency of PSII and photosynthetic election transport rate and changes in response to light (Jones and Hoegh-Guldberg 2001; Larkum et al. 2006). Photoprotection can reduce the potential for damage, by dissipating excess solar energy as heat via the xanthophyll cycle, a form of NPQ (Demmig-Adams and Adams 1992; Hill and Ralph 2005). In addition, less energy is used in photochemical reactions which results in decreasing the photosynthetic efficiency of PSII (e.g. maximum quantum yield (F_V/F_M) and effective quantum yield ($\Delta F/F_M'$)) (Hill and Ralph 2005). In comparison, long-term photoinhibition results in irreversible photodamage to PSII and a long-term reduction in F_V/F_M and require the resynthesis of damaged photosynthetic proteins (Brown et al. 1999; Hill and Ralph 2005).

In this study, we aimed to investigate foraminiferal movement in response to diurnal fluctuations in light intensity and identify associated changes in the photosynthetic response of symbiotic algae. We assessed the capacity for behavioural movement in benthic foraminifera, quantified the degree of potential stress and revealed whether migration was dependent upon light. Field observation and manipulative experiment were performed. The photosynthetic inhibitor 3-(3,4-dichlorophenyl)-1,1-dimethylurea (DCMU) was used to eliminate the photosynthetic function from symbionts to test the hypothesis that foraminiferal movement is controlled by symbiont photosynthesis.

3.2 MATERIALS AND METHODS

3.2.1 Field observation

Field observations were carried out at Heron Island reef flat, on the Southern Great Barrier Reef, Australia (151°55'E, 23°27'S) in November 2009. To observe the movement of *Marginopora vertebralis* in their natural habitat, the proportion of foraminifera exposed to direct irradiance was assessed to determine the number of individuals that moved to exposed or sheltered locations. Exposed foraminifera were defined as individuals living on the surface of a *Halimeda* thallus and exposed to the sun. The sheltered foraminifera were individuals living inside the shaded, cryptic habitat of a *Halimeda* thallus. The abundance of exposed and sheltered individuals were determined in ten 100 cm^2 quadrats (10x10 cm^2) at five times over the day from pre-dawn to post-dusk (0430, 0900, 1200, 1500 and 1900 h) for three consecutive days. Water temperature and light intensity at the foraminiferal sampling depth in the subtidal reef flat were recorded every 10 and 5 mins, respectively, for three consecutive days using submersible data recorders (Odyssey, New Zealand).

To investigate the photosynthetic performance of the exposed and sheltered foraminifera in the field, rapid light curves (RLCs) were performed at the same time each day, using a 6 mm diameter fibre-optic on a Diving-PAM fluorometer (Walz, Germany) (n = 5). RLCs with 10 increasing actinic light intensities (0, 44, 78, 112, 153, 214, 303, 435, 634

and 950 μmol photons m^{-2} s^{-1}) were applied, with 0.8 s saturating flashes (> 4500 μmol photons m^{-2} s^{-1}) between each actinic light intensity every 10 s. Effective quantum yield of PSII ($\Delta F/F_M'$; Schreiber 2004), maximum relative electron transport rate ($rETR_{max}$), minimum saturating irradiance (I_k) and initial slope (α) of rapid light curves (RLCs) were calculated using the curve fitting protocols outlined in Ralph and Gademann (2005) with Sigma Plot (v10.0, SPSS Inc.).

3.2.2 Laboratory experiment

To determine whether foraminiferal movement is controlled by symbionts photosynthesis and investigate the movement of foraminifera in the laboratory, *Marginopora vertebralis* samples were collected by hand from Heron Island reef flat and maintained in outdoor 1 L aquaria with flow-through seawater (pH 8.1, 26 ºC, 33 ppt). The movement of foraminifera was investigated in four experimental treatments: exposed and sheltered, with and without the photosynthetic inhibitor 3-(3,4-dichlorophenyl)-1,1-dimethylurea (DCMU; 0.25 μM). Four independent tanks were used for each treatment and ten foraminifera were placed in each independent tank. DCMU (0.25 μM; w/v mixed in MilliQ water) was added to the seawater eliminate photosynthetic function in the symbiotic algae (Ter Kuile et al. 1989a) to test whether foraminiferal movement was controlled by symbiont photosynthetic activity. In both with and without DCMU tanks, foraminifera in exposed treatments were placed on a sandy substrate, while those in the sheltered treatments were given access to thalli of *Halimeda opuntia* for shading. The horizontal movement (number of foraminifera exposed to direct sunlight in each treatment) was determined five times per day from pre-dawn to post-dusk (0430, 0900, 1200, 1500 and 1900 h). Water temperature and light intensity were recorded in each tank as detailed above for field observations.

PSII photochemical efficiency was determined through measures of chlorophyll *a* fluorescence using a Diving-PAM fluorometer. Steady state light curves (SSLCs; Kramer et al. 2004; Sinutok et al. 2011) with one irradiance step (372 μmol photons m^{-2} s^{-1}) applied for 300 s, 0.8 s saturating flashes (> 4500 μmol photons m^{-2} s^{-1}), were

performed at 0600, 0900, 1200, 1500 and 1800 h after 10 mins of dark adaptation. The maximum quantum yield of PSII (F_V/F_M), the effective quantum yield of PSII (Y(II)), the capacity for photoprotection (non-photochemical quenching (Y(NPQ)) and the level of photoinhibition (non-regulated heat dissipation (Y(NO)) were determined from each SSLC (Kramer et al. 2004; Ulstrup et al. 2006).

Photosynthetic pigment concentration from the foraminiferal symbionts (chlorophyll (chl) *a* and c_2) was determined using the standard spectrophotometric method of Ritchie (2008) at the end of the 3 day experiment. Chlorophyll *a* and c_2 were extracted by homogenising samples in 3 ml of 90% acetone at 4 °C for 24 h. Samples were centrifuged at 1500 *g* for 10 mins and the supernatant placed into a quartz cuvette in a spectrophotometer (Varian, Australia), with absorbance measured at 630 and 664 nm.

Four foraminiferal samples from each treatment were collected for xanthophyll pigment determinations at 0430 h of the first day and at 1900 h on the final day (day 3) and immediately snap frozen and stored in liquid nitrogen. Reverse-phase high performance liquid chromatography (HPLC) was used to detect the concentration of the xanthophyll pigments diatoxanthin (Dt) and diadinoxanthin (Dn) as described in Hill et al. (2012). Dt and Dn showed the de-epoxidation of xanthophylls, Dn to Dt, which is a photoprotective mechanism to avoid long-term photodamage (Falkowski and Raven 2007). Xanthophylls were extracted by crushing the samples (n = 4) with a mortar and pestle in 100% acetone and filtering through GF/C filter paper (Whatman) and a 0.2 µm PTFE 13 mm syringe filter (Micro-Analytix Pty. Ltd.). The extracted samples were stored in amber-coloured HPLC glass vials at -80 ºC overnight (Heukelem and Thomas 2001). The HPLC consisted of a pump system with inline degasser, programmable autoinjector, temperature-controlled autosampler, temperature controlled column oven compartment, photodiode array detector, and Empower Pro software (Waters Australia Pty. Ltd.). The pigments were detected using a photo-diode array detector at 450 nm and 665 nm with 20 nm bandwidth (Heukelem and Thomas 2001). Calibration and quality assurance was performed by external calibration standards (DHI, Denmark). Peaks were integrated using Empower Pro software with manual confirmation. The de-epoxidation state of

xanthophyll pigments was calculated as the relative proportion of Dt to the total xanthophyll pool (Dt+Dn) (Ulstrup et al. 2008; Hill et al. 2012). Dt, Dn and the total xanthophyll pool (Dt+Dn) were determined as μg g^{-1} fresh weight (fw).

At the end of the experiment, algal symbionts were isolated from the foraminifera by crushing the foraminiferal test with a glass rod in 3 ml of 0.2 μm filtered seawater (n = 4). Symbiont density was determined as the number of cells per mm^2 using a haemocytometer. Four replicate counts were made per sample and averaged for each replicate.

3.2.3 Statistical analysis

To determine any significant differences among treatments in foraminiferal abundance, number of foraminifera in sun-exposed regions, and chlorophyll fluorescence parameters (F_V/F_M, Y(II), Y(NPQ), Y(NO), $\Delta F/F_M'$, $rETR_{max}$, I_k, α) over time, repeated-measures analysis of variance (rmANOVA) tests were performed. One-way ANOVA tests were used to compare treatments at the initial and final time points for chlorophyll *a*, and c_2 concentration, xanthophyll pigments and ratios, and symbiont density (SPSS Version 17). All tests were performed with a significance level of 95% and Tukey's HSD post hoc tests were used to identify the statistically distinct groups. If data did not meet the assumptions of normality (Kolmogorov-Smirnov test) and equal variance (Levene's test), the data were transformed using $\log_{10}$ or square root.

3.3 RESULTS

3.3.1 Field observation

The irradiance on Heron Island reef flat from 9-11 November 2009 ranged from 0 at pre-dawn to a maximum of 1117 ± 46 μmol photons m^{-2} s^{-1} at solar noon (1253 h). The sea surface temperature fluctuated over the day, with a low of 23.6 ± 1 ºC at pre-dawn and a maximum of 28.8 ± 0.5 ºC at 1305 h with a tidal transition from flood to ebb at 1400 h (Fig. 3.1A).

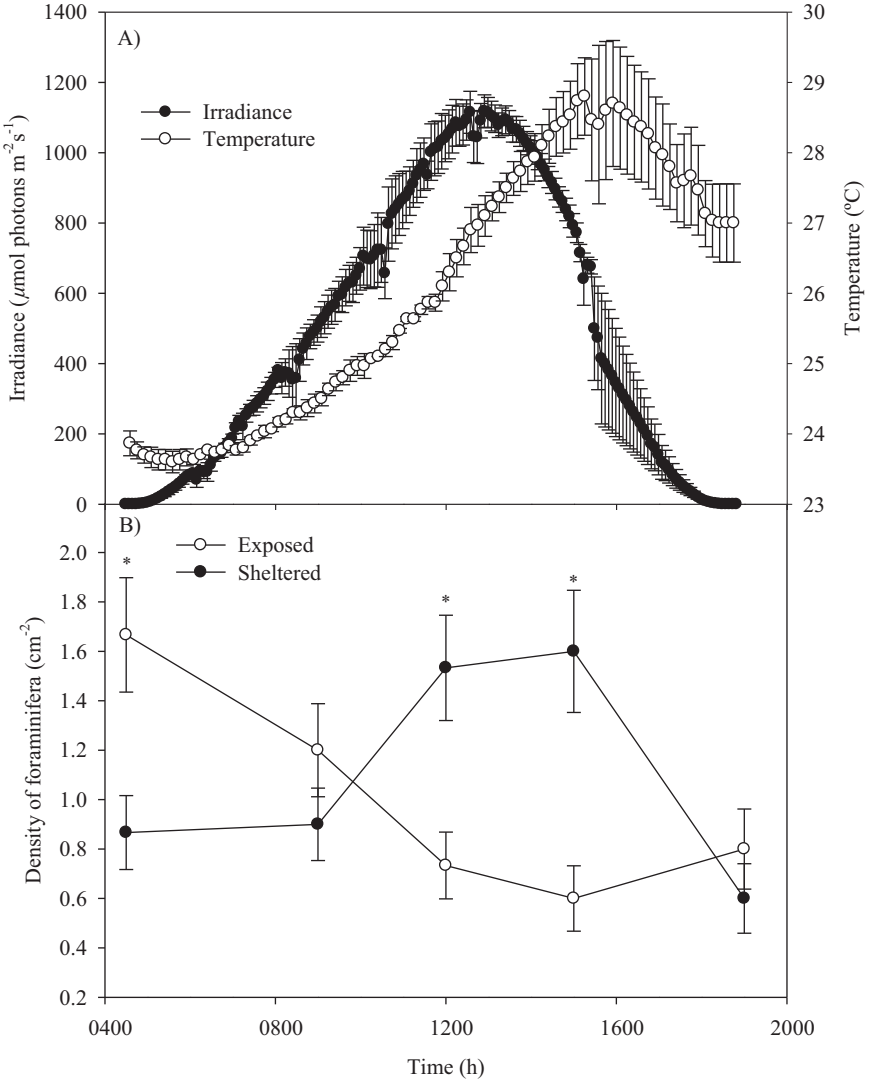

Figure 3.1: A) Irradiance (μmol photon m^{-2} s^{-1}) (closed circles) and seawater temperature (ºC) (open circles) on Heron Island reef flat from 0430 to 1900 h. Data represent mean from three consecutive days ± SE (n = 3) and B) Density (cm^{-2}) of exposed (open circles) and sheltered (closed circles) foraminifera on Heron Island reef flat from 0430 to 1900 h. Data represent mean ± SE (n = 10). * indicates significant differences between sheltered and exposed.

Observations of the number of exposed versus sheltered foraminifera in the field revealed significant differences over the sampling time (P = 0.027; Fig. 3.1B). Foraminifera were most abundant in sheltered habitats at 1200 and 1500 h (1.5 ± 0.2 and 1.6 ± 0.2 cm^{-2}; P = 0.002 and 0.001, Fig. 3.1B), while at 0430 h, foraminifera were most abundant in exposed areas when the habitat experienced very low irradiances (were in the dark) (P = 0.005). The number of individuals in the exposed habitat decreased compared to sheltered habitats at 1200 and 1500 and 1900 h (0.7 ± 0.1, 0.6 ± 0.1 cm^{-2}).

Rapid light curves (RLCs) revealed the highest initial effective quantum yield of PSII ($\Delta F/F_M'$) occurred before actinic light application (maximum quantum yield) in the foraminifera located on exposed surfaces of *Halimeda* at 0430 h (0.618 ± 0.017) and the lowest at 0900 h (0.441 ± 0.035) (P < 0.001; Fig. 3.2A). $\Delta F/F_M'$ in sheltered foraminifera significantly decreased from 0.663 ± 0.018 at 0430 h to 0.566 ± 0.025 at 0900 h (P < 0.001; Fig. 3.2A). At 0430, 0900 and 1200 h, $\Delta F/F_M'$ in exposed individuals was significantly less than those in sheltered habitats (P < 0.001; Fig. 3.2A). There was no significant difference in relative maximum electron transport rate ($rETR_{max}$) among times of day within either habitat (P > 0.05; Fig. 3.2B), although a significantly higher $rETR_{max}$ was observed in sheltered foraminiferans (12.2 ± 2.2 μmol electrons m^{-2} s^{-1}) than those exposed to direct sunlight (5.5 ± 1.4 μmol electrons m^{-2} s^{-1}) at 0900 h (P < 0.05; Fig. 3.2B). Minimum saturating irradiance (I_k) was not significantly different between exposed and sheltered foraminifera (88 ± 15 to 129 ± 10 μmol photons m^{-2} s^{-1}), except at 0900 h where sheltered individuals had a higher I_k (182 ±32 μmol photons m^{-2} s^{-1}) compared to those exposed to direct sunlight (91 ± 22 μmol photons m^{-2} s^{-1}; Fig. 3.2C). Initial slope (α) was significantly greater for sheltered foraminifera at all time points except 1500 h (P = 0.002; Fig. 3.2D). In both exposed and sheltered foraminifera, significantly higher α values were found at 1500 h compared to other time points (Fig. 3.2D). There was significantly higher rETR in sheltered foraminifera at 0900 h than other times of the day (P = 0.038; Fig. 3.3B). Interestingly, a greater rETR was found in exposed foraminifera at 1200 h (P = 0.021; Fig. 3.3C). There were no significant

differences in rETR between sheltered and exposed foraminifera at 0430, 1500 and 1900 h ($P > 0.05$; Fig. 3.3A, D, E).

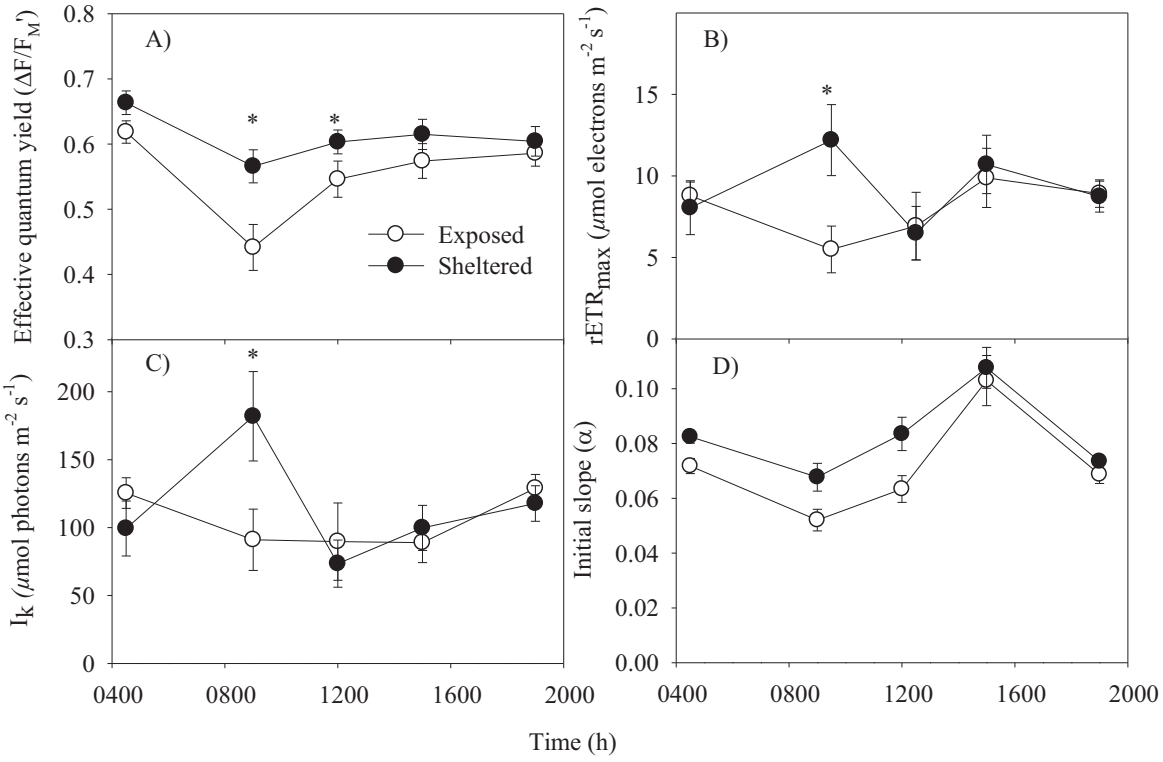

Figure 3.2: A) Effective quantum yield of PSII ($\Delta F/F_M'$), B) maximum relative electron transport rate ($rETR_{max}$; μmol electrons m^{-2} s^{-1}) and C) minimum saturating irradiance (I_k; μmol photons m^{-2} s^{-1}) of exposed (open circles) and sheltered (closed circles) foraminifera on Heron Island reef flat from 0430 to 1900 h. Data represent mean ± SE ($n = 5$). * indicates significant differences between sheltered and exposed.

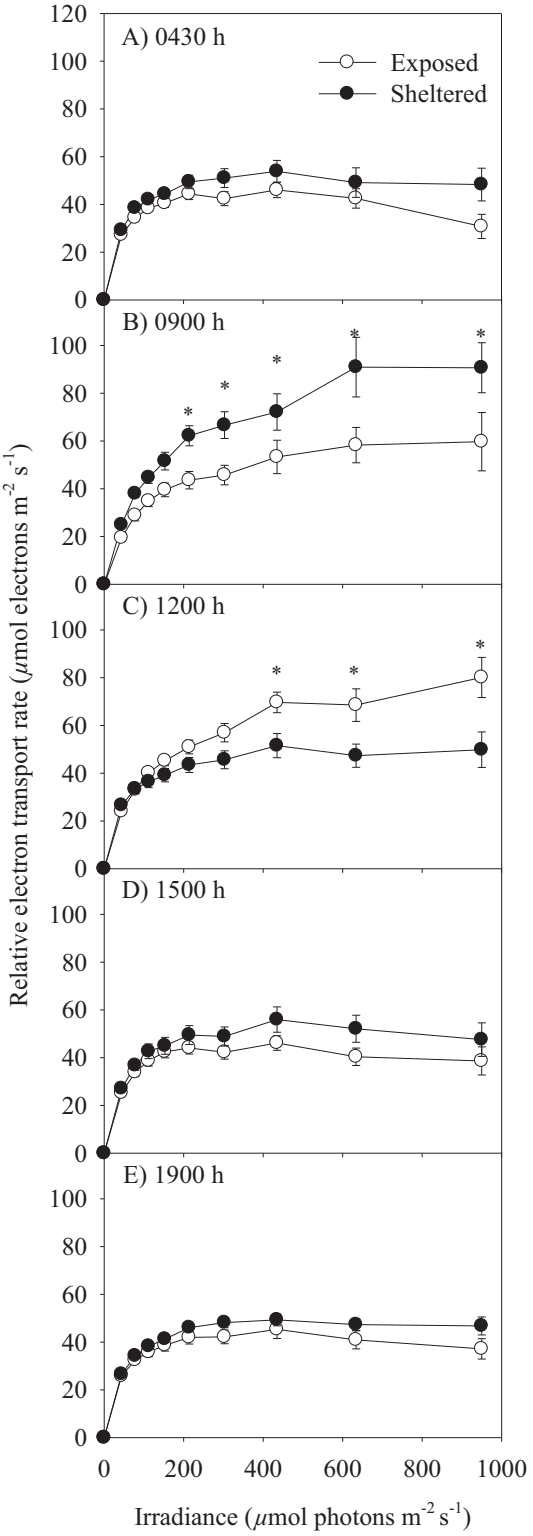

Figure 3.3: Rapid light curves (relative electron transport rate (rETR vs. irradiance) from exposed (open circles) and sheltered (closed circles) foraminifera at 10 irradiance steps (0 to 950 μmol photons m^{-2} s^{-1}) on Heron Island reef flat from 0430 (A), 0900 (B), 1200 (C), 1500 (D) and 2000 h (E). Data represent mean ± SE (n = 5).

3.3.2 Laboratory experiment

To investigate the dependence of foraminiferal movement on symbiont photosynthesis, the horizontal movement of foraminifera in both the exposed and sheltered treatments (with and without DCMU) were recorded. The water temperature fluctuated over the day, with a low of 24.1 ± 0.1 ºC at pre-dawn and a maximum of 27.1 ± 0.1 ºC at 1115 h. Irradiance ranged from 0 at pre-dawn to a maximum of 1580 ± 67 μmol photons m^{-2} s^{-1} at 0923 h (Fig. 3.4A). The shade provided by *Halimeda* thalli reduced ambient irradiance by 70-90%. The numbers of foraminifera exposed to the sun in the sheltered treatment (without DCMU) significantly decreased at 0900 h from 0430 h ($P = 0.001$), reaching the lowest abundance at 1200 and 1500 h. A significant increase was observed at 1900 h compared to 1200 and 1500 h ($P < 0.001$; Fig. 3.4B); however, the number of foraminifera in shade at 1900 h was still significantly lower than at 0430 h. In comparison, when treated with DCMU, the number of sun-exposed foraminifera in the sheltered treatment declined after 0430 h and showed no subsequent change up to 1900 h even though movements were observed (Fig 3.4B). Foraminifera were also observed to move in both exposed treatments (with and without DCMU); however, as no source of shade was provided, the number exposed to the sun remained constant and was significantly higher than the counts in the sheltered treatments ($P < 0.001$).

F_V/F_M and Y(II) showed the same response in both exposed and sheltered treatments over time within each of the two DCMU treatments. Without DCMU, F_V/F_M and Y(II) significantly decreased from 0430 to 1200 h ($P < 0.001$; Fig. 3.5A-B) and had a significant recovery by 1500 h. F_V/F_M and Y(II) were close to zero and constant over time in the presence of DCMU ($P > 0.05$; Fig. 3.5A-B). Within the + and – DCMU treatments, there were no significant differences in Y(NO) and Y(NPQ) between both exposed and sheltered treatments ($P > 0.05$; Fig. 3.5C-D). However, Y(NO) was higher and Y(NPQ) lower in DCMU treated foraminifera (P values < 0.001; Fig. 3.5C-D). No significant change occurred over time in either Y(NO) or Y(NPQ) ($P > 0.05$; Fig. 3.5C-D).

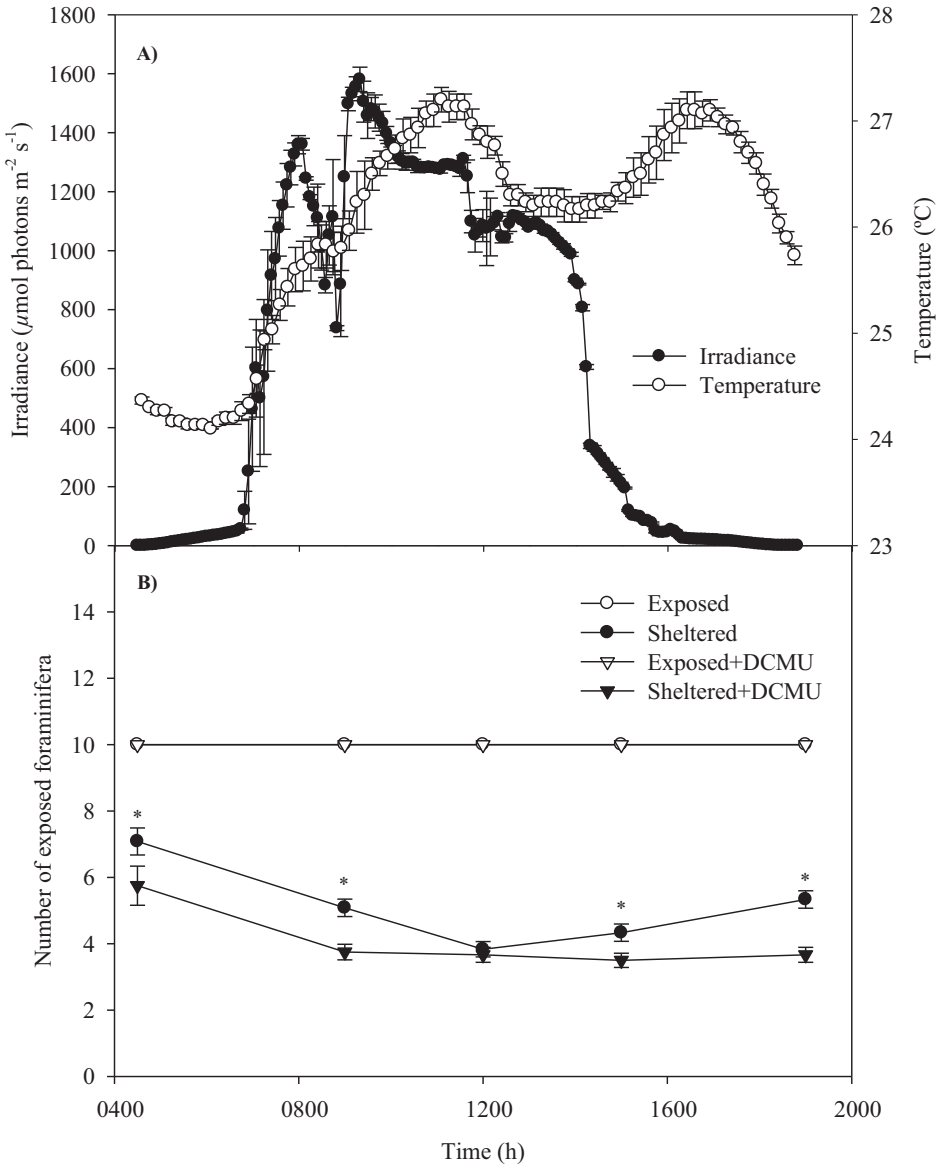

Figure 3.4: A) Irradiance (μmol photon m^{-2} s^{-1}) (closed circles) and seawater temperature (ºC) (open circles) from 0430 to 1900 h. Data represent mean from three consecutive days ± SE (n = 3). B) Number of foraminifera exposed to the sun in exposed (open circles), sheltered (closed circles), exposed with DCMU (open triangles) and sheltered with DCMU (closed triangles) treatments from 0430 to 1900 h. Data represent mean ± SE (n = 4). * indicates significant differences between sheltered and exposed.

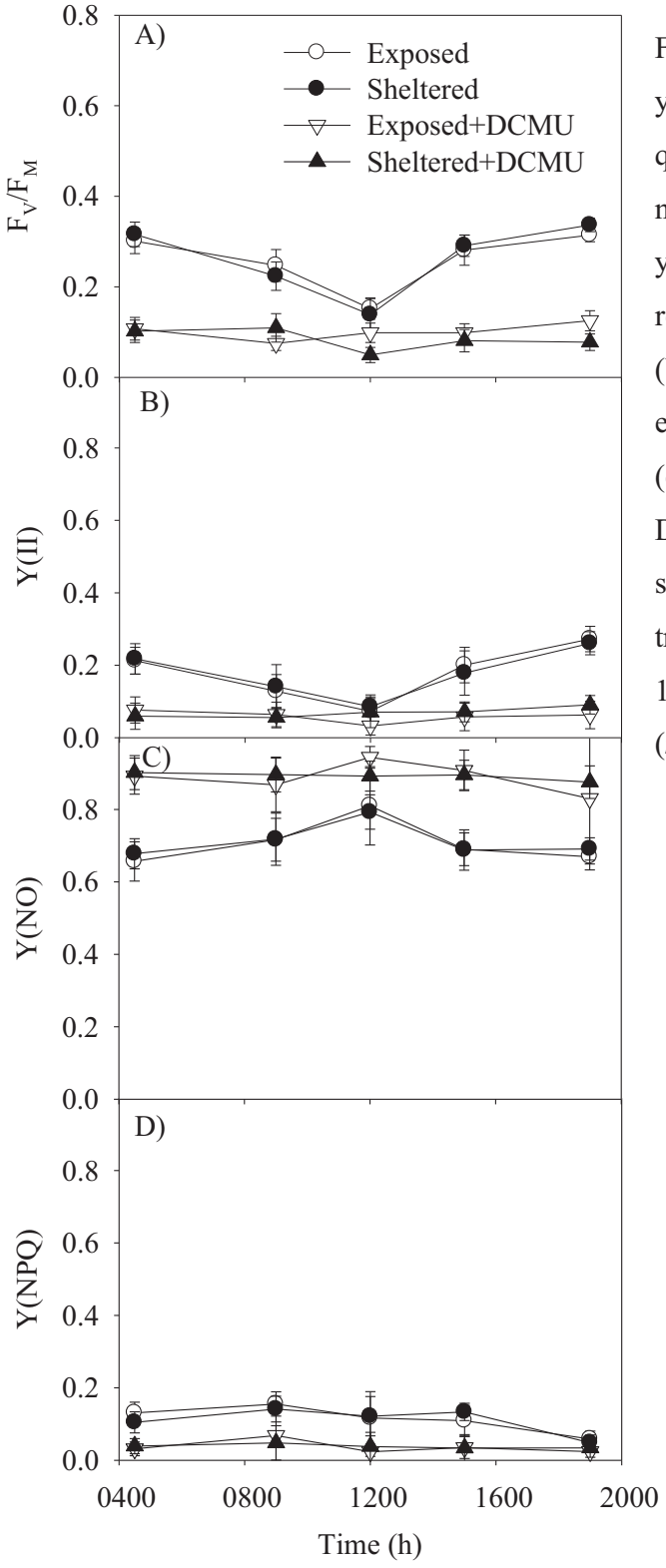

Figure 3.5: A) Maximum quantum yield of PSII (F_V/F_M), B) effective quantum yield of PSII (Y(II)), C) non-photochemical quenching yield (Y(NPQ)), and D) non-regulated heat dissipation yield (Y(NO)) from foraminifera in exposed (open circles), sheltered (closed circles), exposed with DCMU (open triangles) and sheltered with DCMU (closed triangles) treatments from 0430 to 1900 h. Data represent mean ± SE (n = 4).

Chlorophyll *a* and c_2 concentrations within *M. vertebralis*, and the density of algal symbionts, were not significant different (3 days later) across all four treatments (± shelter, ± DCMU; P > 0.05; Fig. 3.6).

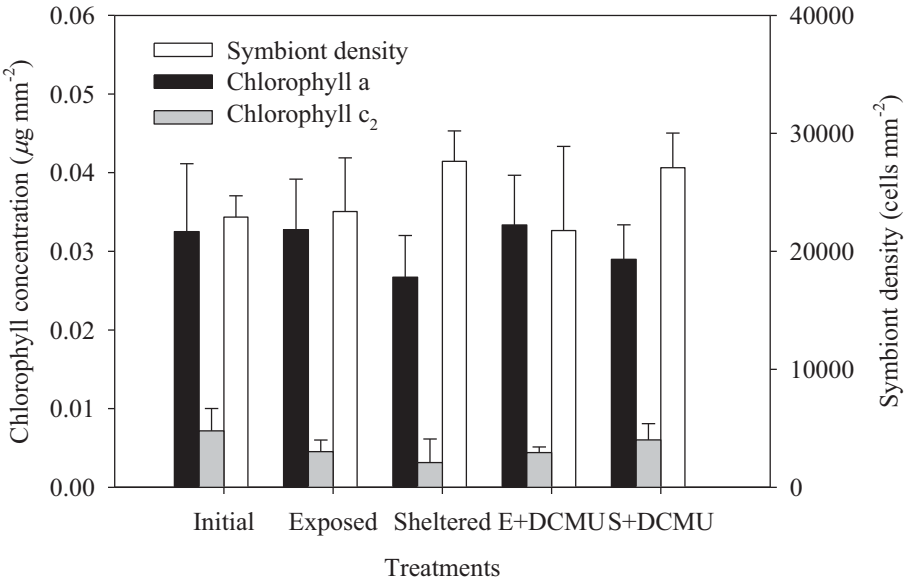

Figure 3.6: Chlorophyll *a* and c_2 concentration (μg mm^{-2}) and symbiont density (cells mm^{-2}) in foraminifera before experimentation (initial) and at the end of the experiments in the exposed, sheltered, exposed with DCMU (E+DCMU) and sheltered with DCMU (S+DCMU) treatments. Data represent mean + SE (n = 4).

In addition, measurements of xanthophyll pigments also revealed no significant change in Dt/(Dt+Dn) between the initial (day 1 at 0430 h) and final (day 3 at 1900 h) time point in exposed and sheltered foraminifera in the absence of DCMU (P > 0.05; Fig. 3.7A). However, a significantly lower Dt/(Dt+Dn) was observed in foraminifera exposed to DCMU for 3 days compared to the initial measurement (P < 0.001; Fig. 3.7A). A significantly greater Dt+Dn pool was found in exposed foraminifera on day 3 without DCMU, compared to all other treatments and the initial measurement (P = 0.031; Fig. 3.7A), while there were no significant differences in the Dt+Dn pool between initial measurements and other treatments (P > 0.05; Fig. 3.7A).

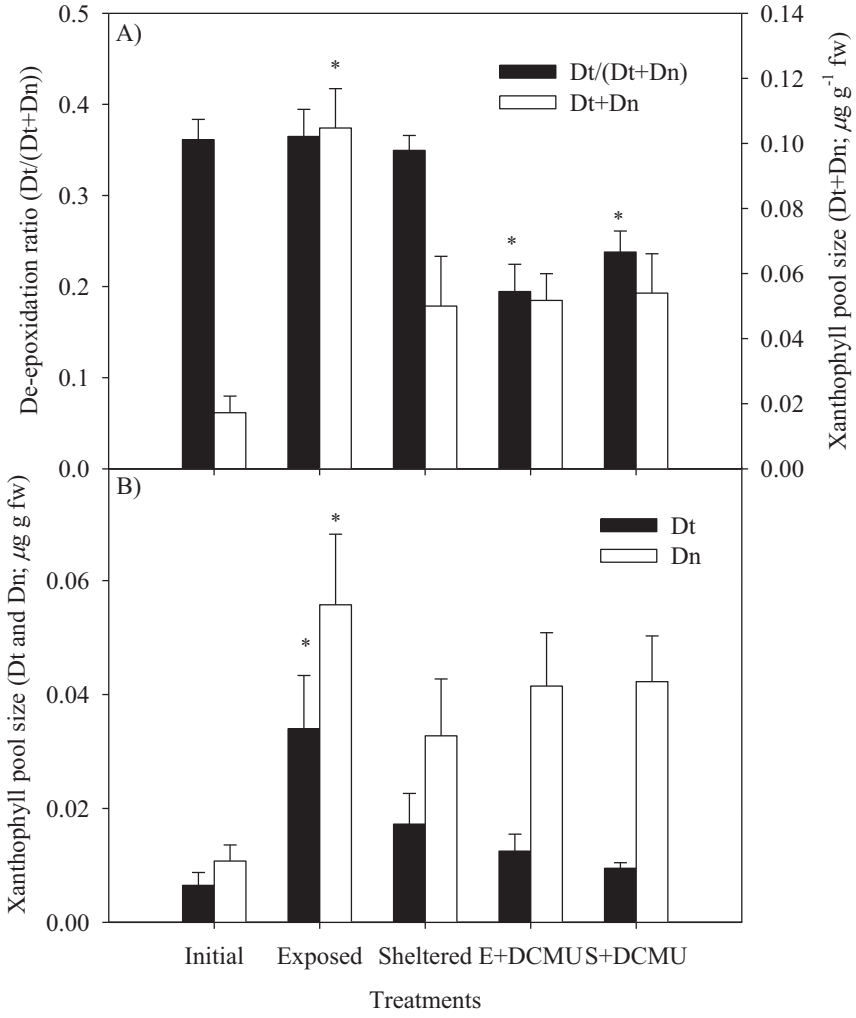

Figure 3.7: A) De-epoxidation ratio (diatoxanthin to total pool of diatoxanthin and diadinoxanthin; Dt/Dt+Dn) and total pool size of diatoxanthin and diadinoxanthin (Dt+Dn; μg g^{-1} fw). B) Diatoxanthin and diadinoxanthin (μg g^{-1} fw) from foraminifera in control, exposed, sheltered, exposed with DCMU (E+DCMU) and sheltered with DCMU (S+DCMU) treatments. Data represent mean + SE (n = 4).

The concentration of each individual pigment was greater in exposed foraminifera without DCMU, compared to initial measurements (P = 0.029 and 0.038 for Dt and Dn, respectively; Fig. 3.7B). Each individual pigment concentration in other treatments was

otherwise stable ($P > 0.05$; Fig. 3.7B) and Dn was the main contributor to the increase in the total pool size.

3.4 DISCUSSION

Our results demonstrate for the first time the capacity for movement in the benthic symbiotic foraminifer, *M. vertebralis*, in response to diurnal changes in irradiance. This movement was directed and had beneficial effects on symbiont photosynthetic performance. From observations in the field, *M. vertebralis* abundance was found to be significantly higher in sheltered areas at midday under high irradiance, indicating that an over-excitation of the photosystems is likely to be the main driver influencing this phototactic movement of benthic symbiotic foraminifera.

The effective quantum yield of PSII ($\Delta F/F_M'$) of exposed foraminifera declined by 30% when the light intensity reached 500 μmol photons m^{-2} s^{-1} at 0900 h, indicating a reduction in photosynthetic efficiency due to high irradiance (White and Critchley 1999; Ralph and Gademann 2005). However, $\Delta F/F_M'$ in exposed foraminifera significantly increased at 1200 and 1500 h, despite incident irradiance increasing. This may be a consequence of the motile capacity of *M. vertebralis*, with the possibility that individuals measured in exposed areas may have recently moved into this space and not received the full morning of direct sunlight. Similar to the exposed foraminifera, although less severe, $\Delta F/F_M'$ in sheltered individuals declined at 0900 h, indicating that sheltered foraminifera experienced lower light stress than the exposed foraminifera. Due to the motile capacity, the decline in $\Delta F/F_M'$ in sheltered foraminifera at 0900 h could be due to some of the exposed foraminifera moving to sheltered regions after 0900 and 1200 h.

Understanding the light history and the influence of photosynthesis in foraminiferal symbionts could identify associated changes in the photosynthetic response of symbiotic algae. RLCs have been used to quantify the light history and acclimation state of photosynthetic marine phototrophs (Ralph and Gademann 2005). In general, low-light

adapted and high-light adapted sessile organisms (such as seagrass, macroalgae, and coral) show clearly different patterns in RLC parameters (I_k, α, $rETR_{max}$) where high-light adapted phototrophs exhibit a higher I_k, a higher rETR and a lower α due to a slower decline in $\Delta F/F_M'$ with increasing light intensity (Ralph and Gademann 2005). The minimum saturating irradiance (I_k; Ralph and Gademann 2005) values in this November study (60-210 μmol photons m^{-2} s^{-1}) are higher compared to the benthic diatom-bearing foraminifera *Amphistergina* spp., *Calcarina* spp. and *Heterostergina depressa* from Edward Island, Australia (Nobes et al. 2008). In this previous study, the foraminifera received a midday irradiance of 1200 μmol photons m^{-2} s^{-1} and exhibited an I_k of 43 μmol photons m^{-2} s^{-1} (Nobes et al. 2008). This indicates that the dinoflagellate-bearing foraminifera *M. vertebralis* from Heron Island (0.3-2 m depth; maximum irradiance: 1163 μmol photons m^{-2} s^{-1}) was photoadapted to a higher light intensity. This could be related to the difference in morphology (thickness of the test), light history (deeper versus shallower species), migration behaviour (movement rate) and symbiont consortium (diatoms versus dinoflagellates) (Röttger and Krüger 1990; Nobes et al. 2008). High-light adaptation enables a greater capacity to cope with high light intensities (Ralph and Gademann 2005) and results in smaller and slower photoinhibitory effects (Shick et al. 1995) and faster recovery (Henley et al. 1991; Hanelt et al. 1993). The diurnal pattern in $\Delta F/F_M'$ observed in foraminifera was not consistent with the more widely observed solar maximum downregulation of PSII photochemical efficiency seen in other phototrophs (Häder et al. 1999; Winters et al. 2003) as we found some recovery of $\Delta F/F_M'$ at midday where the maximum light intensity occurred. We suggest this unusual response arose due to the capacity for movement in foraminifera. This ability may provide a means to reduce the impact of light stress by moving away from direct sunlight once irradiance becomes saturating. In addition, because the same foraminifera were not measured at each time of sampling, at 1200 h, foraminifera which recently moved into sunlight would have had a higher photochemical efficiency, compared to individuals which had received direct sunlight for the whole morning. In the laboratory experiment, however, the down-regulation of photochemistry was observed in both the exposed and sheltered treatment as significant

reductions in photosynthetic efficiency (F_V/F_M and Y(II)) were found at midday when high irradiance occurred (Fig. 3.5A-B). The recovery of F_V/F_M and Y(II) in the afternoon when irradiance declined, indicates that *M. vertebralis* can recover from saturating irradiances by activating photoprotective mechanisms.

To confirm that light-dependent movement occurs in these foraminiferans, we recorded the location of individuals in aquaria from sun-exposed and sheltered treatments. When given shelter in *Halimeda* thalli, foraminifera moved horizontally into shaded areas once irradiance exceeded 1400 μmol photons m^{-2} s^{-1} from 0900 to 1500 h. Once irradiance dropped below 20 μmol photons m^{-2} s^{-1} at 1900 h, individuals moved out to exposed areas. It is likely that foraminifera moved into the shaded areas to avoid over-saturating light that could cause photoinhibition, which may result in bleaching. Chlorophyll concentration and symbiont density in foraminifera is influenced by temperature, pH, spectral quality and quantity of photosynthetic active radiation (Williams and Hallock 2004; Sinutok et al. 2011). Exposure to high light intensity may also lead to bleaching or loss of symbiont. As the endosymbionts play a vital role in calcification and growth of the host, expulsion of endosymbionts and bleaching could have a negative impact on calcification, growth and result in mortality of foraminiferal host. However, our results showed that the chlorophyll *a* and c_2 concentrations and symbiont density were constant over all treatments suggesting that no chlorophyll degradation, symbiont loss or bleaching occurred (Fig. 3.6).

The exposed and sheltered foraminifera treated with the photosynthetic inhibitor DCMU did not show significant movement during the day except in the sheltered treatment from 0430 to 0900 h where +DCMU foraminifera moved into shade. Adding DCMU blocks the electron transport in PSII, so that the symbiont photosynthesis is inhibited. There was some movement at dawn before complete PSII inhibition occurred, once PSII was damaged due to the consequences of the DCMU presence in light, then movement ceased. The lack of movement between the sheltered and exposed areas once photosynthesis was inhibited indicated that there is a light-driven communication between the host foraminifera and the host movement was tightly coupled to

photosynthesis. This suggests the presence of light-dependant communication between the algal symbionts and host foraminiferan, where changes in symbiont physiology were linked to host movement. We therefore suggest that host behaviour can be influenced by the photosynthetic activity of the algal symbionts. Our study is consistent with Zmiri et al. (1974) who observed that no negative phototactic responses in *A. radiata* occurred under low light conditions (<2 μmol photons m^{-2} s^{-1}). Positive and negative phototaxis was also observed in *A. lobifera* when exposed to low light (1.35-13.5 μmol photon m^{-2} s^{-1}) and higher light level (>150 μmol photons m^{-2} s^{-1}), respectively (Lee et al. 1980). It is suggested that phototactic behaviour is the primary mechanism for modulating the light exposure in the symbiont-bearing foraminifera (Williams and Hallock 2004). This behaviour provides an advantage in avoiding photoinhibition and bleaching by moving away from over-saturating irradiance, to more optimal light fields when it is over-saturating or increasing light availability when light conditions are sub-saturating.

Adding DCMU caused a reduction in de-epoxidation in both exposed and sheltered treatments because proton gradient, which is an important process in xanthophyll cycle activation, was not present across the thylakoid membranes (Ridley 1977). As a result, a decrease in xanthophylls pigments occurred. The proportion of Dt to the total xanthophyll pool (Dt+Dn) shows the de-epoxidation of xanthophylls, Dn to Dt which is a photoprotective mechanism to avoid long-term photodamage (Falkowski and Raven 2007). Our result showed that there were no significant differences in degree of de-epoxidation between exposed and sheltered treatments and initial measurement. This may be explained by the time of sample collection for HPLC (0430 and 1900 h) may not induce the de-expoxidation state of xanthophylls pigments. However, the level of photoprotective xanthophyll (Dt+Dn) was significantly higher at exposed foraminifera comparing to sheltered foraminifera and initial measurement (Fig. 3.7A-B). The increase in the photoprotective xanthophyll pools were from the increases in both Dt and Dn indicating that light stress induces the synthesis of photoprotective pigments as a mechanism for photoprotection. The symbionts of *M. vertebralis* therefore have the

capacity to reduce the photosynthetic pressure from saturating irradiances by activating photoprotective mechanisms.

Our results indicated that the phototactic behaviour in foraminifera provides a competitive advantage over co-existing sessile organisms (such as coral and macroalgae) under future predicted increase in irradiance and UV radiation by enhancing their ability to cope with over-saturating irradiance and adjusting their light environment. By attaching to the calcifying macroalga *Halimeda* (Hallock 1981a,b) or seagrasses (Severin 1987), foraminifera can move upward to the top of the plants when requiring more light (positive phototaxis) and move downward or horizontally to shaded areas to avoid excess light (negative phototaxis). This behaviour could help avoid long-term photoinhibition, loss of photosynthetic pigments and expulsion of zooxanthellae from the foraminiferal host (bleaching) that could occur under prolonged high-light stress (Talge and Hallock 2003). In addition, by harbouring the mixed community of endosymbionts which can vary their photophysiology and susceptibility to bleaching under different light and temperature conditions (e.g. *Symbiodinium* sp. clade A, C, F, H; Ulstrup et al. 2008; Fay et al. 2009), the phototactic behaviour along with the mixed community of endosymbionts would provide enhanced growth and fitness of the holobiont in shallow coral reef habitats (Hallock 2000). Our study suggested that the movement ability of benthic symbiotic foraminifera *M. vertebralis* is light-related and controlled by the photophysiology of the symbiont, therefore, the phototactic behaviour is the primary mechanism for modulating the light exposure in the symbiont-bearing foraminifera and benefits to the foraminiferal host.

CHAPTER 4:

WARMER MORE ACIDIC CONDITIONS CAUSE DECREASED PRODUCTIVITY AND CALCIFICATION IN SUBTROPICAL CORAL REEF SEDIMENT-DWEELING CALCIFIERS

4.0 WARMER MORE ACIDIC CONDITIONS CAUSE DECREASED PRODUCTIVITY AND CALCIFICATION IN SUBTROPICAL CORAL REEF SEDIMENT-DWEELING CALCIFIERS

All laboratory work, data collection, data analyses and write up were undertaken by me. Richard Wuhrer assisted with the SEM analysis. Michael Johnson assisted with the confocal microscope set up.

Sinutok S, Hill R, Doblin MA, Wuhrer R, Ralph PJ (2011) Warmer more acidic conditions cause decreased productivity and calcification in subtropical coral reef sediment-dwelling calcifiers. *Limnology and Oceanography* 56(4): 1200-1212.

4.1 INTRODUCTION

Since the beginning of the industrial revolution, human activities such as the burning of fossil fuels, industrialization, deforestation and intensive agricultural activities have raised atmospheric CO_2 concentrations (Gattuso and Lavigne 2009). As a consequence, surface seawater temperature has increased by an average of 0.6°C over the last century (Houghton 2009). Moreover, a 35% increase in atmospheric CO_2 concentration (from pre-industrial levels of 28.4 Pa to approximately 38.9 Pa today) has lead to ocean acidification by elevating the dissolved CO_2 concentration in the surface ocean, which lowers pH (Solomon et al. 2007). The rate of change is 100-1000 times faster than the most rapid changes in temperature and CO_2 in at least the last 420,000 years (Hoegh-Guldberg et al. 2007). Models parameterized with CO_2-emission trends for 1990-1999 (so-called 'SRES scenarios'; Solomon et al. 2007) predict that CO_2 concentrations will rise 150-250% (to $\leq$ 101 Pa) by the year 2100 (Friedlingstein et al. 2006). The surface ocean pH is already 0.1 units lower than pre-industrial values (Orr et al. 2005), which is equivalent to a 30% increase in H^+ ions (Raven et al. 2005) and is predicted to decrease by a further 0.4 to 0.5 units by 2100 (Raven et al. 2005; Lough 2007).

An increase in sea temperature and atmospheric CO_2 will influence the health and survivorship of marine organisms, especially calcifying species, such as molluscs, crustaceans, echinoderms (Doney et al. 2009), corals (Reynaud et al. 2003; Jokiel et al. 2008), calcareous algae (Jokiel et al. 2008), foraminifera (Hallock 2000), and some phytoplankton (Raven et al. 2005; Iglesias-Rodriguez et al. 2008). Temperature influences physiological processes including photosynthesis, respiration and calcification (Howe and Marshall 2002; Necchi 2004). In reef-building (scleractinian) corals, warmer temperatures increase the rate of calcification (Lough and Barnes 2000), although increases beyond a thermal threshold as small as 1-2°C above summer averages can lead to mass coral bleaching events (large areas of coral colonies expelling symbiotic algae) and sometimes death (Hoegh-Guldberg 1999).

Ocean acidification has been suggested to have a positive effect on organisms such as seagrass and non-calcifying macroalgae, which utilise CO_2 as the substrate for carbon fixation in photosynthesis (Gao et al. 1993b; Short and Neckles 1999). However, ocean acidification is likely to have a negative effect on calcified organisms by decreasing the availability of carbonate ions (CO_3^{2-}) and hence the organisms' ability to produce their calcium carbonate skeleton (Feely et al. 2004). Acidification has been shown to reduce calcification, recruitment, growth and productivity in the articulated coralline alga, *Corallina pilulifera* Postels and Ruprecht, as well as crustose coralline algae (CCA) when exposed to elevated pCO_2 (partial pressure of CO_2) seawater (Kuffner et al. 2007; Anthony et al. 2008). Reduced abundance of CO_3^{2-} ions could also lead to an increase in calcium carbonate dissolution in the future (Feely et al. 2004).

Synergistic effects of elevated temperature and carbon dioxide partial pressure (pCO_2) have had limited examination, but Reynaud et al. (2003) observed 50% lower calcification rates in the scleractinian coral *Stylophora pistillata* Esper compared to either high temperature or low pH conditions in isolation. Whereas, in the corals *Acropora intermedia* Brook and *Porites lobata* Dana, Anthony et al. (2008) found that combined ocean acidification and warming scenarios (rather than ocean acidification conditions in isolation) resulted in bleaching, reduced productivity, as well as calcium

carbonate dissolution and erosion in *A. intermedia* and *P. lobata* and in the CCA species, *Porolithon onkodes* (Heydrich) Foslie.

Sediment producing species, *Halimeda* and symbiont bearing foraminifera, are prominent, co-existing taxa in shallow reef systems, and play a vital role in tropical and sub-tropical ecosystems as producers of sediment in coral reefs (Hallock 1981a). However, there is limited evidence of the effects of ocean warming and acidification in these two important carbonate sediment producers. Elevated seawater temperatures of 30ºC to 35ºC reduced the growth rate in the benthic foraminifera, *Rosalina leei* Hedley and Wakefield (Nigam et al. 2008) and induced algal symbiont loss in *Amphistegina gibbosa* d'Orbigny when temperatures reached 32ºC (Talge and Hallock 2003). Borowitzka and Larkum (1976b) showed an inhibition in calcification in *Halimeda tuna* (Ellis and Solander) Lamouroux when seawater pH was dropped from 8.0 to 7.5. A more recent study found thinner aragonite crystals and higher crystal density in *H. tuna* and *H. opuntia* grown in pH 7.5, when compared to those grown at a pH of 8.1 (Robbins et al. 2009). Research on symbiotic and non-symbiotic planktonic foraminifera (*Orbulina universa* d'Orbigny and *Globigerina sacculifers* Brady, respectively) and symbiotic benthic foraminifera (*Marginopora kudakajimensis* Gudmundsson) showed a decrease in shell weight with decreasing availability of the carbonate ion in seawater (Kuroyanagi et al. 2009). These results indicate that a decrease in calcification is likely in these organisms under the acidified conditions which are expected to occur in the future. However, there have been no studies on the combined effect of elevated temperature and CO_2 concentration on the photosynthetic marine calcifiers, *Halimeda* sp. and benthic foraminifera.

Halimeda spp. precipitates calcium carbonate as aragonite while many foraminifera precipitate high-Mg-calcite. The current saturation state of aragonite (Ω-aragonite = 3 to 4) is greater than the high-magnesium calcite mineral (Ω -high-magnesium calcite = 2 to 3) (Kleypas et al. 1999; ISRS 2008) which means that organisms which precipitate high-magnesium calcite are expected to have more difficulty in producing their $CaCO_3$ skeleton under elevated pCO_2 conditions, compared to organisms which precipitate

$CaCO_3$ as aragonite (Kleypas et al. 1999). Thus the hypothesis tested in this study was that the calcifying macroalga, *Halimeda* would perform better than benthic foraminifera under high CO_2 conditions and that all organisms would show greater effects under the combined effects of elevated CO_2 and temperature.

4.2 MATERIALS AND METHODS

4.2.1 Experimental design

Whole specimens of *Halimeda macroloba* Decaisne (thallus size of 13-18 cm long), *Halimeda cylindracea* Decaisne (15-20 cm long), and *Marginopora vertebralis* Quoy and Gaimard (0.3-0.6 cm diameter) were collected by hand from the Heron Island reef flat at low tide at 0.3 m depth in the Southern Great Barrier Reef of Australia (151º55'E, 23º26'S). The symbiont bearing foraminifera *M. vertebralis* hosts the symbiotic alga *Symbiodinium* sp. in interior shell chambers (Pawlowski et al. 2001). The specimens of these species were maintained in a 500 L aquarium with artificial seawater (pH 8.1, 26ºC, salinity 33) under 250 μmol photons m^{-2} s^{-1} (at water surface) on a 12:12 h light:dark cycle. Mature segments of *H. macroloba* (0.8-1.1 cm long) and *H. cylindracea* (1.5-2.0 cm long) from the middle part of the thallus and *M. vertebralis* (320 each species) were randomly allocated to one of four temperature treatments (28°C, 30°C, 32°C, and 34°C) in combination with one of four pH treatments (8.1, 7.9, 7.7, and 7.4; the current and predicted pH values for the years 2065, 2100, and 2200, respectively, and equivalent to pCO_2 38.5, 60.8, 101, and 203 Pa in this experiment) (Houghton 2009)). Within each tank, samples of each of the three species were placed in separate, open petri-dishes, so there was no direct physical interaction between specimens. Samples were ramped from 26°C and a pH of 8.1 to their treatment conditions over 1 week and maintained in the 16 treatments for a further four weeks (n = 4). The tanks set at ambient pH levels of 8.1 and 28ºC acted as controls. The water salinity in the 100 L experimental tanks was maintained at 33 and the light intensity at the sample height was 300 μmol photons m^{-2} s^{-1} on a 12:12 h light:dark cycle (on at 06:00 h and off at 18:00 h). The treatment tanks were 0.2 m deep, consistent with

sampling depth. The carbonate hardness (concentration of CO_3^{2-} + HCO_3^-), calcium, nitrate and phosphate concentration were maintained at 2.3, 10, <0.0016, and <0.0005 mmol L^{-1}, respectively, and monitored weekly using test kits (Aquasonic Pty). The concentration of CO_2 in both treatments and controls was maintained by CO_2 gas bubbling through the water held in the sump before it was recirculated to the aquaria containing the samples. Carbon dioxide dosing was automated using a pH-controller (Tunze) connected to a solenoid valve on a CO_2 gas line. CO_2 gas was bubbled through the seawater once pH increased beyond the target pH and was maintained at a precision of ± 0.01 pH units. pH electrodes (National Bureau of Standards (NBS scale); Tunze), each connected to a pH-controller, were calibrated every week, during which time, no detectable drift in pH was found. Water temperature in each treatment was controlled by water heaters and chillers (Hailea, China) to ± 0.1°C. Water changes (20%) to each treatment were performed every week using seawater media set to the required pH using CO_2 bubbling prior to addition. Salinity was measured daily with a salinity meter (Salt 6, Eutech Instruments), while total alkalinity (TA) was measured weekly by titrating 30 g of seawater with 0.1 mol L^{-1} hydrochloric acid using an autotitrator (Mettler Toledo; Gattuso et al. 1993). From each treatment tank, TA was determined as the average from three independent samples of water. Dissolved inorganic carbon concentrations were calculated using the CO2SYS program (version 01.05; Brookhaven National Laboratory) (Lewis and Wallace 1998). A summary of the TA, dissolved inorganic carbon (DIC, CO_2, CO_3^{-2}, HCO_3^-), CO_2 partial pressure (pCO_2), and saturation state of seawater with respect to calcite (Ω_c) and aragonite (Ω_a) from each pH (8.1, 7.9, 7.7, 7.4) and temperature (28ºC, 30ºC, 32ºC, 34ºC) treatment are shown in Table 4.1. There was no significant difference in TA among the 16 pH and temperature treatments and pCO_2, CO_2, CO_3^{-2}, HCO_3^-, DIC, Ω_c, and Ω_a remained consistent within each pH treatment.

4.2.2 Mortality assessment

Mortality in *H. macroloba* and *H. cylindracea* was determined by presence of bleached and disintegrated segments, while mortality in *M. vertebralis* was determined by bleached and broken tests. In addition, the lack of variable fluorescence from measures

of Pulse Amplitude Modulated (PAM) fluorometry (indicative of photosynthetic activity by algal symbionts) were an indication of mortality.

4.2.3 Photosynthesis

Photosynthetic condition was determined through measures of chlorophyll *a* fluorescence, oxygen production, photosynthetic pigment concentration and, for foraminifera, algal symbiont density. To avoid diel and non-steady state variability, steady state light curves (SSLCs), with 1 irradiance step (372 μmol photons m^{-2} s^{-1} applied for 300 s) were performed with a 6 mm diameter fibre-optic on a Diving-PAM fluorometer (Walz) every week at 10:00 h over the duration of the experiment, following 10 minutes of dark adaptation (Diving-PAM settings: measuring intensity <0.15 μmol photons m^{-2} s^{-1}, saturating intensity >4500 μmol photons m^{-2} s^{-1}, saturating width = 0.8 s, gain = 2, damping = 2). Photosystem II (PSII) photosynthetic efficiency was determined through weekly measures of maximum quantum yield (F_V:F_M) and effective quantum yield (Y(II)). In addition, the capacity for photoprotection (non-photochemical quenching yield (Y(NPQ)) and level of photoinhibition (non-regulated heat dissipation yield (Y(NO)) was determined through SSLCs (Kramer et al. 2004).

Oxygen production was measured using a needle-type fibre optic oxygen micro-sensor PSt1 connected to a Micro TX3 transmitter (Presens). After 10 minutes of dark adaptation, the samples were placed in 10 mL glass bottles filled to the top with treatment water, the bottles sealed and then placed in a water bath (Julabo) set to the relevant treatment temperature. The sensor was inserted through a re-sealable hole in the bottle lid to determine the oxygen production over 5 minutes under 300 μmol photons m^{-2} s^{-1} of irradiance and rates calculated according to Ulstrup et al. (2005).

Photosynthetic pigment concentration (chlorophyll (Chl) *a* and *b* for *H. macroloba* and *H. cylindracea* and chlorophyll *a* and c_2 for *M. vertebralis*) was determined using the standard spectrophotometric method of Ritchie (2008) at the beginning and end of the 5-week experiment.

Table 4.1: Parameters of the carbonate system; total alkalinity (TA), CO_2 partial pressure (pCO_2), dissolve inorganic carbon (CO_2, CO_3^{-2}, HCO_3^-, DIC), and saturation state of seawater with respect to calcite (Ω_c) and aragonite (Ω_a) from each pH (8.1, 7.9, 7.7, 7.4) and temperature (28ºC, 30ºC, 32ºC, 34ºC). Data represent Mean ± SE (n = 3).

Treatment		TA	pCO_2	CO_2	CO_3^{-2}	HCO_3^-	DIC	Ω_c	Ω_a
pH	Temp (ºC)	(mmol kg^{-1})	(Pa)	(mmol kg^{-1})	(mmol kg^{-1})	(mmol kg^{-1})	(mmol kg^{-1})		
8.1	28	2.314±0.187	32.2±2.6	0.008±0.001	0.280±0.035	1.635±0.135	1.923±0.160	6.03±0.95	4.04±0.61
8.1	30	2.647±0.190	36.8±2.7	0.008±0.001	0.340±0.030	1.842±0.145	2.190±0.166	7.40±0.55	4.99±0.63
8.1	32	2.695±0.189	36.9±2.6	0.008±0.001	0.365±0.042	1.835±0.138	2.209±0.162	8.02±0.73	5.44±0.60
8.1	34	2.392±0.190	32.2±2.6	0.007±0.001	0.338±0.035	1.579±0.133	1.924±0.160	7.50±0.74	5.13±0.60
7.9	28	2.685±0.169	66.9±4.6	0.016±0.002	0.231±0.004	2.140±0.170	2.387±0.170	3.34±0.10	3.34±0.09
7.9	30	2.624±0.168	65.1±4.5	0.016±0.002	0.240±0.003	2.058±0.173	2.314±0.173	3.52±0.15	3.52±0.10
7.9	32	2.607±0.170	64.6±4.5	0.015±0.002	0.238±0.003	2.044±0.180	2.297±0.182	3.49±0.12	3.49±0.10
7.9	34	2.309±0.170	56.3±4.6	0.012±0.002	0.235±0.004	1.743±0.175	1.990±0.176	3.57±0.14	3.57±0.12
7.7	28	2.532±0.110	108.0±4.7	0.027±0.001	0.148±0.018	2.172±0.080	2.347±0.101	2.14±0.44	2.14±0.33
7.7	30	2.565±0.108	110.0±4.7	0.025±0.001	0.160±0.019	2.185±0.082	2.370±0.099	2.36±0.52	2.36±0.32
7.7	32	2.427±0.110	104.0±4.8	0.024±0.001	0.162±0.018	2.042±0.083	2.228±0.110	2.41±0.49	2.41±0.34
7.7	34	2.691±0.109	115.0±4.8	0.025±0.001	0.191±0.020	2.244±0.080	2.460±0.095	2.90±0.49	2.90±0.33
7.4	28	2.696±0.136	247.0±12.5	0.062±0.004	0.085±0.008	2.495±0.145	2.642±0.133	1.84±0.16	1.23±0.15
7.4	30	2.568±0.129	236.0±12.2	0.056±0.005	0.087±0.007	2.362±0.135	2.505±0.132	1.89±0.15	1.28±0.15
7.4	32	2.827±0.134	262.0±12.7	0.059±0.005	0.102±0.008	2.588±0.130	2.749±0.139	2.26±0.18	1.53±0.17
7.4	34	2.526±0.135	235.0±12.5	0.051±0.005	0.098±0.005	2.295±0.140	2.444±0.135	2.18±0.15	1.49±0.16

Chlorophyll *a*, *b*, and c_2 were extracted by soaking samples in 3 mL of 90% acetone at 4°C in darkness for 24 hours. Samples were centrifuged at 1500 *g* for 10 minutes and the supernatant placed into a quartz cuvette in a spectrophotometer (Varian, Australia) and absorbance measured at 630, 647, and 664 nm. Chlorophyll concentrations were determined using the equations of Ritchie (2008) and the results were expressed in μg mm^{-2}.

Algal symbiont density in the foraminifera was investigated using a Confocal microscope (Nikon A1). For each individual foraminiferan, four randomly selected interrogation areas were chosen from the edge, middle, and center of the test (shell). Algal symbionts in the chambers within each area were counted and expressed in terms of surface area.

4.2.4 Calcification

Calcification was determined using the buoyant weight technique (Jokiel et al. 2008) with comparisons made between measurements at the start and end of the experimental period. The buoyant weight technique is a reliable measure of calcification, inferred from changes in skeletal weight (Langdon et al. 2010). It was determined by weighing each sample in seawater of known density and applying Archimedes's principle to compute the dry weight of the sample in the air (Jokiel et al. 1978; Langdon et al. 2010). Weight was measured using an electronic balance with accuracy to 0.1 mg. The samples were placed on a glass petri-dish hung below the balance using nylon thread suspended in seawater. The density of water at salinity 33 and 25ºC was 1026.42 kg m^{-3} (Jokiel et al. 1978), and the density of *H. macroloba*, *H. cylindracea*, and *M. vertebralis* at salinity 33 and 25ºC were 2052.37, 5384.9, and 2733.98 kg m^{-3}, respectively (Jokiel et al. 1978).

Images of aragonite and magnesium calcite crystals were examined for size and abundance analysis using a field emission gun scanning electron microscope (FEGSEM; Zeiss Supra 55VP). The instrument was operated at 20 kV with 30 μm aperture, ~4 mm working distance in hivac mode and imaged using the secondary In-lens detector.

Samples were mounted on aluminium stubs using carbon adhesive tape and then placed in a carbon coating unit (Balzers) operated at 40 mm working distance. An area of 9 μm^2 was selected and the crystal abundance was determined (n=4 per sample with 10 measurements per replicate) along with crystal width, which was calculated using a spatial analysis software (University of Texas Health Science Center, San Antonio, Image Tool version 3; University of Texas).

4.2.5 Statistical analysis

To determine any significant differences among treatments in growth rate, chlorophyll *a*, *b*, and c_2 concentration, chlorophyll fluorescence parameters (F_V:F_M, Y(II), Y(NPQ), Y(NO)), oxygen production, and crystal density and width over time, repeated-measures analysis of variance (rmANOVA) tests were performed. One-way ANOVA tests were used to compare treatments at the initial or final time point (Statistical Package for the Social Sciences (SPSS) version 17). All tests were performed with a significance level of 95% and Tukey's Honesty Significant Difference post hoc tests were used to identify the statistically distinct groups. If data did not meet the assumptions of normality (Kolmogorov-Smirnov test) and equal variance (Levene's test), the data were transformed using $\log_{10}$ or square root. Differences in symbiont density among treatments were tested using Friedman test at 95% significance level.

4.3 RESULTS

4.3.1 Calcification and mortality

The calcification rates of *H. macroloba*, *H. cylindracea*, and *M. vertebralis* were slightly positive in the control treatment and were highly negative in the other treatments, indicating dissolution of calcium carbonate. Calcification rate was significantly reduced by elevated temperature (34ºC) at all pH levels (p<0.05). Calcification rate of *H. macroloba* at pH 7.4 and 34ºC (-1.24±0.70 mg $CaCO_3$ day^{-1}) was significantly lower than the control (0.02±0.01 mg $CaCO_3$ day^{-1}) (p<0.001; Fig. 4.1A-D). In *H. cylindracea*, calcification rate significantly declined at pH 7.7 and 7.4 in 34ºC treatments (p<0.001;

Fig. 4.1E-H), while in *M. vertebralis* calcification rate significantly decreased at pH 7.9, 7.7, and 7.4 at 30ºC, 32ºC, and 34ºC ($p<0.05$; Fig. 4.1I-L). Foraminiferal mortality was first observed at day 21 of the experiment in pH 7.4, 30ºC and 34ºC, while in *H. macroloba* and *H. cylindracea*, mortality was found at day 28 in pH 8.1, 7.9, 7.4 at 34ºC and pH 8.1 at 34ºC, respectively.

Halimeda macroloba and *H. cylindracea* had 100% mortality at the end of the experiment at pH 7.4 and 34ºC while 100% mortality of *M. vertebralis* was observed at pH 7.7 and 7.4 in the 32ºC and 34ºC treatments. At lower pH treatments (all except control) and higher temperature (32ºC and 34ºC) treatments, the symbiont density of foraminifera significantly decreased ($p<0.001$; Fig. 4.2A-E) and foraminiferal bleaching and death were observed.

4.3.2 Pigment content

After 5 weeks, the chlorophyll *a* and *b* concentration in *H. macroloba* significantly declined at pH 8.1, 7.9 and 7.7 with 34ºC and 7.4 with 32ºC and 34ºC treatments ($p<0.001$; Fig. 4.3A-E). However, no significant change was detected in chlorophyll *a* and *b* concentration in pH 8.1, 7.9, and 7.7 with 28ºC, 30ºC, and 32ºC treatments over the 5 week experiment ($p>0.05$; Fig. 4.3A-E). The chlorophyll *a* and *b* concentration in *H. cylindracea* after 5 weeks significantly declined at pH 8.1 and 7.9 with 34ºC and pH 7.4 with 28ºC and 34ºC treatments ($p<0.001$; Fig. 4.3F-J). In *M. vertebralis*, chlorophyll *a* and c_2 concentration significantly decreased in pH 7.9, 7.7, and 7.4 at all temperature treatments and in pH 8.1 at 34ºC treatment ($p<0.001$; Fig. 4.3K-O).

4.3.3 Chlorophyll a fluorescence

Maximum quantum yield (F_V:F_M) and effective quantum yield (Y(II); data not shown) in the control treatment did not significantly vary in *H. macroloba*, *H. cylindracea*, and *M. vertebralis*' symbionts ($p>0.05$; Fig. 4.4A, 4.4E and 4.4I).

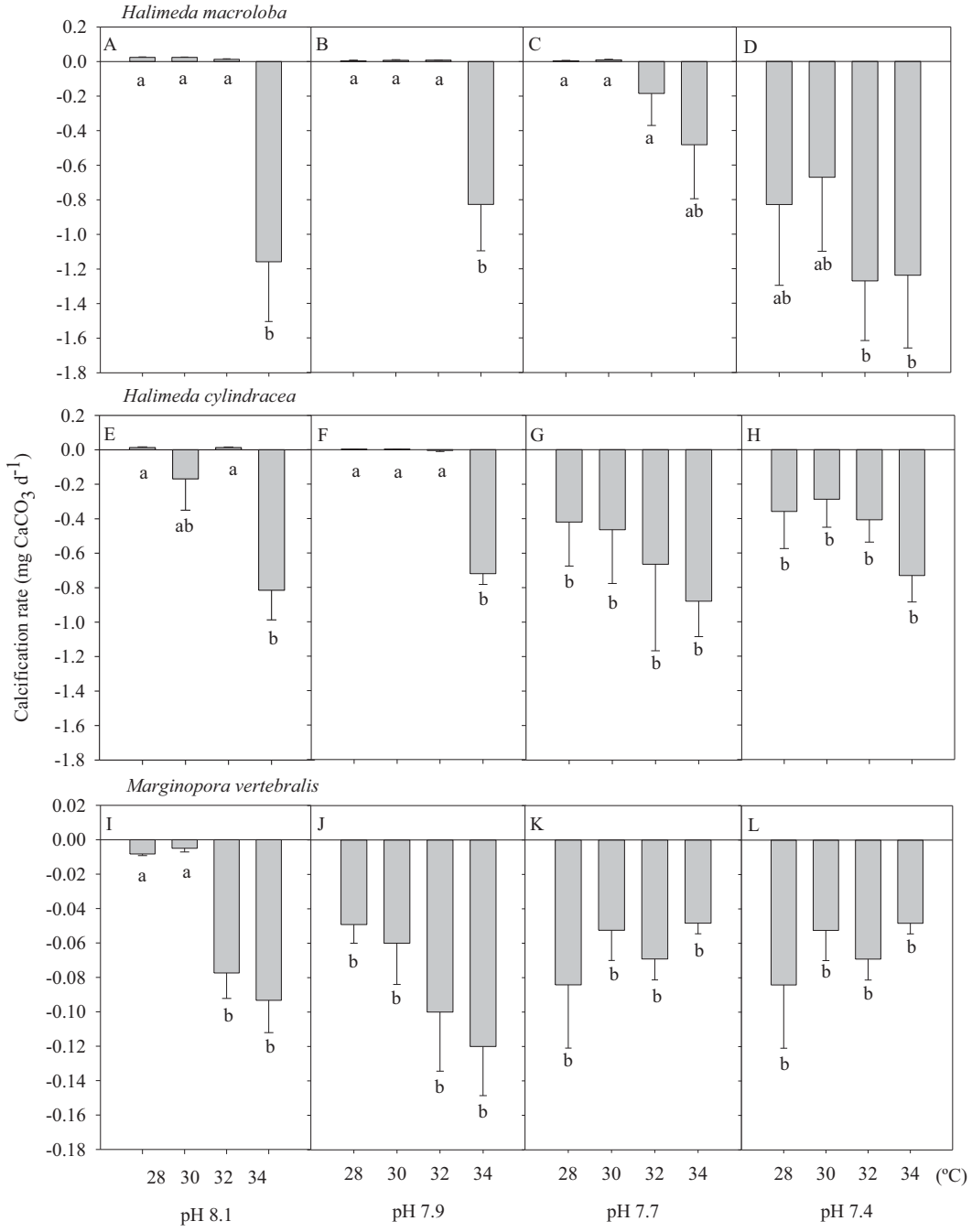

Figure 4.1: Calcification rate (mg $CaCO_3$ day^{-1}) over the 5 week period in (A-D) *H. macroloba*, (E-H) *H. cylindracea*, and (I-L) *M. vertebralis* in each pH and temperature treatment. Data represent means (n = 4, SEM).

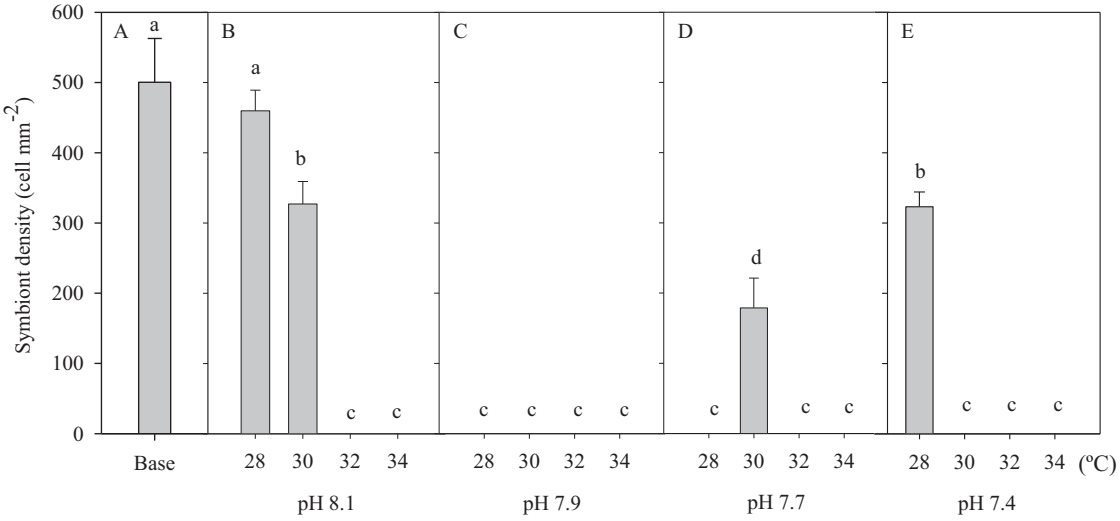

Figure 4.2: Symbiont density (cells mm^{-2}) of *M. vertebralis* at (A) time zero (base) and after five weeks for each of the four temperature treatments (28, 30, 32 and 34°C) at pH (B) 8.1, (C) 7.9, (D) 7.7, and (E) 7.4. No bar indicates the absence of symbionts. Data represent means (n = 4, SEM).

A significant decrease in F_V:F_M and Y(II) was found in all species when exposed to elevated CO_2 (pH 7.4 in all temperature treatments) and temperature (32ºC and 34ºC in all pH treatments) over the length of the experiment (p<0.001; Fig. 4.4A-D, 4.4E-H, and 4.4I-L). In *H. macroloba,* F_V:F_M declined to zero after being treated under 34ºC at all pH treatments for 28 days (p<0.001; Fig. 4.4A-D). F_V:F_M of *H. cylindracea* decreased to zero after 28 days at 34ºC, in pH 8.1, 7.9, and 7.7 treatments (p<0.001; Fig. 4.4E-H). In *M. vertebralis*' symbionts, F_V:F_M significantly decreased at 34ºC and all pH treatments after 14 days of experimentation and also reached zero within 14 days in pH 8.1 and 34ºC treatment (p<0.001; Fig. 4.4I-L). At lower temperature (28ºC and 30ºC) with lower pH treatments (pH 7.7 and 7.4), F_V:F_M (p<0.001; Fig. 4.4A-D, 4.4E-H, and 4.4I-L), and Y(II) (p<0.001; data not shown) of *H. macroloba*, *H. cylindracea*, and *M. vertebralis* significantly decreased after 5 weeks of experimentation. Moreover, there was a greater decrease in F_V:F_M and Y(II) in all species when exposed to the combined treatment of

elevated temperature and CO_2. The capacity for photoprotection (non-photochemical quenching yield (Y(NPQ)), and level of photoinhibition (non-regulated heat dissipation yield (Y(NO)) were similar over time in all pH and temperature treatments prior to mortality (p>0.05; data not shown).

4.3.4 Oxygen production

The rate of oxygen production of *H. macroloba*, *H. cylindracea*, and *M. vertebralis*' symbionts significantly decreased when exposed to elevated CO_2 to pH 7.4 for 18 days (p<0.001, Fig. 4.5A-D, 4.5E-H, and 4.5I-L). Higher temperature (34ºC) significantly lowered the oxygen production rate in *H. macroloba* only when maintained at a pH of 8.1. Greatest oxygen production of *H. macroloba* was found at pH 8.1, 30ºC (14.06±1.47 μmol L^{-1}) on day 0, while the lowest oxygen production was found at 34ºC in all pH treatments on day 35 (0±0 μmol L^{-1}) (Fig. 4.5A-D). Similarly, *H. cylindracea* had its highest and lowest oxygen production on day 0, pH 7.9, 34ºC and at pH 8.1, 7.9, and 7.4 treatments (14.85±4.82 and 0.0±0.0 μmol L^{-1}), respectively, while in *M. vertebralis*' symbionts the highest and lowest oxygen production was found on day 18, pH 7.9, 34ºC and on day 27 and day 35, 32ºC and 34ºC at all pH treatments (11.71±4.17 and 0.0±0.0 μmol L^{-1}; Fig. 4.5E-H and 4.5I-L).

4.3.5 Calcification

After 5 weeks, the calcium carbonate crystal width of *H. macroloba*, *H. cylindracea*, and *M. vertebralis* significantly decreased when exposed to elevated CO_2 at pH 7.7 and 7.4 (p<0.05; Figs. 4.6, 4.7). Elevated temperature had no effect on the crystal width in *H. macroloba* (p =0.562) or *H. cylindracea* (p=0.926), but caused a significant decrease in the crystal width of *M. vertebralis* at 32ºC and 34ºC in all pH treatments (p<0.001; Fig. 4.6). In contrast, crystal abundance in the foraminifera increased significantly at high CO_2 under pH 7.9, 7.7, and 7.4 and high temperature at 32ºC and 34ºC (p<0.001) from 25.46±0.77 number μm^{-2} in the control to 39.93±0.43 number μm^{-2} at pH 7.4 and 34ºC. However, there was no significant difference in crystal abundance of *H.*

macroloba and *H. cylindracea* among pH and temperature treatments (p>0.05).

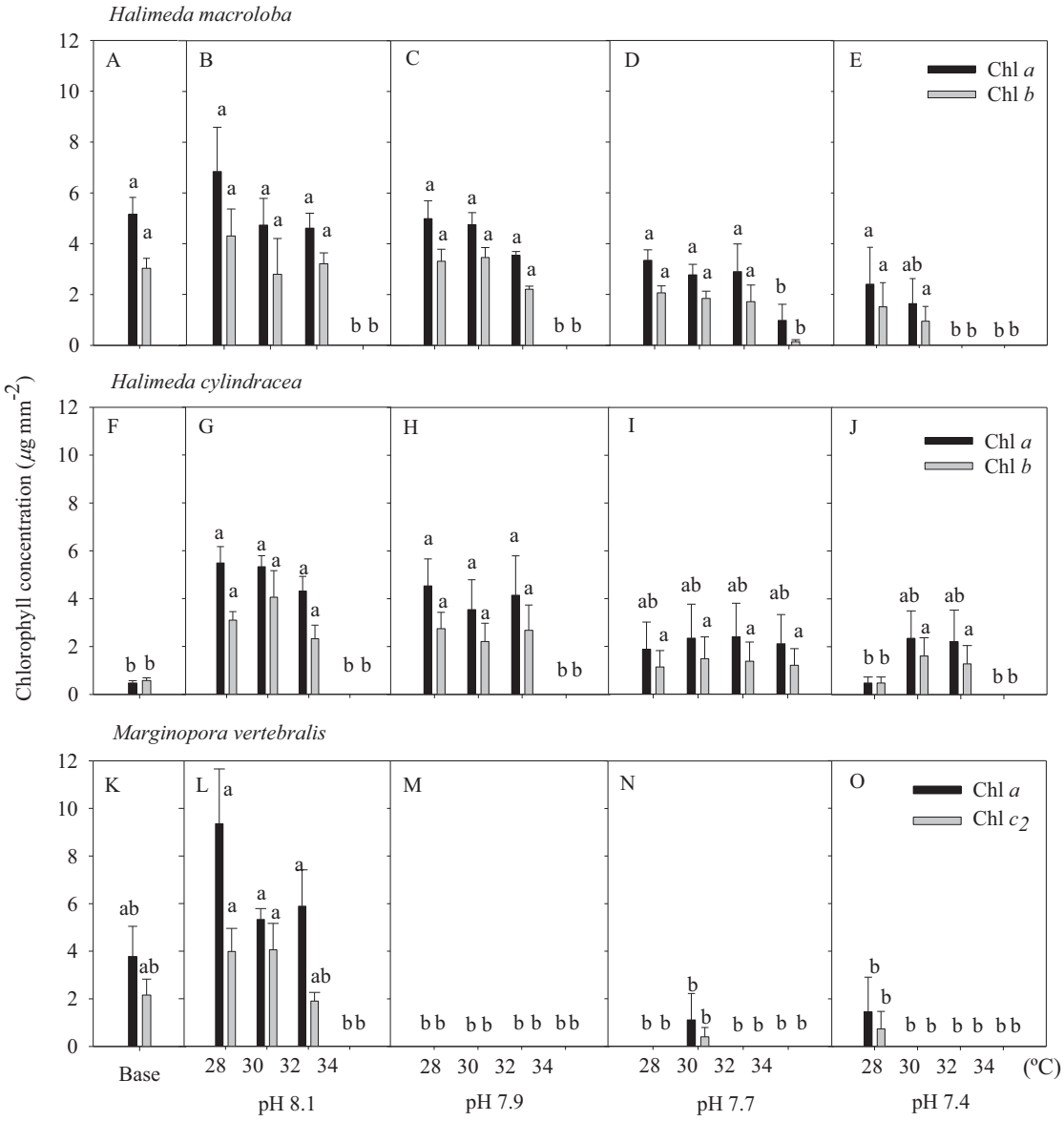

Figure 4.3: Chlorophyll *a* and *b* concentration (μg mm^{-2}) in (A-E) *H. macroloba* and (F-J) *H. cylindracea* and chlorophyll *a* and c_2 concentration (μg mm^{-2}) in (K-O) *M. vertebralis* at time zero (base) and each pH and temperature treatment at week 5. No bar indicates the absence of chlorophyll. Data represent means (n = 4, SEM).

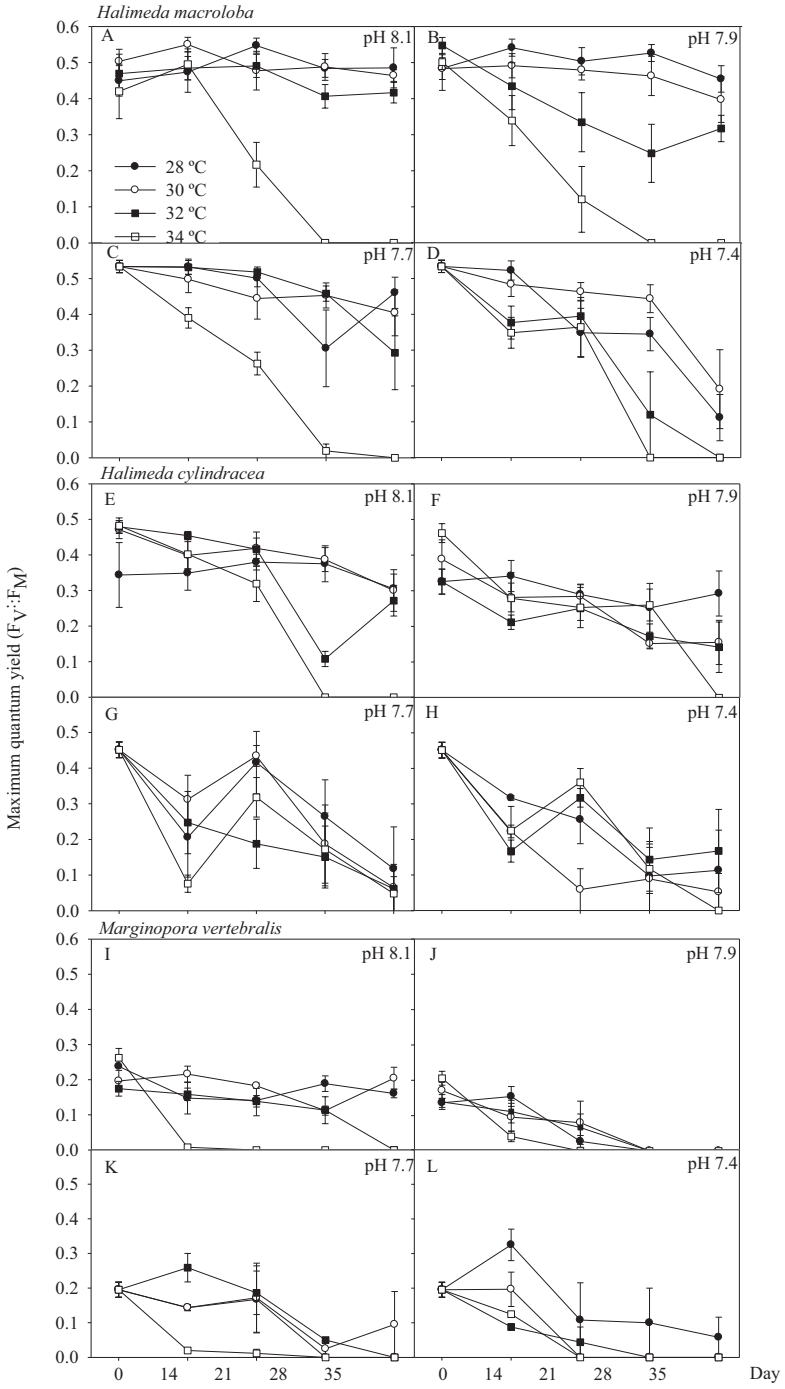

Figure 4.4: Maximum quantum yield (F_V:F_M) of (A-D) *H. macroloba*, (E-H) *H. cylindracea*, and (I-L) *M. vertebralis* in each pH and temperature treatment over the length of the experimental period. Data represent means (n = 4, SEM).

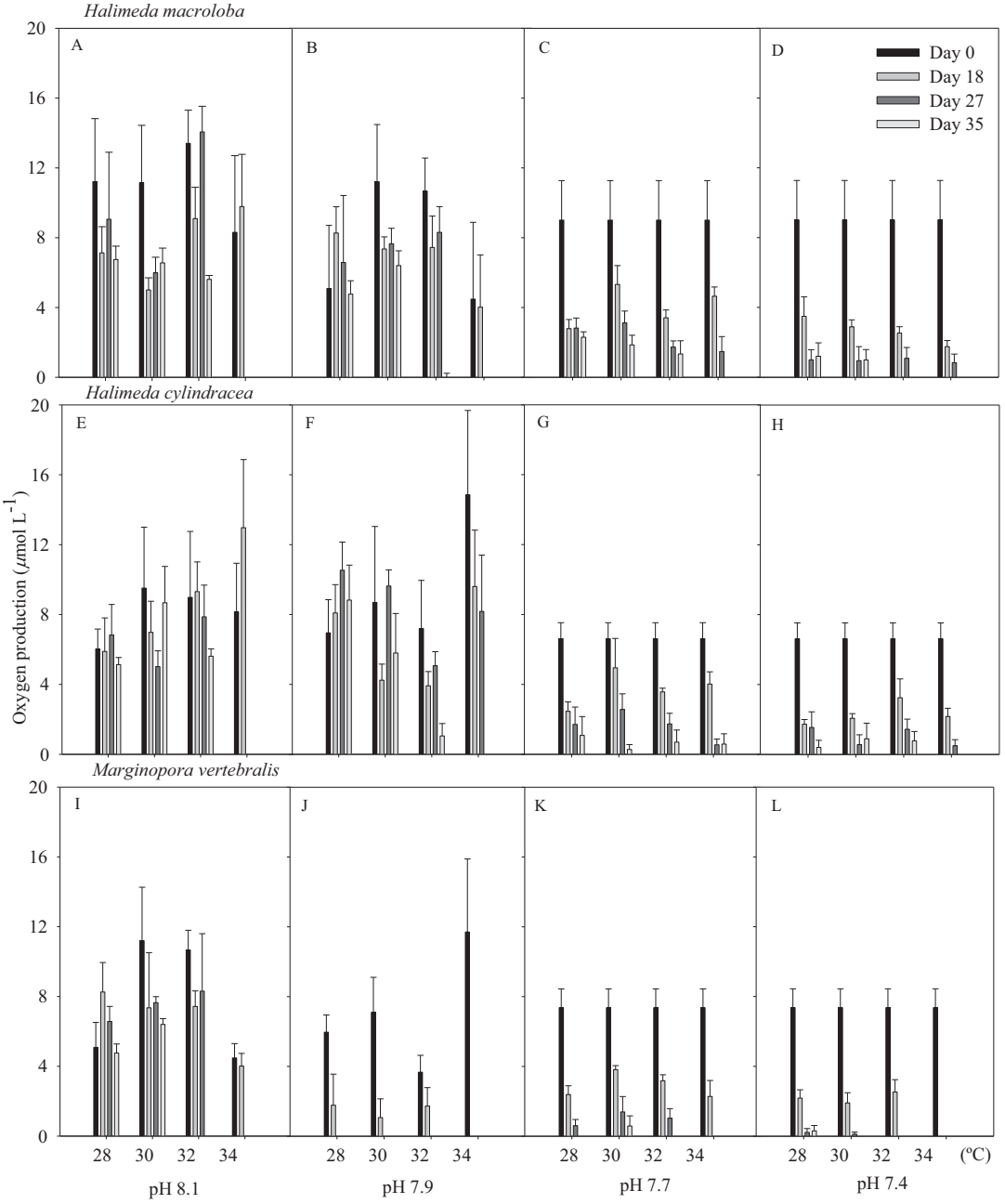

Figure 4.5: Oxygen production (μmol O_2 L^{-1}) in (A-D) *H. macroloba*, (E-H) *H. cylindracea*, and (I-L) *M. vertebralis* in each pH and temperature treatment over the length of the experimental period. Data represent means (n = 4, SEM).

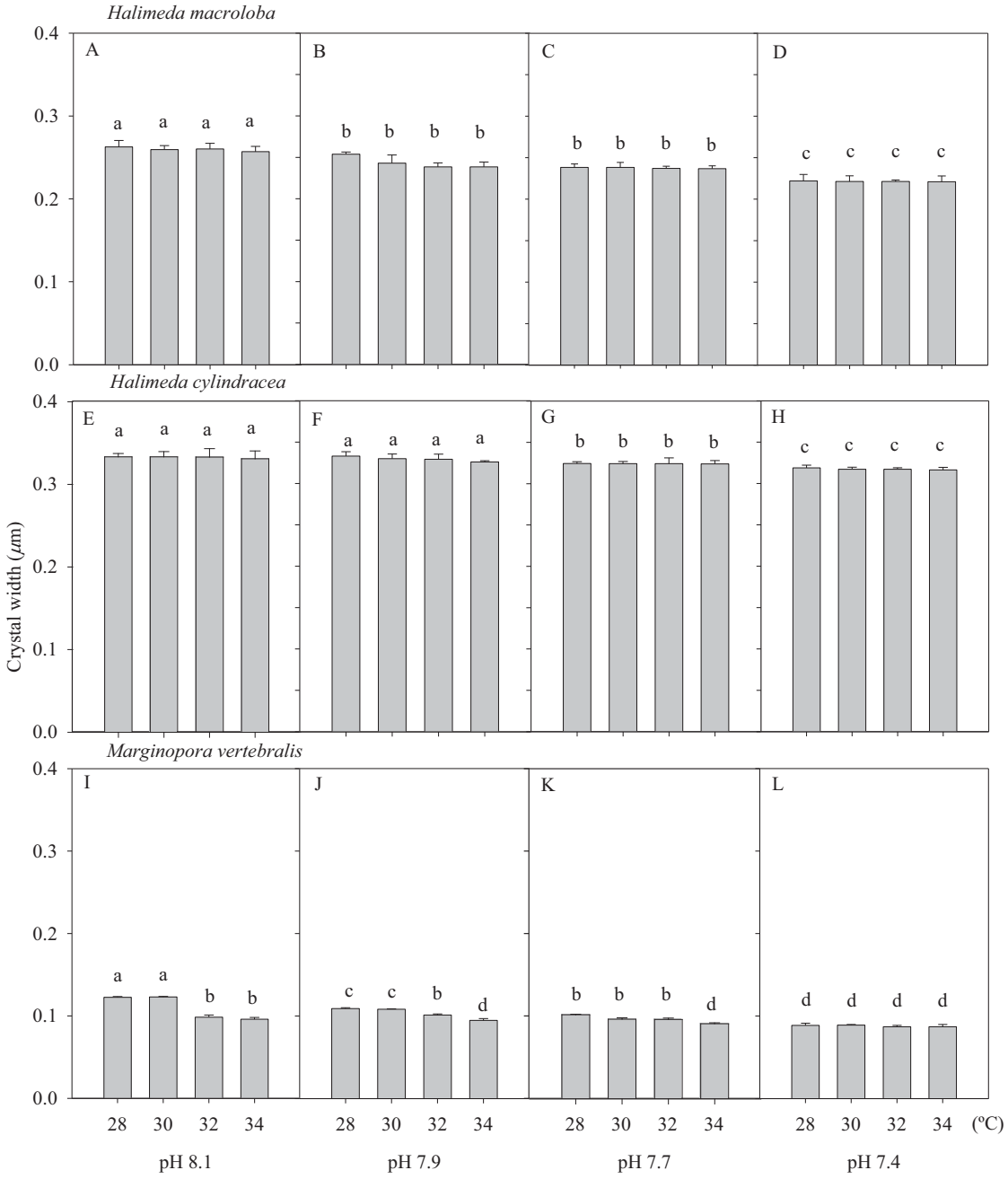

Figure 4.6: Crystal width (μm) in (A-D) *H. macroloba*, (E-H) *H. cylindracea*, and (I-L) *M. vertebralis* under pH and temperature conditions at the end of the 5th week. Data represent means (n = 4, SEM).

Halimeda macroloba

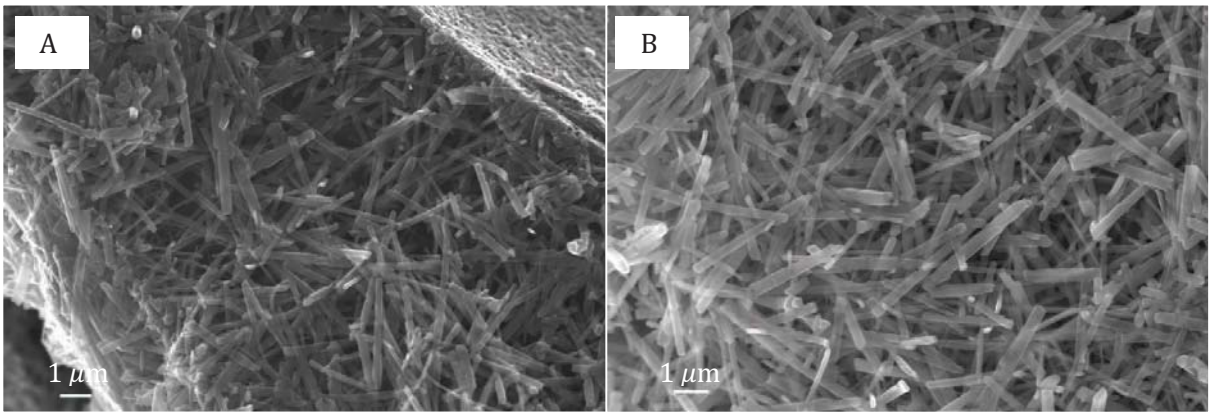

Halimeda cylindracea

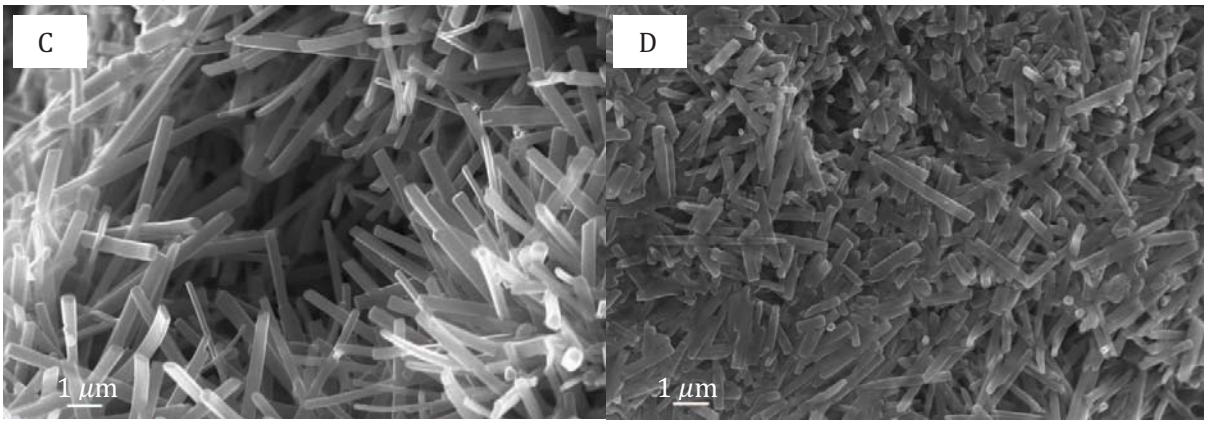

Marginopora vertebralis

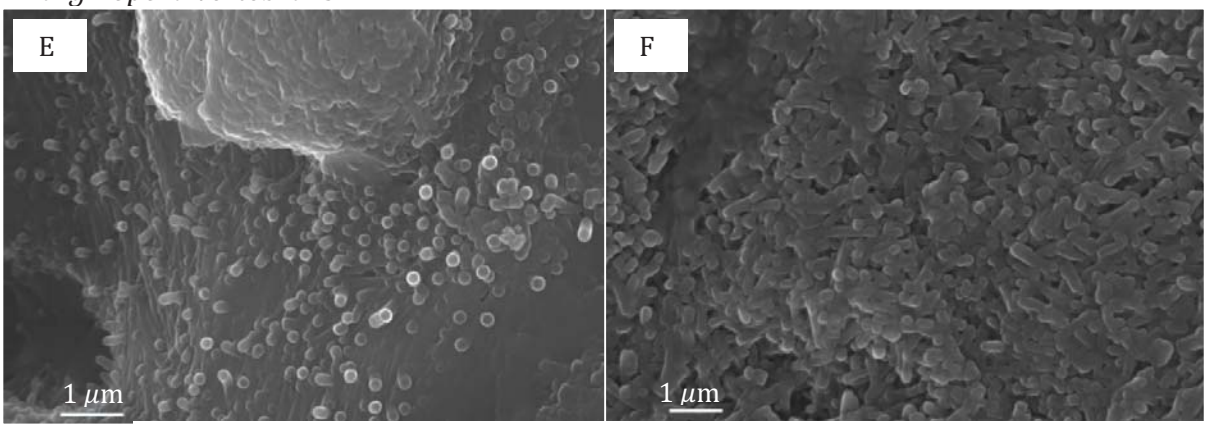

Control (pH 8.1, 28˚C) pH 7.4, 34˚C

Figure 4.7: SEM photographs of crystals in (A-D) *H. macroloba*, (E-H) *H. cylindracea*, and (I-L) *M. vertebralis* in control (pH 8.1, 28ºC) and pH 7.4, 34ºC treatment at the end of the 5th week.

4.4 DISCUSSION

This is the first investigation on the combined effects of elevated temperature and ocean acidification on photosynthesis and calcification in the photosynthetic marine calcifying algae *H. macroloba* and *H. cylindracea*, and the benthic symbiotic foraminifera *M. vertebralis*. As we hypothesised, the calcifying macroalga, *Halimeda* performed better than benthic foraminifera under high CO_2 conditions and the combined factors had a more detrimental (synergistic) effect on growth, photosynthesis and calcification in all species. Unexpectedly, elevated temperature and lowered pH (34ºC and pH 7.4) caused mortality in *H. macroloba* and *H. cylindracea* within 4 weeks and in *M. vertebralis* within 3 weeks. The causes of this mortality are likely due to damage to the symbionts, as indicated by changes in photosynthetic pigments, chlorophyll *a* fluorescence (F_V:F_M, Y(II)) and oxygen production. There was a decline in chlorophyll *a*, *b*, and c_2 concentrations in lower pH treatments (pH 7.7 and 7.4) after 5 weeks, indicative of chlorophyll degradation, decreased photosynthetic unit size and/or a decrease in the number of PSII reaction centers. There was also a significant decline in photosynthetic efficiency and primary production after 28 days of exposure to 32ºC and 34ºC, and pH 7.4 conditions in all three species (Figs. 4.4, 4.5). It is clear that elevated CO_2 and temperature conditions cause a reduction in the photosynthetic efficiency of PSII. Heat stress is likely to damage PSII, possibly by damaging the D1 protein and disrupting the thylakoid membrane stability (Allakhverdiev et al. 2008) while pH stress may disrupt the CO_2 accumulation pathway at the site of Rubisco or interfere with electron transport via the thylakoid proton gradients (Anthony et al. 2008).

Lower pH and higher temperature (all treatments except control pH and 28ºC, 30ºC) significantly triggered the bleaching and death of *M. vertebralis*. Symbiont expulsion is suggested to occur when the symbionts are damaged through photoinhibition (Hallock et al. 2006). Promotion of photooxidative reactions is likely under the stress conditions of pH and temperature applied here, through the degradation of D1 protein (Talge and Hallock 2003). Alternatively, the symbionts may be digested by the host when they are damaged (Hallock et al. 2006). Our results are consistent with the recent study of Talge

and Hallock (2003) which demonstrated that bleaching in the foraminifera *Amphistegina gibbosa* can be triggered by thermal stress.

Rising pCO_2 will inhibit calcification in calcifying organisms by decreasing the availability of CO_3^{2-} ions required for the deposition of calcium carbonate skeletons. However, in photosynthetic organisms (e.g., fleshy algae and seagrass), rising pCO_2 is expected to promote photosynthesis and hence enhance growth due to the greater abundance of substrate (CO_2) required for carbon fixation (Gao et al. 1993b; Short and Neckles 1999). Therefore the relationship between CO_2 abundance, photosynthesis and growth is dependent upon whether or not the organism calcifies.

This study demonstrated that increased CO_2 (yielding potentially more substrate available for carbon uptake) did not lead to increased production in any organisms, suggesting that the main effect was one of pH affecting the overall metabolism of the organisms.

There was however, a dramatic effect on calcification rates. Calcification rate was negative in *H. macroloba*, *H. cylindracea*, and *M. vertebralis* under the highest pCO_2 treatment, with high magnesium calcite species experiencing greater decline than aragonite forming species. The calcification rate of the control did not change over time. The application of heat caused increasingly negative calcification rates in all species, with *M. vertebralis* being most sensitive under all pCO_2 treatments at the highest temperature (pH 8.1, 7.9, 7.7, 7.4 and 34ºC; Fig. 4.1). The extreme CO_2 treatment of our experiments created the greatest reduction in CO_3^{2-} saturation state (to 1.23±0.15 for Ω_a and 1.84±0.16 for Ω_c; Table 4.1) which virtually prevented calcification in all three organisms and increased the potential for dissolution of the calcium carbonate structure. Increased temperature above the optimum temperature for these species will have a negative effect on calcification by decreasing enzyme activity and photosynthetic CO_2 fixation (Borowitzka 1986; Gonzalez-Mora et al. 2008). Thinner aragonite and calcite crystals were observed in the two *Halimeda* species when exposed to high pCO_2 (pH 7.7 and 7.4) and *M. vertebralis* when exposed to high pCO_2 and elevated temperature

conditions (pH 7.7, 7.4 and 32ºC and 34ºC) (Figs. 4.6, 4.7). Crystal density in *M. vertebralis* increased with higher pCO_2 and temperature levels (pH 7.9, 7.7, 7.4, and 32 and 34ºC), however, there was no change in calcium carbonate crystal abundance in *H. macroloba* and *H. cylindracea* at elevated pCO_2 and temperature conditions. Previous studies on *H. opuntia* and *H. tuna* that found a reduction in crystal width and increase in crystal abundance with decreasing pH, indicates that the crystallization may be initiated and terminated more frequently with increasing pCO_2 (Robbins et al. 2009). The decrease in crystal width and increase in crystal density in *M. vertebralis* in this study shows that calcification in this high-magnesium calcite species (*M. vertebralis*) is more sensitive to lower pH and higher temperature than in the aragonite forming species of *Halimeda* spp. This finding is consistent with the prediction of Kleypas et al. (1999) based on calcium carbonate saturation state where the saturating threshold is lowest in high-magnesium calcite depositing species.

Furthermore, photosynthetic marine calcifiers may experience conditions which reduce calcification rate, but enhance photosynthetic rate (e.g., low pH, high CO_2 availability). In this study, although rising pCO_2 resulted in an increase in dissolved CO_2 and HCO_3^{2-} availability (substrates for photosynthesis), the increase in these carbon species might be too small to promote photosynthesis and growth, but large enough to reduce calcification (Reynaud et al. 2003).

Exposure to elevated temperature (to 32ºC and 34ºC) alone or reduced pH (to pH 7.7 and 7.4) alone reduced photosynthesis and calcification in *H. macroloba, H. cylindracea,* and *M. vertebralis.* However, there was a strong synergistic effect of elevated temperature and reduced pH, with dramatic reductions in photosynthesis and calcification in all three species. It is suggested that rising temperature and pCO_2 can exceed the threshold for survival of these species. Subsequent mortality may be the cause of the reduce calcification and photosynthesis. A simultaneous reduction in pH and higher temperature will result in the greatest effect to these species. It is likely that the elevated temperature of 32ºC and the pCO_2 concentration of 101 Pa are the upper limit for survival of these species at our site of collection (Heron Island on the Great

Barrier Reef, Australia). However when taking into account the effects of high solar radiation (including ultraviolet light), this upper limit of survival may be an overestimate (i.e., the upper limit of survival may be below 32ºC and 101 Pa pCO_2) as Gao and Zheng (2010) showed that photosynthesis and calcification are dramatically reduced under high irradiance in combination with elevated CO_2 concentration.

Under the predicted climate change scenarios of rising ocean temperatures and ocean acidification, the vulnerability of calcifying algae and foraminifera is of great concern. With some predictions estimating that atmospheric CO_2 concentrations will reach 101 Pa by 2100 and 203 Pa by 2200 (Friedlingstein et al. 2006; Houghton 2009), and ocean temperature rise by 2-6°C over the next 100-200 years (Houghton 2009), the survival of these photosynthetic marine calcifiers is under threat. Furthermore, non-calcifying macroalgae which may benefit from near-future climate change scenarios (Gao et al. 1993b; Hobday et al. 2006), are expected to exhibit a competitive advantage over calcifying species (Fabry et al. 2008; Martin and Gattuso 2009). The loss of these calcifying keystone species will affect many other associated species such as fish communities in the future (Kleypas and Yates 2009). Consequent changes in community structure and habitat structure for many marine organisms could very well influence trophic interactions and habitat availability for other coral reef organisms. The loss of these sediment producing species will also reduce the sediment turnover rate and decrease the amount of carbonate sands in the marine environment.

CHAPTER 5:

MICROENVIRONMENTAL CHANGES SUPPORT EVIDENCE OF PHOTOSYNTHESIS AND CALCIFICATION INHIBITION IN *HALIMEDA* UNDER OCEAN ACIDIFICATION AND WARMING

5.0 MICROENVIRONMENTAL CHANGES SUPPORT EVIDENCE OF PHOTOSYNTHESIS AND CALCIFICATION INHIBITION IN *HALIMEDA* UNDER OCEAN ACIDIFICATION AND WARMING

All laboratory work, data collection, data analyses and write up were undertaken by me. Michael Kühl assisted with the microsensor set up.

5.1 INTRODUCTION

The anthropogenic use of fossil fuels, industrialization, deforestation and agricultural activities has raised the concentration of carbon dioxide (CO_2) in the atmosphere and increased CO_2 dissolution into the surface ocean (Gattuso and Lavigne 2009). This has stimulated global warming and more acidic conditions, i.e., a pH decrease in the ocean's surface layer. The latter affects the inorganic carbon speciation inducing further changes in seawater chemistry including a reduction in carbonate ion (CO_3^{2-}) abundance and a decreased aragonite saturation state (Feely et al. 2004) leading to a decrease in the capacity for marine calcifiers to produce their $CaCO_3$ skeleton (Diaz-Pulido et al. 2007; Fujita et al. 2011; Sinutok et al. 2011). Under such conditions, non calcifying macrophytes such as seagrasses and fleshy algae may therefore have benefits over calcifying algae, as evidenced in naturally high CO_2 regions, such as the volcanic vents off Ischia Island, Italy (Hall-Spencer et al. 2008). These studies point towards likely consequences of acidification for marine ecosystems and predict an expected reduction in calcifier diversity and abundance, which will result in significant changes to habitat structure and function (Gao et al. 1993b; Hall-Spencer et al. 2008; Kleypas and Yates 2009).

Halimeda is a sediment-dwelling, calcifying siphonalean green macroalga, which is widely distributed in tropical and subtropical marine environments, where it plays a major role as a carbonate sediment producer. In coral reef ecosystems, *Halimeda* is known to produce around 2.2 kg of $CaCO_3$ m^{-2} y^{-1}, which is equivalent to the rate of production by scleractinian corals (Smith and Kinsey 1976; Drew 1983). *Halimeda* thus

provides essential ecological services as a habitat forming bioengineer in these marine ecosystems (Drew 1983). The algal thallus consists of articulated, plate-like and calcified segments, which are joined together by small, uncalcified nodes forming branching chains (Blaxter et al. 1980). *Halimeda* precipitates $CaCO_3$ in the form of aragonite into the intercellular (utricular) space of its segments (Borowitzka et al. 1974; Borowitzka and Larkum 1977). New segments can be formed rapidly, involving a complex sequence of local decalcification, filament extension and chloroplast migration from old segments overnight, followed by onset of calcification (Larkum et al. 2011).

The current saturation state of aragonite, Ω_a, is 3.5-4.0 for the Pacific region and is expected to decline ~30 % by 2050 under predicted future climate scenarios (Kleypas et al. 1999; Guinotte et al. 2003). Elevated pCO_2 has previously been shown to reduce calcification, growth and productivity in the articulate coralline alga *Corallina pilulifera* and *C. officinalis* and crustose coralline algae (Kuffner et al. 2007; Anthony et al. 2008; Hofmann et al. 2012). Combined effects of elevated temperature and pCO_2 cause bleaching, calcium carbonate dissolution, and erosion in the reef-building corals *Acropora intermedia* and *Porites lobata* (Anthony et al. 2008). Recently, Sinutok et al. (2011) showed that pCO_2 levels representative of modelled climate scenarios for the years 2100 and 2200 (Houghton 2009) significantly reduced calcification and photosynthetic efficiency in *Halimeda*. Such impairment was attributed to lower seawater pH and reduced abundance of CO_3^{2-} as already shown by Borowitzka and Larkum (1976b), leading to a decline in calcification rate, calcium carbonate crystal size, photosynthetic pigment content (chlorophyll *a* and *b*) and photosynthetic efficiency. The decline of photosynthesis and calcification was amplified by concurrent exposure to elevated temperatures, i.e., 2-6°C above typical summer average seawater temperature. While bulk seawater characteristics had an obvious impact on photosynthesis and calcification, the microenvironmental conditions and regulatory mechanisms involved in such impairment of photosynthesis and calcification in *Halimeda* under elevated pCO_2 and temperature remain unknown.

Microsensors enable mapping of the physico-chemical microenvironment of marine calcifying organisms at high spatio-temporal resolution (De Beer and Larkum 2001; Al-Horani 2005; Köhler-Rink and Kühl 2005). Oxygen (O_2), carbon dioxide (CO_2), pH, and calcium (Ca^{2+}) microsensors have been used to study the photosynthesis and calcification in *Halimeda discoidea.* De Beer and Larkum (2001) showed that calcium dynamics and calcification in *H. discoidea* is determined by the pH at the segment surface and they hypothesized that acidification of seawater would decrease the calcification rate. Here, I investigate the effects of ocean acidification and ocean warming on the microenvironment and photosynthesis of *Halimeda* spp. using O_2 microsensors and chlorophyll *a* fluorometry and present the first data on how the microenvironment, photosynthesis and respiration of *Halimeda* is affected by changing pCO_2 and temperature conditions.

5.2 MATERIALS AND METHODS

5.2.1 Sample collection and experimental design

Halimeda macroloba and *Halimeda cylindracea* specimens (thallus length of 13-20 cm) were collected by hand from Heron Island reef flat (Southern Great Barrier Reef, Australia; 151º55'E, 23º27'S) at low tide at 0.3-m depth and maintained at the University of Technology, Sydney for 2 months in a 500 L aquarium with artificial seawater (26°C, pH 8.1, salinity of 33) under an incident irradiance (PAR, 400-700 nm) of 250 μmol photons m^{-2} s^{-1} over a 12h:12h light-dark cycle. Seawater concentrations of carbonate, calcium, nitrate and phosphate were maintained at 2.3, 10, <0.0016 and 0.0005 mM, respectively. Whole specimens of *Halimeda* were randomly allocated to one of four treatments (1 sample per tank, 4 tanks per treatment): i) control (pH 8.1 and 28°C; equivalent to current summer temperature average at Heron Island and a pCO_2 of 400 μatm), ii) elevated temperature only (pH 8.1 and 32°C), iii) reduced pH only (pH 7.7 and 28°C), and iv) a combination of both low pH and high temperature (pH 7.7 and 32°C). The elevated temperature and decreased pH treatments represent conditions predicted by current climate change models for the year 2100, equivalent to a 4°C

temperature rise and a pCO_2 concentration of 1200 µatm (Houghton 2009). Samples were ramped from 26°C and a pH of 8.1 to their treatment conditions over one week and were maintained for another four weeks in their treatments. pCO_2 and temperature were controlled using pH controllers (7020/2, Tunze, Germany) connected to CO_2 bubblers, and water thermostats (TC10, Teco, Italy), as described in Sinutok et al. (2011). Salinity was set at 33 and quantum irradiance (PAR) at the sample surface was 300 µmol photons m^{-2} s^{-1} on a 12:12 h light:dark cycle (light on at 0900 hrs and light off at 2100 hrs). The water quality was maintained identical to the holding tank with carbonate, calcium, nitrate and phosphate concentrations of 2.3, 10, <0.0016 and 0.0005 mM, respectively. Total alkalinity (TA) was measured weekly by titrating 30 g of seawater with 0.1 M HCl in an autotitrator (DL50, Mettler Toledo). The speciation of dissolved inorganic carbon (DIC) into CO_2, CO_3^{-2} and HCO_3^-, the CO_2 partial pressure (pCO_2), and the saturation state of seawater with respect to aragonite (Ω_a) were determined using CO2SYS (version 01.05; Brookhaven National Laboratory; Lewis and Wallace 1998). A summary of the TA, total inorganic carbon (DIC), DIC speciation, pCO_2, and Ω_a from each temperature (28°C, 32°C) and pH (8.1, 7.7) treatment is shown in Table 5.1.

5.2.2 Calcification

Whole specimen calcification rates were determined using the buoyant weight technique (Jokiel et al. 2008; Ries et al. 2009; Sinutok et al. 2011) with weight comparisons made between measurements at the start and end of the experimental period. The buoyant weight technique is a reliable measure of calcification by weighing each sample in seawater of known density and applying Archimedes' principle to compute the dry weight of the sample in the air (Jokiel et al. 1978; Langdon et al. 2010). Samples were placed on a glass Petri-dish hung below an electronic balance (AB204-S, Mettler Toledo, USA; accuracy ~0.1 mg) using nylon thread suspended in seawater.

5.2.3 Variable chlorophyll a fluorescence

Photosynthetic performance of *Halimeda* was quantified every 10 d over the duration of the experiment by variable chlorophyll fluorescence measurements using a 6 mm diameter fibre-optic probe connected to a Diving-PAM fluorometer (Walz, Germany). Photosystem II (PSII) photochemical efficiency was measured as the maximum quantum yield of PSII (F_V/F_M) at 0900 hrs (before lights were turned on) and the effective quantum yield ($\Delta F/F_M'$) at 1300 hrs, after which the maximum excitation pressure over photosystem II (Q_m) was calculated. The parameter Q_m quantifies non-photochemical quenching and is defined as $Q_m = 1 - (\Delta F/F_M')/(F_V/F_M)$ according to Iglesias-Prieto et al. (2004).

5.2.4 Photosynthetic pigment concentration

Concentrations of chlorophyll (Chl) *a* and *b* were determined in extracts of *Halimeda* samples using the spectrophotometric method of Ritchie (2008) at the beginning and end of the 5 week experiment, and expressed in μg Chl g^{-1} fresh weight (fw) of *Halimeda*. Chl *a* and *b* were extracted by grinding samples in 4 ml of 90% acetone at 4°C followed by extraction in darkness for 24 hours. Subsequently, samples were centrifuged at 1500 *g* for 10 mins, after which the supernatant was transferred to a quartz cuvette and its absorbance measured at 647 and 664 nm on a spectrophotometer (Cary 50, Varian, Australia).

5.2.5 Oxygen microsensors

Microsensor measurements of O_2 concentration were performed in a 2 l flow chamber as described by Köhler-Rink and Kühl (2000) at the start of the experiment, and after 3 and 5 weeks. Segments of *H. macroloba* (0.8-1.2 cm long) and *H. cylindracea* (1.5-2.0 cm long) from the treatment tanks were placed on the bottom of the chamber, with a water flow of 2.5 cm s^{-1} maintained by a submersible aquarium pump.

Table 5.1 Parameters of the carbonate system; total alkalinity (TA), CO_2 partial pressure (pCO_2), dissolved inorganic carbon species (DIC; CO_2, CO_3^{-2}, HCO_3^-), total DIC, and saturation state of seawater with respect to aragonite (Ω_a) from each pH (8.1, 7.7) and temperature (28ºC, 32ºC) treatment used in this study. Data represent means (n = 3, ± S.E.).

Treatment		TA	pCO_2	CO_2	CO_3^{-2}	HCO_3^-	DIC	Ω_a
pH	Temp (ºC)	(mmol kg^{-1})	(µatm)	(mmol kg^{-1})	(mmol kg^{-1})	(mmol kg^{-1})	(mmol kg^{-1})	
8.1	28	2.327±0.002	380.8±0.4	0.010±0.001	0.239±0.024	1.745±0.020	1.993±0.020	3.87±0.01
8.1	32	2.326±0.036	444.9±7.4	0.010±0.002	0.239±0.039	1.742±0.030	1.881±0.033	3.97±0.07
7.7	28	2.512±0.030	1208.1±14.6	0.032±0.004	0.122±0.015	2.219±0.027	2.373±0.028	1.97±0.02
7.7	32	2.508±0.015	1394.2±8.6	0.034±0.002	0.123±0.007	2.212±0.014	2.369±0.014	2.05±0.01

The thallus surface O_2 concentration and rate of O_2 production was determined under quantum irradiances of 0, 80, 150, 230, 570, and 900 µmol photons m^{-2} s^{-1}, as controlled by a fibre optic halogen lamp (KL-2500, Schott, Germany) equipped with a collimating lens and a heat filter. The O_2 microsensor was mounted on a motorized micromanipulator (Oriel Encoder Mike, United States) which, along with data acquisition, was regulated by Profix software (Pyro-Science, Denmark).

Oxygen concentration profiles and the rate of gross photosynthetic O_2 production were measured at the surface (0 to 300 µm) of *H. macroloba* and *H. cylindracea* using an O_2 microelectrode (OX-100, Unisense, Denmark) connected to a picoammeter (PA2000, Unisense, Denmark) and a strip chart recorder (BD12E, Kipp&Zonen, The Netherlands). The microelectrode had an outer tip diameter of 100 µm, a 90% response time of <8 s, and a stirring sensitivity of <1.5%. A linear calibration of the microelectrode was performed at chamber temperature in air-saturated seawater and O_2-free seawater (made anoxic by addition of sodium dithionite). A proxy for gross photosynthesis (P_y; nmol O_2 cm^{-3} s^{-1}) at the specimen surface of *Halimeda* spp. was estimated after a short experimental light-dark shift by measuring the rate of O_2 depletion over the first 10 s after darkening (Revsbech et al. 1981; Köhler-Rink and Kühl 2000). According to the limitation of microsensor response time (<8 s), the gross photosynthesis from this measurement is underestimated and represents an integral over a large sample volume, however it can still be used to compare between treatments.

The local diffusive O_2 flux (J; nmol O_2 cm^{-2} s^{-1}), i.e., the O_2 uptake rate in darkness and the net O_2 production rate in light, was calculated from measured steady-state O_2 concentration profiles by Fick's first law (Köhler-Rink and Kühl 2000): $J = -D_0 (dC/dz)$ where D_0 is the molecular diffusion coefficient in seawater at experimental salinity and temperature, and dC/dz is the linear slope of the O_2 concentration profile in the diffusive boundary layer (DBL) above the *Halimeda* thallus surface. I note that the presence of the microsensor above the *Halimeda* thallus can compress the diffusive boundary layer leading to a locally accelerated flow around the microsensor tip (Glud et al. 1995).

However, as flow conditions were identical between treatments, diffusive fluxes can still be compared.

5.2.6 Statistical analysis

To identify significant differences ($\alpha = 0.05$) among treatments in calcification, Chl *a* and *b* concentration, a series of one-way and two-way analysis of variance (ANOVA) tests were performed (SPSS v17). To determine significant differences among treatments and over time in chlorophyll fluorescence parameters (F_V/F_M, $\Delta F/F_M'$, Q_m), O_2 concentration at the thallus surface, diffusive O_2 flux, and proxy gross photosynthesis, mixed-design factorial ANOVA tests, with pH and temperature as between-subject independent variables and time as a within-subject independent variable (repeated measures factor) were performed. Tukey's Honestly Significant Difference post hoc tests were used to identify statistically distinct groups. If data did not meet the assumptions of normality (Kolmogorov-Smirnov test) and equal variance (Levene's test), the data were transformed using $\log_{10}$ or square root.

5.3 RESULTS

5.3.1 Calcification rate

The calcification rates of *H. macroloba* and *H. cylindracea* were slightly positive in the control (pH 8.1, 28ºC; <0.5% increase per day; Table 5.2) and the elevated temperature treatment (pH 8.1, 32ºC; <0.3% per day), but were negative in the elevated pCO_2 treatments both at control and elevated temperature (pH 7.7, 28ºC and pH 7.7, 32ºC; -0.2 to -1.6% per day; Table 5.2). *H. macroloba* and *H. cylindracea* had significantly lower calcification in the reduced pH treatments at both 28ºC and 32ºC than in the control treatment ($P = 0.003$ and $P < 0.001$, respectively; Table 5.2). The calcification rate of *H. macroloba* in the elevated CO_2 and elevated temperature treatment was not significantly different from calcification in *H. cylindracea* in the same treatment ($P > 0.05$).

Table 5.2 Calcification rate (% increase day^{-1}) and chlorophyll (Chl) *a* and *b* concentration (μg g^{-1} fw) of *Halimeda macroloba* and *Halimeda cylindracea* after 5 weeks in each pH and temperature treatment. Data represent means (n = 4, mean ± S.E.). * signifies $P < 0.05$.

	Calcification rate (% per day)	Chl *a* (μg g^{-1} fw)	Chl *b* (μg g^{-1} fw)
H. macroloba			
Time 0	-	42.1±5.8	24.5±3.0
pH 8.1, 28ºC	0.45±0.07	45.8±5.1	32.5±3.8
pH 8.1, 32ºC	0.26±0.14	39.4±3.6	24.5±2.7
pH 7.7, 28ºC	-0.51±0.16	28.5±2.1	18.2±2.5
pH 7.7, 32ºC	-1.57±0.71	29.7±2.5	20.8±3.6
P value			
- pH	0.003*	0.005*	0.012*
- Temperature	0.123	0.529	0.412
- pH*Temperature	0.269	0.374	0.115
H. cylindracea			
Time 0	-	43.6±3.3	28.9±1.7
pH 8.1, 28ºC	0.38±0.14	43.3±2.5	24.1±2.3
pH 8.1, 32ºC	0.26±0.18	34.5±1.3	21.3±2.1
pH 7.7, 28ºC	-0.29±0.08	29.4±1.2	17.3±2.7
pH 7.7, 32ºC	-0.31±0.04	26.2±0.7	16.0±1.9
P value			
- pH	<0.001*	<0.001*	0.014*
- Temperature	0.586	0.011*	0.375
- pH*Temperature	0.697	0.189	0.732

5.3.2 Photosynthetic pigment concentration

Initial Chl *a* and *b* concentrations were 42.1 ± 5.8 and 24.5 ± 3.0 μg g^{-1} (mean ± SE) in *H. macroloba* and 43.6 ± 3.3 and 28.9 ± 1.7 μg g^{-1} (mean ± SE) in *H. cylindracea*, respectively (Table 5.2). After 5 weeks, there were no significant changes in Chl *a* and *b* concentration in *H. macroloba* in the control (pH 8.1, 28ºC; $P = 0.651$ for Chl *a*; $P = 0.151$ for Chl *b*) and elevated temperature treatments (pH 8.1, 32ºC; $P = 0.788$ for Chl *a*; $P = 0.997$ for Chl *b*) or in the control treatment for *H. cylindracea* (pH 8.1, 28ºC; $P = 0.946$ for Chl *a*; $P = 0.146$ for Chl *b*). In *H. cylindracea* at pH 8.1, 32ºC, Chl *a* concentration significantly declined to 34.5 ± 1.3 μg g^{-1} (mean ± SE; $P < 0.046$),

whereas there were no significant changes in Chl *b* concentration ($P > 0.05$; Table 5.2). The Chl *a* and *b* concentration in *H. macroloba* and *H. cylindracea* significantly declined at pH 7.7 within the 28 and 32ºC treatment ($P < 0.05$; Table 5.2).

5.3.3 Variable chlorophyll fluorescence

The maximum quantum yield (F_V/F_M), effective quantum yield ($\Delta F/F_M'$) and maximum excitation pressure on PSII (Q_m) in the control treatment remained constant over the experimental period in both species of *Halimeda*, ranging between 0.73-0.79, 0.70-0.77, and 0.01-0.08, respectively ($P > 0.05$; Fig. 5.1a, d). There was, however, a significant decrease (50-70%) in F_V/F_M and $\Delta F/F_M'$ in *H. macroloba* and *H. cylindracea* at week 5 under elevated CO_2 and temperature treatments (pH 8.1, 32ºC, pH 7.7, 28ºC and pH 7.7, 32ºC; $P < 0.001$; Fig. 5.1a-b, d-e). Both *Halimeda* species under elevated CO_2 and temperature showed very large Q_m values (0.2-0.6) at week 5. At this time, *H. macroloba* exhibited significantly higher Q_m values under elevated CO_2 in both temperature treatments ($P < 0.022$; Fig. 5.1c), whereas *H. cylindracea* showed significantly higher Q_m values in all treatments except the control ($P < 0.038$; Fig. 5.1f).

5.3.4 O_2 microenvironment

Oxygen concentration profiles measured towards the thallus surface of *H. macroloba* and *H. cylindracea* were affected by irradiance, pCO_2, temperature, and time of exposure to elevated pCO_2 and temperature ($P < 0.05$; Figs. 5.2-5.4). Initially, in all light treatments, the O_2 concentration surpassed the ambient O_2 concentration in the surrounding water (209 µM) at the upper boundary of the diffusive boundary layer ~150 µm above the *H. macroloba* segment surface, and reached an O_2 concentration of 277-306 µM at the segment surface (Fig. 5.2a). In the dark, the ambient O_2 concentration decreased from 209 µM at 150 µm above the *H. macroloba* segment to 117 µM at the segment surface (Fig. 5.2a). The O_2 concentration at the segment surface in all light treatments was higher compared to when in darkness ($P < 0.001$; Fig. 5.2a).

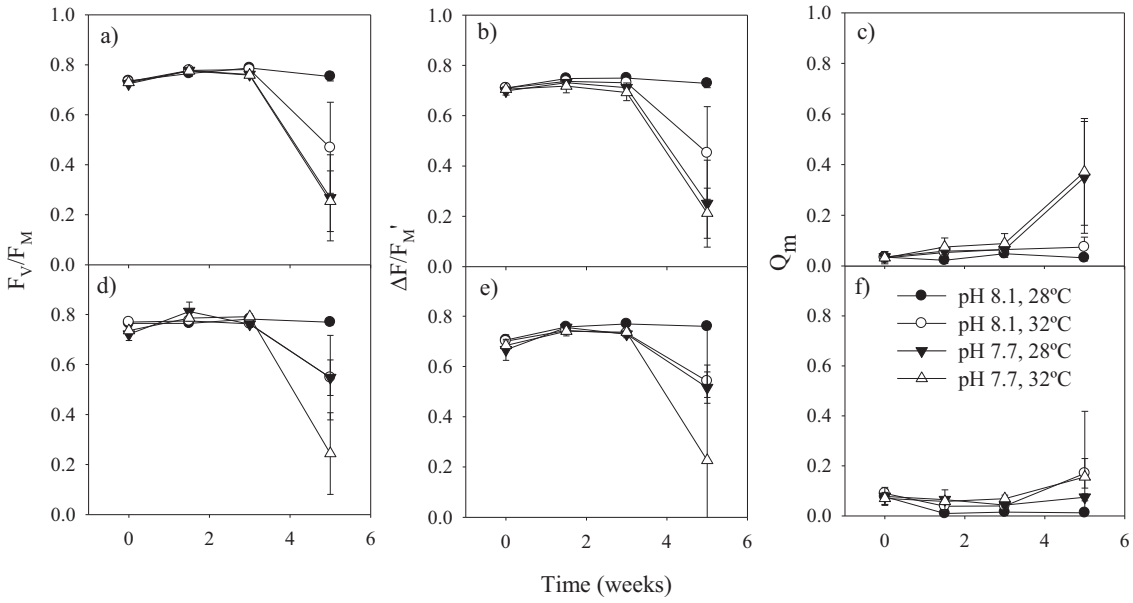

Figure 5.1 Maximum quantum yield (F_V/F_M), effective quantum yield ($\Delta F/F_M'$), and maximum excitation pressure over photosystem II (Q_m) of a-c *Halimeda macroloba* and d-f *Halimeda cylindracea* in each pH and temperature treatment over the length of the experimental period. Data represent means (n = 4, ± SE).

After 3 and 5 weeks, the O_2 concentration profiles in *H. macroloba* showed different responses in each pH and temperature treatment (Fig. 5.3a-h). O_2 concentration at segment surface changed over time and between pH and temperature treatments (P < 0.001; Fig. 5.2a, 5.3a-h). After 3 weeks, the control treatment of *H. macroloba* showed an increasing O_2 concentration at the segment surface reaching ~230-330 µM in all light treatments and a decrease in O_2 concentration to 202 µM under dark conditions (Fig. 5.3a). Significant increases in segment surface O_2 concentration were found in the pH 8.1, 32ºC treatment reaching 333-461 µM at all irradiance levels (P < 0.001), whereas segment surface O_2 concentration significantly decreased to 180 µM in the dark (P < 0.001; Fig. 5.3b). There were significant decreases in segment surface O_2 concentration in the pH 7.7, 28ºC treatment at 570 and 900 µmol photons m^{-2} s^{-1} (P < 0.001; Fig. 5.3c). After 5 weeks, the pH 8.1, 32ºC treatment showed no significant changes in O_2

concentration at the segment surface ($P > 0.05$; Fig. 5.3f). Similar observations were seen at pH 7.7 and both temperature treatments at 3 and 5 weeks in *H. macroloba* (Fig. 5.3c-d, g-h).

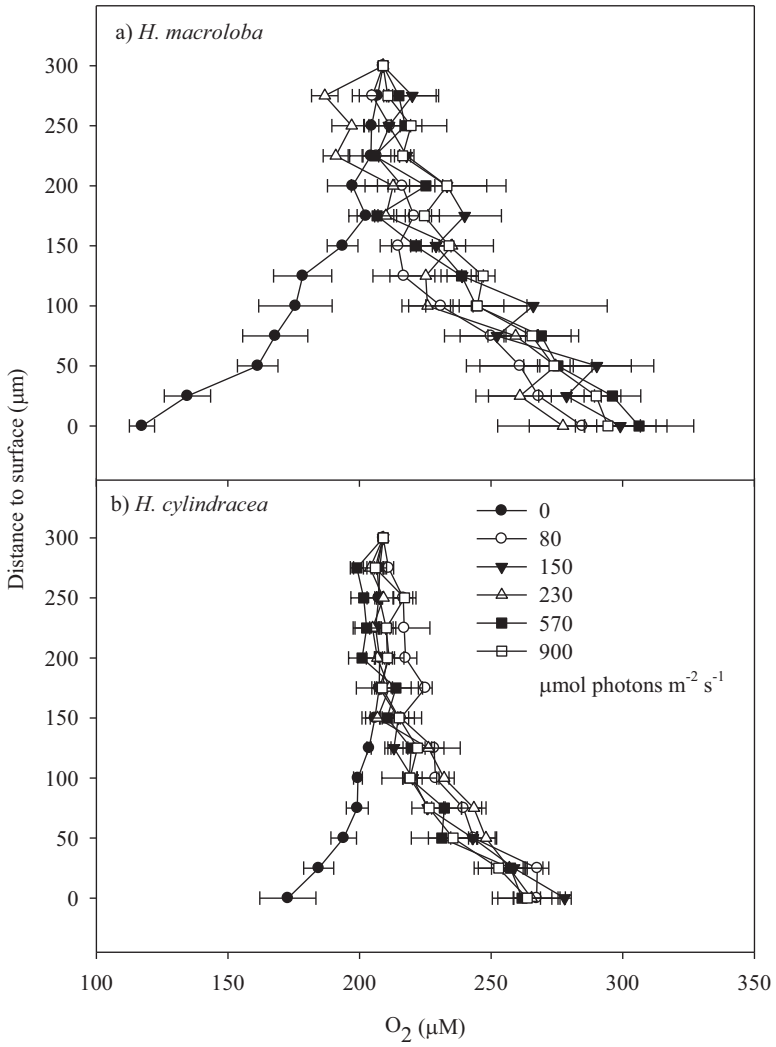

Figure 5.2: Oxygen concentration profile towards the thallus surface measured at week 1 from a) *Halimeda macroloba* and b) *Halimeda cylindracea* at each experimental irradiance (0, 80, 150, 230, 570 and 900 µmol photons m^{-2} s^{-1}). Data represent means (n = 4, ± SE).

In *H. cylindracea* at the start of the experiment, the ambient O_2 concentration increased from 209 μM at 125 μm above the segment to 260-277 μM at the segment surface when in light. A decrease to 172 μM was found at the tissue surface when in darkness (Fig. 5.2b). There were significant changes in O_2 concentration at shell surface over time and between pH and temperature treatments ($P < 0.001$; Fig. 5.2b, 5.4a-h). At 3 weeks, *H. cylindracea* in the control treatment and pH 8.1, 32ºC treatment, a significant increase in O_2 concentration was found when reaching the segment surface at about 265-580 and 336-400 μM, respectively, in all light treatments ($P < 0.001$; Fig. 5.4a-b). In addition, a significant decrease in O_2 concentration was found when reaching the segment surface at about 128 and 184 μM in darkness, respectively ($P < 0.001$; Fig. 5.4a-b). No significant changes in O_2 concentration at the segment surface were observed at 3 and 5 weeks at pH 7.7 in both temperature treatments and at 5 weeks in the pH 8.1, 32ºC treatment ($P > 0.05$; Fig. 5.4c-d, f-h).

5.3.5 Gross photosynthesis and O_2 flux

Estimated rates of gross photosynthesis and O_2 flux, i.e., net photosynthesis, of both *Halimeda* species were influenced by CO_2 and time of exposure to elevated CO_2 and temperature ($P < 0.001$; Figs. 5.5-5.6). In *H. macroloba*, gross photosynthesis decreased with elevated pCO_2 (pH 7.7 at both temperatures; $P < 0.001$; Fig. 5.5a) and long term exposure (5 weeks) to elevated pCO_2 and temperature ($P < 0.001$; Fig. 5.5b). Gross photosynthesis in *H. cylindracea* also declined at week 5 at pH 7.7 at 28 and 32°C ($P < 0.001$; Fig. 5.5d).

After 3 weeks, a significant decrease in the rate of O_2 efflux in light was observed in both species under elevated CO_2 conditions (pH 7.7, at both temperatures; $P < 0.001$; Fig 6a, c). After 5 weeks, the rate of O_2 efflux in both species decreased under elevated CO_2 treatments (pH 7.7, at both temperatures for 70-80% ($P < 0.001$; Fig. 5.6b, d).

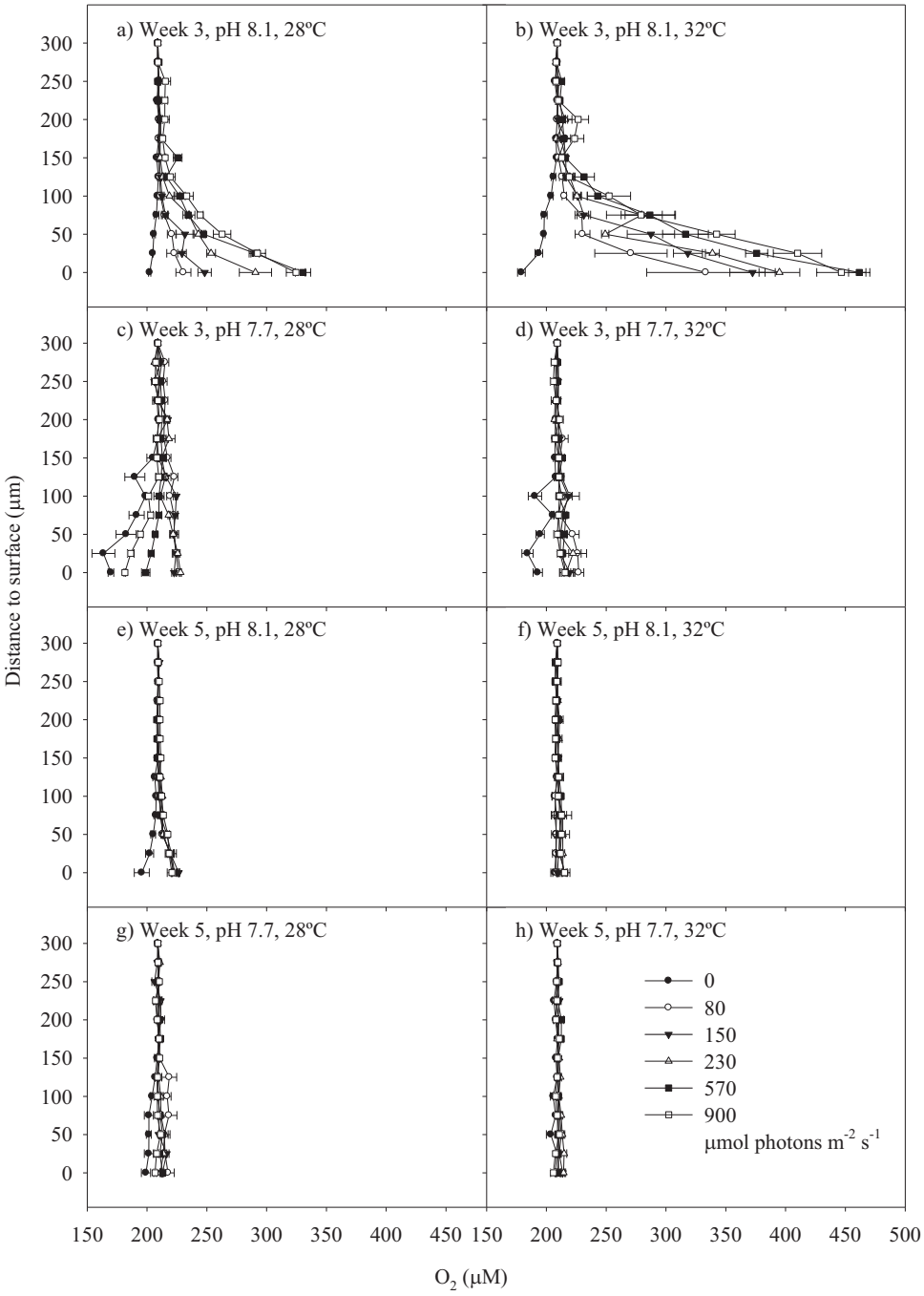

Figure 5.3: Oxygen concentration profile towards the thallus surface measured at a-d week 3 and e-h week 5 from *Halimeda macroloba* at each pH and temperature treatment

at each experimental irradiance (0, 80, 150, 230, 570, and 900 µmol photons m^{-2} s^{-1}). Data represent means (n = 4, ± SE).

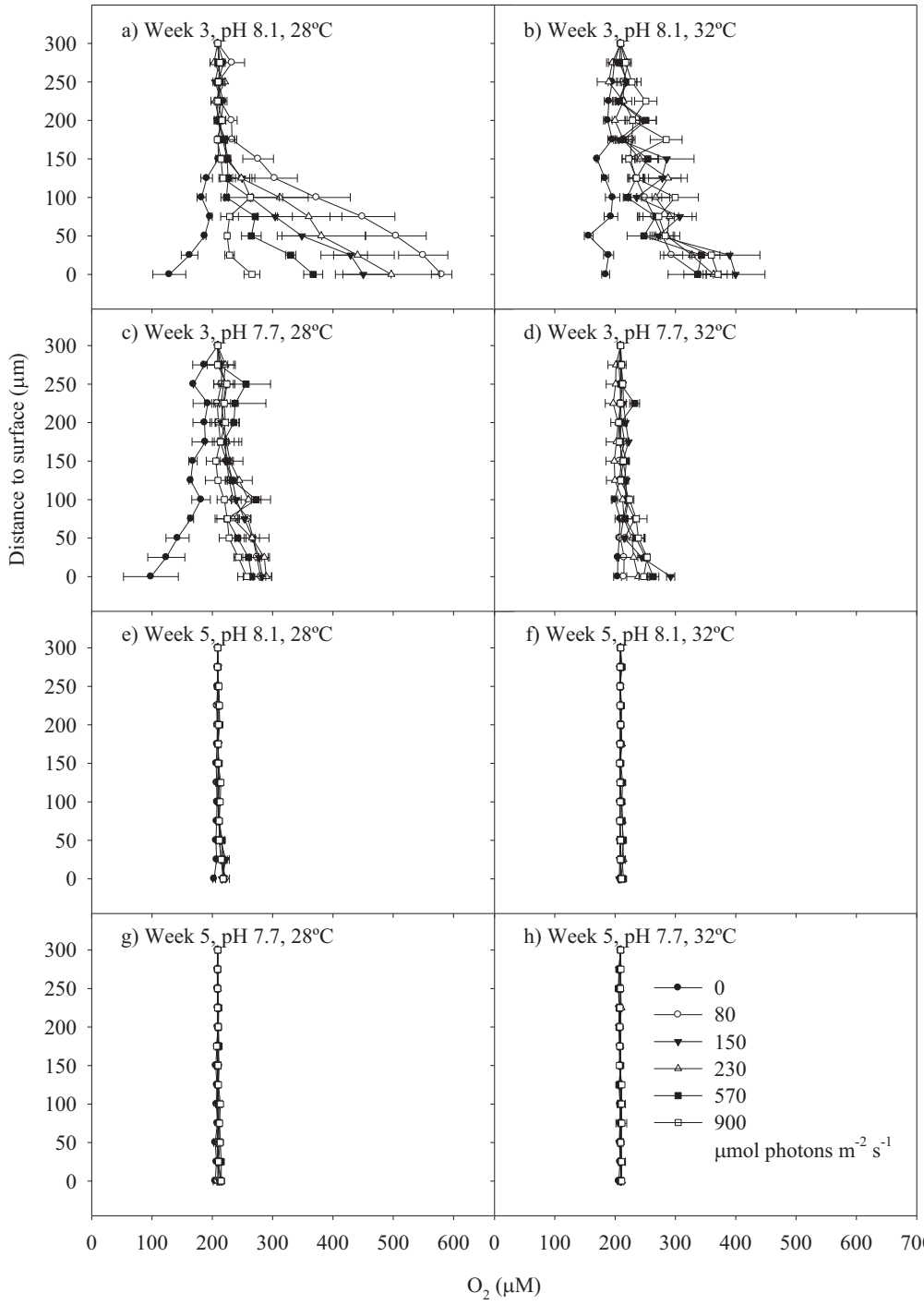

Figure 5.4: Oxygen concentration profile towards the thallus surface measured at a-d week 3 and e-h week 5 from *Halimeda cylindracea* at each experimental pH and temperature treatment at each irradiance (0, 80, 150, 230, 570, and 900 µmol photons m^{-2} s^{-1}). Data represent means (n = 4, ± SE).

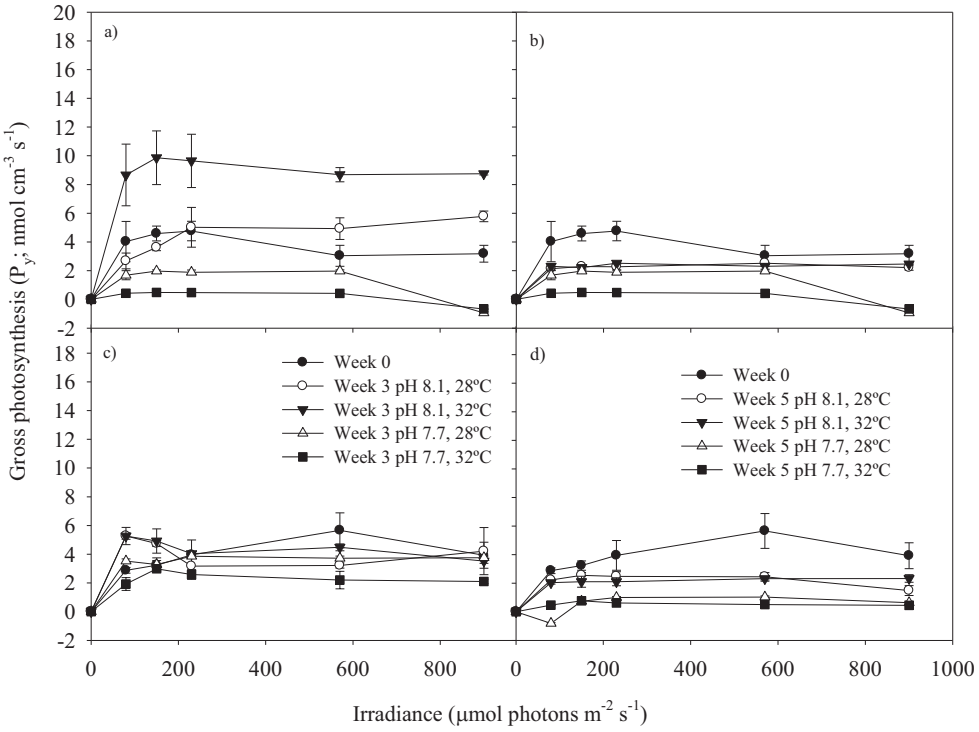

Figure 5.5: Gross photosynthesis estimates (P_y; nmol O_2 cm^{-3} s^{-1}) at the thallus surface measured at week 1, 3 and 5 from a-b *Halimeda macroloba* and c-d *Halimeda cylindracea* in each pH and temperature treatment. Data represent means (n = 4, ± SE).

5.4 DISCUSSION

Previous application of pH and O_2 microsensors have demonstrated their ability to resolve the dynamic microenvironment of calcifying reef algae, corals and foraminifera at high spatio-temporal resolution (e.g., De Beer and Larkum 2001; Al-Horani 2005; Köhler-Rink and Kühl 2005) but this is the first study to investigate the combined effects of elevated temperature and pCO_2 on the O_2 microenvironment of *Halimeda.*

These results showed strong effects of elevated temperature and pCO_2 on the microenvironment around the segments of two *Halimeda* species, as well as strong reductions in physiological performance.

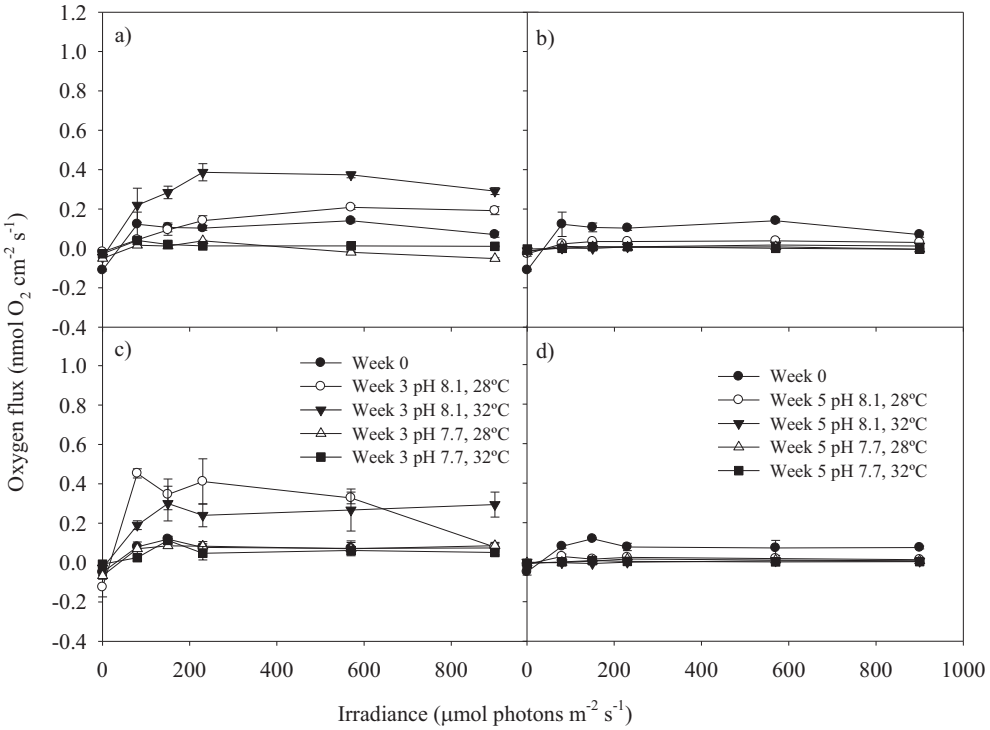

Figure 5.6: Diffusive O_2 flux (nmol O_2 cm^{-2} s^{-1}) at the thallus surface measured at week 1, 3 and 5 from a-b *Halimeda macroloba* and c-d *Halimeda cylindracea* in each pH and temperature treatment. Data represent means (n = 4, ± SE).

5.4.1 Temporal changes in productivity in response to ocean acidification and ocean warming

In the control treatment, over the length of the 5 week experiment, there was net O_2 production in the light, which was reversed in darkness due to respiration. Short-term exposure (3 weeks) to elevated temperature (32ºC) and current pCO_2 (400 µatm) increased the productivity of both species, with increasing O_2 concentration and O_2 flux at the segment surface and increasing gross photosynthesis, while long-term exposure (5

weeks) to elevated temperature led to a decrease in the productivity of both species. These observations are consistent with a previous study, where high O_2 production was found after short-term (18 days) exposure to elevated temperature, while long-term exposure (35 days) resulted in decreased productivity and metabolism in these species (Sinutok et al. 2011). Although short-term exposure to elevated temperature (32ºC) may lead to increasing productivity and metabolism in this species, however, 32ºC was found to be an upper limit for survival in these species. Exposure to 32ºC for 5 weeks may damage PSII, possibly by damaging the D1 protein and disrupting the thylakoid membrane stability (Allakhverdiev et al. 2008). This suggests that the acclimation for thermal stress is limited. After 3 and 5 weeks under elevated CO_2 and temperature, the rate of O_2 consumption in darkness and net O_2 production in light decreased even further. This suggests that ocean acidification compounds the reduction in photosynthetic activity and elevated photoinhibition under temperature stress.

5.4.2 Ocean acidification is more influential than ocean warming in reducing *Halimeda* productivity

Although the CO_2 uptake during photosynthesis is mainly occurred at the cell wall surface facing into the intercellular space (Borowitzka and Larkum 1976b), De Beer and Larkum (2001) observed that photosynthetic CO_2 uptake in *Halimeda* leads to an increase in extracellular pH at the thallus surface, whereas CO_2 and H^+ production from respiration and calcification leads to a decrease in pH. This study showed that elevated CO_2 conditions, and thus increased availability for carbon uptake, did not lead to increased O_2 production in these species, suggesting that pH may be the main factor inhibiting metabolism of *Halimeda*. A reduction in pH may disrupt the CO_2 accumulation pathway at the site of Rubisco or disrupt electron transport via the thylakoid proton gradients (Anthony et al. 2008). A reduction in photosynthesis due to these stressors will consequently have an impact on calcification due to the loss of elevated intracellular pH at the site of calcification.

Calcification is promoted under high pH conditions, as the speciation of dissolved inorganic carbon is favoured towards carbonate (Table 5.1), which was clearly shown in Borowitzka and Larkum (1976b). Therefore, any alterations of intracellular pH will influence calcification rate. Reduced pH as a direct consequence of ocean acidification as well as through the inhibition of photosynthesis are therefore likely to slow the rate of calcification (Borowitzka and Larkum 1976b; De Beer and Larkum 2001). Rising CO_2 will inhibit calcification by decreasing the availability of CO_3^{2-} ions required for calcium carbonate precipitation (De Beer and Larkum 2001; Feely et al. 2004; Ries 2011a,b). Although pH seems the main factor affecting *Halimeda* species and elevated temperature leads to an increase in aragonite saturation state (less solubility of $CaCO_3$) as shown in Table 1 (Weyl 1959), heat stress also has an impact on their PSII photochemical efficiency (Warner et al. 1999; Hill et al. 2004; Sinutok et al. 2011).

5.4.3 Intracellular mechanisms of calcification and the interaction with respiration and production

The physico-chemical microenvironment surrounding *Halimeda* segments is influenced by physiological processes (calcification, photosynthesis and respiration) and environmental parameters (temperature, pH, flow and light) (Borowitzka and Larkum1976b; Borowitzka 1986; De Beer and Larkum 2001; Al-Horani 2005). The pH in the DBL surrounding *Halimeda* increases due to CO_2 uptake for photosynthesis in the light, whereas pH decreases due to CO_2 and H^+ release from respiration and calcification (De Beer and Larkum 2001). pH and light also influence Ca^{2+} dynamics. In the light, the Ca^{2+} concentration in seawater decreases due to Ca^{2+} diffusion for calcification (De Beer and Larkum 2001).

It has been proposed that calcification promotes photosynthesis by providing a proton source through the calcium carbonate deposition producing H_2O and CO_2, which will enhance $CaCO_3$ nucleation (Borowitzka 1989; McConnaughey 1989; McConnaughey and Whelan 1997). These protons promote the conversion of HCO_3^- to CO_2, which is used in the dark reactions of photosynthesis (McConnaughey 1989; McConnaughey and

Whelan 1997). Many studies have shown that calcification in *Halimeda* is influenced by light, CO_3^{2-}, CO_2 and pH of the intercellular space, as well as photosynthetic rate (Stark et al. 1969; Borowitzka and Larkum 1976a, 1976b; Borowitzka 1977). Photosynthetic CO_2 uptake by the enzyme Rubisco in the Calvin cycle elevates intracellular pH and CO_3^{2-} content (McConnaughey 1989). Borowitzka and Larkum (1976b) showed that the rate of calcification is proportional to the photosynthetic rate; for every mole of $CaCO_3$ precipitated, 4-8 moles of CO_2 must be fixed in photosynthesis. In this study, I observed that calcification rates declined with decreasing pH, with a concomitant decline in photosynthetic efficiency. This suggests that calcification in these species is closely coupled photosynthesis, such that a decrease in photosynthetic efficiency leads to a decrease in calcification.

5.4.4 Ocean acidification and ocean warming as drivers of calcification and photosynthesis inhibition in *Halimeda*

Negative calcification rates were observed in *H. macroloba* and *H. cylindracea* under high pCO_2 conditions, independent of treatment temperature, suggesting that dissolution of the calcium carbonate structure occurred primarily in response to shifts in carbonate chemistry, rather than increased temperature. The elevated pCO_2 in the treatments changed the carbonate chemistry of seawater by decreasing the availability of CO_3^{2-} ions required for calcification and resulted in a decreased aragonite saturation state (Ω_a) to 1.97 ± 0.02 and 2.05 ± 0.01 (mean ± SE) at pH 7.7, 28ºC and 32ºC, respectively (Table 5.1). This finding is consistent with previous studies that observed negative calcification rates and decreasing aragonite crystal width in *Halimeda* spp. (Sinutok et al. 2011) under ocean acidification and ocean warming conditions.

Increases in pCO_2 are expected to promote photosynthesis and growth in some marine phototrophs such as seagrasses and non-calcifying macroalgae, due to an increased availability of inorganic carbon sources for photosynthesis (Gao et al. 1993b; Short and Neckles 1999; Palacios and Zimmerman 2007). However, we found that 5 weeks at elevated pCO_2 lead to a decline in Chl *a* and *b* concentrations in both temperature

treatments, indicating decreased chlorophyll production or pigment degradation in *Halimeda*, leading to less capacity for light absorption and photosynthesis. Reductions of PSII photochemical efficiency (F_V/F_M and $\Delta F/F_M'$) were observed at elevated pCO_2 and temperature treatments, similar to previous findings (Sinutok et al. 2011) indicating a loss of functional PSII reaction centers, downregulation of photochemistry, and/or photoinhibition. In addition, increases in the maximum excitation pressure (Q_m), an indicator of non-photochemical quenching, were observed under elevated pCO_2 and temperature stress. Values close to 1 were observed in the high CO_2 and temperature treatment, indicating that most of the PSII reaction centres are closed under maximum irradiance increasing the potential for photoinhibition (Iglesias-Prieto et al. 2004).

Under ocean acidification and ocean warming conditions, the reductions in PSII photochemical efficiency (F_V/F_M and $\Delta F/F_M'$) and increases in the maximum excitation pressure (Q_m) suggested that the level of non-photochemical quenching was elevated via heat dissipation. Both observations indicated a decrease in physiological performance and the onset of a combination of photoprotective processes and photoinhibition in these species under pH and thermal stress (Iglesias-Prieto et al. 2004; Kuguru et al. 2010). Our results from O_2 microprofiles support the photosynthetic pigment and chlorophyll fluorescence data, showing decreasing O_2 production with declining Chl *a* and *b* concentrations and a decreased photosynthetic efficiency under pH and/or heat stress (Table 5.2; Fig. 5.1-5.6).

5.4.5 Ecological implications

A recent study in a naturally high CO_2 region at volcanic vents off Ischia Island, Italy, observed high seagrass production and a lack of calcifying organisms (e.g. *Halimeda* and corals) at pH 7.6 and $\Omega_a < 2.5$ (Hall-Spencer et al. 2008). This study is consistent with those findings and indicates that rising pCO_2 and temperature will have a negative impact on photosynthesis and calcification in *Halimeda* leading to a reduction of its abundance and primary productivity on coral reefs. I found strong effects of temperature and pCO_2 on the microenvironment of two *Halimeda* species, as well as significant

reductions in physiological performance. As an ecosystem engineer and a key sediment producer, the loss or severe decline of *Halimeda* from reef ecosystems will thus have a dramatic impact on carbonate accumulation, sediment turnover, habitat structure, as well as trophic food webs associated with these species.

CHAPTER 6:

OCEAN ACIDIFICATION AND WARMING ALTER MICROSCALE PHOTOSYNTHESIS AND CALCIFICATION OF THE SYMBIONT-BEARING FORAMINIFERA *MARGINOPORA VERTEBRALIS*

6.0 OCEAN ACIDIFICATION AND WARMING ALTER MICROSCALE PHOTOSYNTHESIS AND CALCIFICATION OF THE SYMBIONT-BEARING FORAMINIFERA *MARGINOPORA VERTEBRALIS*

All laboratory work, data collection, data analyses and write up were undertaken by me. Michael Kühl assisted with the microsensor set up.

Sinutok S, Hill R, Doblin MA, Kühl M, Ralph PJ (2012) Microenvironmental changes support evidence of photosynthesis and calcification inhibition in *Halimeda* under ocean acidification and warming. *Coral Reefs* 31:1201-1213.

6.1 INTRODUCTION

Climate change is expected to have significant impacts on near-shore marine ecosystems and their resident organisms (Johnson and Marshall 2007). Human activities such as burning of fossil fuels, industrialization, deforestation and agricultural activities have led to an increasing release and accumulation of greenhouse gases in the atmosphere (Gattuso and Lavigne 2009). Enhanced CO_2 levels drive a rise of ocean temperature and onset of more acidic conditions in the ocean's surface layer (reduced pH) (Doney et al. 2009). As a consequence of chemical shifts in the carbonate system of seawater, the abundance of carbonate ions (CO_3^{2-}) and the calcite saturation state (Ω_c) is declining, reducing the capacity for calcifiers to produce their $CaCO_3$ skeleton (Diaz-Pudilo et al. 2007). Elements such as magnesium (Mg) are incorporated into biogenic calcium carbonate during calcification and the degree of Mg incorporation is influenced by physical and chemical conditions at the calcification site (e.g., temperature, pH, Mg content in seawater; Ries 2006; Dissard et al. 2010). The incorporation of Mg leads to an even lower saturation state, and Mg-calcite calcifiers (e.g. foraminifera *Marginopora vertebralis*, crustose coralline alga (CCA) *Lithophyllum cabiochae*) will be more sensitive to the increasing atmospheric CO_2 levels than calcite depositing species (Kleypas et al. 1999).

Benthic foraminifera are calcifying amoeboid protists with reticulated pseudopods, i.e., fine cytoplasmic strands that can branch out and merge to form a network. Many species have algal symbionts, which come from a variety of algal groups such as diatoms, dinoflagellates, unicellular chorophytes, unicellular rhodophytes and cyanobacteria (Nobes and Uthicke 2008). The benthic foraminifer, *Marginopora vertebralis*, hosts several species of dinoflagellates, i.e., *Gymnodinium obesum* Schiller, *Gymnodinium rotundatum* Klebs and *Symbiodinium microadriaticum* Freudenthal (Ross 1972; Pawlowski et al. 2001; Lee et al. 2009). These benthic foraminifera play a vital role in tropical and sub-tropical ecosystems as carbonate sediment producers; in the Pacific they have been shown to contribute up to 1 kg $CaCO_3$ m^{-2} y^{-1} (Langer et al. 1997).

Foraminifera will be significantly affected by lower oceanic pH and a reduced abundance of CO_3^{2-} resulting both in reduced calcification (growth and calcium carbonate crystal size) and photosynthetic efficiency (Sinutok et al. 2011). Microsensors for O_2, CO_2, pH and Ca^{2+} have previously been used to study photosynthesis and calcification in planktonic symbiotic foraminifera *Globigerinoides sacculifer* and *Orbulina universa* (Jørgensen et al. 1985; Rink et al. 1998) and the benthic symbiotic foraminifera *M. vertebralis*, *Amphistegina lobifera*, and *Amphisorus hemprichii* (Köhler-Rink and Kühl 2000, 2001). These studies have shown that the O_2 and pH microenvironment of symbiont-bearing foraminifera is strongly affected by photosynthesis and respiration in combination with the presence of a diffusive boundary layer that impedes solute exchange with the surrounding seawater (Köhler-Rink and Kühl 2000, 2001). Further studies showed that the CO_2 supply for photosynthetic O_2 evolution can be derived both from ambient seawater and internal mechanisms that include respiration, calcification and enzymatic dehydration of HCO_3^- to CO_2 through the enzyme carbonic anhydrase (Köhler-Rink and Kühl 2001, 2005). Carbonic anhydrase, which stabilises the O_2 evolving complex and PSII function (Villarejo et al. 2002) as well as supplies CO_3^{2-} ions at the site of calcification (Al-Horani et al. 2003), can be inhibited by a reduction in pH and increasing light stress (De Beer and Larkum 2001; Satoh et al. 2001). However, there have been no studies to date on the effect of

elevated temperature and CO_2 concentration on the photosynthesis of benthic foraminifera. In this study, I use O_2 microsensors and variable chlorophyll *a* fluorescence techniques to quantify effects of ocean acidification and ocean warming on the photosynthesis and calcification of benthic foraminifera.

6.2 MATERIALS AND METHODS

6.2.1 Sample collection and experimental design

Specimens of the imperforate foraminifer *M. vertebralis* were collected from Heron Island reef flat (Southern Great Barrier Reef, Australia; 151˚55'E, 23˚26'S), and maintained in a 500 L holding tank with artificial seawater (26°C, pH 8.1, salinity 33) under an irradiance of 250 µmol photons m^{-2} s^{-1} over a 12:12 h light:dark cycle at the University of Technology, Sydney. Specimens were randomly allocated to one of two temperature treatments (28°C and 32°C) in combination with one of two pH treatments (pH 8.1 or pH 7.7; the current and predicted pH values for the years 2100 (A1F1), respectively, and equivalent to a pCO_2 of 400 and 1200 µatm; Houghton, 2009). The treatment tanks were ramped from 26°C and a pH of 8.1 to their final conditions over one week and were then maintained at their treatment conditions for a further four weeks (n = 4). The control tanks were set at pH 8.1 and 28ºC. pCO_2 and temperature were controlled using pH controllers (7020/2, Tunze, Germany) connected to CO_2 aerators and water heaters (TC10, Teco, Italy), as described in Sinutok et al. (2011). Irradiance was 300 μmol photons m^{-2} s^{-1} on a 12:12 h light:dark cycle (on at 09:00 h and off at 21:00 h) and salinity 33. The water quality was identical to the holding tank with carbonate hardness, calcium, nitrate and phosphate concentrations of 2.3, 10, <0.0016 and 0.0005 mM, respectively. Total alkalinity was measured weekly by titrating 30 g of seawater with 0.1 M HCl in an autotitrator (DL50, Mettler Toledo, United States). The dissolved inorganic carbon (DIC) speciation (CO_2, CO_3^{2-} and HCO_3^-), CO_2 partial pressure (pCO_2), and the saturation state of seawater with respect to calcite (Ω_c) were determined using CO2SYS (Lewis and Wallace, United States; Table 6.1).

Table 6.1. Parameters of the carbonate system; total alkalinity (TA), CO_2 partial pressure (pCO_2), dissolve inorganic carbon (DIC; CO_2, CO_3^{-2}, HCO_3^-), and saturation state of seawater with respect to calcite (Ω_c) from each pH (8.1, 7.7) and temperature (28ºC, 32ºC) treatment. Mean ± SE (n = 3).

Treatment		TA	pCO_2	CO_2	CO_3^{-2}	HCO_3^-	DIC	Ω_c
pH	Temp (ºC)	(mmol kg^{-1})	(µatm)	(mmol kg^{-1})	(mmol kg^{-1})	(mmol kg^{-1})	(mmol kg^{-1})	
8.1	28	2.327±0.002	380.8±0.4	0.010±0.001	0.239±0.024	1.745±0.020	1.993±0.020	5.83±0.01
8.1	32	2.326±0.036	444.9±7.4	0.010±0.002	0.239±0.039	1.742±0.030	1.881±0.033	5.90±0.09
7.7	28	2.512±0.030	1208.1±14.6	0.032±0.004	0.122±0.015	2.219±0.027	2.373±0.028	2.97±0.04
7.7	32	2.508±0.015	1394.2±8.6	0.034±0.002	0.123±0.007	2.212±0.014	2.369±0.014	3.04±0.02

6.2.2 Calcification

Calcification rates were determined using the buoyant weight technique (Jokiel et al. 1978; Ries et al. 2009; Sinutok et al. 2011) with wet weight comparisons made between measurements at the start and end of the experimental period using an electronic balance with an accuracy of 0.1 mg (AB204-S, Mettler Toledo, USA). For weighing, individual foraminifera were placed on a glass Petri-dish hung below an electronic balance using nylon thread suspended in seawater.

6.2.3 Chlorophyll a fluorescence

Variable chlorophyll *a* fluorescence measurements were done with a 6mm diameter fibre-optic attached to a Diving-PAM fluorometer (Walz GmbH, Effeltrich, Germany). Measurements were done every 10 days over the duration of the experiment to assess the photosynthetic performance of *M. vertebralis*. Photosystem II (PSII) photochemical efficiency was determined through measures of the maximum quantum yield of PSII (F_V/F_M) at 09:00 h and the effective quantum yield ($\Delta F/F_M'$) at 1300 h, after which the maximum excitation pressure of photosystem II (Q_m) was calculated as $Q_m = 1 - (\Delta F/F_M'$ at 13:00 h / F_V/F_M at 0900 h) as a proxy for photoinhibition (Iglesias-Prieto et al. 2004).

6.2.4 Photosynthetic pigment concentration

Chlorophyll (Chl) *a* and c_2 concentrations (in μg g^{-1} fresh weight (fw)) were determined at the beginning and end of the 5-week experiment using the spectrophotometric method of Ritchie (2008). Individual specimens of *M. vertebralis* were extracted by grinding samples in 3 mL of 90% acetone at 4°C followed by extraction in darkness for 24 hours (n = 4). Samples were then centrifuged at 1500 x g for 10 mins, whereafter the supernatant was placed into a quartz cuvette for absorbance measurements at 630 and 664 nm in a spectrophotometer (Cary 50, Varian, Australia).

6.2.5 Oxygen microsensor

Microsensor measurements of O_2 concentration were performed according to Köhler-Rink and Kühl (2000) at the start of the experiment, and after week 3 and week 5 on individual *M. vertebralis* specimens mounted in a 2 L flow chamber (n = 4). For this, a foraminifer from the treatment tanks was placed on the bottom of the flow chamber, with laminar water flow maintained at 2.5 cm s^{-1} by a submersible aquarium pump. Temperature and salinity were maintained at 28ºC and salinity at 33, respectively. Microsensor measurements were done under photon irradiances of 0, 80, 150, 230, 570, and 900 μmol photons m^{-2} s^{-1}. Irradiance was provided by a fiber optic halogen lamp (KL-2500, Schott GmbH, Germany) equipped with a collimating lens and a heat filter as well as a spectrally neutral screen with various densities for adjusting irradiance. The O_2 microsensor was mounted on a motorized micromanipulator (Encoder Mike, Oriel, United States), which, along with data acquisition, was controlled by a PC running dedicated software (Profix, Pyro-Science, Denmark).

Photosynthetic rates and O_2 concentration profiles were conducted from the overlying water downwards into the specimen surface (0 to 300 µm from the surface) and were measured with an O_2 microelectrode (OX-100, Unisense, Denmark) connected to a picoammeter (PA2000, Unisense, Denmark) and a strip chart recorder (BD12E, Kipp&Zonen, The Netherlands). The microelectrode had an outer tip diameter of 100 µm, a 90% response time of <8 s, and a stirring sensitivity <1.5%. A linear calibration of the microelectrode was done at each experimental temperature in air-saturated seawater and O_2-free seawater made anoxic by addition of sodium dithionite. A proxy for gross photosynthesis (P_y; nmol O_2 cm^{-3} s^{-1}) at the shell surface was measured using the light-dark shift technique (Revsbech et al 1981; Köhler-Rink and Kühl 2000) by estimating the rate of O_2 depletion over the first 10 seconds after the rapid transition to darkness. A more precise determination of gross photosynthesis was hampered by the slow response of the relatively large microsensor used in this study but the measurements still allowed for comparison of gross photosynthesis estimates in the different treatments. The diffusive O_2 flux (J; nmol O_2 cm^{-2} s^{-1}) through the diffusive

boundary layer (DBL) was calculated from measured steady-state O_2 concentration profiles using Fick's first law: $J = -D_0 (dC/dz)$, where D_0 is the molecular diffusion coefficient in seawater at the experimental salinity and temperature, and dC/dz is the linear slope of the O_2 concentration profile in the DBL.

6.2.6 Statistical analysis

Two-way analysis of variance (ANOVA) tests were performed (in SPSS, IBM) to determine any significant differences among treatments in calcification, chlorophyll *a* and c_2 concentration, variable chlorophyll fluorescence parameters (F_V/F_M, $\Delta F/F_M'$, Q_m), O_2 concentration at the shell surface, diffusive O_2 flux, and gross photosynthesis estimates. Repeated-measures analysis of variance (rmANOVA) tests were performed to determine any significant differences over time in variable chlorophyll fluorescence parameters (F_V/F_M, $\Delta F/F_M'$, Q_m), O_2 concentration at shell surface, diffusive O_2 flux, and gross photosynthesis estimates. All tests were performed with a significance level of 95% and Tukey's Honestly Significant Difference post hoc tests were used to identify statistically distinct groups. If data did not meet the assumptions of normality (Kolmogorov-Smirnov test) and equal variance (Levene's test), the data were transformed using $\log_{10}$ or square root.

6.3 RESULTS

6.3.1 Calcification rate

The calcification rates of *M. vertebralis* were slightly positive in the control (pH 8.1, 28ºC; 0.11±0.03% increase day^{-1}) and elevated temperature treatment (pH 8.1, 32ºC; 0.06±0.03% day^{-1}), but were negative under elevated CO_2 at both optimal and elevated temperature treatments (pH 7.7, 28ºC and pH 7.7, 32ºC; -0.1 to -0.4% day^{-1}; $P < 0.001$; Table 6.2).

Table 6.2: Calcification rate (% increase day^{-1}) and chlorophyll (Chl) *a* and c_2 concentration (μg g^{-1} fw) of *Marginopora vertebralis* after 5 weeks in each pH and temperature treatment. Data represent means (n = 4, mean ± S.E.). * signifies P <0.05.

	Calcification rate (% per day)	Chl *a*	Chl c_2
pH 8.1, 28ºC	0.11±0.03	16.3±0.7	6.2±1.2
pH 8.1, 32ºC	0.06±0.03	6.1±0.3	3.1±0.7
pH 7.7, 28ºC	-0.14±0.03	6.3±0.5	4.5±0.2
pH 7.7, 32ºC	-0.42±0.09	5.9±0.3	3.1±0.4
P value			
- pH	<0.001*	<0.001*	0.440
- Temperature	0.010*	<0.001*	0.060
- pH*Temperature	0.062	<0.001*	0.458

6.3.2 Photosynthetic pigment concentration

After 5 weeks, Chl *a* and Chl c_2 concentrations in *M. vertebralis* were 16.3±0.7 and 6.2±1.2 μg g^{-1} fw, respectively in the control treatment. Chl *a* significantly decreased at pH 7.7 in both temperature treatments and at pH 8.1 under elevated temperature 32ºC (P <0.001; Table 2). In contrast, Chl c_2 was the same in pH and temperature treatments (P >0.05; Table 6.2).

6.3.3 Chlorophyll *a* fluorescence

The maximum quantum yield of PSII (F_V/F_M), effective quantum yield ($\Delta F/F_M'$) and maximum excitation pressure of PSII (Q_m) in the control treatment did not change over the experimental period (P >0.05; Fig. 6.1). A significant decrease in F_V/F_M and $\Delta F/F_M'$ was found in week 3 of the experiment in both the pH 7.7, 28ºC and pH 7.7, 32ºC treatments (P <0.001; Fig. 6.1A-B) and by the end of the experiment this significant decline was found in all treatments, except the control (P <0.001; Fig. 6.1A-B). Under elevated CO_2 and temperature, *M. vertebralis* showed very large Q_m values (0.2-1) at the end of the experiment. The Q_m significantly increased in week 3 in both the pH 7.7,

28ºC and pH 7.7, 32ºC treatments (P <0.001; Fig. 6.1C) and at the end of the experiment, this was found in all treatments, except the control (P <0.001; Fig. 6.1C).

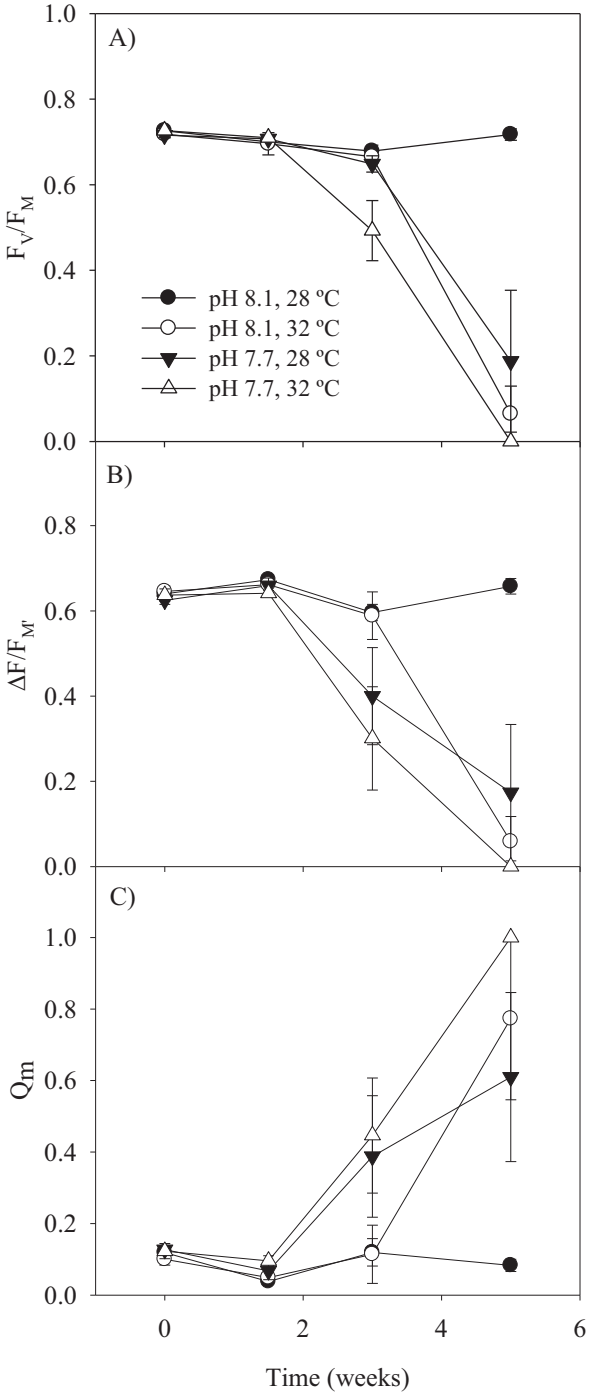

Figure 6.1: Maximum quantum yield of PSII (F_V/F_M; A), effective quantum yield ($\Delta F/F_M'$; B), and maximum excitation pressure of photosystem II (Q_m; C) for *M. vertebralis* in each pH and temperature treatment over the length of the experimental period. Data represent means (*n* = 4, ± S.E.M.).

6.3.4 Oxygen microenvironment

Oxygen concentration profiles of *M. vertebralis* were strongly affected by irradiance, CO_2, temperature, and time of exposure to elevated CO_2 and temperature ($P < 0.05$; Fig. 6.2-3). At the beginning of the experiment (time 0), the ambient O_2 concentration of 209 µM started to increase ~125 µm above the shell and reached 235-275 µM at the shell surface under all light conditions, whereas an O_2 concentration of only 199 µM was reached at the shell surface when in darkness (Fig. 6.2), which is less than bulk water O_2 concentration.

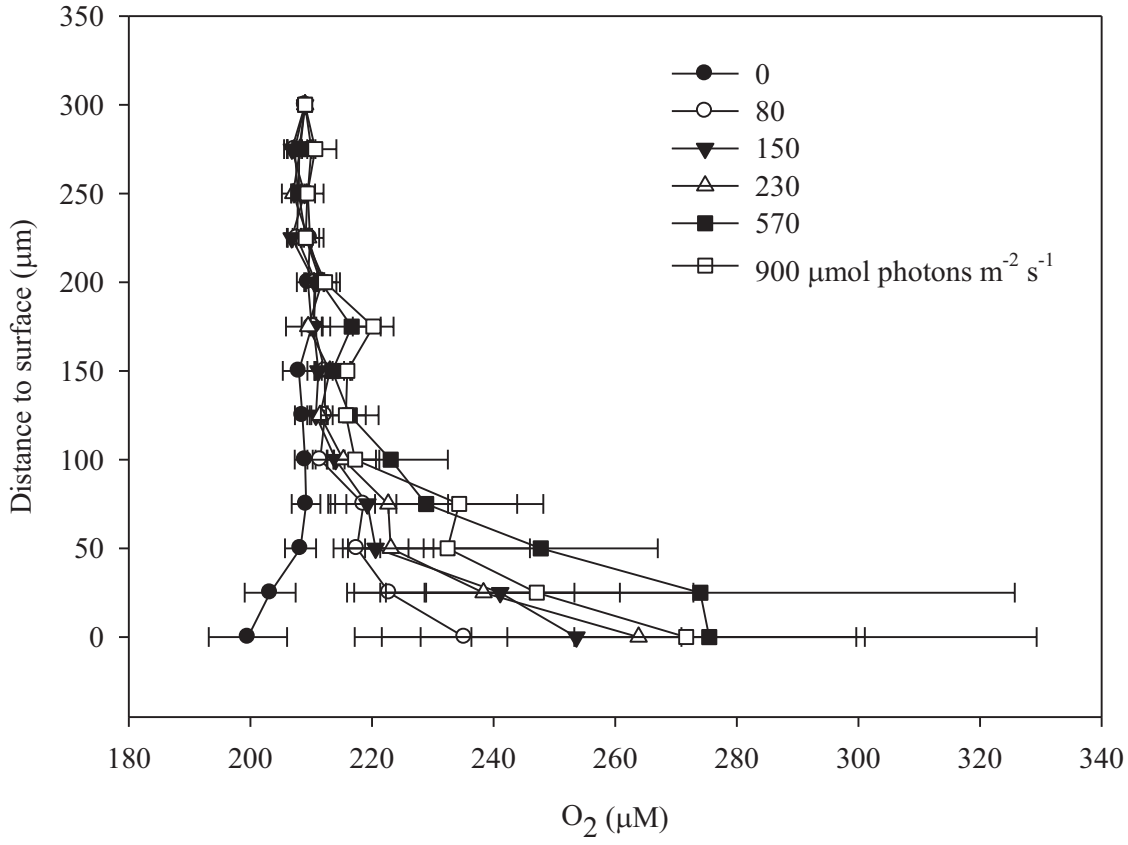

Figure 6.2: Oxygen concentration profile measured towards the shell surface of *M. vertebralis* measured at week 1 under increasing irradiance (0, 80, 150, 230, 570, and 900 μmol photons m^{-2} s^{-1}). Data represent means (n = 4, ± S.E.M.).

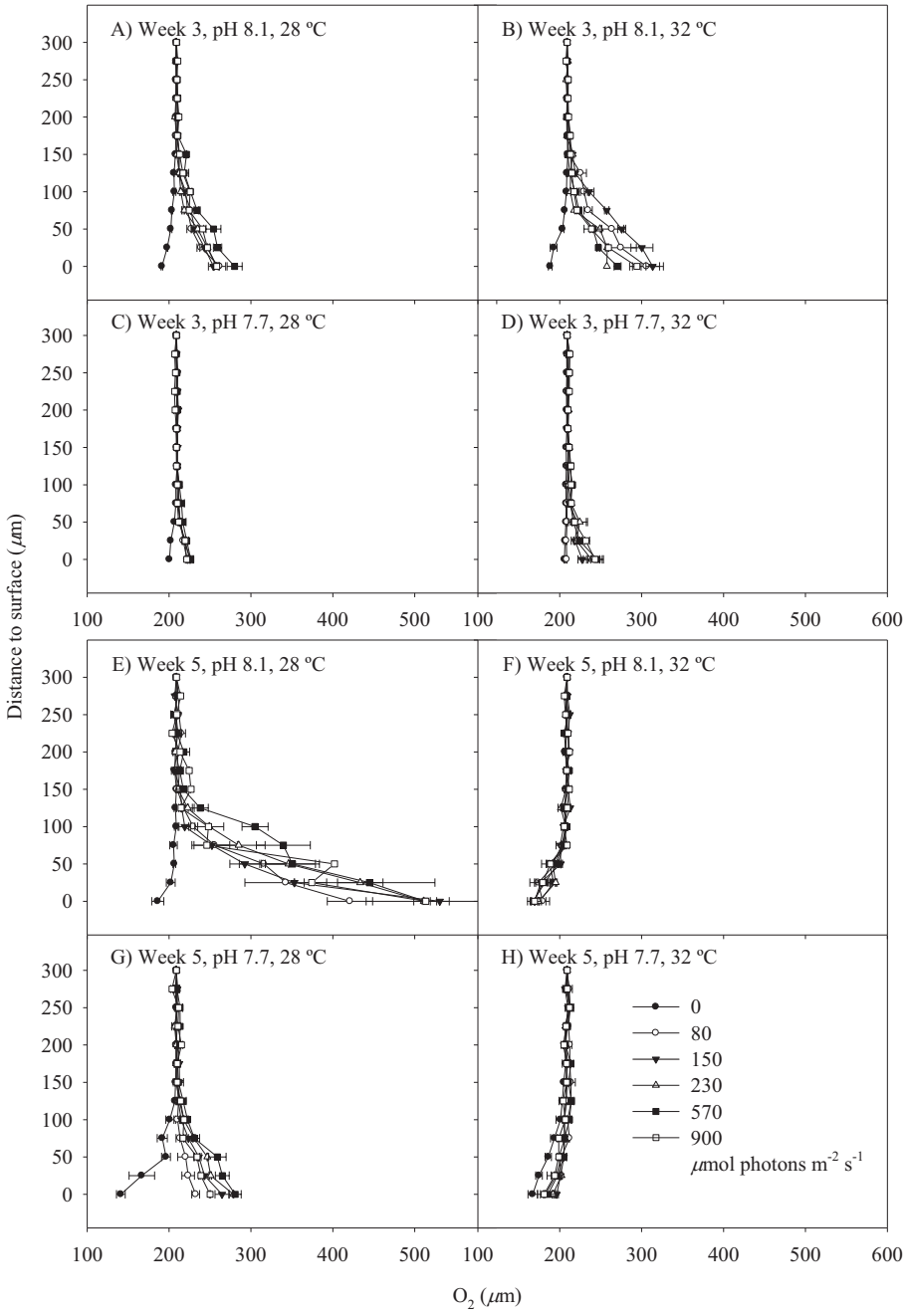

Figure 6.3: Oxygen concentration profile measured towards the shell surface of *M. vertebralis* at week 3 and week 5 in specimens from each pH and temperature treatment at each irradiance (0, 80, 150, 230, 570, and 900 μmol photons m^{-2} s^{-1}). Data represent means (n = 4, ± S.E.M.).

After 3 weeks, *M. vertebralis* in the control (Fig. 6.3A) and pH 8.1, 32ºC (Fig. 6.3B) treatments showed increases in O_2 concentration at the shell surface to ~254-280 and ~257-313 µM under all irradiances, and decreases in shell surface O_2 concentration of ~191 and ~188 µM in darkness, respectively. At pH 7.7 in both temperature treatments after 3 weeks, O_2 concentration at the shell surface slightly increased to ~221-226 and ~208-245 µM for all irradiances and exhibited a slightly decrease to ~200 and ~205 µM at the shell surface in darkness (Fig. 6.3C-D). At 5 weeks, *M. vertebralis* in the control and pH 7.7, 28ºC treatments showed increases in O_2 concentration at the shell surface (Fig. 6.3E, G). However, after 5 weeks in the pH 8.1, 32ºC and pH 7.7, 32ºC treatments, there was no change in O_2 concentration at the shell surface (167-179 and 166-196 µM O_2, respectively), between light and dark conditions (Fig. 6.3F, H).

6.3.5 Gross photosynthesis and O_2 flux

The rate of gross photosynthesis and O_2 flux at the shell surface of *M. vertebralis* was influenced both by the CO_2 and temperature and the time of exposure to elevated CO_2 and temperature ($P < 0.001$; Fig. 6.4). Decreases in mean gross photosynthesis were observed at pH 8.1, 32ºC and pH 7.7 for all temperature treatments ($P < 0.001$; Fig. 6.4A, B). After 3 weeks, a significant decrease in the rate of O_2 efflux was observed at elevated CO_2 and temperature (pH 7.7, at all temperature; $P < 0.001$; Fig. 6.4C). A net O_2 influx decreased through time, with week 5 showing strong decreased compared to week 3 both in light (80 to 900 μmol photons m^{-2} s^{-1}) as well as in darkness in the elevated CO_2 and temperature (32ºC, at all pH) treatments after 5 weeks (Fig. 6.4D).

6.4 DISCUSSION

The photosynthesis and calcification of the Mg-calcite depositing benthic foraminifer, *M. vertebralis* was negatively affected by both elevated CO_2 and temperature. The negative calcification rate observed under conditions of high CO_2 and temperature indicates a breakdown in the calcification process and increasing calcium carbonate dissolution. An increase in pCO_2 leads to a reduction in CO_3^{2-} ions (the substrate

required for calcium carbonate precipitation) and a lowering of the Mg-calcite saturation state (Ω_c), consequently inhibiting calcification. Our results are consistent with other studies on foraminiferal showing decreased calcification rate and carbonate dissolution under elevated pCO_2 conditions (Lombard et al. 2010; Fujita et al. 2011; Haynert et al. 2011; Sinutok et al. 2011). However, the degree of ocean acidification impact on foraminiferal calcification can vary with foraminiferan test types and calcium carbonate polymorphs (calcite, low Mg-calcite and high Mg-calcite; Fujita et al. 2011).

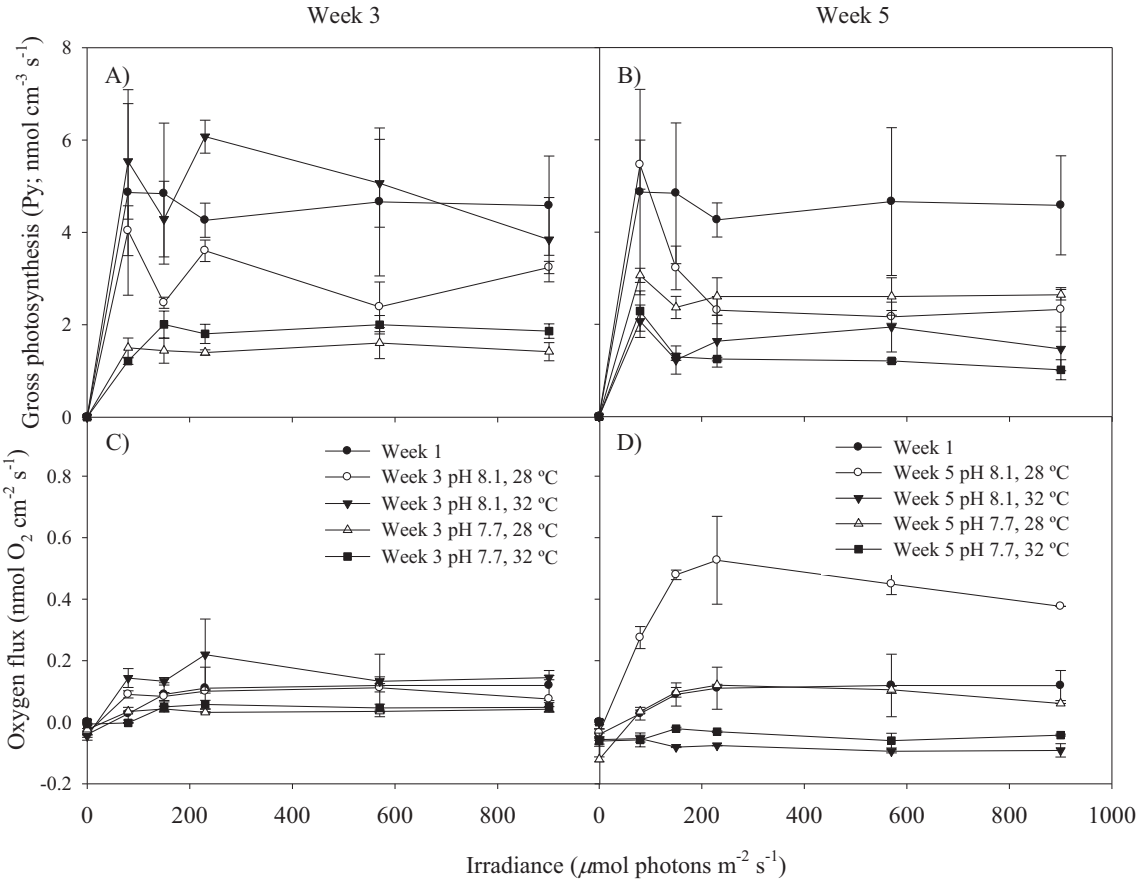

Figure 6.4: Gross photosynthesis estimates (P_y; nmol O_2 cm^{-3} s^{-1}; A-B) and the diffusive O_2 flux (nmol O_2 cm^{-2} s^{-1}; C-D) at the shell surface *M. vertebralis* measured at week 1 and 3 (A, C) and 5 (B, D) on specimens from each pH and temperature treatment. Data represent means (n = 4, ± S.E.M.).

Recent studies on imperforate (porcelaneous) symbiotic foraminifera (*Marginopora kudakajimensis* and *Amphisorus hemprichii*) showed that their test weight and calcification showed a strong decrease with increasing pCO_2 (Fujita et al. 2011; Kuroyanagi et al. 2009). In comparison, perforate (hyaline) symbiotic foraminifera (*Baculogypsina sphaerulata* and *Calcarina gaudichaudii*), show a smaller degree of ocean acidification impact where calcification was enhanced at intermediate pCO_2 levels (580 and 770 μatm), but reduced at a higher level (970 μatm) (Fujita et al. 2011). Such differences were explained by different uptake mechanisms of dissolved inorganic carbon. In the porcelaneous foraminifera, dissolved inorganic carbon uptake into the test increased linearly with the carbonate concentration outside the test, whereas DIC uptake into the test in hyaline foraminifera is less influenced by the carbonate concentration outside the test (Ter Kuile et al. 1989b; Fujita et al. 2011). The hyaline species has an internal Ci pool in the form of a carbon concentrating mechanism, which is used for calcification. The internal Ci pool, the intracellular pH and the ratio between dissolved CO_2, HCO_3^-, and CO_3^{2-} in hyaline species can be modified by both foraminiferal protoplasm and the photosynthesis of algal symbionts (Ter Kuile et al. 1989a; De Nooijer 2009; Fujita et al. 2011). However, this mechanism doesn't exist in porcelaneous foraminifera such as *M. vertebralis* used in this study.

This study showed *M. vertebralis* had negative growth rates under elevated CO_2 at both optimal and elevated temperature treatments (pH 7.7, 28ºC and pH 7.7, 32ºC) indicating $CaCO_3$ dissolution. Recent studies have shown that *M. vertebralis* has a higher growth rate at 22ºC as compared to 28ºC (Reymond et al. 2011) and that an elevated temperature of 32ºC and a pCO_2 of 1000 μatm is the upper limit for survival of this species on the southern Great Barrier Reef (Sinutok et al. 2011). No change in growth rate was observed in the low Mg-calcite species *Amphistergina gibbosa* (McIntyre-Wressnig et al. in press), whereas reduced growth rates were observed in the high-Mg test producing species *Archaias angulatus* (McIntyre-Wressnig in press), *M. kujakajimensis* (Kuroyanagi et al. 2009) and *A. hemprichii*, *B. sphaerulata*, and *C. gaudichaudii* (Fujita et al. 2011) when exposed to elevated pCO_2. This is consistent with

the prediction that foraminifera, which precipitate high Mg-calcite, will be more sensitive to increasing pCO_2 than those depositing aragonite or low Mg-calcite (Kleypas et al. 1999). De Nooijer et al. (2009) showed that both high and low Mg-calcite depositing foraminifera are able to elevate internal pH by at least one pH unit at the site of calcification to promote calcite precipitation. Under elevated CO_2 conditions, more energy is therefore required to reach the same pH level for calcite precipitation and maintain the same rate of calcification, leading to changes in energy partitioning and hence growth. Under elevated CO_2 conditions, slower growth rate, calcification rate or less reproduction then may be observed in these species.

The symbiont-bearing foraminifera *M. vertebralis* is known to host several species of dinoflagellates, which are sensitive to environmental perturbations (Hallock et al. 2006; Uthicke and Nobes 2008; Reymond et al. 2011). Our results showed a decrease in Chl *a* concentration with increasing pCO_2 and temperature after 5 weeks. Sinutok et al. (2011) found a similar decrease in photosynthetic pigments in the same species indicating symbiont expulsion and/or damage due to photoinhibition (Hallock et al. 2006). After day 20 of our experiment, there was a significant decrease in the effective quantum yield ($\Delta F/F_M'$) observed at pH 7.7 in all temperature treatments indicating down-regulation of photochemistry (Warner et al. 2011). Significant declines in both maximum quantum yield and effective quantum yield of PSII (F_V/F_M and $\Delta F/F_M'$) in this study indicated photoinhibition of the symbiotic algae under high CO_2 and temperature treatments (pH 8.1, 32ºC; pH 7.7, 28ºC and 32ºC treatments) after 30 days (Maxwell and Johnson 2000). Increases in the maximum excitation pressure (Q_m), an indicator of non-photochemical quenching, were observed under pH and heat stress (pH 8.1, 32ºC; pH 7.7, 28ºC and 32ºC) providing further evidence for onset of chronic photoinhibition (Iglesias-Prieto et al. 2004). In other symbiont-bearing species (e.g. the diatom-harbouring foraminifera *A. radiata*, *H. depressa*, and *C. hispida*; Schmidt et al. 2011), as well as in corals, a reduction in photosynthetic efficiency (F_V/F_M) and an increase in Q_m were observed under thermal stress (32ºC) (Warner et al. 2006; Abrego et al. 2008). The pH and temperature stress may trigger photoinhibition through the degradation of the D1

protein (Allakhverdiev et al. 2008), the production of reactive oxygen species in PSII (Talge and Hallock 2003) and the disruption of photoprotective mechanism such as the xanthophyll cycle (Anthony et al. 2008).

While the O_2 microenvironment of *M. vertebralis* was affected by light, temperature, and pCO_2, temperature was the main factor influencing the microenvironment of this species. Our study is consistent with Köhler-Rink and Kühl (2000, 2001), where photosynthesis of endosymbionts led to an increase in O_2 concentration, and dark respiration led to a decrease in O_2 concentration towards the foraminifera shell surface. Gross photosynthesis and O_2 flux significantly decreased when *M. vertebralis* was exposed for longer periods (5 weeks) of elevated CO_2 and temperature (Fig. 6.4). These results are in agreement with a previous study, where long-term exposure (35 days) led to a decrease in primary productivity in this species (Sinutok et al. 2011).

Our results showed that although elevated CO_2 has a negative effect on primary productivity in *M. vertebralis*, temperature is likely to have a greater impact on gross photosynthesis and O_2 flux than pCO_2 as we observed negative fluxes and negative gross photosynthesis at high temperature in both CO_2 treatments in week 5 and elevated CO_2 and elevated temperature treatments decreased fluxes by 50% and 80% from control, respectively. Elevated CO_2 may induce a disruption in the CO_2 uptake pathway for photosynthesis or interfere with the electron transport and the thylakoid proton gradients (Anthony et al. 2008), but the capacity of foraminifera to increase their intracellular pH by at least one pH unit through the conversion of HCO_3^- to CO_3^{2-} may elevate the threshold for CO_2 stress (De Nooijer et al. 2009). If healthy foraminifera produce 1 kg $CaCO_3$ m^{-2} y^{-1}, I can predict a 4-fold reduction to 0.25 kg $CaCO_3$ m^{-2} y^{-1} under pH 7.7, 32 ºC.

Shell surface pH was not measured in this study. However, it has been shown that symbiont photosynthesis increases the O_2 concentration and pH at the shell surface in *M. vertebralis*, *A. hemprichii* and *A. lobifera* in the light (Köhler-Rink and Kühl 2000, 2001). At higher irradiance, when photoinhibition occurred, the O_2 concentration and

pH at the shell surface decreased (Köhler-Rink and Kühl 2000; Sinutok et al. submitted). The changes in pH at shell surface support the notion of biological induction of $CaCO_3$ precipitation (Köhler-Rink and Kühl 2000, 2001) and suggest that pH dynamics from photosynthesis and irradiance can influence the calcification in *M. vertebralis*. Therefore, in these results, a reduction in primary productivity and O_2 concentration at the shell surface when exposed to elevated CO_2 and temperature could lead to a decrease in shell surface pH and result in inhibition of calcification (Köhler-Rink and Kühl 2005). At elevated CO_2 and temperature, the inhibition of the external and internal enzyme carbonic anhydrase and calcification will also lead to a decrease in photosynthesis and productivity (De Beer and Larkum 2001; Satoh et al. 2001; Köhler-Rink and Kühl 2001, 2005). On the other hand, a reduction in photosynthesis can lead to a decrease in local pH and subsequent decrease in CO_3^{2-} and thereby decrease calcification (Köhler-Rink and Kühl 2005).

$CaCO_3$ precipitation in foraminifera is influenced by the carbonate chemistry of the surrounding seawater (Köhler-Rink and Kühl 2000). While ocean acidification lowers carbonate ion availability in the seawater (Feely et al. 2004), physiological processes such as photosynthesis can greatly influence and offset these reductions (Anthony et al. 2011). On a coral reef, photoautotrophs can decrease the pCO_2 flux and elevate aragonite saturation state (Ω_a) of seawater at the local scale (Anthony et al. 2011). *M. vertebralis* is commonly found attached to macroalgae, such as the calcareous green alga *Halimeda* sp. (Sinutok et al. 2011). Under optimal CO_2, temperature and light conditions, photosynthesis in *Halimeda* sp. has the capacity to alter the carbonate chemistry through the uptake of CO_2 and an associated rise in pH on its thallus surface (De Beer and Larkum 2001). Therefore, *Halimeda* photosynthesis influences the seawater chemistry on the surface and the immediate vicinity of its thallus and may thus indirectly favour calcification of the attached foraminifera. Conversely, when exposed to elevated CO_2 and temperature conditions, photosynthetic efficiency and primary productivity of *Halimeda* decreases (Sinutok et al. 2011), thus removing the capacity for locally alleviation of ocean acidification impacts. Given the vulnerability of both

foraminifera and *Halimeda* to climate change-induced heating and acidification of seawater, this association may not provide a sufficient buffer against ocean acidification in the future.

These results indicate that predicted levels of future ocean acidification and ocean warming can have strong effects on the photosynthesis and calcification of *M. vertebralis.* Interestingly, effects of natural ocean acidification can be observed in a volcanic CO_2 vent area around the island of Ischia, Italy, in the Mediterranean Sea, where foraminiferal diversity and abundance was reduced from 25 species at pH of 8.17, to 4 species at pH 7.6 (Dias et al. 2010). Reductions in abundance and diversity of symbiont-bearing benthic foraminifera will have a dramatic impact on carbonate sediment production and turnover on coral reefs. Shifts in community structure may occur by a dominance of species that benefit from elevated CO_2 and temperature conditions (Diaz-Pulido et al. 2007). The use of microsensors in this study demonstrated their advantages in investigating the physico-chemical microenvironment of *M. vertebralis* under simulated climate change scenarios at a scale enabling precise measurements of foraminiferal photophysiology. Further investigation of climate change impacts using different microsensors (e.g., Ca^{2+}, pH, CO_2) will allow for a deeper understanding the dynamic microenvironment of foraminiferal species.

CHAPTER 7:

OCEAN ACIDIFICATION AND WARMING WILL INCREASE VULNERABILITY OF *HALIMEDA* SP. TO BREAKAGE AND REMOVAL

7.0 OCEAN ACIDIFICATION AND WARMING WILL INCREASE VULNERABILITY OF *HALIMEDA* SP. TO BREAKAGE AND REMOVAL

I was responsible for most of laboratory work, data collection, data analyses and the majority of writing. Mark Berkahn was instrumental in assisting me with the X-ray diffraction and data analyses. David Bishop was mostly responsible for the ICP-MS analyses.

7.1 INTRODUCTION

The anthropogenic release of carbon dioxide (CO_2) into the atmosphere is resulting in more acidic and warmer conditions in the ocean's surface layers (Solomon *et al*. 2007). As a consequence of the shift in carbon chemistry, the abundance of carbonate ions (CO_3^{2-}) will decline, reducing the capacity for calcifiers to deposit their $CaCO_3$ skeleton (Doney *et al*., 2009). Reduced calcification has been demonstrated to impact growth rates and $CaCO_3$ crystal size in calcareous organisms, with potentially serious implications for mechanical strength (Sinutok *et al*. 2011). Increase in calcium carbonate dissolution and reduced calcification in the future may result in changing community composition and habitat structure for many marine organisms (Feely *et al*. 2004; Kleypas *et al*. 2006). Additionally, increases in temperature will elevate sea level, increase precipitation and evaporation, leading to more intense storms (Walsh & Ryan 2000; Knutson & Tuleya 2004). According to some predictions, storm intensity will increase by 2-11% by 2100 (Emanuel, 2005; Knutson *et al*. 2010).

Changes in storm activity will have fitness consequences for sessile organisms living on coral reefs. One such organism is *Halimeda*, a calcareous alga that has multiple important roles as an ecosystem engineer (Kleypas & Yates 2009), a dominant sediment producer (Drew 1983), a source of food for herbivores (Smith *et al*. 2004), and shelter and nursery grounds for invertebrates (Hillis-Colinvaux 1980). *Halimeda* individuals are rigid, grow vertically and are therefore exposed to hydrodynamic forces produced by surface waves (DeWreede 2006). Intermittently, these forces become severe during

tropical storms (Emanuel 2005; Madin & Connolly 2006). Furthermore, reef carbonate materials, including *Halimeda* structural materials and the reef substratum to which they attach, are expected to become weaker due to ocean acidification (Madin *et al.* 2008) and ocean warming (Anthony *et al*. 2008), which would increase rates of removal from the substrate and hence lead to mortality.

Species of *Halimeda* are classified according to the shape, size and internal structure of their segments (Verbruggen 2005), with each species having a different growth form that suits a particular habitat niche (Price *et al*. 2011). Some species grow in sandy substrata in intertidal to subtidal regions and form a bulbous holdfast, a mass of rhizoids which entrain sand and form hemispherical to cylindrical masses (Verbruggen 2005; Anderson *et al*. 2006), as found in *Halimeda macroloba* Decaisne and *Halimeda cylindracea* Decaisne. In several species, the thallus is attached to rock surface by a single, small holdfast (Verbruggen 2005). Studies have shown that algae adapt their morphology to reduce the effect of wave action (Koehl 1984; Koehl & Alberte 1988; Carrington 1990; Pratt & Johnson 2002), and holdfast morphology might also be influenced by water motion (Anderson *et al*. 2006). Thallus strength in wave-swept macroalgae is often greater than required to avoid breakage from mechanical stress imposed on the thallus, suggesting that they are over-engineered for resisting wave forces (Mach *et al.* 2007). In addition to affecting the organism directly, increased water motion also has indirect effects, such as altering nutrient availability, light penetration, temperature, salinity, and sediment characteristics (e.g., grain size; Denny 1988; Hurd 2000; Hoogenboom & Connolly 2009). Wave-exposed sites usually have little or no sediment deposition, small variation in temperature, salinity, and nutrients, and large sediment grains (Lobban & Harrison 1994; van Keulen & Borowitzka 2003). In contrast, sheltered habitats have a much greater loading of smaller sediment particles (leading to increased re-suspension = turbidity), along with daily or seasonal variation in temperature, salinity and nutrient concentration (Lobban & Harrison 1994, van Keulen & Borowitzka 2003). Holdfast and thallus characteristics are therefore hypothesised to

be the result of wave motion, sediment composition, and other environmental factors, and will be assessed in *Halimeda* for the first time in this study.

The biomechanical properties of hardness, stiffness, toughness, stress, strain, strength, breaking and removing force and drag force, have previously been studied in macroalgae (Armstrong 1987; Lin & Dai 1996; Carrington *et al*. 2001; Stewart 2006). An investigation of some of the biomechanical properties (force to remove, force to break, and strength) of *Halimeda incrassata*, a coenocytic (multinucleate-unicellular) alga, showed that in situations of stress, whole individuals detach from the substratum rather than experience a break in the thallus in more than 95% of cases (DeWreede 2006). Another study of biomechanical properties and holdfast morphology of coenocytic algae, *Udotea flabellum*, *Penicillus capitatus*, *P. pyriformis*, and *H. gracilis*, by Anderson *et al*. (2006) revealed no significant correlation between holdfast volume and force-to-remove because holdfast tenacity (resistance to removal) was determined by a combination of factors such as sediment shear strength (sediment compaction), holdfast surface area, and rhizoid strength. These factors are likely to play an important role in influencing their capacity to persist on coral reefs under conditions where thallus strength may be reduced.

Halimeda consists of plate-like, calcified segments which are jointed together by uncalcified nodes. These form branching chains to produce a bushy thallus (Hillis-Collinvaux, 1980). *Halimeda* segments consist of i) uncalcified walls, comprised of microfibrils containing xylan, ii) branching filaments without cross walls, called utricles, and iii) calcified structures predominantly in the form of aragonite (Hillis-Colinvaux, 1980). It has been suggested that the calcified structure or $CaCO_3$ polymorph (e.g. aragonite, calcite) and the material properties of the alga, both influence the shear strength and toughness of *Halimeda* segments (Padilla 1985; Onoda *et al.* 2008). Therefore, changes in chemical composition, may contribute to differences in mechanical properties (Padilla 1985; Onoda *et al.* 2008). A recent study on the impact of ocean acidification on *H. opuntia* and *H. taenicola* showed that there are species-specific responses to ocean acidification in terms of calcification and photosynthesis due

to anatomical and physiological differences between species (Price *et al*. 2011). *H. macroloba* and *H. cylindracea* are in the same lineage (section *Rhipsalis*; Verbruggen 2005) where they develop erect thalliwith bulbous holdfast, three to many layers of moderately inflated utricles and nodal medullary filaments generally fusing into a single unit (Hillis-Colinvaux 1980; Verbruggen & Kooistra 2004). However, these species are different in bulbous holdfast size, segment size and shape, and utricle size. *H. cylindracea* consists of cylindrical segments (1.5 mm thickness) with dichotomous branching and smaller peripheral utricles and a massive bulbous holdfast for attachment. *H. macroloba* consists of large, undulating or lobed segments (1 mm thickness) with polychotomous or dichotomous branching and a smaller bulbous holdfast (Hillis-Colinvaux 1980; Verbruggen & Kooistra 2004). The morphological (e.g. branching, percentage of $CaCO_3$, segment thickness) and anatomical (e.g. utricle, siphon pattern, intercellular space size, the fusion of the siphons between node and segment) characteristics of the algae may play a role in physiological and biomechanical properties (e.g. toughness and strength), but this has not yet been assessed.

During calcification, elements such as strontium (Sr) and magnesium (Mg) are incorporated into the calcium carbonate matrix of the *Halimeda* (Dissard *et al*. 2010). Mg:Ca and Sr:Ca ratios are influenced by the physical and environmental conditions such as pH and temperature (Dissard *et al*. 2010), CO_3^{2-}, Mg and Sr content in seawater (Ries 2006), and growth rate (Cléroux *et al*. 2008). An increase in CO_3^{2-} concentration was found to decrease the Mg:Ca ratio in the high-Mg calcite foraminifera, species *Orbulina universa* d'Orbigny and *Globigerina bulloides* d'Orbigny (Russell *et al*. 2004), but had no affect on the Mg:Ca ratio in *Ammonia tepida* Cushman (Dissard *et al*. 2010). However, the Sr:Ca ratio has been shown to increase with increasing CO_3^{2-} concentration in *A. tepida* (Dissard *et al*., 2010) and *O. universa* (Lea *et al*., 1999; Russell *et al*. 2004), yet not with the non-symbiont foraminiferal species *G. bulloides* (Russell *et al*. 2004). The responses to CO_3^{2-} concentration (or pH) may be species-specific depending on whether it photosynthesizes, as the impact of pH from photosynthetic activity may affect the calcification rate in symbiotic species (Russell *et*

al. 2004; Dissard *et al*. 2010). By determining the Mg:Ca and Sr:Ca ratios, I examined the impact of ocean acidification and ocean warming on the elemental incorporation during calcification.

This study uses innovative methodologies, such as a penetrometer, inductively coupled plasma mass spectroscopy (ICP-MS) and X-ray diffraction, to examine for the first time the effects of ocean acidification and ocean warming on the mechanical integrity and skeletal mineralogy of two common and widespread species of *Halimeda*. Specifically, our objectives were to (1) understand and quantify changes in biomechanical and morphological properties in these species at different wave exposures in their natural reef habitats and (2) investigate the effects of carbonate availability and temperature on biomechanical properties and skeletal mineralogy. Reductions in carbonate availability were hypothesised to weaken calcified structures and water temperature was expected to augment this weakening, resulting in decreased mechanical integrity and increased susceptibility to storm- and predatory-induced mortality.

7.2 MATERIALS AND METHODS

7.2.1 Effects of wave motion on biomechanical and morphological properties of *Halimeda* spp.

The biomechanical properties (force required to remove, force required to break, and tensile strength) of *Halimeda macroloba* and *Halimeda cylindracea* (n = 30) from exposed and sheltered regions of Heron Island reef flat (Southern Great Barrier Reef; 151º55'E, 23º26'S) were determined at a low tide of 0.5 m depth. The exposed site was close to the reef crest on the western side of the reef, while the sheltered site was at Shark Bay at the southern end of Heron Island. The average water velocities from exposed and sheltered areas were measured using an acoustic doppler velocity meter (Vectrino, Nortek AS, Norway) and were 0.131±0.001 and 0.031±0.001 m s^{-1} (Mean±SE), respectively, suggesting a greater than fourfold difference in velocity between the sites. A digital spring device was used to measure both the force required to

remove the whole thallus and the force required to break the thallus in Newtons (30 thalli of each species) by clamping the *Halimeda* blades with clips hooked to a spring device and pulling the spring device upwards vertically until the thallus either uprooted from the substratum or the thallus broke. The ratio of uprooting to breakages for each site and species was calculated. The tensile strength (Pa) was calculated by dividing the force-to-break (in Newtons) by the elliptical cross-sectional area of the break (m^2). Following biomechanical measurements, the same *Halimeda* thalli were collected to measure morphological properties (length, width, dry weight of blade and holdfast, blade surface area, holdfast volume, uncalcified node size). The blade surface area was measured using spatial analysis software (University of Texas Health Science Center, San Antonio, Image Tool version 3; University of Texas). The holdfast volume was quantified using the water displacement technique in a graduated cylinder (Anderson *et al*., 2006). Rhizoid thickness (at 1 cm below basal segment) was measured under a stereomicroscope (Leica MZ16; Leica Microsystems, Switzerland) using instrument-specific software (Leica Application Suite V.3.7.0, Leica Microsystems, Switzerland) (n = 10 per holdfast, 30 holdfasts per site, n = 300 in total). The composition of sediment trapped within the holdfast was investigated using sieve analysis, to separate grains into eight size classes (<63, 63-125, 125-250, 250-500, 500-1000, 1000-2000, 2000-4000, and >4000 μm).

7.2.2 Effects of ocean acidification and ocean warming on biomechanical properties of *Halimeda* spp.

Specimens of *H. macroloba* and *H. cylindracea* (thallus lengths of 13-20 cm) were collected by hand from the Heron Island reef flat (the exposed habitat only) at low tide and transported alive to the University of Technology, Sydney. The specimens of these species were randomly allocated to one of two temperature treatments (28 and 32°C) in combination with one of two pH treatments (8.1 and 7.7; the current and predicted pH values for present day (Houghton *et al*., 2001) and the year 2100 (A1F1; Houghton, 2009), respectively, and equivalent to pCO_2 400, and 1000 μatm in this experiment. Samples were ramped from 26°C and a pH of 8.1 to their treatment conditions over 1

week and maintained under those 4 treatments for a further four weeks (n = 4). The tanks (n = 4 per treatment) set to pH 8.1 and 28ºC were the controls. Light intensity, salinity, pCO_2 and temperature were controlled as described in Sinutok *et al*. (2011). The carbonate hardness, dissolved calcium, nitrate, and phosphate concentration, total alkalinity (TA), dissolved inorganic carbon (DIC) speciation (CO_2, CO_3^{-2} and HCO_3^-), CO_2 partial pressure (pCO_2), and the saturation state of seawater with respect to calcite (Ω_c) and aragonite (Ω_a) were measured as described in Sinutok *et al*. (2011) (n = 3). A summary of the seawater chemistry from each treatment are shown in Table 7.1.

The contribution of precipitated $CaCO_3$ to the total mass of *H. macroloba* and *H. cylindracea* was investigated by dissolving *Halimeda* segments in 5% HCl and measuring the dry weights before and after $CaCO_3$ dissolution using an electronic balance (Mettler Toledo, USA; accuracy to 0.1 mg) (n = 30). After 5 weeks, calcification rate of the whole specimen was determined using the buoyant weight technique as described in Sinutok *et al.* (2011) (Jokiel *et al*. 2008). The *Halimeda* segments from each pH and temperature treatment (5 segments per sample, 4 replicates per treatment) were collected to examine the biomechanical properties of shear strength (maximum force per unit fracture area), punch strength (maximum force per unit area of punch) and punch toughness (energy per unit volume to fracture) using a penetrometer (model 5542, Instron, USA) as described in Onoda *et al*. (2008). Testing software (Bluehill 2 version 2.12, Instron, USA) was used to record the force applied to the sample and create a force-displacement curve. Shear strength, punch strength and punch toughness were then calculated from force-displacement curves (R program Version 2.12.0) according to Onoda *et al*. (2008). Shear strength determines the force applied on organic materials and calcified structures at the site of fracture and is related to grazing resistance (Sanson *et al.*, 2001; Onoda *et al.* 2008), while punch strength indicates the force applied on the area of punch and is controlled by organic tissue and the calcified structure (Onoda *et al.* 2008). Punch toughness indicates the total energy that is required to fracture and is mainly controlled by the organic, viscoelastic materials and is related to herbivore resistance (Choong *et al.* 1992).

Table 7.1: Parameters of the carbonate system; total alkalinity (TA), CO_2 partial pressure (pCO_2), dissolve inorganic carbon (DIC; CO_2, CO_3^{-2}, HCO_3^-), and saturation state of seawater with respect to calcite (Ω_c) and aragonite (Ω_a) from each pH (8.1, 7.7) and temperature (28ºC, 32ºC) treatment used in experiments. Data represent mean ± S.E. (n = 3).

Treatment		TA	pCO_2	CO_2	CO_3^{-2}	HCO_3^-	Total DIC	Ω_c	Ω_a
pH	Temp (ºC)	(mmol kg^{-1})	(µatm)	(mmol kg^{-1})	(mmol kg^{-1})	(mmol kg^{-1})	(mmol kg^{-1})		
8.1	28	2.369±0.003	388.1±0.6	0.010±0.001	0.242±0.036	1.779±0.027	2.031±0.038	5.88±0.01	3.87±0.01
8.1	32	2.302±0.005	440.2±1.1	0.010±0.002	0.235±0.055	1.726±0.041	1.971±0.046	5.71±0.01	3.76±0.01
7.7	28	2.422±0.009	1041.2±3.9	0.030±0.007	0.116±0.043	2.141±0.081	2.287±0.086	2.82±0.01	1.85±0.01
7.7	32	2.453±0.002	1055±0.7	0.030±0.002	0.118±0.008	2.169±0.015	2.318±0.016	2.85±0.01	1.88±0.01

7.2.3 Effects of ocean acidification and ocean warming on skeletal mineralogy of *Halimeda* spp.

Inductively coupled plasma mass spectroscopy (ICP-MS) and X-ray diffraction were used to investigate the Mg:Ca and Sr:Ca ratios and percentage of aragonite and Mg-calcite, respectively, on specimens maintained for 5 weeks under the previously described experimental pH and temperature treatments. Segments of *Halimeda* spp. were cleaned, rinsed with deionised water, dried and digested with 2% (w/w) nitric acid for ICP-MS analysis (Agilent Technologies 7500cs; Le Cornec & Corrège 1997). Samples (n = 4 per treatment) were introduced to the ICP-MS via a concentric nebuliser (Micromist Glass expansion) and a double pass spray chamber (Scott type) cooled to 2°C. The sample solution and the spray chamber waste were carried with the aid of a peristaltic pump. The ICP operating parameters and the lens conditions were selected to maximise the sensitivity of a 1% HNO_3:HCl solution containing 1 ng ml^{-1} of Li, Co, Y, Ce and Tl. Calibration curves were constructed and the results analysed using instrument specific software (Masshunter, Agilent Technologies).

To analyse the percentage of aragonite and Mg-calcite, segments of *Halimeda* spp. were cleaned and rinsed with deionised water, dried and ground into a powder (1-5 μm) with a mortar and pestle (n = 4 per treatment). To determine the quantities of the aragonite and Mg-calcite mineralogies, X-ray diffraction patterns were collected using a diffractometer (Siemens D5000) with a graphite post monochromator. The radiation used was copper k alpha (1.5406 angstroms) deployed at a beam power of 40 kV and 30 mA, with beam collimation consisting of a 1º divergence angle, 2 mm antiscatter slit and a 0.2 mm receiving slit. The data were acquired using a scan range of 22 to 89.5º (two theta), at a step size of 0.02º and a count time of 8 s per step. The data were then fitted using the Rietveld method and the instrument-specific software package (Siroquant v3 Sietronics, Australia) which enabled all samples to achieve a good fit with the Chi-squared values below 3 for all samples.

7.2.4 Statistical analysis

To determine if the thalli in each treatment were over-engineered (more removals than breakages) or under-engineered (more breakages than removals) (probability (p) = 0.5; α = 0.05), the numbers of uprooting and breakages were analysed using a Binomial test (R v2.14.0). To determine any significant differences (α = 0.05) among wave exposure, temperature and pCO_2 treatments, analysis of variance (ANOVA) tests were performed (SPSS v17). Tukey's Honestly Significant Difference post-hoc tests were used to identify statistically distinct groups. If data did not meet the assumptions of normality (Kolmogorov-Smirnov test) and equal variance (Levene's test), the data were transformed using $\log_{10}$ or square root.

7.3 RESULTS

7.3.1 Effects of wave motion on biomechanical and morphological properties of *Halimeda* spp.

At the exposed site, more force was required to uproot *H. macroloba* thalli (18.15±2.34 N) than at the sheltered site (10.34±1.19 N; P = 0.003; Fig. 7.1a). *H. cylindracea* displayed a similar trend (exposed: 17.27±3.49 N; sheltered: 13.78±2.13 N; P > 0.05), however, differences were not statistically significant. The force required to break thalli of the two species at the exposed site (11.80±1.46 and 11.10±1.55 N for *H. macroloba* and *H. cylindracea*, respectively) was markedly higher than for the sheltered site (4.20±1.20 and 5.84±1.25 N for *H. macroloba* and *H. cylindracea*, respectively; P values < 0.001; Fig. 7.1b). Despite some of these differences being driven by morphology (below), *H. macroloba* and *H. cylindracea* thalli from the exposed site also had significantly greater tensile strength (73.0±27.1 and 57.0±10.9 kPa, respectively) than the thalli from the sheltered site (14.6±2.6 and 29.9±7.0 kPa, respectively; P = 0.041 and 0.047; Fig. 7.1c). *H. macroloba* and *H. cylindracea* showed similar patterns in ratios of uprooting to breakages, where they were far more likely to break (i.e., the thalli were under-engineered) in the exposed site (p = 0.25 and 0.25, respectively; P = 0.023).

In the sheltered site, they were equally likely to break or uproot and thalli were neither over-engineered nor under-engineered (p = 1.14 in *H. macroloba* and p = 0.76 in *H. cylindracea*; P > 0.05).

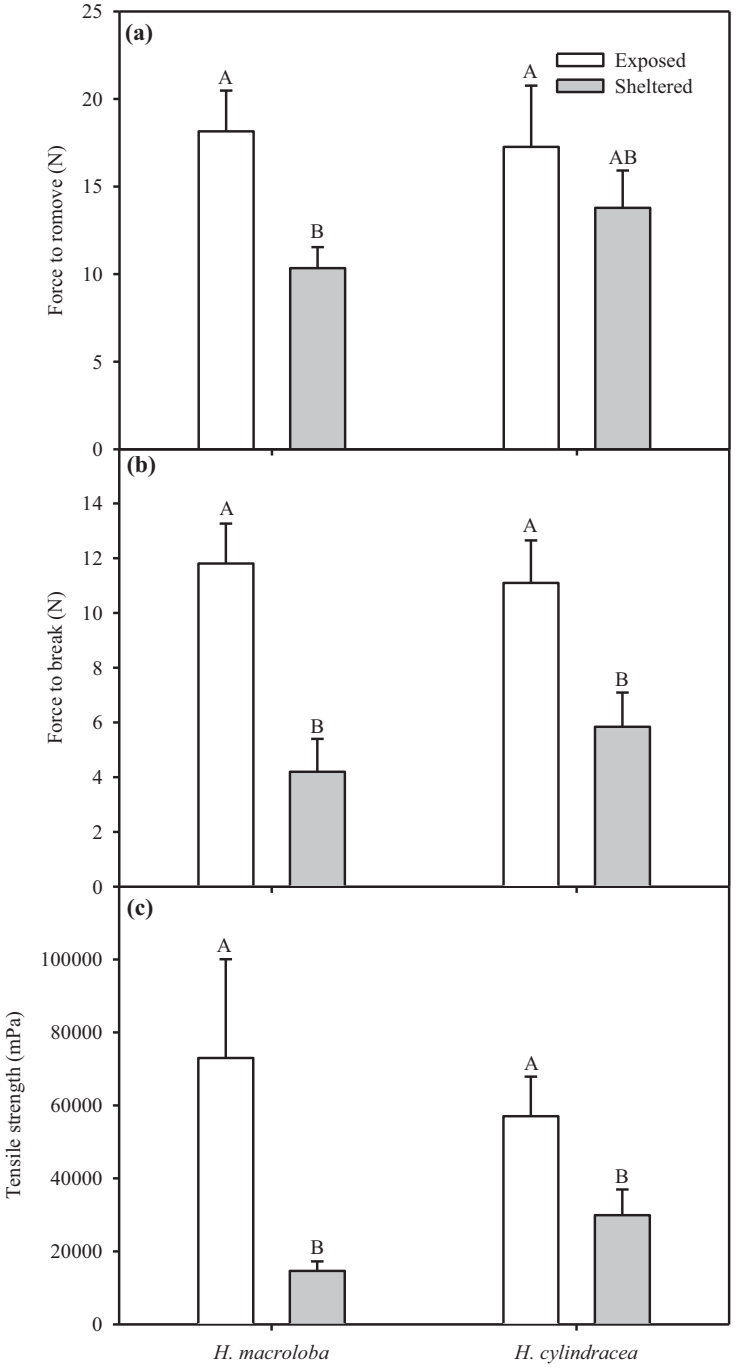

Figure 7.1: Biomechanical properties of *H. macroloba* and *H. cylindracea* from exposed (white bars) and sheltered (grey bars) sites within Heron Island lagoon. a) force required to remove (N); b) force required to break (N); and c) tensile strength (mPa). Data represent mean + S.E. (*n* = 30). A, B indicates significant differences.

H. cylindracea samples from the exposed site had larger blade surface area and holdfast volume (60.86±3.66 cm^2; 44.01±6.74 cm^3) compared to thalli found at the sheltered site (39.16±2.95 cm^2; 22.19±2.31 cm^3; $P < 0.001$ and $P = 0.005$; Fig. 7.2a,b). *H. cylindracea* from the exposed site had a significantly greater blade and holdfast dry weight (9.35±0.83 g for blade and 48.95±8.77 g for holdfast dry weight for *H. cylindracea*) than sheltered thalli (4.97±0.53 g for blade and 19.24±3.06 g for holdfast dry weight, respectively; $P < 0.001$ and $P = 0.006$; Fig. 7.2c). Larger uncalcified nodes were also found at the exposed site (5.96±0.42 vs. 4.47±0.14 mm; $P < 0.002$; Fig. 7.2d) in *H. cylindracea*. In *H. macroloba*, there were no significant differences between exposed and sheltered blade surface area and holdfast volume (49.25±3.65 and 39.34±5.74 cm^2 for blade surface area; 23.20±1.63 and 18.22±2.06 cm^3 for holdfast volume; P values > 0.05; Fig. 7.2a,b) or exposed and sheltered blade dry weight (5.19±0.49 and 4.15±0.67 g; $P > 0.05$; Fig. 7.2c). However, significantly greater holdfast dry weight was found at the exposed site (24.56±1.74 g) compared to the sheltered site (15.83±2.34 g; $P = 0.005$; Fig. 7.2c), while larger uncalcified nodes were found at the sheltered site (6.43±0.25 vs. 5.53±0.25 mm; $P = 0.015$; Fig. 7.2d). Exposure had no effect on rhizoid thickness in the holdfast of *H. macroloba* (33.4±0.6 and 32.1±0.6, respectively; $P = 0.054$) or *H. cylindracea* (33.6±0.7 and 32.1±0.6, respectively; $P = 0.407$).

In the substrate associated with *Halimeda* holdfasts, there were significant differences in sediment composition between exposed and sheltered areas ($P < 0.001$; Fig 7.3a). A significantly greater proportion of < 250 and 1000-4000 μm sediment grains were found at the sheltered site, whereas a significantly larger proportion of 250-1000 and > 4000 μm sediment grains was found at the exposed site. Significant differences in sediment composition were also found in the *Halimeda* holdfasts in exposed and sheltered sites (P values < 0.05; Fig 7.3b), but there was no significant difference between sediment composition between species (P values > 0.05; Fig 7.3b). There were greater proportions of larger sized sediment grains in the exposed site holdfasts compared to the sheltered specimens. A significantly greater proportion of < 500 μm sediment was found at the

sheltered site, whereas a significantly larger proportion of 500-2000 μm sediment was found at the exposed site (Fig 7.3b).

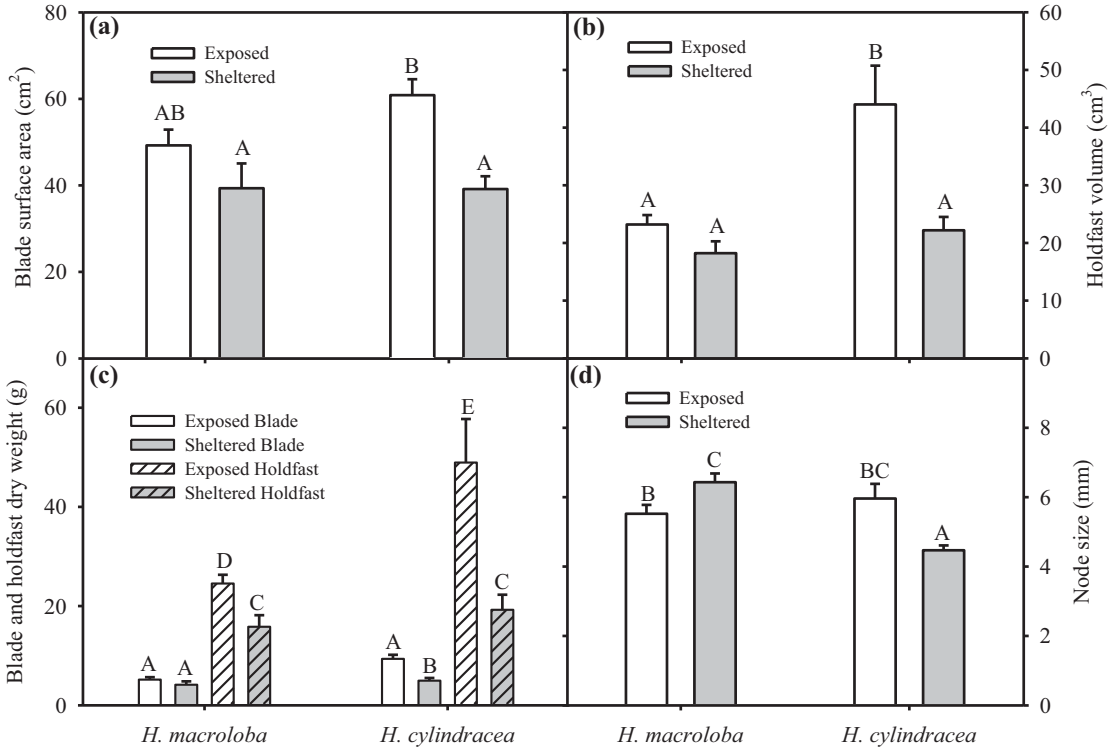

Figure 7.2: Morphological properties of *H. macroloba* and *H. cylindracea* from exposed (white bars) and sheltered (grey bars) sites within Heron Island lagoon. a) blade surface area (cm^2); b) holdfast volume (cm^3); c) blade (no cross-hatching) and holdfast (cross-hatching) dry weight (g); and D) node size (mm). Data represent mean + S.E. (n = 30). A, B, C, D, E indicates significant differences.

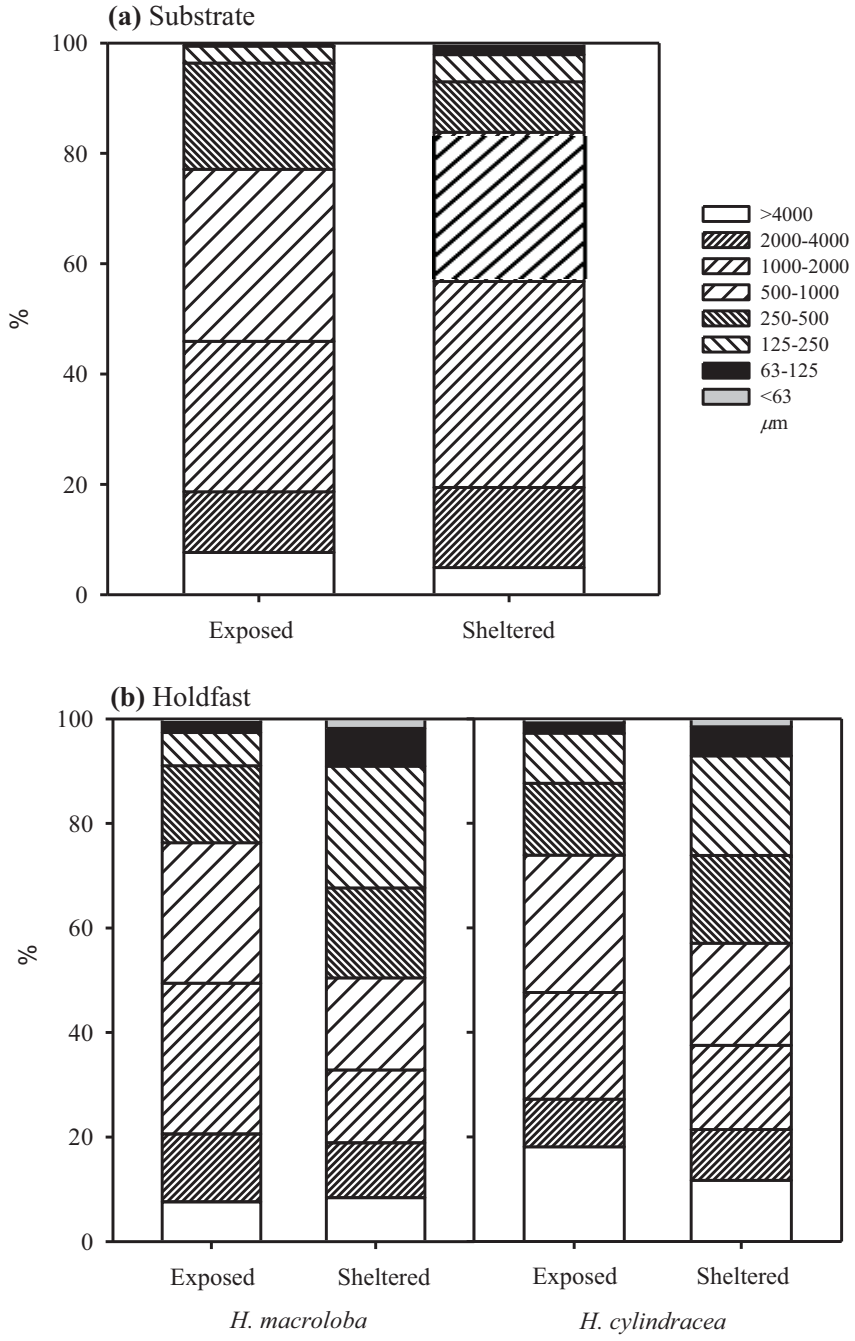

Figure 7.3: Sediment composition divided into eight size fractions (>4000, 2000-4000, 1000-2000, 500-1000, 250-500, 125-250, 63-125, and <63 μm) from the substrate (a) and trapped within the holdfast (b) of *H. macroloba* and *H. cylindracea* from exposed and sheltered sites within Heron Island lagoon. Data represent mean (n = 30).

7.3.2 Effects of ocean acidification and ocean warming on biomechanical properties of *Halimeda* spp.

Overall, *H. cylindracea* had greater calcium carbonate precipitation (86% $CaCO_3$) relative to *H. macroloba* (81% $CaCO_3$). At the end of the experiment, the calcification rates of *H. macroloba* and *H. cylindracea* were significantly greater in the control treatment and significantly reduced at pH 8.1 32ºC, pH 7.7 28°C and pH 7.7 32ºC ($P = 0.004$ and $P < 0.001$ for *H. macroloba* and *H. cylindracea*, respectively; Fig. 7.4a,b).

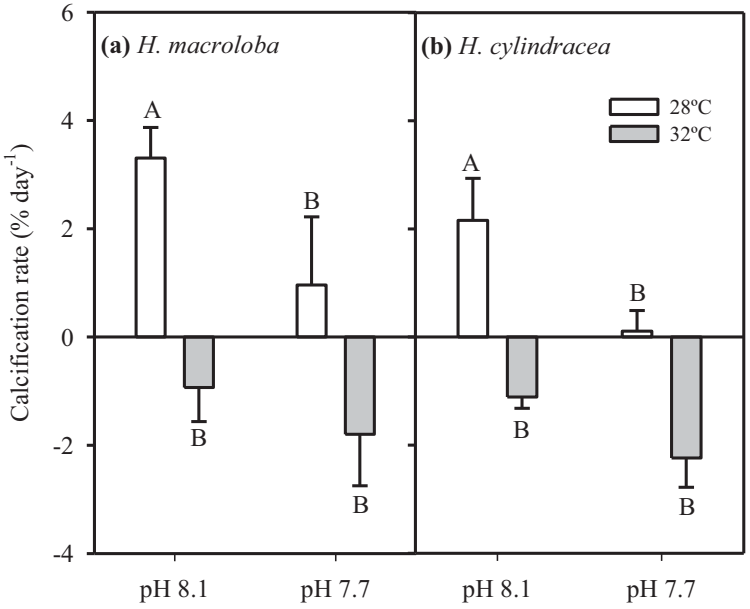

Figure 7.4: Calcification rate (% day^{-1}) over the 5 week period for *H. macroloba* (a), and *H. cylindracea* (b) at pH 8.1 and 7.7 and temperatures 28°C (white bars) and 32°C (grey bars). Data represent mean ± S.E. ($n = 4$). A, B indicates significant differences.

H. macroloba showed variable shear strength, punch strength and punch toughness under elevated CO_2 and temperature. Shear strength and punch toughness were significantly greater at high CO_2 and optimal temperature (pH 7.7 28ºC; 1.12±0.23 mPa and 2.99±1.45 J mm^{-2}; $P = 0.024$ and 0.005; Fig. 7.5a,c). However, there was no significant difference between the control, current CO_2 and elevated temperature, and

elevated CO_2 and temperature treatments in shear strength (0.80±0.12, 0.63±0.11 and 0.80±0.11 mPa; P = 0.305; Fig. 7.5a) and punch toughness (1.21±0.41, 0.72±0.22 and 1.06±0.27 J mm^{-2}; P = 0.237; Fig. 7.5c). In contrast, punch strength showed a significant reduction at elevated CO_2 and temperature (P = 0.027; Fig. 7.5b).

In *H. cylindracea*, there were significant differences between CO_2 and temperature treatments (P < 0.05; Fig. 7.5d,e,f). Shear strength and punch strength were highest in the control treatment (0.85±0.05 and 4.00±0.32 mPa), followed by the current CO_2, elevated temperature treatment (pH 8.1 32ºC; 0.22±0.03 and 1.87±0.11 mPa), elevated CO_2 with optimal temperature treatment (pH 7.7 28ºC; 0.71±0.04 and 2.66±0.13 mPa) and elevated CO_2 and temperature treatment (pH 7.7 32ºC; 0.23±0.02 and 20.6±0.13 mPa; P < 0.001; Fig. 7.5d,e). Punch toughness was significantly reduced in the 32°C treatments compared to 28°C treatments, independent of pH (pH 8.1 32ºC and pH 7.7 32ºC) (P < 0.001; Fig. 7.5f).

7.3.3 Effects of ocean acidification and ocean warming on skeletal mineralogy of *Halimeda* spp.

After 5 weeks, the Mg:Ca and Sr:Ca ratios in *H. macroloba* were significantly higher in the pH 7.7 32ºC treatment (80.9±1.9 and 30.4±2.3 mmol mol^{-1}) compared to the control (pH 8.1 28ºC; 40.6±3.3 and 24.2±0.4 mmol mol^{-1}, respectively; P < 0.001; Fig. 7.6a). In *H. cylindracea*, the Sr:Ca ratio was significantly lower under elevated CO_2 and temperature conditions, with values of 26.2±0.5 mmol mol^{-1} in the control (pH 8.1 28ºC) and 19.3±0.9 mmol mol^{-1} in the pH 7.7 32ºC treatment (P < 0.05; Fig. 7.6b).

X-ray diffraction analysis showed that the $CaCO_3$ polymorph in *H. macroloba* and *H. cylindracea* varied with pH and temperature. Approximately 98-100% of $CaCO_3$ was aragonite in all samples, with the remainder identified as Mg-calcite. The percentage of Mg-calcite in *H. macroloba* was significantly higher in the elevated CO_2 and optimal temperature treatment (pH 7.7 28ºC; 1.58±0.54%) than in other treatments (P = 0.037; Fig. 7.7). In *H. cylindracea*, the Mg-calcite percentage was significantly greater in the

elevated temperature and CO_2 treatment (pH 7.7 32ºC; 1.00±0.29%) (P = 0.011; Fig. 7.7).

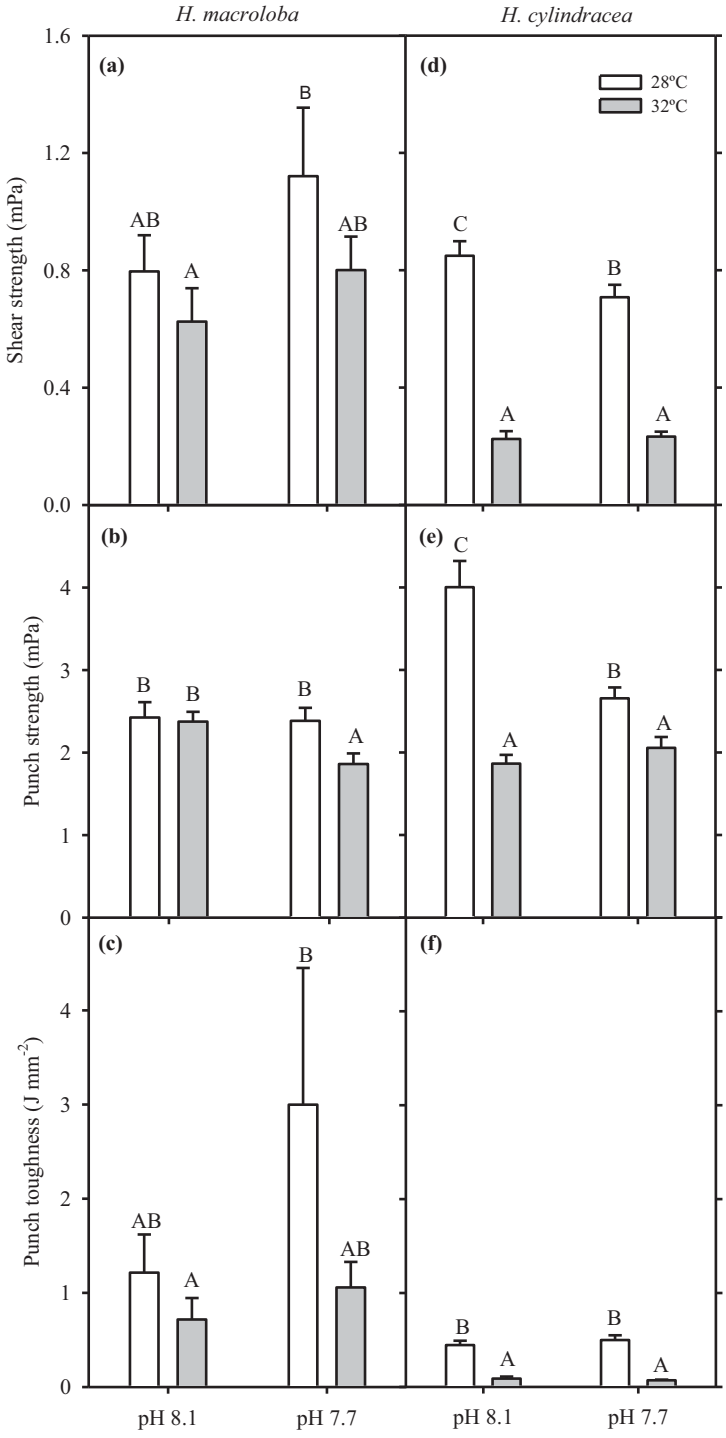

Figure 7.5: Biomechanical properties of (shear strength (mPa) (a,d), punch strength (mPa) (b,e) and punch toughness (J mm^{-2}) (c,f) from *H. macroloba* and *H. cylindracea* at pH 8.1 and 7.7 and temperatures 28°C (white bars) and 32°C (grey bars). Data represent mean + S.E. (*n* = 4). A, B, C indicates significant differences.

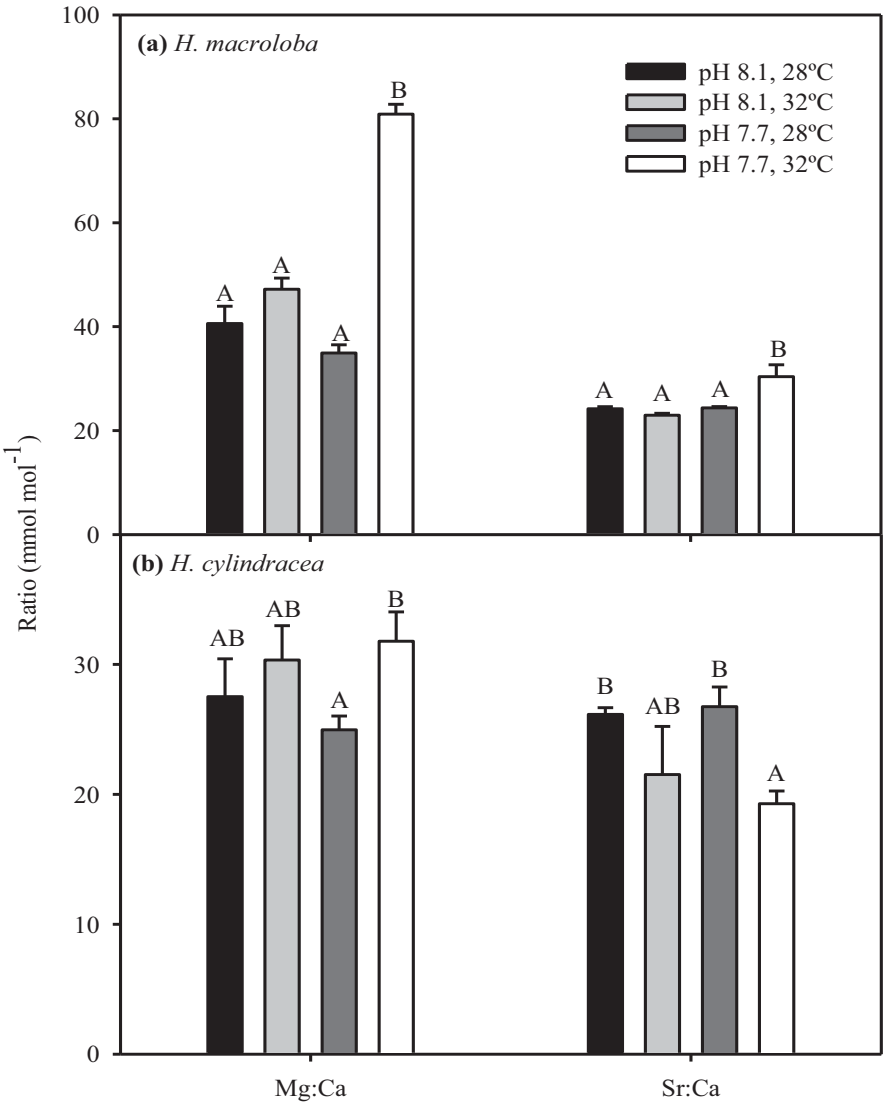

Figure 7.6: Mg:Ca and Sr:Ca ratios (mmol mol^{-1}) from *H. macroloba* (a) and *H. cylindracea* (b) in each of the two pH and two temperature treatments. Data represent mean + S.E. (n = 4). A, B indicates significant differences.

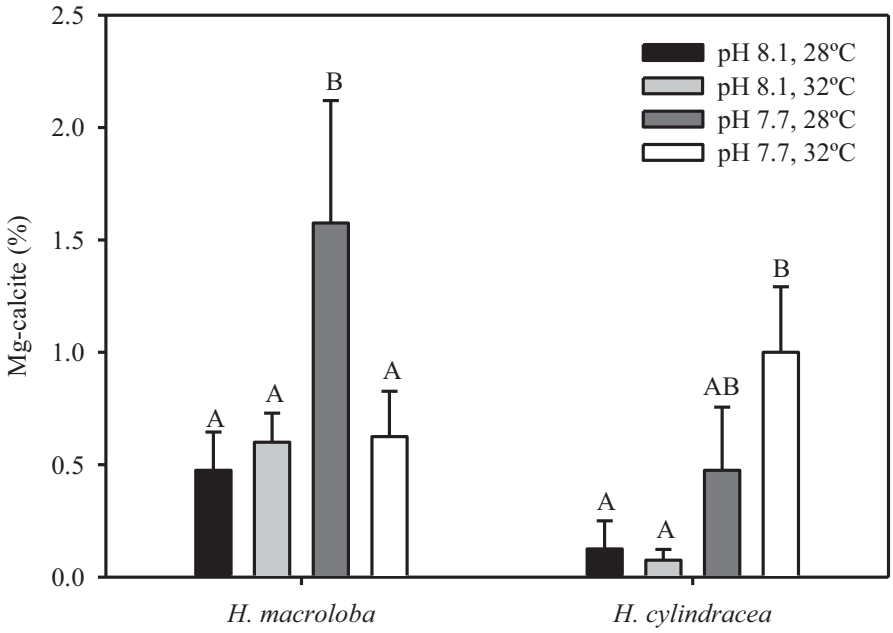

Figure 7.7: Percentage of Mg-calcite from *H. macroloba* and *H. cylindracea* in each of the two pH and two temperature treatments. Data represent mean + S.E. (n = 4). A, B indicates significant differences.

7.4 DISCUSSION

The most significant finding of this study was that *Halimeda* has an intrinsic capacity to withstand hydrodynamic exposure, as shown by the phenotypic differences in architecture and mechanical strength of thalli from different habitats. *H. macroloba* and *H. cylindracea* thalli consist of calcified segments joined together by uncalcified nodes which form a branching chain and a massive bulbous holdfast attached to sand particles (Verbruggen, 2005; Anderson *et al*., 2006) allowing their thalli to be flexible to avoid breakage and remain in the sediment. Wave exposure influences the thallus engineering such that the above ground thallus / below ground holdfast varied with the environment. Experimentation revealed that temperature was the main factor influencing calcification and led to the dissolution of the calcium carbonate skeleton. There was however a

combined effect of temperature and CO_2 on the calcification of both *Halimeda* species, leading to higher risk of thallus breakage or removal from the substrate under future climate change scenarios.

7.4.1 Adaptations of *Halimeda* to wave exposure on coral reefs

Water motion is an important physical parameter influencing morphology and distribution of algae (Carrington, 1990; Pratt & Johnson, 2002). Intertidal macroalgae reduce hydrodynamic forces imposed on their thalli by bending and changing their morphology to reduce drag (Boller & Carrington 2006; Martone *et al*. 2010). Our results showed that several external (e.g. sediment compaction, wave exposure) and internal (e.g., thallus morphology, thallus strength, degree of calcification) factors determine the likelihood of algal uprooting or breaking. Water motion influenced the biomechanical properties of *Halimeda* spp. At the exposed site, more force was required to remove *H. macroloba* thalli from the substratum and more force was required to break *H. macroloba* and *H. cylindracea* thalli (Fig. 7.1). In addition, tensile strength of these species at the exposed site was significantly greater than those at the sheltered site (Fig. 7.1). The greater force to remove is likely to be a result of larger holdfast volume at the exposed site (Fig. 7.1, 2b; DeWreede 2006), but was concomitant with a larger blade and node size in *H. cylindracea*. However, in *H. macroloba* the only differences between sites were the heavier holdfasts and smaller node size in exposed thalli. Although there were no differences in blade area between these species, the differences in segment size and shape (cylindrical shape in *H. cylindracea* and lobed shape in *H. macroloba*) and holdfast volume may lead to different drag force and therefore different impacts from wave motion. The cylindrical shape of *H. cylindracea* may result in a lower drag coefficient and lower drag force than the lobe shape of *H. macroloba* (Denny 1988), suggesting that *H. macroloba* may be more vulnerable to drag.

Anderson *et al*. (2006) found more force was required to remove *H. gracilis* with a large thallus surface area from the substratum compared to individuals with a smaller thallus surface area. In general, *Halimeda* thalli display flattened, calcified segments joined by

uncalcified nodes (Hillis-Colinvaux 1980). These morphological features, along with low stiffness (resistance to deformation) and low tensile strength (compared to other biological materials, e.g., wood, shell and bone; Denny *et al*. 1989) lead to higher flexibility in these macroalgae, thus increasing their ability to cope with mechanical forces (Denny *et al*. 1989; Martone *et al*. 2010). This characteristic is also found in other coenocytic algae such as the tropical green algae *Penicillus dumetosus* and *P. pyriformes* which are upright and flattened perpendicular to the direction of incoming waves (DeWreede 2006). The segmentation in *Halimeda* allows their thalli to bend, reconfigure and avoid breakage and removal (Martone & Denny 2008*a*, 2008*b*; Martone *et al*. 2010). Flattening and bending may lead to reduced destructive torsion (rotational) forces and decreasing drag forces on their thalli (DeWreede 2006). However, *Halimeda* are only flexible at the joint, rather than the whole thallus like fleshy algae. Greater deposition of calcium carbonate in *H. cylindracea* (86% $CaCO_3$) relative to *H. macroloba* (81% $CaCO_3$) may contribute to greater stiffness and tensile strength resulting in greater damage or removal by wave motion. In addition, the force required to remove may be influenced by several other factors, such as holdfast surface area, rhizoid strength, and external factors such as sediment shear strength and compaction of sediments where the holdfast is attached. Thus, a site with a higher degree of wave exposure and compact sediments may result in a smaller holdfast plug than counterparts in sheltered areas with a looser substrate (Anderson *et al*. 2006).

For both species, the number of uprootings versus breakages were equal at the sheltered site suggesting that the thallus in the sheltered site is neither over-engineered nor under-engineered and is dependent on sediment composition, an external factor. In contrast, *Halimeda* thalli were more likely to break at the exposed site, suggesting that thallus strength is the factor limiting plant integrity (an organism controlled factor and under natural selection) and the thallus is under-engineered. These findings are different from an investigation of *H. incrassata*, where in situations of stress, whole individuals detached from the substratum rather than the thallus breaking (DeWreede 2006). The dislodgement of whole *Halimeda* individuals is fatal as they have no ability to re-attach

(Anderson *et al*. 2006), however *Halimeda* fragments from breakages are able to re-attach and generate a new thallus via vegetative reproduction (Walters & Smith 1994; Walters *et al*. 2002; DeWreede 2006). Consequently, breakages rather than uprootings in an exposed site are likely to be an advantage to survive under hydrodynamic forces, suggesting increased fitness of under-engineered thalli.

In addition, the sediment composition of the substrate and *Halimeda* holdfasts were significantly different between the exposed and sheltered areas. It is likely that the sediment accumulation in holdfasts is a result of sediment selection by the alga. In *Halimeda*, the sediment selection process may be partially dependent on the availability of sediment size in the substrate, rhizoid thickness, the capacity for rhizoid sediment selection and accumulation and other unknown factors. In addition, the sediment selection may be advantageous in increasing sediment compaction and holdfast strength (holdfast tenacity) for increasing their capacity to attach to the sediment. These results showed that there was no significant difference in rhizoid thickness between individuals at exposed and sheltered sites and that may indicate that several factors influence sediment selection.

7.4.2 Impact of climate change to biomechanical properties of *Halimeda*

Elevated CO_2 and temperature have been shown to have a negative effect on calcified organisms by decreasing the availability of carbonate ions (CO_3^{2-}) and reducing their ability to produce the calcium carbonate skeletons (Feely *et al*. 2004; Sinutok *et al*. 2011). Our results showed a negative rate of calcification in both species of *Halimeda* under current CO_2, and elevated temperature (pH 8.1 32ºC) and elevated CO_2 and temperature (pH 7.7 32ºC) treatments (Fig. 7.4). This result suggests that temperature was the main factor influencing calcification and led to the dissolution of the calcium carbonate skeleton (negative growth; Fig. 7.4). In the more heavily calcified species, *H. cylindracea*, a reduction in shear strength and punch strength was found in all treatments compared to the control (Fig. 7.5). Punch toughness in this species was also found to decrease after exposure to elevated temperature, independent of pH.

A recent study on *Halimeda* calcification using environmental scanning electron microscopy revealed that aragonite crystal width decreased when exposed to elevated CO_2 (pH 7.7 and 7.4) and temperature (32 and 34ºC) (Sinutok *et al*. 2011). Reductions in strength and toughness of *Halimeda* may be related to this decrease in the calcium carbonate crystal size and the decline in calcification. We suggested that the morphological (e.g., branching, percentage of $CaCO_3$, segment thickness) and anatomical (e.g., utricle, siphon pattern, intercellular space size, the fusion of the siphons between node and segment) characteristics of the algae could lead to differences in physiological and biomechanical properties (toughness and strength). The differences in the magnitude of biomechanical properties of these species to elevated CO_2 and temperature may be due to anatomical, morphological and physiological differences. The influence of other material properties, such as xylan content, may also play a role, although this is yet to be investigated.

7.4.3 Shifts in *Halimeda* skeletal mineralogy in response to climate change

CO_2 and temperature are known to influence the calcium carbonate precipitation in marine calcifying organisms, e.g., corals, foraminifera and calcifying algae (Gao *et al*. 1993*b*; Gattuso *et al*. 1998; Reynaud *et al*. 2003; Anthony *et al*. 2008; Sinutok *et al*. 2011). Ries (2006) observed that the Mg:Ca ratio in the crustose coralline alga *Neogoniolithon* sp. is related to the Mg:Ca of surrounding seawater. Ries (2011) also found that the Mg:Ca ratio in some high-Mg calcite species (serpulid worm, *Hydroides crucigera* and red alga, *Neogoniolithon* sp.) varied with CO_2, suggesting that CO_2 concentration has an impact on skeletal mineralogy in some, but not all, marine calcifiers. The incorporation of Mg^{2+} and Sr^{2+} into the aragonite and calcite crystal structure is controlled by several environmental and biological factors, such as temperature, pH, and salinity; however the exact mechanisms are yet to be resolved (Littler 1972; Weber, 1973; Berger *et al*., 1997; Cohen *et al*. 2001; Reynaud *et al*. 2007; Cohen *et al*. 2009). The concentrations of Mg^{2+} and Sr^{2+} in the aragonite-depositing alga *Bornetella sphaerica* were found to positively correlate with temperature. Chave (1954) also observed more Mg^{2+} incorporation with increasing temperature in several marine

algae. In the coral genus *Acropora*, a 30% increase in the Mg:Ca ratio was observed when temperature increased from 21 to 29ºC and a 9% increase was found when light intensity increased from 100 to 400 μmol photons m^{-2} s^{-1} (Reynaud *et al*. 2007). However, there was a 4.5% decrease in the Sr:Ca ratio with increasing temperature and no significant change in response to irradiance. These findings suggest there is a strong biological control over the incorporation of Mg^{2+} and Sr^{2+} in some marine calcifiers (Reynaud *et al*. 2007).

The causes of changes in Mg:Ca and Sr:Ca ratios with temperature and CO_2 are not well known (Cohen *et al*. 2001; Cohen *et al*. 2009; Ries 2011b). Several studies suggested that the Mg:Ca ratio increases and Sr:Ca ratio decreases with increasing calcification rate (Weber 1973; Cohen & Gaetani 2010). Sr^{2+} is larger and heavier than Ca^{2+} so it may diffuse to the calcification site more slowly than Ca^{2+}. As a consequence, species with high calcification rates could have lower Sr^{2+} incorporation (Weber 1973). However, some studies suggest that Mg:Ca and Sr:Ca ratios in coral are independent of the skeletal growth rate (Wei *et al*. 2000; Mitsuguchi *et al*. 2003). My results showed varied responses - there was an increase in Mg:Ca and Sr:Ca ratios in *H. macroloba* and a decrease in Sr:Ca under the elevated CO_2 and elevated temperature treatment (pH 7.7, 32ºC) where the calcification rate was reduced. These results may suggest that under CO_2 and temperature stress, the calcification process at the ionic level in these species was disrupted and these changes in Mg:Ca and Sr:Ca ratios were due to biological effects (such as Ca^{2+} ATPase (Ca^{2+} transport enzyme) and calcification rate) influenced by environmental conditions (Marshall & McCulloch 2002).

Ries (2011b) studied the % Mg-calcite in species which are known to precipitate their $CaCO_3$ skeleton with > 97% aragonite (e.g., *Halimeda incrassata* and the temperate coral *Oculina arbuscula*) and found that there were no changes in % calcite under elevated CO_2 treatments (pH 7.48-8.03). However, the proportion of high to low Mg-calcite (i.e., more and less soluble phases of $CaCO_3$) increased with increasing CO_2 in organisms producing comparable proportions of calcite and aragonite (i.e., the calcareous serpulid worm *Hydroides crucigera* and the whelk *Urosalpinx cinerea*,

respectively) (pH 7.42-8.03) (Ries 2011b). The differences between these organisms may be related to their plasticity to elevated CO_2 conditions. In contrast to Ries (2011b), my findings show an increase in the percentage of the less soluble low Mg-calcite under elevated CO_2 conditions. Both *Halimeda* species were comprised of > 97% aragonite with the magnitude of changes in low Mg-calcite and aragonite less than 2%. It is likely that the inconsistency between Ries (2011b) and our study may be explained by differences in the resolution of X-ray diffraction methods. Here, our resolution was 0.1%, while the detection limit of Ries (2011b) method was 3%. Our data suggest that *Halimeda* spp. could respond to elevated CO_2 conditions by producing more, less soluble low Mg-calcite. Changes in the mineralogy of calcium carbonate have also been observed in several studies in response to the surrounding seawater (Stanley *et al*. 2002; Ries 2005; Stanley *et al*. 2010). The high Mg-calcite species *Amphiroa* spp. was found to produce low Mg-calcite when exposed to low Mg:Ca seawater and the Mg:Ca ratio of the calcite in *H. incrassata* increased with high Mg:Ca seawater, suggesting that the Mg:Ca ratio in the surrounding water strongly influences the $CaCO_3$ precipitation in these calcifying algae (Stanley *el. al*. 2002; Stanley *et al*. 2010).

7.4.4 Ecological implications

In shallow reef habitats, *Halimeda* are known to be consumed by herbivorous fish such as parrotfish (Earle 1972; Mathieson *et al.* 1975; Wolf 1985; Paul & Van Alstyne 1988). However, *Halimeda* has two defensive mechanisms to protect against herbivores: 1) producing the diterpenoids, Halimedatrial and Halimedatetraacetate, as a chemical defense (Paul & Fenical 1984, 1986), and 2) calcifying as a structural defense (Paul & Fenical 1984, 1986; Paul & Van Alstyne 1988). Newly produced segments contain a high concentration of defensive chemicals, however, after 16 hours when the segment is fully calcified (Hay *et al*. 1988), the concentration of defensive chemicals decreases and the structural defence increases (Hay *et al*. 1988). Padilla (1989, 1993) suggested that calcification strengthens the thallus and minimizes the probability of tissue loss from herbivory damage. As a consequence, decreases in calcification, strength and toughness in *Halimeda* due to ocean acidification and ocean warming may lead to increasing

susceptibility to herbivory. Although *H. macroloba* may be more vulnerable to drag under increasing flow velocity, more heavily calcified species, *H. cylindracea* may be more vulnerable to ocean warming and acidification. In addition, under the predicted increase in storm severity, with intensity increases of 2-11% by 2100 (Walsh & Ryan 2000; Knutson & Tuleya 2004; Emanuel 2005; Knutson *et al*. 2010), my results suggested the weakened structure of both species of *Halimeda* would increase the risk of thallus breakage or removal from the substrate.

7.4.5 Conclusions

These findings suggest that these two species of calcifying macroalgae are highly sensitive to the future climate change scenarios of elevated temperature and more acidic oceans, and that *Halimeda* may be one of the "losers" under future climate change. As this species is a dominant sediment producer and ecosystem/habitat engineer, the loss of these marine species may decrease the sediment turnover rate and the carbonate sand availability in the marine environment. In addition, it may affect other associated species such as herbivorous fish and invertebrate communities (Diaz-Pulido *et al.* 2007; Kleypas & Yates 2009). Shifts in community structure may occur and the reefs may be dominated by non-calcifying macroalgae, which are expected to benefit from future climate change (Gao *et al*. 1993*a*). There is also great potential for cascading effects on trophic interactions and habitat availability for other coral reef organisms.

CHAPTER 8:

GENERAL DISCUSSION

8.0 GENERAL DISCUSSION

8.1 SUMMARY OF EXPERIMENTS TO DETERMIN THE IMPACTOF OCEAN ACIDIFICATION AND OCEAN WARMING ON ARAGONITE AND MG-CALCITE SPECIES

This thesis represents the first research to provide insight into the combined effect of elevated CO_2 and temperature on two important coral reef sediment producers: the aragonite-depositing species of macroalga *Halimeda* spp. and the Mg-calcite-depositing species of foraminifera, *Marginopora vertebralis*. Responses were determined in terms of photosynthetic performance, calcification, skeletal mineralogy and biomechanical integrity. The research was performed at a variety of scales: from individuals to the microenvironmental boundary layer and intracellular scales. This study uses innovative methodologies, such as a microsensor technique, a penetrometer, inductively coupled plasma mass spectroscopy (ICP-MS) and X-ray diffraction, to examine for the first time the effects of ocean acidification and ocean warming on the microenvironmental changes in *Halimeda* and foraminifera and the mechanical integrity and skeletal mineralogy of two common and widespread species of *Halimeda*. IPCC predicted emission scenarios (A1F1; pCO_2 ~1000 µatm; pH ~7.7 in 2100) were used for these studies and this will be useful for predicting the impact of ocean acidification and warming on important aragonite- and Mg-calcite-depositing species on coral reefs in the near future under climate change.

8.1.1 Effects on primary production

Photosynthetic efficiency, pigmentation and productivity of *H. macroloba*, *H. cylindracea* and *M. vertebralis* under elevated CO_2 and temperature were investigated using chlorophyll *a* fluorescence, spectrophotometry and oxygen microsensors from a number of experiments to understand on how ocean acidification and warming affect primary production of these species. Photosynthesis in *Halimeda* spp. and *M. vertebralis* were investigated at both an organism scale (PAM fluorometry and oxygen optode) and

a microscale (O_2 microsensor). O_2 microsensor techniques allow for mapping of the physico-chemical microenvironment of these species at high a spatio-temporal resolution (De Beer and Larkum 2001; Köhler-Rink and Kühl 2005). PAM fluorometry allows the measurement of PSII photochemical efficiency and determination of the onset of stress in photosynthetic organisms (Silva et al. 2009). Ocean acidification and warming caused negative impacts on photosynthetic efficiency (F_V/F_M, Y(II)) and pigmentation (Chl *a* and *b* in *H. macroloba* and *H. cylindracea* and Chl *a* and c_2 in *M. vertebralis*) after 5 weeks (Chapter 4, 5, 6; Sinutok et al. 2011). Data from the study using O_2 microsensors (Chapter 5, 6) showed that 5 weeks of exposure to elevated CO_2 and temperature decreased the gross photosynthesis and O_2 flux of *H. macroloba* and *H. cylindracea*. These results are in agreement with previous measurements (Chapter 4), which used a respirometry chamber. Here, 35 days of exposure to elevated CO_2 and temperature led to a decrease in primary productivity in these species, suggesting that microscale photosynthesis and respiration influence the primary productivity of the whole organism. These results indicated chlorophyll degradation, decreased photosynthetic unit size, a decrease in the number of PSII reaction centers and a loss of functional PSII units, down-regulation of photochemistry and/or photoinhibition leading to less capacity for light absorption and photosynthesis (Chapter 4; Sinutok et al. 2011). Increases in the maximum excitation pressure (Q_m), an indicator of non-photochemical quenching under the high CO_2 and temperature treatment (pH 7.7, 32ºC) indicates potential for photoinhibition (Chapter 5, 6; Iglesias-Prieto et al. 2004). Exposure to either elevated temperature or elevated CO_2 both reduced photosynthesis of these species. There was also a strong additive effect of elevated temperature and pH on photosynthesis in these species (Chapter 4; Sinutok et al. 2011). Heat stress is likely to damage PSII, by damaging the D1 protein and disrupting the thylakoid membrane stability (Allakhverdiev et al. 2008), whereas pH stress may disrupt the CO_2 accumulation pathway at the site of Rubisco or interfere with electron transport via the thylakoid proton gradients (Anthony et al. 2008; Sinutok et al. 2011). The production of reactive oxygen species in PSII (Talge and Hallock 2003) and the disruption of photoprotective mechanism such as the xanthophyll cycle (Anthony et al. 2008) may

also occur under pH and thermal stress.

In foraminifera, the bleaching and subsequent death under elevated CO_2 and temperature (all except control CO_2 and 28 and 30ºC) suggested that symbionts were expelled or damaged through photoinhibition (Chapter 4; Hallock et al. 2006; Sinutok et al. 2011). These results are consistent with the study which demonstrated thermal stress triggered bleaching in the foraminifera *Amphistegina gibbosa* (Talge and Hallock 2003). Bleaching in foraminifera was caused by the deterioration of symbionts and host endoplasm degradation, which was triggered by several stressors including high irradiance, ultraviolet radiation, salinity, temperature and CO_2 (Talge and Hallock 1995; 2003; Sinutok et al. 2011), and can be assessed by a decline in PSII chemical efficiency (F_V:F_M), symbiont density and chlorophyll concentration (Schmidt et al. 2011). Talge and Hallock (2003) observed pseudopodial activity in bleached foraminifera, indicating that the host ectoplasm continues to feed and produce new chambers. Unbleached foraminifera can gain energy from autorophic nutrition, but the bleached foraminifera must rely on heterotrophic feeding to meet metabolic demands. The broken shells observed in bleached foraminifera indicated that photosynthate from algal symbionts is essential for host shell maintenance and construction (Toler and Hallock 1998).

Halimeda has an ability to utilise HCO_3^{2-} for photosynthesis (Borowitzka and Larkum 1976b). Rising pCO_2 leads to an increase in dissolved CO_2 and HCO_3^{2-} availability surrounding the organisms and may result in enhanced photosynthesis (Gao et al. 1993b). This research, however, showed that elevated CO_2 led to a decrease in productivity (O_2 production; Chapter 4, 5, 6; Sinutok et al. 2011). This suggested that these *Halimeda* species may not be carbon-limited or there is down-regulation of Rubisco and the carbonic enhydrase (CA) enzyme (Sobrino et al. 2009; Raven et al. 2011).

8.1.2 Effects on calcification

Negative calcification rates were observed in all species tested when exposed to elevated CO_2 (Chapter 4, 5, 6; Sinutok et al. 2011). The combination of heat and CO_2 stress caused an increased inhibition of calcification rate as well as dissolution of the $CaCO_3$ structure. Rising CO_2 will inhibit calcification by decreasing availability of CO_3^{2-} ions, which are required for $CaCO_3$ deposition and result in a decreased aragonite and calcite saturation state (Furla et al. 2000; Feely et al. 2004; Ries 2011a,b). Increasing temperature beyond optimum levels for these species had a negative impact on calcification, possibly by decreasing enzyme activity and photosynthetic CO_2 fixation (Borowitzka 1986; Hallock 2000; Gonzalez-Mora et al. 2008; Sinutok et al. 2011). Thinner aragonite and calcite crystals were observed in *H. macroloba* and *H. cylindracea* when exposed to high CO_2 (pH 7.7 and 7.4) and in *M. vertebralis* when exposed to elevated CO_2 and temperature (pH 7.7 and 7.4, and 32 and 34ºC). There was also an increase in crystal density in *M. vertebralis* under high CO_2 and elevated temperature (7.9, 7.7 and 7.4, and 32 and 34ºC) (Chapter 4; Sinutok et al. 2011). A previous study on *H. opuntia* and *H. tuna* found a reduction in crystal width and an increase in crystal abundance with decreasing pH, which indicated that crystallisation may be initiated and terminated more frequently with increasing CO_2 (Robbins et al. 2009). My findings suggested that the decline in CO_3^{2-} ion availability under elevated CO_2 is likely to be the main factor affecting calcification rate and crystallisation in these species (Chapter 4, 5, 6; Sinutok et al. 2011). Under predicted increases in pCO_2 and temperature in the near future, this study suggests that the rate of calcification of two major groups of sediment-producers, *Halimeda* and foraminifera, will decline. As a consequence, there will be a decrease in the sediment turnover rate and the amount of carbonate sands in the marine environment of coral reefs.

8.1.3 Link between photosynthesis and calcification

It has been proposed that calcification promotes photosynthesis by providing a proton source through $CaCO_3$ precipitation, which produces H_2O and CO_2 (Borowitzka 1989;

McConnaughey 1989; McConnaughey and Whelan 1997). On the other hand, photosynthetic CO_2 uptake by the enzyme Rubisco in the Calvin cycle elevates intracellular pH and CO_3^{2-} content, promoting calcification (McConnaughey 1989). pH and O_2 at the diffusion boundary layer (DBL) surrounding *Halimeda* and foraminifera has been shown to increase due to CO_2 uptake for photosynthesis in the light. In contrast, during darkness and photoinhibitory light exposure (>570 µmol photon m^{-2} s^{-1}), pH and O_2 at the DBL decreased due to CO_2 and H^+ release from respiration and calcification (Chapter 5, 6; Köhler-Rink and Kühl 2000; De Beer and Larkum 2001). For these results, a reduction in primary productivity and O_2 concentration at the specimen surface when exposed to elevated CO_2 and temperature could lead to a decrease capacity for photosynthesis to elevate pH at the surface and inhibit calcification (Chapter 5, 6; De Beer and Larkum 2001; Satoh et al. 2001; Köhler-Rink and Kühl 2001, 2005). This study suggests that calcification in these particular species is closely coupled with photosynthesis (chapter 5, 6). Two species of scleractinian coral have been found to survive under acidic conditions (pH 7.3-7.6), maintaining endosymbiont photosynthesis without calcium carbonate skeletons (Fine and Tchernov 2007). *Halimeda* and foraminifera under elevated CO_2 and temperature conditions may not be able to respond like corals (Fine and Tchenov 2007), due to a decrease in productivity and calcification and a close link between photosynthesis and calcification observed in this study. This prediction is supported by a lack of *Halimeda* and foraminifera at volcanic vents off Ischia Island, Italy and in Papua New Guinea (pH < 7.7 amd Ω_a < 2.9; Hall-Spencer et al. 2008; Dias et al. 2010; Fabricius et al. 2011).

8.1.4 Effects on skeletal mineralogy

During $CaCO_3$ precipitation, elements such as strontium (Sr^{2+}) and magnesium (Mg^{2+}) are incorporated into the $CaCO_3$ matrix (Dissard et al. 2010). The degree of elemental incorporation is controlled by several environmental and biological factors, such as temperature, pH, salinity, calcification rate, and the Mg^{2+} and Sr^{2+} contents in seawater (Chave 1954; Littler 1972; Weber 1973; Berger et al. 1997; Cohen et al. 2001; Ries 2006; Reynaud et al. 2007; Cohen et al. 2009; Ries 2011b). However, the response of

Mg:Ca and Sr:Ca ratios to these factors varied between species suggesting several additional factors may influence the Mg^{2+} and Sr^{2+} incorporation. Ries (2006) observed that the Mg:Ca ratio in the crustose coralline alga *Neogoniolithon* sp. is related to the Mg:Ca of surrounding seawater. Ries (2011b) also found that the Mg:Ca ratio in some high-Mg calcite species (calcifying serpulid worm *Hydroides crucigera* and red alga, *Neogoniolithon* sp.) varied with CO_2, suggesting that CO_2 concentration has an impact on skeletal mineralogy in some, but not all, marine calcifiers. This research on *Halimeda* observed varied responses with an increase in Mg:Ca and Sr:Ca ratios in *H. macroloba* and a decrease in Sr:Ca ratio in *H. cylindracea* under elevated CO_2 and temperature (pH 7.7, 32ºC) (Chapter 7). Little is known about mechanisms of change in Mg:Ca and Sr:Ca ratios. In the aragonite-depositing alga *Bornetella sphaerica*, Mg^{2+} and Sr^{2+} concentrations were found to be positively correlated with temperature. Mg:Ca ratio in the coral genus *Acropora* increased with increasing temperature and light intensity but the Sr:Ca ratio decreased with increasing temperature (Reynaud et al. 2007). Some studies with coral have suggested that Mg:Ca and Sr:Ca ratios are independent of the skeletal growth rate (Wei et al. 2000; Mitsuguchi et al. 2003). However, several studies found that Mg:Ca ratio increased and Sr:Ca ratio decreased with increasing calcification rate (Weber 1973; Cohen and Gaetani 2010). Our results suggested that that the crystallization and calcification process at the ionic level in these species were disrupted and these changes in elemental ratios may be due to biological effects (such as Ca^{2+} transport enzyme Ca^{2+} ATPase and calcification rate) which is influenced by environmental conditions (such as pH and temperature) (Marshall and McCulloch 2002).

Environmental parameters, such as Mg and Sr concentrations in seawater, were found to influence the production of $CaCO_3$ polymorphs in several species (Stanley et al. 2002; Ries et al. 2006; Stanley et al. 2010). This research showed that both *Halimeda* species produced more, low Mg-calcite under elevated CO_2 conditions (Chapter 7), and suggested that *Halimeda* spp. could respond to elevated CO_2 by producing more of the low soluble $CaCO_3$ polymorph. This plasticity in $CaCO_3$ precipitation will provide a

greater capacity to cope with a high CO_2 environment and may lead to less $CaCO_3$ dissolution. These findings are consistent with other studies on scleractinian corals producing aragonite, which can produce calcite in artificial seawater with an ambient Mg:Ca ratio that favours the precipitation of the calcite polymorph (Ries et al. 2006). The high Mg-calcite alga *Amphiroa* sp. was able to produce low Mg-calcite when exposed to low Mg:Ca seawater and the Mg:Ca ratio of the calcite in *H. incrassate* increased with high Mg:Ca surrounding seawater (Stanley et al. 2002; Stanley et al. 2010). These findings suggested that the skeletal mineralogy of calcifying organisms is partially controlled by the seawater chemistry and the Mg:Ca ratio in the surrounding environment which strongly influences the $CaCO_3$ precipitation in these calcifying algae (Stanley et al. 2002; Ries et al. 2006; Stanley et al. 2010).

The degree of impact by elevated CO_2 and temperature on calcification is influenced by the calcium carbonate polymorph (Kleypas et al. 1999). The decrease in crystal width and the increase in crystal density in *M. vertebralis*, when compared to *H. macroloba* and *H. cylindracea* (Chapter 4; Sinutok et al. 2011), showed that the aragonite-depositing species *Halimeda* performed better than Mg-calcite-depositing benthic foraminifera under high CO_2 and temperature conditions. This finding is consistent with the prediction of Kleypas et al. (1999) based on calcium carbonate saturation state where the saturation state of aragonite ($\Omega_a = 3$) is higher than that of the high Mg-calcite (Ω_c = 2-3) leading to higher solubility of high Mg-calcite compared to aragonite. *Halimeda* has shown the capacity to produce 4 times more low Mg-calcite, which is less soluble under elevated CO_2 conditions (Chapter 7). An increase in the low Mg-calcite polymorph ratio with increasing CO_2 has been observed in the organisms producing comparable proportions of calcite and aragonite (approximately 50% calcite and 50% aragonite, including calcareous serpulid worm *Hydroides crucigera* and the whelk *Urosalpinx cinerea*) (Ries 2011b). Interestingly, there were no changes in high to low Mg-calcite proportion in calcite species (e.g., sea urchin *Arbacia punctulata*, shrimp *Penaeus plebejus*, and oyster *Crassostrea virginica*) (Ries 2011b). I did not investigate the capacity in producing the less soluble polymorph of $CaCO_3$ in *M. vertebralis* (low

Mg-calcite) under elevated CO_2 and temperature, because X-Ray diffraction required a large sample size which was not feasible with the size of individual foraminifera. However, it is predicted that there may be less plasticity in $CaCO_3$ production under stress in *M. vertebralis* compared to *Halimeda*, because higher energy is required to precipitate low Mg-calcite in the Mg-saturated seawater that favours the production of high Mg-calcite crystals (Toler et al. 2001).

8.1.5 Effects on morphological and biomechanical properties

Ocean acidification and warming have a negative effect on $CaCO_3$ precipitation by reducing calcification rates (Chapter 4, 5, 7), changing $CaCO_3$ polymorphs and Mg:Ca and Sr:Ca ratios (Chapter 7), and decreasing aragonite crystal size (Chapter 4; Sinutok et al. 2011), which can lead to the dissolution of the $CaCO_3$ skeleton (Chapter 4, 7; Sinutok et al. 2011). Reductions in strength and toughness in *Halimeda* may be related to the changes in these parameters. In addition, the morphological (e.g., branching, percentage of $CaCO_3$, segment thickness) and anatomical (e.g., utricle, siphon pattern, intercellular space size, the fusion of the siphon between node and segment) properties of the algae may be impacted by CO_2 and temperature and could lead to differences in physiological and biomechanical properties (strength and toughness) (Padilla 1985; Onoda et al. 2008; Price et al. 2011). Both *H. macroloba* and *H. cylindracea* have an erect thallus with bulbous holdfast, with three to many layers of moderately inflated utricles and nodal siphons generally fusing into a single unit (Fig. 8.1; Hillis-Colinvaux 1980; Verbruggen and Kooistra 2004). However, these species are different in the size of the bulbous holdfast, segment size and shape, utricle size and segment branching pattern. *H. cylindracea* consists of cylindrical segments (1.5 mm thickness) with dichotomous branching and smaller peripheral utricles and a massive bulbous holdfast (Fig. 8.1). In contrast, *H. macroloba* consists of large, undulating or lobed segments (1 mm thickness) with polychotomous or dichotomous branching and a smaller bulbous holdfast (Fig. 8.1; Hillis-Colinvaux 1980; Verbruggen and Kooistra 2004). *H. cylindracea* had higher calcium carbonate deposition rates relative to *H. macroloba* (86 compared to 81% $CaCO_3$). However, the impact of future climate change on these morphological and

anatomical characteristics are still unresolved and require further investigation.

Biomechanical and morphological properties of *Halimeda* from different wave exposure habitats and the impact of ocean acidification and warming on the mechanical integrity of *Halimeda* were examined in Chapter 7. Several environmental (e.g., sediment compaction, sediment shear strength, wave exposure; Anderson et al. 2006) and internal (e.g., thallus morphology, thallus strength, degree of calcification; Boller and Carrington 2006; Martone et al. 2010) factors determine the likelihood of algae uprooting or breaking. More force was required to remove *H. macroloba* from exposed habitat than from sheltered habitat and more force was required to break *H. macroloba* and *H. cylindracea* thalli from exposed habitat. This suggests the biomechanical properties of these species are influenced by the degree of wave exposure (Chapter 7; Fig. 8.1). It may be predicted that *Halimeda* thalli from other reefs could have an ability to adapt their biomechanical properties according to their wave environment. In addition, morphological plasticity may reduce hydrodynamic forces imposed on their thalli (Boller and Carrington 2006; Martone et al. 2010). Exposed thalli of *H. cylindracea* exhibit larger blade and holdfast size while *H. macroloba* did not show the same trend. Lobed-shape-segments in *H. macroloba* may lead to higher drag force than the cylindrical morphology of *H. cylindracea*, suggesting that *H. macroloba* may be more vulnerable to drag (Chapter 7; Fig. 8.1). To resist wave forces, thallus strength must be greater than required to avoid breakage from mechanical stress imposed on the thallus (Mach et al. 2007). Here I found that the thallus in sheltered sites were neither over-engineered nor under-engineered and was dependent on sediment composition of the substratum. In contrast, an exposed thallus is likely to break rather than uproot suggesting that an exposed thallus is under-engineered and the thallus strength is the factor limiting plant integrity. The thallus breakage may be advantageous over uprooting due to the ability to re-attach and generate a new thallus via vegetative reproduction in broken thalli (Walters and Smith 1994; Walters et al. 2002; DeWreede 2006) whilst dislodgement and uprooting of a thallus is fatal (Anderson et al. 2006) (Chapter 7). These results suggested that *Halimeda* has an intrinsic capacity to withstand exposure,

as shown by the phenotypic differences in morphology and mechanical strength of thalli from different degrees of wave exposure.

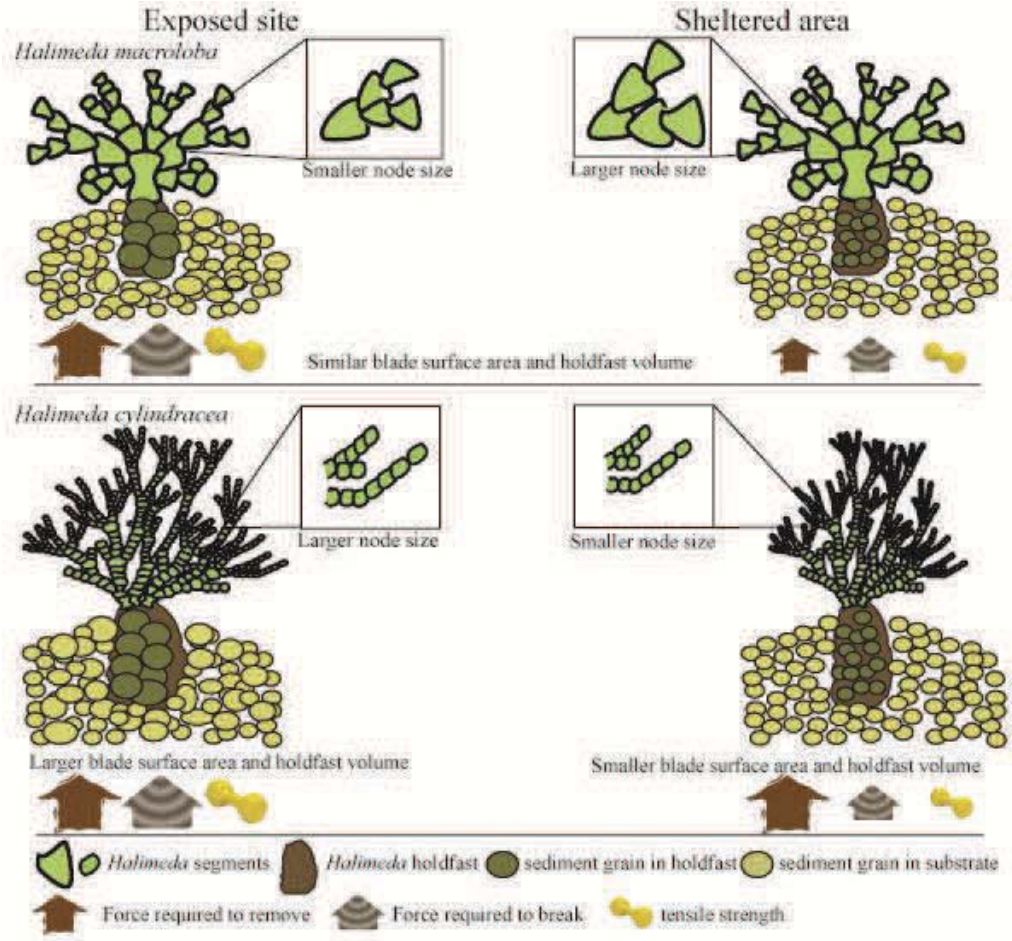

Figure 8.1 Summary of effects of wave exposure on morphological and biomechanical properties in *H. macroloba* and *H. cylindracea* showing the differences in blade surface area, holdfast volume, node size, sediment grain size in holdfast and sediments between *H. macroloba* and *H. cylindracea* from exposed and sheltered habitats.

H. cylindracea (86% $CaCO_3$) has greater deposition of calcium carbonate relative to *H. macroloba* (81% $CaCO_3$) and this may contribute to greater stiffness and tensile strength. I observed that elevated CO_2 and temperature had a greater impact on more heavily calcified species, *H. cylindracea* than the less heavily calcified species, *H. macroloba* (Chapter 7), suggesting that *H. cylindracea* may be more vulnerable to

elevated CO_2 and temperature conditions. The differences in the magnitude of biomechanical properties of these species may be due to these anatomical, morphological and physiological differences (Chapter 7).

8.2 IMPLICATIONS FOR THE CORAL REEF ECOSYSTEM

The data in this thesis suggests that elevated CO_2 concentrations of 1000 µatm and a high temperature of 32ºC are the upper limit for survival of these species from the site of collection (Heron Island on the Great Barrier Reef, Australia) (Chapter 4; Sinutok et al. 2011). However, when taking into account other impacts (e.g., high solar radiation, ultraviolet light), which is known to dramatically reduce photosynthesis and calcification, this upper limit of survival may be an overestimate (Chapter 2, 3, 4; Gao and Zheng 2010; Sinutok et al. 2011). Gao and Zheng (2010) showed that photosynthesis and calcification are dramatically reduced under the combination of high irradiance and elevated CO_2 condition. Therefore, the upper limit of survival for these species may be below 32ºC and 1000 µatm.

8.2.1 Interactions between *Halimeda* and benthic symbiont-bearing foraminifera

Chapter 3 indicated that the mobility of benthic symbiotic foraminifera *M. vertebralis* is light-related and controlled by the photophysiology of the symbiont. Therefore, the phototactic behaviour is the primary mechanism for modulating the light exposure in the symbiont-bearing foraminifera and benefits to the foraminiferal host. Phototactic behaviour in foraminifera provides a competitive advantage over co-existing sessile organisms (such as coral and macroalgae) under future predicted increase in irradiance and UV radiation by enhancing their ability to cope with over-saturating irradiance and adjusting their light environment. By attaching to the calcifying macroalga *Halimeda* (Hallock 1981a,b) or seagrasses (Severin 1987), foraminifera can move upward to the top of the plants when requiring more light (positive phototaxis) and move downward or horizontally to shaded areas to avoid excess light (negative phototaxis). This behaviour could help avoid long-term photoinhibition, loss of photosynthetic pigments and

expulsion of zooxanthellae from the foraminiferal host (bleaching) that could occur under prolonged high-light stress (Talge and Hallock 2003).

While ocean acidification lowers carbonate ion availability in the seawater (Feely et al. 2004), physiological processes of phototrophs such as photosynthesis can locally decrease pCO_2, increase pH and increase the aragonite saturation state, offsetting these reductions and reducing ocean acidification impacts at the local scale (Anthony et al. 2011). In contrast, physiological process in calcifiers (e.g., calcification in corals) can elevate pCO_2, decrease pH and decrease the saturation state of aragonite leading to increasing ocean acidification effects in downstream habitats (Anthony et al. 2011). Under optimal CO_2, temperature and light conditions, photosynthesis in *Halimeda* sp. has the capacity to alter the external carbonate chemistry and pH through the uptake of CO_2 and associated rise in pH on its thallus surface (De Beer and Larkum 2001). The calcification in *M. vertebralis*, which is commonly attached to *Halimeda* will be therefore indirectly favoured. Conversely, under high CO_2 and temperature conditions, the primary productivity and photosynthetic efficiency of *Halimeda* decreases (Chapter 4; Sinutok et al. 2011) and may result in decreasing pH and reducing the capacity for local alleviation of acidification impacts (De Beer and Larkum 2001). Given the vulnerability of both foraminifera and *Halimeda* to climate change-induced heating and acidification of seawater, this association may not provide a sufficient buffer against ocean acidification in the future. It is suggested that coral reefs dominated by *Halimeda* and foraminifera may experience an elevation of pCO_2 and a decline in saturation state of aragonite and may lead to increasing ocean acidification effects.

8.2.2 Biotic interactions of *Halimeda* on coral reefs

In *Halimeda* there are two important defensive mechanisms against herbivores: 1) producing diterpenoid compounds, Halimedatrial and Halimedatetraacetate, as chemical defense, and 2) calcifying to generate structural defence (Paul and Fenical 1984; Paul and Van Alstyne 1988; Padilla 1989, 1993). Under ocean acidification and warming (pH 7.7, 32ºC), calcification, strength and toughness will decrease in *Halimeda* (Chapter 7).

The weakened structure may lead to increasing susceptibility to herbivory and increasing the risk of thallus breakage or removal from the substrate under predicted increases in storm severity (Walsh and Ryan 2000; Knutson and Tuleya 2004; Emanuel 2005; Knutson et al. 2010). *Halimeda* may have to rely on chemical defence by producing more diterpenoids under elevated CO_2 and temperature; however, the calcification-chemical defence interactions have not yet been investigated.

Under the predicted climate change scenarios of rising ocean acidification and warming, the survival of these photosynthetic marine calcifiers is under threat (Chapter 4; Sinutok et al. 2011). *H. macroloba*, *H. cylindracea* and *M. vertebralis* may be classed as "losers" under future climate change. Non-calcifying macroalgae, epiphytic algae and seagrass (Gao et al. 1993; Short and Neckles 1999), which may perform better under future climate change, may benefit and exhibit a competitive advantage over calcifying macroalgae and may be classed as "winners" (Beach et al. 2003; Fabry et al. 2008; Hall-Spencer et al. 2008; Martin and Gattuso 2009). The coral reefs may be dominated by non-calcifying algae and epiphytic algae. The loss of these keystone species may also reduce the primary productivity on coral reefs and affect other associated species such as herbivorous fish and invertebrate communities (Llobet et al. 1991; Vroom et al. 2003; Diaz-Pulido et al. 2007; Kleypas and Yates 2009), leading to shifts in community structure and result in changing trophic interactions and reduction in habitat availability for many marine organisms.

8.2.3 Abiotic interactions of benthic photosynthetic calcifiers on coral reefs

These species are the main sediment and carbonate sand producers on coral reefs. Therefore, the loss of these species and the dissolution of calcium carbonate sand produced from these species under warmer, more acidic oceanic conditions will lead to a reduction in sediment turnover rate and carbonate sand availability in the marine environment.

8.3 THESIS SUMMARY

8.3.1 Conceptual model on the impacts of ocean acidification and warming

Figure 8.2 summarises the impact of elevated CO_2 and temperature on *H. macroloba* and *H. cylindracea*. Impacts under optimal and elevated temperature are described in the presence and absence of elevated CO_2. Decreases in calcification occurred in both species; however, the results on strength, toughness, Mg:Ca and Sr:Ca ratios and Mg-calcite were not consistent between species. The greatest impact was found under the combined conditions of elevated CO_2 and temperature, which lead to rapid $CaCO_3$ dissolution and changes in skeletal mineralogy in both species. In addition, mechanical integrity was also lost in *H. cylindracea*. These impacts are expected to result in greater susceptibility to herbivory and a higher risk of thallus breakage or removal from the substrate under the predicted increase in storm severity.

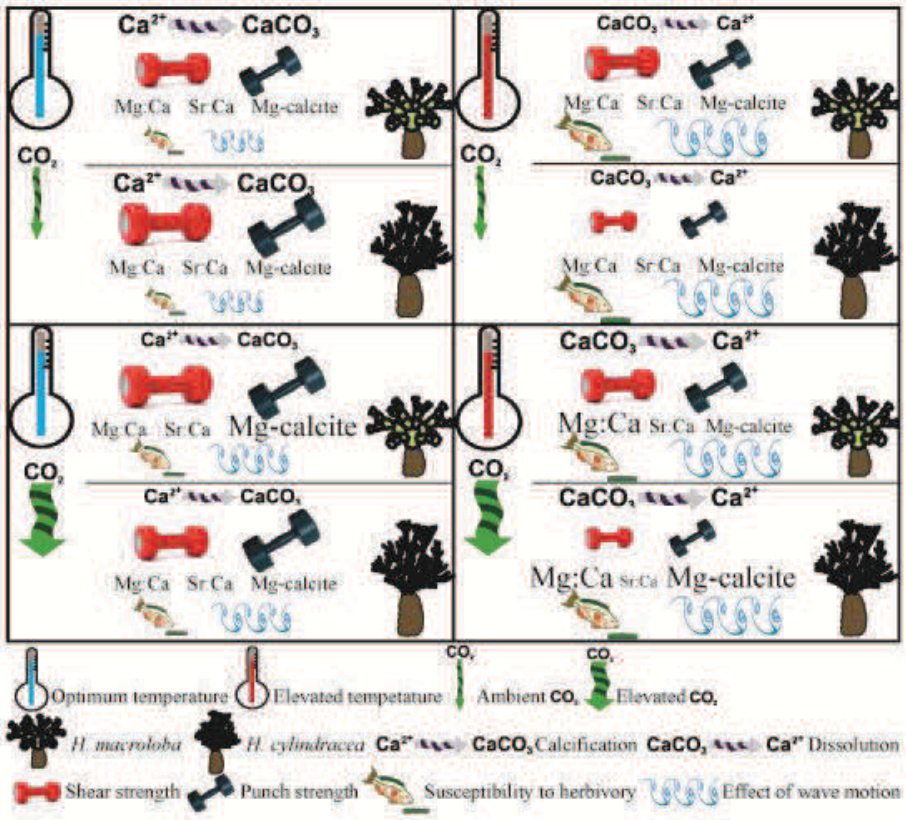

Figure 8.2 Summary of effects of elevated CO_2 and/or temperature on calcification, mechanical strength, skeletal mineralogy and risk of herbivory and thallus breakage/removal in *H. macroloba* and *H. cylindracea.*

8.3.2 Summary of key findings

8.3.2.1 In the short-term, irradiance was not found to influence photosynthetic efficiency, photoprotective mechanisms and calcification in *Halimeda macroloba*, *Halimeda cylindracea* and *Halimeda opuntia.*

8.3.2.2 The mobility of benthic symbiotic foraminifera *M. vertebralis* is influenced by light and the photophysiology of the symbiont, therefore the phototactic behavior is an effective mechanism for modulating the light exposure in the symbiont-bearing foraminifera.

8.3.2.3 pH is the main factor affecting the O_2 microenvironment around the segments of two *Halimeda* species; however, temperature has more effect on the foraminifera species. There were strong additive effects of elevated temperature and CO_2 on the O_2 microenvironment around the segments of two *Halimeda* species and the foraminifera shell, as well as strong reductions in physiological performance.

8.3.2.4 *Halimeda* has an intrinsic capacity to withstand exposure, as shown by the phenotypic differences in architecture and mechanical strength of thalli from different habitats.

8.3.2.5 There was an additive effect of temperature and CO_2 on the calcification (growth and crystal size) of both *Halimeda* species, leading to higher risk of thallus breakage and removal from the substrate under future climate change scenarios.

8.3.2.6 Calcification in high Mg-calcite species (*M. vertebralis*) was more sensitive to elevated temperature and CO_2 than in the aragonite-forming species of

Halimeda spp.

8.3.2.7 The elevated temperature of 32ºC and the pCO_2 concentration of 1000 µatm are the upper limit for survival of these species at Heron Island reef (Great Barrier Reef, Australia). However, this prediction may be an overestimate when taking into account the effects of high solar radiation and ultraviolet light.

In summary, *H. macroloba*, *H. cylindracea* and *M. vertebralis* may be classed as "losers" under future climate change.

8.4 PERSPECTIVE FOR FUTURE RESEARCH

This research has provided a new understanding of the combined and individual effects of ocean acidification and warming on photosynthesis and calcification in aragonite-forming species *Halimeda* sp. and Mg-calcite foraminifera *M. vertebralis.* The impact on skeletal mineralogy (Mg:Ca and Sr:Ca ratios, aragonite and Mg-calcite polymorph and crystal) and mechanical integrity (strength and toughness) in *H. macroloba* and *H. cylindracea* were examined. However, the impact of future climate change on the morphological (e.g., branching, percentage of $CaCO_3$, segment thickness) and anatomical (e.g., utricle, siphon pattern, intercellular space size, the fusion of the siphon between node and segment) characteristics are still unresolved and require further investigation. It will be important to focus on the microenvironmental changes in pH, Ca^{2+} and CO_2 at the surface of *Halimeda* and foraminifera because it will provide a better understanding of how ocean acidification will impact the physiology at a microscale. Interactions of chemical (diterpenoids, Halimedatrial and Halimedatetraacetate) and structural (calcification) herbivore defence mechanisms in *Halimeda* will also provide insight to *Halimeda*-herbivore interactions and trophic interactions. The experimental studies under different stressors (CO_2, temperature, irradiance, UV, tropical storm, salinity and nutrients) are needed to understand the interactive effects between these stressors, which are predicted to occur in the near

future (Wernberg et al. 2012). Furthermore, the results from these predominantly laboratory-based experiments must be validated in the field and the studies of the impact of these climate change scenarios at a community level are necessary because they can provide more information on the shifts in species composition, interaction effects between species and predict potential winners and losers under future climate change.

REFERENCES

Referencing format consistent with the journal Marine Biology

REFERENCES

Abel KM, Drew EA (1985) Response of *Halimeda* metabolism to various environmental parameters The Fifth International Coral Reef Congress, Tahiti 5: 21-26

Abrego D, Ulstrup KE, Willis BL, van Oppen MJH (2008) Species-specific interactions between algal endosymbionts and coral hosts define their bleaching response to heat and light stress. Proceedings of the Royal Society B: Biological Sciences 275: 2273-2282

Al-Horani FA (2005) Effects of changing seawater temperature on photosynthesis and calcification in the scleractinian coral *Galaxea fascicularis*, measured with O_2, Ca^{2+} and pH microsensors. Scientia Marina 69: 347-354

Al-Horani FA, Al-Moghrabi SM, de Beer D (2003a) Microsensor study of photosynthesis and calcification in the scleractinian coral, *Galaxea fascicularis*: active internal carbon cycle. Journal of Experimental Marine Biology and Ecology 288: 1-15

Al-Horani FA, Al-Moghrabi SM, de Beer D (2003b) The mechanism of calcification and its relation to photosynthesis and respiration in the scleractinian coral *Galaxea fascicularis*. Marine Biology 142: 419-426

Allakhverdiev SI, Kreslavski VD, Klimov VV, Los DA, Carpentier R, Mohanty P (2008) Heat stress: an overview of molecular responses in photosynthesis. Photosynthesis Research 98: 541-550

Allen JF (2003) State transitions—a question of balance. Science 299: 1530-1532

Anderson K, Close L, DeWreede RE, Lynch BJ, Ormond C, Walker M (2006) Biomechanical properties and holdfast morphology of coenocytic algae (Halimedales, Chlorophyta) in Bocas del Toro, Panama. Journal of Experimental Marine Biology and Ecology 328: 155-167

Anthony KRN, Kleypas JA, Gattuso J-P (2011) Coral reefs modify their seawater carbon chemistry – implications for impacts of ocean acidification. Global Change Biology 17: 3655-3666

Anthony KRN, Kline DI, Diaz-Pulido G, Dove S, Hoegh-Guldberg O (2008) Ocean acidification causes bleaching and productivity loss in coral reef builders. Proceedings of the National Academy of Sciences 105(45): 17442-17446

Armstrong SL (1987) Mechanical properties of the tissues of the brown alga *Hedophyllum sessile* (C. Ag.) Setchell: variability with habitat. Journal of Experimental Marine Biology and Ecology 114: 143-151

Aro EM, Virgin I, Andersson B (1993) Photoinhibition of photosystem II motivation, protein damage and turnover. Biochimica et Biophysica Acta 1143: 113-134

Atwell BJ, Kriedemann PE, Turnbull CGN (1999) Plants in action: adaptation in nature, performance in cultivation. Macmillan Education, Victoria

Bach SD (1979) Standing crop, growth and production of calcareous Siphonales (Chlorophyta) in a South Florida Lagoon. Bulletin of Marine Science 29: 191-201

Baker NR (2008) Chlorophyll fluorescence: a probe of photosynthesis in vivo. Annual Review of Plant Physiology 59: 89-113

Ballesteros E (1991) Seasonality of growth and production of a deep-water population of *Halimeda tuna* (Chlorophyceae, Caulerpales) in the North-Western Mediteranean. Botanica Marina 34: 291-301

Barnes DJ, Chalker BE (1990) Calcification and photosynthesis in reef-building corals and algae. In: Dubinsky Z (ed) Coral reefs. Ecosystems of the world. Elsevier, Amsterdam, pp 109-131

Beach K, Walters L, Borgeas H, Smith C, Coyer J, Vroom P (2003) The impact of *Dictyota* spp. on *Halimeda* populations of Conch Reef, Florida Keys. Journal of Experimental Marine Biology and Ecology 297: 141-159

Beach K, Walters L, Vroom P, Smith C, Coyer J, Hunter C (2003) Variability in the ecophysiology of *Halimeda* (Chlorophyta, Bryopsidales) on Conch Reef, Florida Keys, USA. Journal of Phycology 39: 633-643

Berger LS, Kaever MJ, Reichel MB (1997) Influence of ecological conditions on magnesium and strontium content and ultrastructure of the calcareous skeleton of

Bornetella sphaerica (Zarnadini), Dasycladales. Paläontologische Zeitschrift 71: 189-195

Bijma J, Hönisch B, Zeebe RE (2002) Impact of the ocean carbonate chemistry on living foraminiferal shell weight: Comment on ‘‘Carbonate ion concentration in glacial-age deep waters of the Caribbean". Geochemistry Geophysics Geosystems 3: 1064-1077

Boardman K (1977) Comparative photosynthesis of sun and shade plants. Annual Review of Plant Physiology 28: 355-377

Bohm EL, Goreau TF (1973) Rates of turnover and net accretion of calcium and the role of calcium binding polysaccharides during calcification in the calcareouse alga *Halimeda opuntia* (L.). International Reviews of Hydrobiology 58: 723-740

Boller ML, Carrington E (2006) *In situ* measurement of hydrodynamic forces imposed on *Chondrus crispus* Stackhouse. Journal of Experimental Marine Biology and Ecology 337: 159-170

Borowitzka MA (1977) Algal calcification. Oceanography and Marine Biology: an Annual Review 15: 189-223

Borowitzka MA (1981) Photosynthesis and calcification in the articulated coralline red algae *Amphiroa anceps* and *A. foliacea*. Marine Biology 62: 17-23

Borowitzka MA (1984) Calcification in aquatic plants. Plant, Cell and Environment 7: 457-466

Borowitzka MA (1986) Physiology and biochemistry of calcification in the Chlorophyceae. In: Leadbeter B, Riding H (eds) Biomeneralization in the lower plants and animals. Oxford University Press, pp 107-124

Borowitzka MA (1989) Carbonate calcification in algae - initiation and control. In: Mann S, Webb J, Williams RJP (eds) Biomineralization: Chemical and biochemical perspectives. VCH, Weinheim, pp 63-94

Borowitzka MA, Larkum AWD (1976a) Calcification in the green alga *Halimeda* II. The exchange of Ca^{2+} and the occurrence of age gradients in calcification and photosynthesis. Journal of Experimental Botany 27: 864-878

Borowitzka MA, Larkum AWD (1976b) Calcification in the green alga *Halimeda* III. The sources of inorganic carbon for photosynthesis and calcification and a model of the mechanism of calcification. Journal of Experimental Botany 27: 879-893

Borowitzka MA, Larkum AWD (1976c) Calcification in the green alga *Halimeda* IV. The action of metabolic inhibitors on photosynthesis and calcification. Journal of Experimental Botany 27: 894-907

Borowitzka MA, Larkum AWD (1977) Calcification in the green alga *Halimeda*. I. An ultrastructure study on thallus development. Journal of Phycology 13: 6-16

Borowitzka MA, Larkum AWD, Nockolds CE (1974) A scanning electron microscope study of the structure and organization of the calcium carbonate deposits of algae. Phycologia 13: 195-203

Brown BE, Ambarsari I, Warner ME, Fitt WK, Dunne RP, Gibb SW, Cummings DG (1999) Diurnal changes in photochemical efficiency and xanthophyll concentrations in shallow water reef corals: evidence for photoinhibition and photoprotection. Coral Reefs 18: 99-105

Brown BE, Downs CA, Dunne RP, Gibb SW (2002) Preliminary evidence for tissue retraction as a factor in photoprotection of coral incapable of xanthophyll cycling. Journal of Experimental Marine Biology and Ecology 277: 129-144

Buddemeier RW, Kleypas JP, Aronson RB (2004) Coral reefs and global climate change: Potential contributions of climate change to stresses on coral reef ecosystems. Pew Center on Global Climate Change

Campbell DA, Cockshutt AM, Porankiewicz-Asplund J (2003) Analysing photosynthetic complexes in uncharacterized species or mixed microalgal communities using global antibodies. Physiologia Plantarum 119: 322-327

Carnicas E, Jiménez C, Niell FX (1999) Effects of changes of irradiance on the pigment composition of *Gracilaria tenuistipitata* var. *liui* Zhang et Xia. Journal of Photochemistry and Photobiology B: Biology 50: 149-158

Carrington E, Grace SP, Chopin T (2001) Life history phases and the biomechanical properties of the red alga *Chondrus crispus* (Rhodophyta). Journal of Phycology 37: 699-704

Carrington EC (1990) Drag and dislodgment of an intertidal macroalga: consequences of morphological variation in *Mastocarpus papillatus* Kützing. Journal of Experimentai Marine Biology and Ecology 139: 185-200

Chave KE (1954) Aspects of the biogeochemistry of magnesium 2. Calcareous sediments and rocks. The Journal of Geology 62: 587-599

Chen M, Li A-F, Zhou B-C (2002) Structural analysis of peptides of PSII light-harvesting complexes in siphonous green algae, *Codium fragile*. Acta Botanica Sinica 44: 147-151

Choong MF, Lucas PW, Ong JSY, Pereira B, Tan HTW, Turner IM (1992) Leaf fracture toughness and sclerophylly: their correlations and ecological implications. New Phytologist 121: 597-610

Cléroux C, Cortijo E, Anand P, Labeyrie L, Bassinot F, Caillon N, Duplessy J-C (2008) Mg/Ca and Sr/Ca ratios in planktonic foraminifera: proxies for upper water column temperature reconstruction. Paleoceanography 23: PA3214

Clifton KE, Clifton LM (1999) The phenology of sexual reproduction by green algae (Bryopsidales) on Caribbean coral reefs. Journal of Phycology 35: 24-34

Cohen AL, Gaetani GA (2010) Ion partitioning and the geochemistry of coral skeletons: Solving the mystery of the "vital effect". In: Prieto M, Stoll H (eds) European Mineralogical Union, Notes in mineralogy: "Ion partitioning in ambient temperature aqueous systems: from fundamentals to applications in climate proxies and environmental geochemistry" 10: 399-415

Cohen AL, Layne GD, Hart SR (2001) Kinetic control of skeletal Sr/Ca in a symbiotic coral: Implications for the paleotemperature proxy. Paleoceanography 16: 20-26

Cohen AL, McCorkle DC, de Putron S, Gaetani GA, Rose KA (2009) Morphological and compositional changes in the skeletons of new coral recruits reared in acidified seawater: Insights into the biomineralization response to ocean acidification. Geochemistry Geophysics Geosystems 10. DOI: 10.1029/2009GC002411

Costanza R, d'Arge R, Groot Rd, Farberk S, Grasso M, Hannon B, Limburg K, Naeem S, O'Neill RV, Paruelo J, Raskin RG, Sutton P, Belt Mvd (1997) The value of the world's ecosystem services and natural capital. Nature 387: 253-260

Cruz S, Serôdio J (2008) Relationship of rapid light curves of variable fluorescence to photoacclimation and non-photochemical quenching in a benthic diatom. Aquatic Botany 88: 256-264

De Beer D, Larkum AWD (2001) Photosynthesis and calcification in the calcifying algae *Halimeda discoidea* studied with microsensors. Plant, Cell and Environment 24: 1209-1217

Déath G, Lough JM, Fabricius KE (2009) Declining coral calcification on the Great Barrier Reef. Science 323: 116-119

Demes KW, Bell SS, Dawes CJ (2009) The effects of phosphate on the biomineralization of the green alga, *Halimeda incrassata* (Ellis) Lam. Journal of Experimental Marine Biology and Ecology 374: 123–127

Demmig-Adams B, Adams WWI (1992) Photoprotection and other responses of plants to high light stress. Annual Review of Plant Physiology 43: 599-626

Denny M, Brown V, Carrington E, Kraemer G, Miller A (1989) Fracture mechanics and the survival of wave-swept macroalgae. Journal of Experimental Marine Biology and Ecology 127: 211-228

Denny MW (1988) Biology and the mechanics of the wave-swept environment. Princeton University Press, New Jersey

De Nooijer LJ, Toyofuku T, Kitazato H (2009) Foraminifera promote calcification by elevating their intracellular pH. Proceedings of the National Academy of Sciences 106: 15374-15378

DeWreede RE (2006) Biomechanical properties of coenocytic algae (Chlorophyta, Caulerpales). Science Asia 32: 57-62

Dias BB, Hart MB, Smart CW, Hall-Spencer JM (2010) Modern seawater acidification: the response of foraminifera to high-CO_2 conditions in the Mediterranean Sea. Journal of the Geological Society, London 167: 843-846

Diaz-Pulido G, McCook LJ, Larkum AWD, Heike K. Lotze, Raven JA, Schaffelke B, Smith JE, Steneck RS (2007) Vulnerability of macroalgae of the Great Barrier Reef to climate change. In: Johnson JE, Marshall PA (eds) Climate change and the Great Barrier Reef. Great Barrier Reef Marine Park Authority and Australian Greenhouse Office, Australia, pp 153-192

Dissard D, Nehrke G, Reichart GJ, Bijma J (2010) Impact of seawater pCO_2 on calcification and Mg/Ca and Sr/Ca ratios in benthic foraminifera calcite: results from culturing experiments with *Ammonia tepida*. Biogeosciences 7: 81-93

Dissard D, Nehrke G, Reichart GJ, Nouet J, Bijma J (2009) Effect of the fluorescent indicator calcein on Mg and Sr incorporation into foraminiferal calcite. Geochemistry Geophysics Geosystems 10. DOI: 10.1029/2009GC002417

Doney SC, Fabry VJ, Feely RA, Kleypas JA (2009) Ocean acidification: The other CO_2 problem. Annual Review of Marine Science 1: 169-192

Drew EA (1979) Physiological aspects of primary production in seagrasses. Aquatic Botany 7: 139-150

Drew EA (1983) *Halimeda* biomass, growth rates and sediment generation on reefs in the Central Great Barrier Reef Province. Coral Reefs 2: 101-110

Drew EA, Abel KM (1990) Studies on *Halimeda* III. A daily cycle of chloroplast migration within segments. Botanica Marina 33: 31-45

Drew EA, Abel KM (1995) Studies on *Halimeda*. V. Effect of temperature on chloroplast migration in this Siphonous green alga. Biological Rhythm Research 26: 48-54

Duguay LE (1983) Comparative laboratory and field studies on calcification and carbon fixation in foraminiferal-algal associations. Journal of Foraminiferal Research 13: 252-261

Duguay LE, Taylor DL (1978) Primary production and calcification by the Soritid foraminifer *Archais angulatus* (Fichtel & Moll). Journal of Protozoology 25: 356-361

Dupont S, Thorndyke MC (2009) Impact of CO_2-driven ocean acidification on invertebrates early life-history - What we know, what we need to know and what we can do. Biogeosciences Discussions 6: 3109-3131

Earle SA (1972) The influence of herbivores on the marine plants of Great Lameshur Bay, with an annotated list of plants. In: Collett BB, Earle SA (eds) Results of the tektite program: ecology of coral reef fishes. Science Bulletin of Los Angeles County Natural History Museum, pp 17-44

El-Manawy IM, Shafik MA (2008) Morphological characterization of *Halimeda* (Lamouroux) from different biotopes on the Red Sea coral reefs of Egypt. American-Eurasian Journal of Agricultural & Environmental Sciences 3: 532-538

Emanuel K (2005) Increasing destructiveness of tropical cyclones over the past 30 years. Nature 436: 686-688

Erez J (2003) The source of ions for biomineralization in foraminifera and their implications for paleoceanographic proxies. Mineralogy and Geochemistry 54: 115-149

Fabricius KE, Langdon C, Uthicke S, Humphrey C, Noonan S, Déath G, Okazaki R, Muehllehner N, Glas MS, Lough JM (2011) Losers and winners in coral reefs acclimatized to elevated carbon dioxide concentrations. Nature Climate Change 1: 165-169

Fabry VJ, Seibel BA, Feely RA, Orr JC (2008) Impacts of ocean acidification on marine fauna and ecosystem processes. International Council for the Exploration of the Sea Journal of Marine Science 65: 414-432

Fagoonee I, Wilson HB, Hassell MP, Turner JR (1999) The dynamics of zooxanthellae populations: a long-term study in the field. Science 283: 843-845

Falkowski PG, Raven JA (2007) Aquatic photosynthesis. Princeton University Press, New Jersey

Fay SA, Weber MX, Lipps JH (2009) The distribution of *Symbiodinium* diversity within individual host foraminifera. Coral Reefs 28: 717-726

Feely RA, Sabine CL, Lee K, Berelson W, Kleypas J, Fabry VJ, Millero FJ (2004) Impact of anthropogenic CO_2 on the $CaCO_3$ system in the oceans. Science 305: 362-366

Figueroa FL, Salles S, Aguileral J, Jiménez C, Mercadol J, Viñegla B, Flores-Moya A, Altamirano M (1997) Effects of solar radiation on photoinhibition and pigmentation in the red alga *Porphyra leucosticta*. Marine Ecology Progress Series 151: 81-90

Fine M, Tchernov D (2007) Scleractinian coral species survive and recover from decalcification. Science 315: 1811

Fitt WK, McFarland FK, Warner ME, Chilcoat GC (2000) Seasonal patterns of tissue biomass and densities of symbiotic dinoflagellates in reef corals and relation to coral bleaching. Limnology and Oceanography 45: 677-685

Fong P, Boyer KE, Kamer K, Boyle KA (2003) Influence of initial tissue nutrient status of tropical marine algae on response to nitrogen and phosphorus additions. Marine Ecology Progress Series 262: 111-123

Fraile I, Mulitza S, Schulz M (2009) Modeling planktonic foraminiferal seasonality: Implications for sea-surface temperature reconstructions. Marine Micropaleontology 72: 1-9

Franklin LA, Larkum AWD (1997) Multiple strategies for a high light existence in a tropical marine macroalga. Photosynthesis Research 53: 149-159

Franklin LA, Seaton GGR, Lovelock CE, Larkum AWD (1996) Photoinhibition of photosynthesis on a coral reef. Plant, Cell and Environment 19: 825-836

Friedlingstein P, Cox P, Betts R, Bopp L, Bloh WV, Brovkin V, Cadule P, Doney S, Eby M, Fung I, Bala G, John J, Jones C, Joos F, Kato T, Kawamiya M, Knorr W, Lindsay IK, Mathews HD, Raddatz T, Rayner P, Reick C, Roeckner E, Schnitzler K-G, Strassmann R, Weaver AJ, Yoshikawa C, Zeng N (2006) Climate–carbon cycle feedback analysis: Results from the C^4MIP model intercomparison. Journal of Climate 19: 3337-3353

Fujita K, Hikami M, Suzuki A, Kuroyanagi A, Sakai K, Kawahata H, Nojiri Y (2011) Effects of ocean acidification on calcification of symbiont-bearing reef foraminifers. Biogeosciences 8: 2089-2098

Furla P, Galgani I, Durand I, Allemand D (2000) Sources and mechanisms of inorganic carbon transport for coral calcification and photosynthesis The Journal of Experimental Biology 203: 3445-3457

Gao K, Aruga Y, Asada K, Ishihara T, Akano T, Kiyohara M (1993a) Calcification in the articulated coralline alga *Corallina pilulifera*, with special reference to the effect of elevated CO_2 concentration. Marine Biology 117: 129-132

Gao K, Aruga Y, Asada K, Kiyohara M (1993b) Influence of enhanced CO_2 on growth and photosynthesis of the red algae *Gracilaria* sp. and *G. chilensis*. Journal of Applied Phycology 5: 563-571

Gao K, Zheng Y (2010) Combined effects of ocean acidification and solar UV radiation on photosynthesis, growth, pigmentation and calcification of the coralline alga *Corallina sessilis* (Rhodophyta). Global Change Biology 16: 2388-2398

Gattuso J-P, Frankignoulle M, Bourge I, Romaine S, Buddemeier RW (1998) Effect of calcium carbonate saturation of seawater on coral calcification. Global and Planetary Change 18: 37-46

Gattuso J-P, Gao K, Lee K, Rost B, Schulz KG (2010) Guide for best practices in ocean acidification research and data reporting. Publications Office of the European Union, Luxembourg

Gattuso J-P, Lavigne H (2009) Technical note: Approaches and software tools to investigate the impact of ocean acidification. Biogeosciences 6: 2121–2133

Gattuso J-P, Pichon M, Delesalle B, Frankignoulle M (1993) Community metabolism and air-sea CO_2 fluxes in a coral reef ecosystem (Moorea, French Polynesia). Marine Ecology Progress series 96: 259-267

Glud RN, Gundersen JK, Revsbech NP, Jørgensen BB (1995) Effects on the diffusive boundary layer imposed by microelectrodes. Limnology and Oceanography 39: 462-467

Goldstein ST (1999) Foraminifera: A biological overview. In: Gupta BKS (ed) Modern foraminifera. Kluwer Academic Publishers, Great Britain, pp 37-55

Gonzalez-Mora B, Sierro FJ, Flores JA (2008) Controls of shell calcification in planktonic foraminifers. Quaternary Science Reviews 27: 956-961

Govindjee (1995) Sixty-three years since Kautsky: Chlorophyll a fluorescence. Australian Journal of Plant Physiology 22: 131-160

Gross O (2000) Influence of temperature, oxygen and food availability on the migrational activity of bathyal benthic foraminifera: evidence by microcosm experiments. Hydrobiologia 426: 123-137

Gudmundsson G (1994) Phylogeny, ontogeny and systematics of recent Soritacea Ehrenberg 1839 (Foraminiferida). Micropaleontology 40: 101-155

Guinotte JM, Buddemeier RW, Kleypas JA (2003) Future coral reef habitat marginality: temporal and spatial effects of climate change in the Pacific basin. Coral Reefs 22: 551-558

Häder D-P (2008) Photoinhibition and UV response in the aquatic environment. In: Demmig-Adams B, III WWA, Mattoo AK (eds) Photoprotection, photoinhibition, gene regulation, and environment. Springer, Dordrecht, pp 87-105

Häder D-P, Figueroa FL (1997) Photoecophysiology of marine macroalgae. Photochemistry and Photobiology 66: 1-14

Häder D-P, Gröniger A, Hallier C, Lebert M, Figueroa FL, Jiménez C (1999) Photoinhibition by visible and ultraviolet radiation in the red macroalga *Porphyra umbilicalis* grown in the laboratory. Plant Ecology 145: 351-358

Häder D-P, Lebert M, Sinha RP, Barbieri ES, Helbling EW (2002) Role of protective and repair mechanisms in the inhibition of photosynthesis in marine macroalgae. Photochemical and Photobiological Sciences 1: 809-814

Häder D-P, Porst M, Herrmannl H, Schäferl J, Santas R (1996) Photoinhibition in the Mediterranean green alga *Halimeda tuna* Ellis et Sol measured in situ. Photochemistry and Photobiology 64: 428-434

Haikali BE, Bensoussan N, Romano J-C, Bousquet V (2004) Estimation of photosynthesis and calcification rates of *Corallina elongata* Ellis and Solander, 1786, by measurements of dissolved oxygen, pH and total alkalinity. Scientia Marina 68: 45-56

Hall DO, Rao KK (1994) Photosynthesis. Cambridge University Press, Cambridge

Hallock P (1981a) Algal symbiosis: A mathematical analysis. Marine Biology 62: 249-255

Hallock P (1981b) Light dependence in *Amphistegina*. Journal of Foraminiferal Research 11: 40-46

Hallock P (1999) Symbiont-bearing foraminifera. In: Gupta BKS (ed) Modern foraminifera. Kluwer Academic Publishers, Great Britain, pp. 123-139

Hallock P (2000) Symbiont-bearing foraminifera: harbingers of global change? Micropaleontology 46: 95-104

Hallock P, Lidz BH, Cockey-Burkhard EM, Donnelly KB (2003) Foraminifera as bioindicators in coral reef assessment and monitoring: the foram index Environmental Monitoring and Assessment 81: 221-238

Hallock P, Williams DE, Fisher EM, Toler SK (2006) Bleaching in foraminifera with algal symbionts: Implications for reef monitoring and risk assessment. Forams 29: 108-128

Hall-Spencer JM, Rodolfo-Metalpa R, Martin S, Ransome E, Fine M, Turner SM, Rowley SJ, Tedesco D, Buia M-C (2008) Volcanic carbon dioxide vents show ecosystem effects of ocean acidification. Nature 454: 96-99

Hancke K, Hancke TB, Olsen LM, Johnsen G (2008) Temperature effects on microalgal photosynthesis-light responses measured by O_2 production, Pulse-Amplitude-Modulated fluorescence, and ^{14}C assimilation. Journal of Phycology 44: 501-504

Hanelt D, Huppertz K, Nultsch W (1993) Daily course of photosynthesis and photoinhibition in marine macroalgae investigated in the laboratory and field. Marine Ecology Progress Series 97: 31-37

Hansen HJ (1999) Shell construction in modern calcareous Foraminifera. In: Gupta BKS (ed) Modern foraminifera. Kluwer Academic Publishers, Great Britain, pp 57-70

Harrison PL, Booth DJ (2007) Coral reefs: naturally dynamic and increasingly disturbed ecosystems. In: Connell SD, Gillanders BM (eds) Marine ecology. Oxford University Press, Melbourne, pp 319-377

Haugan PM, Drange H (1996) Effects of CO_2 on the ocean environment. Energy Conversion and Management 37: 1019-1012

Hay ME, Paul VJ, Lewis SM, Gustafson K, Tucker J, Trindell RN (1988) Can tropical seaweeds reduce herbivory by growing at night? Diel patterns of growth, nitrogen content, herbivory, and chemical versus morphological defenses. Oecologia 75: 233-245

Haynert K, Schönfeld J, Riebesell U, Polovodova I (2011) Biometry and dissolution features of the benthic foraminifer *Ammonia aomoriensis* at high pCO_2. Marine Ecology Progress Series 432: 53-67

Henley WJ, Levavasseur G, Franklin LA, Lindley ST, Ramus J, Osmond CB (1991) Diurnal responses of photosynthesis and fluorescence in *Ulva rotundata* acclimated to sun and shade in outdoor culture. Marine Ecology Progress Series 75: 19-28

Heukelem LV, Thomas CS (2001) Computer-assisted high-performance liquid chromatography method development with applications to the isolation and analysis of phytoplankton pigments. Journal of Chromatography A 910: 31-49

Hill R (2008) Coral bleaching: photosynthetic impacts on symbiotics dinoflagellates> Coral reefs and climate change. VDM Publishing House Ltd, Germany

Hill R, Larkum AWD, Frankart C, Kühl M, Ralph PJ (2004) Loss of functional photosystem II reaction centres in zooxanthellae of corals exposed to bleaching conditions: using fluorescence rise kinetics. Photosynthesis Research 82: 59-72

Hill R, Larkum AWD, Prášil O, Kramer DM, Szabó M, Kumar V, Ralph PJ (2012) Light-induced dissociation of antenna complexes in the symbionts of scleractinian corals correlates with sensitivity to coral bleaching. Coral Reefs 31: 963-975

Hill R, Ralph PJ (2005) Diel and seasonal changes in fluorescence rise kinetics of three scleractinian corals. Functional Plant Biology 32: 549-559

Hill R, Ralph PJ (2008) Impact of bleaching stress on the function of the oxygen evolving complex of zooxanthellae from scleractinian corals. Journal of Phycology 44: 299-310

Hillis-Colinvaux L (1980) Ecology and Taxonomy of *Halimeda*: primary producer of coral reefs. In: Blaxter JHS, Russel FS, Young M (eds) Advances in marine Biology 17. Academic Press, New York, pp 1-327

Hobday AJ, Okey TA, Poloczanska ES, Kunz TJ, Richardson AJ (2006) Impacts of climate change on Australian marine life: Part B. Technical report., Canberra, Australia

Hoegh-Guldberg O (1999) Climate change, coral bleaching and the future of the world's coral reefs. Marine and Freshwater Research 50: 839-866

Hoegh-Guldberg O, Mumby PJ, Hooten AJ, Steneck RS, Greenfield P, Gomez E, Harvell CD, Sale PF, Edwards AJ, Caldeira K, Knowlton N, Eakin CM, Iglesias-Prieto R, Muthiga N, Bradbury RH, Dubi A, Hatziolos ME (2007) Coral reefs under rapid climate change and ocean acidification. Science 318: 1738-1742

Hofmann LC, Yildiz G, Hanelt D, Bischof K (2012) Physiological responses of the calcifying rhodophyte, *Corallina officinalis* (L.), to future CO_2 levels. Marine Biology: 1-10

Hofmann M, Schellnhuber H-J (2009) Oceanic acidification affects marine carbon pump and triggers extended marine oxygen holes. Proceedings of the National Academy of Sciences 106: 3017-3022

Hoogenboom MO, Connolly SR (2009) Defining fundamental niche dimensions of corals: Synergistic effects of colony size, light, and flow. Ecology 90: 767-780

Houghton J (2009) Global warming: the complete briefing. Cambridge University Press, United Kingdom

Houghton JT, Ding Y, Griggs DJ, Noguer M, Linden PJvd, Dai X, Maskell K, Johnson CA (2001) IPCC, 2001: Climate change 2001: The scientific basis. Contribution of Working Group I to the third assessment report of the Intergovernmental Panel on Climate Change. Cambridge University Press, Cambridge

Howe SA, Marshall AT (2002) Temperature effects on calcification rate and skeletal deposition in the temperate coral, *Plesiastrea versipora* (Lamarck). Journal of Experimental Marine Biology and Ecology 275: 63-81

Hurd CL (2000) Water motion, marine macroalgal physiology, and production. Journal of Phycology 36: 453-472

Hurd CL, Hepburn CD, Currie KI, Raven JA, Hunter KA (2009) Testing the effects of ocean acidification on algal metabolism: Considerations for experimental designs. Journal of Phycology 45: 1236–1251

Iglesias-Prieto R, Beltrán VH, LaJeunesse TC, Reyes-Bonilla H, Thome PE (2004) Different algal symbionts explain the vertical distribution of dominant reef corals in the eastern Pacific. Proceedings of the Royal Society B: Biological Science 271: 1757-1763

Iglesias-Rodriguez MD, Halloran PR, Rickaby REM, Hall IR, Colmenero-Hidalgo E, Gittins JR, Green DRH, Tyrrell T, Gibbs SJ, von Dassow P, Rehm E, Armbrust EV, Boessenkool KP (2008) Phytoplankton calcification in a high-CO_2 world. Science 320: 336-340

Ilyina T, Zeebe RE, Maier-Reimer E, Heinze C (2009) Early detection of ocean acidification effects on marine calcification. Global Biogeochemical Cycles 23: 1-11

Invers O, Tomàs F, Pérez M, Romero J (2002) Potential effect of increased global CO_2 availability of the depth distribution of the seagrass *Posidonia oceanica* (L.) Delile: A tentative assessment using a carbon balance model. Bulletin of Marine Science 71: 1191-1198

ISRS (2008) Coral reefs and ocean acidification. Briefing paper 5. International Society for Reef Studies: 1-9

Jeffery C, Ross P (2007) NSW Biology. Macmillan, Australia

Jensen PR, Gibson RA, Littler MM, Littler DS (1985) Photosynthesis and calcification in four deep-water *Halimeda* species (Chlorophyceae, Caulerpales). Deep Sea Research 32: 451-464

Jia H-S, Li D-Q (2003) State transition, is it a photochemical or non-photochemical process in leaf in response to irradiance. Acta Botanica Sinica 45: 1428-1433

Jiang CD, Gao HY, Zou Q, Jiang GM (2004) Inhibition of photosynthesis by shift in the balance of excitation energy distribution between photosystems in dithiothreitol treated soybean leaves. Photosynthetica 42: 409-415

Johnson JE, Marshall PA (2007) Climate change and the Great Barrier Reef: A vulnerability assessment. Great Barrier Reef Marine Park Authority and Australian Greenhouse Office, Australia

Jokiel PL, Maracios JE, Franzisket L (1978) Coral growth: buoyant weight technique. In: Stoddard DR, Juhannes RE (eds) Coral reefs: research methods. Monographs on oceanographic methodology. UNESCO, Paris, pp 14

Jokiel PL, Rodgers KS, Kuffner IB, Andersson AJ, Cox EF, Mackenzie FT (2008) Ocean acidification and calcifying reef organisms: a mesocosm investigation. Coral Reefs 27: 473-483

Jones RJ, Hoegh-Guldberg O (2001) Diurnal changes in the photochemical efficiency of the symbiotic dinoflagellates (Dinophyceae) of corals: photoprotection, photoinactivation and the relationship to coral bleaching. Plant, Cell and Environment 24: 89-99

Jørgensen BB, Erez J, Revsbech NP, Cohen Y (1985) Symbiotic photosynthesis in a placktonic foraminiferan *Globigerinoides sacculifer* (Brady), studied with microelectrodes. Limnology and Oceanography 30: 1253-1267

Katz A (1973) The interaction of magnesium with calcite during crystal growth at 25-90°C and one atmosphere. Geochimica et Cosmochimica Acta 37: 1563-1586

Khare N, Nigam R (2000) Laboratory experiment to record rate of movement of cultured benthic foraminifera. ONGC Bulletin 37: 53-61

Kleypas JA, Buddemeier RW, Archer D, Gattuso J-P, Langdon C, Opdyke BN (1999) Geochemical consequences of increased atmospheric carbon dioxide on coral reefs. Science 284: 118-120

Kleypas JA, Feely RA, Fabry VJ, Langdon C, Sabine CL, Robbins LL (2006) Impacts of ocean acidification on coral reefs and other marine calcifiers: A guide for

future research. National Science Foundation, the National Oceanic and Atmospheric Administration, and the U.S. Geological Survey

Kleypas JA, Yates KK (2009) Coral reefs and ocean acidification. Oceanography 22: 108-117

Knutson TR, McBride JL, Chan J, Emanuel K, Holland G, Landsea C, Held I, Kossin JP, Srivastava AK, Sugi M (2010) Tropical cyclones and climate change. Nature Geoscience 3: 157-163

Knutson TR, Tuleya RE (2004) Impact of CO_2-induced warming on simulated hurricane intensity and precipitation: Sensitivity to the choice of climate model and convective parameterization. Journal of Climate 17: 3477-3495

Koehl MAR (1984) How do benthic organisms withstand moving water? American Zoology 24: 57-70

Koehl MAR, Alberte RS (1988) Flow, flapping, and photosynthesis of *Nereocystis luetkeana*: a functional comparison of undulate and flat blade morphologies. Marine Biology 99: 435-444

Köhler-Rink S, Kühl M (2000) Microsensor studies of photosynthesis and respiration in larger symbiotic foraminifera. I The physio-chemical microenvironment of *Marginopora vertibralis*, *Amphistegina lobifera* and *Amphisorus hemprichii*. Marine Biology 137: 473-486

Köhler-Rink S, Kühl M (2001) Microsensor studies of photosynthesis and respiration in the larger symbiont bearing foraminifera *Amphistefina lobifera* and *Amphisorus hemprichii.* Ophelia 55: 111-122

Köhler-Rink S, Kühl M (2005) The chemical microenvironment of the symbiotic planktonic foraminifer *Orbulina universa*. Marine Biology Research 1: 68-78

Kooistra WHCF, Coppejans EGG, Payri C (2002) Molecular systematics, historical ecology, and phylogeography of *Halimeda* (Bryopsidales). Molecular Phylogenetics and Evolution 24: 121-138

Koziol AG, Borza T, Ishida K-I, Keeling P, Lee RW, Durnford DG (2007) Tracing the evolution of the light-harvesting antennae in chlorophyll a/b-containing organisms. Plant Physiology 143: 1802-1816

Kramer DM, Johnson G, Kiirats O, Edwards GE (2004) New fluorescence parameters for the determination of QA redox state and excitation energy fluxes. Photosynthesis Research 79: 209–218

Kuffner IB, Andersson AJ, Jokiel PL, Rodgers KS, Mackenzie FT (2007) Decreased abundance of crustose coralline algae due to ocean acidification. Nature Geoscience 1: 114-117

Kuguru B, Achituv Y, Gruber DF, Tchernov D (2010) Photoacclimation mechanisms of corallimorpharians on coral reefs: Photosynthetic parameters of zooxanthellae and host cellular responses to variation in irradiance. Journal of Experimental Marine Biology and Ecology 394: 53-62

Le Cornec F, Corrège T (1997) Determination of uranium to calcium and strontium to calcium ratios in corals by inductively coupled plasma mass spectrometry. Journal of Analytical Atomic Spectrometry 12: 969-973

Kuroyanagi A, Kawahata H, Suzuki A, Fujita K, Irie T (2009) Impacts of ocean acidification on large benthic foraminifers: Results from laboratory experiments. Marine Micropaleontology 73: 190-195

Langdon C, Gattuso J-P, Anderson A (2010) Measurements of calcification and dissolution of benthic organisms and communities. In: Riebesell U, Fabry VJ, Hansson L, Gattuso J-P (eds) Guide to best practices for ocean acidification research and data reporting. Publication Office of the European Union, Luxembourg, pp 213-232

Langer MR, Silk MT, Lipps JH (1997) Global ocean carbonate and carbon dioxide production: the role of reef foraminifera. Journal of Foraminiferal Research 27: 271-277

Larkum AWD, Drew EA, Ralph PJ (2006) Photosynthesis and metabolism in seagrasses at the cellular level. In: Larkum AWD, Orth RJ, Duarte CM (eds) Seagrass: biology, ecology and conservation. Springer, Netherlands, pp 323-345

Larkum AWD, Salih A, Kühl M (2011) Rapid mass movement of chloroplasts during segment formation of the calcifying Siphonalean green alga, *Halimeda macroloba*. Plos One 6: e20841

Lea DW, Mashiotta TA, Spero HJ (1999) Controls on magnesium and strontium uptake in planktonic foraminifera determined by live culturing. Geochimica et Cosmochimica Acta 63: 2369-2379

Leclercq N, Gattuso J-P, Jaubert J (2000) CO_2 partial pressure controls the calcification rate of a coral community. Global Change Biology 6: 329-334

Lee J, Fine M, Levy O, Morales J (2009) A note on asexual reproduction of a *Marginopora* sp. from a modern deep-water population in the Heron-Wistari Channel, Australia. Journal of Foraminiferal Research 39: 4-7

Lee JJ (2006) Algal symbiosis in larger foraminifera. Symbiosis 42: 63-75

Lee JJ, Bock WD (1976) The importance of feeding in two species of soritid foraminifera with algal symbionts. Bulletin of Marine Science 26: 530-537

Lee JJ, Burnham B, Cevasco ME (2004) A new modern soritid foraminifer, *Amphisorus saurensis* n. sp., from the Lizard Island Group (Great Barrier Reef, Australia). Micropaleontology 50: 357-368

Lee JJ, MaEnery ME, Garrison JR (1980) Experimental studies of larger foraminifera and their symbionts from the Gulf of Elat on the Red Sea. Journal of Foraminiferal Research 10: 31-47

Lee JJ, Sang K, Kuile Bt, Strauss E, Lee PJ, W. W. Faber J (1991) Nutritional and related experiments on laboratory maintenance of three species of symbiont-bearing, large foraminifera. Marine Biology 109: 417-425

Lesser MP (2004) Experimental biology of coral reef ecosystems. Journal of Experimental Marine Biology and Ecology 300: 217-252

Leutenegger S (1984) Symbiosis in benthic foraminifera specificity and host adaptations. Journal of Foraminiferal Research 14: 16-35

Lewis E, Wallace DWR (1998) Program developed for CO_2 system calculations. Carbon Dioxide Information Analysis Center, Tennessee

Lin MC, Dai CF (1996) Drag, morphology and mechanical properties of three species of octocorals. Journal of Experimental Marine Biology and Ecology 201: 13-22

Littler MM (1972) The crustose Corallinaceae. Oceanography and Marine Biology: Annual Review 10: 311-347

Littler MM, Littler DS, Brooks BL (2004) Extraordinary mound-building forms of *Avrainvillea* (Bryopsidales, Chlorophyta): their experimental taxonomy, comparative functional morphology and ecological strategies. Atoll Research Bulletin 515: 1-26

Llobet I, Gill J-M, Hughes RG (1991) Horizontal, vertical and seasonal distributions of epiphytic hydrozoa on the alga *Halimeda tuna* in the Northwestern Mediterranean Sea. Marine Biology 110: 151-159

Lobban CS, Harrison PJ (1994) Seaweed ecology and physiology. Cambridge University Press

Loeblich ARJ, Tappan H (1984) Suprageneric classification of the Foraminiferida (Protozoa). Micropaleontology 30: 1-70

Lombard F, da Rocha RE, Bijma J, Gattuso J-P (2010) Effect of carbonate ion concentration and irradiance on calcification in planktonic foraminifera. Biogeosciences 7: 247-255

Lough J (2007) Climate and climate change on the Great Barrier Reef. In: Johnson JE, Marshall PA (eds) Climate change and the Great Barrier Reef: A vulnerability assessment. Great Barrier Reef Marine Park Authority and Australian Greenhouse Office, pp 15-74

Lough JM, Barnes DJ (1997) Several centuries of variation in skeletal extension, density and calcification in massive *Porites* colonies from the Great Barrier Reef: A proxy for seawater temperature and a background of variability against which to identify unnatural change. Journal of Experimental Marine Biology and Ecology 211: 29-67

Lough JM, Barnes DJ (2000) Environmental controls on growth of the massive coral *Porites*. Journal of Experimental Marine Biology and Ecology 245: 225-243

Mach KJ, Hale BB, Denny MW, Nelson DV (2007) Death by small forces: a fracture and fatigue analysis of wave-swept macroalgae. The Journal of Experimental Biology 210: 2231-2243

Madin JS, Connolly SR (2006) Ecological consequences of major hydrodynamic disturbances on coral reefs. Nature 444: 447-480

Madin JS, O'Donnell MJ, Connelly SR (2008) Climate-mediated mechanical changes to post-disturbance coral assemblages. Biology Letters 4: 490-493

Marshall JF, McCulloch MT (2002) An assessment of the Sr/Ca ratio in shallow water hermatypic corals as a proxy for sea surface temperature. Geochimica et Cosmochimica Acta 66: 3263-3280

Martin S, Gattuso J-P (2009) Response of Mediterranean coralline algae to ocean acidification and elevated temperature. Global Change Biology 15: 2089–2100

Martone PT, Boller M, Burgert I, Dumais J, Edwards J, Mach K, Rowe N, Rueggeberg M, Seidel R, Speck T (2010) Mechanics without muscle: Biomechanical Inspiration from the plant world. Integrative and Comparative Biology 50: 888-907

Martone PT, Denny MW (2008a) To bend a coralline: Effect of joint morphology on flexibility and stress amplification in an articulated calcified seaweed. Journal of Experimental Biology 211: 3421-3432

Martone PT, Denny MW (2008b) To break a coralline: Mechanical constraints on the size and survival of a wave-swept seaweed. Journal of Experimental Biology 211: 3433-3441

Mathieson AC, Fralick RA, Burns R, Flashive W (1975) Phycological studies during Tektite II at St. John, U.S.V.I. In: Earle SA, Lavenberg RE (eds) Results of the tektite program: coral reef invertebrates and plants. Science Bulletin of Los Angeles County Natural History Museum, pp 77-103

Maxwell K, Johnson GN (2000) Chlorophyll fluorescence - a practical guide. Journal of Experimental Botany 51: 659-668

McConnaughey T (1989) Biomineralization mechanisms. In: Crick RE (ed) Origin, evolution, and modern aspects of biomineralization in plants and animals. Plenum Press, New York, pp 57-73

McConnaughey TA, Whelan JF (1997) Calcification generates protons for nutrient and bicarbonate uptake. Earth-Science Reviews 42: 95-117

McNeil BI, Matear RJ, Barnes DJ (2004) Coral reef calcification and climate change: The effect of ocean warming. Geophysical Research Letters 31. DOI: 10.1029/2004GL021541

McQuaid CD, Branch GM (1984) Influence of sea temperature, substratum and wave exposure on rocky intertidal communities: an analysis of fauna and floral biomass. Marine Ecology Progress Series 19: 145-151

Merrett MJ, Armitage TL (1982) The effect of oxygen concentration on photosynthetic biomass production by algae. Planta 155: 95-96

Mitsuguchi T, Matsumoto E, Uchida T (2003) Mg/Ca and Sr/Ca ratios of *Porites* coral skeleton: Evaluation of the effect of skeletal growth rate. Coral Reefs 22: 381-388

Mullineaux CW, Emlyn-Jones D (2005) State transitions: an example of acclimation to low-light stress. Journal of Experimental Botany 56: 389-393

Multer HG, Clavijo I (1989) *Halimeda* investigations: Progress and problems 12th Carribean Geological Conference pp 117-127

Murakami A (1997) Quantitative analysis of 77K fluorescence emission spectra in *Synechocystis* sp. PCC 6714 and *Chlamydomonas reinhardtii* with variable PS I/PS II stoichiometries. Photosynthesis Research 53: 141-148

Murray JW (2006) Ecology and applications of benthic foraminifera. Cambridge University Press, Cambridge

Nancollas GH, Purdie N (1964) The kinetics of crystal growth. Chetmieal Society London Quarterly Review 19: 1-20

Necchi Jnr O (2004) Photosynthetic responses to temperature in tropical lotic macroalgae. Phycological Research 52: 140-148

Nigam R, Kurtarkar SR, Saraswat R, Linshy VN, Rana SS (2008) Response of benthic foraminifera *Rosalina leei* to different temperature and salinity, under laboratory culture experiment. Journal of the Marine Biological Association of the United Kingdom 88: 699-704

Nobes K, Uthicke S (2008) Benthic foraminifera of the Great Barrier Reef: a guild to species potentially useful as water quality indicators. Report to the Marine and Tropical Sciences Research Facility, Cairns

Nobes K, Uthicke S, Henderson R (2008) Is light the limiting factor for the distribution of benthic symbiont bearing foraminifera on the Great Barrier Reef? Journal of Experimental Marine Biology and Ecology 363: 48-57

Onoda Y, Schieving F, Anten NPR (2008) Effects of light and nutrient availability on leaf mechanical properties of *Plantago major*: A conceptual approach. Annals of Botany 101: 727-736

Orr JC, Fabry VJ, Aumont O, Bopp L, Doney SC, Feely RA, Gnanadesikan A, Gruber N, Ishida A, Joos F, Key RM, Lindsay K, Maier-Reimer E, Matear R, Monfray P, Mouchet A, Najjar RG, Plattner G-K, Rodgers KB, Sabine CL, Sarmiento JL, Schlitzer R, Slater RD, Totterdell IJ, Weirig M-F, Yamanaka Y, Yool A (2005) Anthropogenic ocean acidification over the twenty-first century and its impact on calcifying organisms. Nature 437: 681-685

Padilla DK (1985) Structural resistance of algae to herbivores: A biomechanical approach. Marine Biology 90: 103-109

Padilla DK (1989) Algal structure defenses: Form and calcification in resistance to tropical limpets. Ecology 70: 835-842

Padilla DK (1993) Rip stop in marine algae: minimizing the consequences of herbivore damage. Evolutionary Ecology 7: 634-644

Palacios SL, Zimmerman RC (2007) Response of eelgrass *Zostera marina* to CO_2 enrichment: possible impacts of climate change and potential for remediation of coastal habitats. Marine Ecology Progress Series 344: 1-13

Patterson RT, Richardson RH (1987) A taxonomic revision of the unilocular foraminifera Journal of Foraminiferal Research 17: 212-226

Paul VJ, van Alstyne KL (1988) Chemical defense and chemical variation in some tropical Pacific species of *Halimeda* (Halimedaceae; Chlorophyta). Coral Reefs 6: 263-269

Paul VJ, Fenical W (1984) Bioactive diterpenoids from tropical marine algae of the genus *Halirneda*. Tetrahedron 40: 3053-3062

Paul VJ, Fenical W (1986) Chemical defense in tropical green algae, order Caulerpales. Marine Ecology Progress Series 34: 157-169

Pawlowski J, Holzmann M, Fahrni JF, Pochon X, Lee JJ (2001) Molecular identification of algal endosymbionts in large Miliolid foraminifera: 2. Dinoflagellates. Journal of Eukaryotic Microbiology 48: 368-373

Pratt MC, Johnson AS (2002) Strength, drag, and dislodgment of two competing intertidal algae from two wave exposures and four seasons. Journal of Experimental Marine Biology and Ecology 272: 71-101

Price NN, Hamilton SL, Tootell JS, Smith JE (2011) Species-specific consequences of ocean acidification for the calcareous tropical green algae *Halimeda*. Marine Ecology Progress Series 440: 67-78

Pröschold T, Leliaert F (2007) Systematics of the green algae: Conflict of classic and modern approaches. In: Brodie J, Lewis JM (eds) Unravelling the algae: the past, present, and future of algal systematics. CRC Press, Boca Raton, pp 123-153

Ralph PJ, Gademann R (2005) Rapid light curves: A powerful tool to assess photosynthetic activity. Aquatic Botany 82: 222-237

Ralph PJ, Larkum AWD, Kuhl M (2005) Temporal patterns in effective quantum yield of individual zooxanthellae expelled during bleaching. Journal of Experimental Marine Biology and Ecology 316: 17-28

Ralph PJ, Macinnis-Ng CMO, Frankart C (2005) Fluorescence imaging application: effect of leaf age on seagrass photokinetics. Aquatic Botany 81: 69-84

Raven JA, Caldeira K, Elderfield H, Hoegh-Guldberg O, Liss P, Riebesell U, Shepherd J, Turley C, Heap R, Banes R, Quinn R (2005) Ocean acidification due to increasing atmospheric carbon dioxide. The Clyvedon Press Ltd., Cardiff

Raven JA, Giordano M, Beardall J, Maberly SC (2011) Algal and aquatic plant carbon concentrating mechanisms in relation to environmental change. Photosynthesis Research 109: 281-296

Revsbech NP, Jørgensen BB, Brix O (1981) Primary production of microalgae in sediments measured by oxygen microprofile, $H^{14}CO_3^-$ fixation, and oxygen exchange methods. Limnology and Oceanography 26: 717-730

Reymond CE, Uthicke S, Pandolfi JM (2011) Inhibited growth in the photosymbiont-bearing foraminifer *Marginopora vertebralis* from the nearshore Great Barrier Reef, Australia. Marine Ecology Progress Series 435: 97-109

Reynaud S, Ferrier-Pagès C, Meibom A, Mostefaoui S, Mortlock R, Fairbanks R, Alleman D (2007) Light and temperature effects on Sr/Ca and Mg/Ca ratios in the scleractinian coral *Acropora* sp. Geochimica et Cosmochimica Acta 71: 354-362

Reynaud S, Leclercq N, Romaine-Lioud S, Ferrier-Pagès C, Jaubert J, Gattuso J-P (2003) Interacting effects of CO_2 partial pressure and temperature on photosynthesis and calcification in a scleractinian coral. Global Change Biology 9: 1660-1668

Ridley SM (1977) Interaction of chloroplasts with inhibitors: In duction of chlorosis by diuron during prolonged illumination *in vitro*. Plant Physiology 59: 724-732

Riebesell U, Zondervan I, Rost B, Tortell PD, Zeebe RE, Morel FMM (2000) Reduced calcification of marine plankton in response to increased atmospheric CO_2. Nature 407: 364-367

Ries JB (2005) Aragonite production in calcite seas: effect of seawater Mg/Ca ratio on the calcification and growth of the calcareous alga *Penicillus capitatus*. Paleobiology 31: 445-458

Ries JB (2006) Mg fractionation in crustose coralline algae: Geochemical, biological, and sedimentological implications of secular variation in the Mg/Ca ratio of seawater. Geochimica et Cosmochimica Acta 70: 891-900

Ries JB (2011a) A physicochemical framework for interpreting the biological calcification response to CO_2-induced ocean acidification. Geochimica et Cosmochimica Acta 75: 4053-4064

Ries JB (2011b) Skeletal mineralogy in a high-CO_2 world. Journal of Experimental Marine Biology and Ecology 403: 54-64

Ries JB, Cohen AL, McCorkle DC (2009) Marine calcifiers exhibit mixed responses to CO_2- induced ocean acidification. Geology 37: 1131-1134

Ries JB, Stanley SM, Hardie LA (2006) Scleractinian corals produce calcite, and grow more slowly, in artificial Cretaceous seawater. Geology 34: 525-528

Rink S, Kühl M, Bigma J, Spero HJ (1998) Microsensor studies of photosynthesis and respiration in the symbiotic foraminifer *Orbulina universa*. Marine Biology 131: 583-595

Ritchie RJ (2006) Consistent sets of spectrophotometric chlorophyll equations for acetone, methanol and ethanol solvents. Photosynthesis research 89: 27-41

Ritchie RJ (2008) Universal chlorophyll equations for estimating chlorophylls *a, b, c*, and *d* and total chlorophylls in natural assemblages of photosynthetic organisms using acetone, methanol, or ethanol solvents. Photosynthetica 46: 115-126

Robbins LL, Knorr PO, Hallock P (2009) Response of *Halimeda* to ocean acidification: field and laboratory evidence. Biogeosciences Discussions 6: 4895-4918

Rochaix J-D (2011) Reprint of: Regulation of photosynthetic electron transport. Biochimica et Biophysica Acta 1807: 878-886

Rockholm DC, Yamamoto HY (1996) Violaxanthin de-epoxidase: Purification of a 43-kilodalton lumenal protein from lettuce by lipid-affinity precipitation with monogalactosyldiacylglyceride. Plant Physiology 110: 697-703

Rodolfo-Metalpa R, Peirano A, Houlbrèque F, Abbate M, Ferrier-Pagès C (2008) Effects of temperature, light and heterotrophy on the growth rate and budding of the temperate coral *Cladocora caespitosa*. Coral Reefs 27: 17-25

Roger MJR (2001) Handbook of plant ecophysiology techniques. Kluwar Academic Publishers, The Netherlands

Ross CA (1972) Biology and ecology of *Marginopora vertebralis* (Foraminiferida), Great Barrier Reef. Journal of Protozoology 19: 181-192

Rost B, Riebesell U (2004) Coccolithophores and the biological pump: responses to environmental changes. In: Thierstein HR, Young JR (eds) Coccolithophores: from molecular processes to global impact. Springer, Berlin, pp 99-125

Röttger R (1974) Larger foraminifera: Reproduction and early stages of development in *Heterostegina depressa*. Marine Biology 26: 5-12

Röttger R, Irwan A, Schmaljohann R, Franzisket L (1980) Growth of the symbiont-bearing foraminifera *Amphistegina lobifera* and *Heterostegina depressa*. In: Schwemmler W, Schenk HEA (eds) Endocytobiology, endosymbiosis and cell biology. Walter de Gruyther, Berlin, pp 125-132

Röttger R, Krüger R (1990) Observations on the biology of Calcarinidae (Foraminiferida). Marine Biology 106: 419-425

Russell AD, Honisch B, Spero HJ, Lea DW (2004) Effects of seawater carbonate ion concentration and temperature on shell U, Mg, and Sr in cultured planktonic foraminifera. Geochimica et Cosmochimica Acta 68: 4347-4361

Sanson G, Read J, Aranwela N, Clissold F, Peeters P (2001) Measurement of leaf biomechanical properties in studies of herbivory: Opportunities, problems and procedures. Austral Ecology 26: 535-546

Satoh A, Kurano N, Miyachi S (2001) Inhibition of photosynthesis by intracellular carbonic anhydrase in microalgae under excess concentrations of CO_2. Photosynthesis Research 68: 215-224

Schmidt C, Heinz P, Kucera M, Uthicke S (2011) Temperature-induced stress leads to bleaching in larger benthic foraminifera hosting endosymbiotic diatoms. Limnology and Oceanography 56: 1587-1602

Schreiber U (2004) Pulse-Amplitude-Modulation (PAM) fluorometry and saturation pulse method: An overview Advances in photosynthesis and respiration. Kluwer Academic, The Netherlands

Schubert R, Schellnhuber H-J, Buchmann N, Epiney A, Grießhammer R, Kulessa M, Messner D, Rahmstorf S, Schmid J (2006) The future oceans – Warming up, rising high, turning sour. Germanadvisory Council on Global Change, Berlin

Severin KP (1987) Spatial and temporal variation of *Marginopora vertebralis* on seagrass in Papua New Guinea during a six week period. Micropaleontology 33: 368-377

Shick JM, Lesser MP, Dunlap WC, Stochaj WR, Chalker BE, Won JW (1995) Depth-dependent responses to solar ultraviolet radiation and oxidative stress in the zooxanthellate coral *Acropora microphthalma*. Marine Biology 122: 41-51

Short FT, Neckles HA (1999) The effects of global climate change on seagrasses. Aquatic Botany 63: 169-196

Silva J, Sharon Y, Santos R, Beer S (2009) Measuring seagrass photosynthesis: methods and applications. Aquatic Biology 7: 127-141

Simkiss K (1964) Phosphate as crystal poisons of calcification. Biological Reviews 39: 487-505

Sinutok S (2008) Seasonal variation in distribution, density, and life stage of *Halimeda macroloba* Decaisne at Tangkhen Bay, Phuket Province, Thailand. Dissertation, Prince of Songkla University

Sinutok S, Hill R, Doblin MA, Wuhrer R, Ralph PJ (2011) Warmer more acidic conditions cause decreased productivity and calcification in subtropical coral reef sediment-dwelling calcifiers. Limnology and Oceanography 56: 1200-1212

Sinutok S, Pongparadon S, Prathep A (2008) Seasonal variation in density, growth rate and calcium carbonate accumulation of *Halimeda macroloba* Decaisne at Tangkhen Bay, Phuket Province, Thailand. Malaysian Journal of Science 27: 1-8

Six C, Sherrard R, Lionard M, Roy S, Campbell DA (2009) Photosystem II and pigment dynamics among ecotypes of the green alga *Ostreococcus*. Plant Physiology 151: 379-390

Smith AD, Roth AA (1979) Effect of carbon dioxide concentration on calcification in the red coralline alga *Bossiella orbigniana*. Marine Biology 52: 217-225

Smith DF, Wiebe WJ (1977) Rates of carbon fixation, organic carbon release and translocation in a reef-building foraminifer, *Marginopora vertebralis*. Australian Journal of Marine and Freshwater Research 28: 311-319

Smith JE, Smith CM, Vroom PS, Beach KL, Miller S (2004) Nutrient and growth dynamics of *Halimeda tuna* on Conch Reef, Florida Keys: Possible influence of internal tides on nutrient status and physiology. Limnology and Oceanography 49: 1923-1936

Smith SV, Kinsey DW (1976) Calcium carbonate production, coral reef growth, and sea level change. Science 194: 937-939

Sobrino C, Neale PJ, Phillips-Kress JD, Moeller RE, Porter JA (2009) Elevated CO_2 increases sensitivity to ultraviolet radiation in lacustrine phytoplankton assemblages. Limnology and Oceanography 54: 2448-2459

Solomon S, Qun D, Manning M, Chen Z, Marquis M, Averyt KB, Tignor M, Miller HL (2007) Climate change 2007: The physical science basis. Contribution of working group I to the fourth assessment report of the Intergovernmental Panel on Climate Change. Cambridge University Press, New York

Stanley SM, Ries JB, Hardie LA (2002) Low-magnesium calcite produced by coralline algae in seawater of Late Cretaceous composition. Proceedings of the National Academy of Sciences 99: 15323-15326

Stanley SM, Ries JB, Hardie LA (2010) Increased production of calcite and slower growth for the major sediment-producing alga *Halimeda* as the Mg/Ca ratio of seawater is lowered to a "calcite sea" level. Journal of Sedimentary Research 80: 8-16

Stark LM, Almodovar L, Krauss RW (1969) Factors affecting the rate of calcification in *Halimeda opuntia* (L.) Lamouroux and *Halimeda discoidea* Decaisne. Journal of Phycology 5: 305-312

Stewart HL (2006) Hydrodynamic consequences of flexural stiffness and buoyancy for seaweeds: a study using physical models. The Journal of Experimental Biology 209: 2170-2181

Strychar KB, Coates M, Sammarco PW (2004) Loss of *Symbiodinium* from bleached Australian scleractinian corals (*Acropora hyacinthus*, *Favites complanata* and *Porites solida*). Journal of Experimental Marine Biology and Ecology 55: 135-144

Taiz L, Zeiger E (2006) Plant physiology. Sinauer Associates Inc, Massachusetts

Talge HK, Hallock P (1995) Cytological examination of symbiont loss in a benthic foraminifera, *Amphistegina gibbosa*. Marine Micropaleontology 26: 107-113

Talge HK, Hallock P (2003) Ultrastructural responses in field-bleached and experimentally stressed *Amphistegina gibbosa* (Class Foraminifera). Journal of Eukaryotic Microbiology 50: 324-333

Ter Kuile B, Erez J, Padan E (1989a) Competition for inorganic carbon between photosynthesis and calcification in the symbiont-bearing foraminifer *Amphistegina lobifera*. Marine Biology 103: 253-259

Ter Kuile B, Erez J, Padan E (1989b) Mechanisms for the uptake of inorganic carbon by two species of symbiont-bearing foraminifera. Marine Biology 103: 241-251

Toler SK, Hallock P (1998) Shell malformation in stressed *Amphistegina* populations: relation to biomineralization and paleoenvironmental potential. Marine Micropaleontology 34: 107-115

Toler SK, Hallock P, Schijf J (2001) Mg/Ca ratios in stressed foraminifera, *Amphistegina gibbosa*, from the Florida Keys. Marine and Freshwater Research 43: 199-206

Ulstrup KE, Hill R, van Oppen MJH, Larkum AWD, Ralph PJ (2008) Seasonal variation in the photo-physiology of homogeneous and heterogeneous *Symbiodinium consortia* in two scleractinian corals. Marien Ecology Progress Series 361: 139-150

Ulstrup KE, Hill R, Ralph PJ (2005) Photosynthetic impact of hypoxia on in hospite zooxanthellae in the scleractinian coral *Pocillopora damicornis*. Marine Ecology Progress Series 286: 125-132

Ulstrup KE, Ralph PJ, Larkum AWD, Kühl M (2006) Intra-colonial variability in light acclimation of zooxanthellae in coral tissues of *Pocillopora damicornis*. Marine Biology 149: 1325-1335

Uthicke S, Nobes K (2008) Benthic foraminifera as ecological indicators for water quality on the Great Barrier Reef. Estuarine, Coastal and Shelf Science 78: 763-773

Van Keulen M, Borowitzka MA (2003) Seasonal variability in sediment distribution along an exposure gradient in a seagrass meadow in Shoalwater Bay, Western Australia. Estuarine, Coastal and Shelf Science 57: 587-592

Verbruggen H (2005) Resegmenting *Halimeda*: Molecular and morphometric studies of species boundaries within a green algal genus. Dissertation, Ghent University

Verbruggen H, Kooistra W (2004) Morphological characterization of lineages within the calcified tropical seaweed genus *Halimeda* (Bryopsidales, Chlorophyta). European Journal of Phycology 2: 213-228

Villarejo A, Shutova T, Moskvin O, Forssén M, Klimov VV, Samuelsson G (2002) A photosystem II-associated carbonic anhydrase regulates the efficiency of photosynthetic oxygen evolution. The EMBO Journal 21: 1980-1938

Vroom PS, Smith CM, Coyer JA, Walters LJ, Hunter CL, Beach KS, Smith JE (2003) Field biology of *Halimeda tuna* (Bryopsidales, Chlorophyta) across a depth gradient: comparative growth, survivorship, recruitment, and reproduction. Hydrobiologia 501: 149-166

Walsh KJE, Ryan BF (2000) Tropical cyclone intensity increase near Australia as a result of climate change. Journal of Climate 13: 3029-3036

Walters LJ, Smith CM (1994) Rapid rhizoid production in *Halimeda discoidea* Decaisne (Chlorophyta, Caulerpales) fragments: a mechanism for survival after separation from adult thalli. Journal of Experimental Marine Biology and Ecology 175: 105-120

Walters LJ, Smith CM, Coyer JA, Hunter CL, Beach KS, Vroom PS (2002) Asexual propagation in the coral reef macroalga *Halimeda* (Chlorophyta, Bryopsidales): production, dispersal and attachment of small fragments. Journal of Experimental Marine Biology and Ecology 278: 45-65

Warner ME, Fitt WK, Schimidt GW (1999) Damage to photosystem II in symbiotic dinoflagellates: A determinant of coral bleaching. Proceedings of the National Academy of Sciences 96: 8007–8012

Warner ME, LaJeunesse TC, Robison JD, Thur RM (2006) The ecological distribution and comparative photobiology of symbiotic dinoflagellates from reef corals in Belize: Potential implications for coral bleaching. Limnology and Oceanography 51: 1887-1897

Warner ME, Lesser MP, Ralph PJ (2011) Chlorophyll fluorescence in reef-building coral. In: Suggett PJ, Borowitzka MA, Prášil O (eds) Chlorophyll fluorescence in aquatic science: Methods and applications. Springer Science+Business Media B. V., pp 203-222

Weber JN (1973) Incorporation of strontium into reef coral skeletal carbonate. Geochimica et Cosmochimica Acta 37: 2173-2190

Wei G, McCulloch MT, Mortimer G, Deng W, Xie L (2009) Evidence for ocean acidification in the Great Barrier Reef of Australia. Geochimica et Cosmochimica Acta 73: 2332-2346

Wei G, Sun M, Li X, Nie B (2000) Mg/Ca, Sr/Ca and U/Ca ratios of a porites coral from Sanya Bay, Hainan Island, South China Sea and their relationships to sea surface temperature. Palaeogeography, Palaeoclimatology, Palaeoecology 162: 59-74

Wernberg T, Smale DA, Thomsen MS (2012) A decade of climate change experiments on marine organisms: procedures, patterns and problems. Global Change Biology 18: 1491-1498

Weyl PK (1959) The change in solubility of calcium carbonate with temperature and carbon dioxide content. Geochimica et Cosmochimica Acta 17: 214-225

White AJ, Critchley C (1999) Rapid light curves: a new fluorescence method to assess the state of the photosynthetic apparatus. Photosynthesis Research 59: 63-72

Wilkinson C (2002) Status of coral reefs of the world: 2002. Australian Institute of Marine Science, Australia, pp 378

Williams DE, Hallock P (2004) Bleaching in *Amphistegina gibbosa* d'Orbigny (Class Foraminifera): observations from laboratory experiments using visible and ultraviolet light. Marine Biology 145: 641-649

Williams SL (1984) Uptake of sediment ammonium and translocation in a marine green macroalga *Caulerpa cupressoides*. Limnology and Oceanography 29: 374-379

Winters G, Loya Y, Rottgers R, Beer S (2003) Photoinhibition in shallow-water colonies of the coral *Stylophora pistillata* as measured in situ. Limnology and Oceanography 48: 1388-1393

Wolf NG (1985) Food selection and resources partitioning by herbivorous fishes in mixed-species groups. Proceedings of the Fifth International Coral Reef Symposium 4: 23-28

Wollman F-A (2001) State transitions reveal the dynamics and flexibility of the photosynthetic apparatus. The EMBO Journal 20: 3623-3630

Yamazaki J, Kozu A, Fukunaga Y (2006) Characterization of chlorophyll–protein complexes isolated from two marine green algae, *Bryopsis maxima* and *Ulva pertusa*, growing in the intertidal zone. Photosynthesis Research 89: 19-25

Yates KK, Halley RB (2006a) CO_3^{2-} concentration and pCO_2 thresholds for calcification and dissolution on the Molokai reef flat, Hawaii. Biogeoscience 3: 357-369

Yates KK, Halley RB (2006b) Diurnal variation in rates of calcification and carbonate sediment dissolution in Florida Bay. Estuaries and Coasts 29:24-39

Zhang Y, Dawe RA (2000) Influence of Mg^{2+} on the kinetics of calcite precipitation and calcite crystal morphology. Chemical Geology 163: 129-138

Zmiri A, Kahan D, Hochstein S, Reiss Z (1974) Phototaxis and thermotaxis in some species of *Amphistergina* (Foraminifera). Journal of Protozoology 21: 133-138

Zondervan I, Rost Br, Riebesell U (2002) Effect of CO_2 concentration on the PIC/POC ratio in the coccolithophore *Emiliania huxleyi* grown under light-limiting conditions and different daylengths. Journal of Experimental Marine Biology and Ecology 272: 55-70

APPENDIX

APPENDIX

APPENDIX 1 PUBLICATION ARISING FORM CHAPTER 4:

Sinutok S, Hill R, Doblin MA, Wuhrer R, Ralph PJ (2011) Warmer more acidic conditions cause decreased productivity and calcification in subtropical coral reef sediment-dwelling calcifiers. *Limnology and Oceanography* 56(4): 1200-1212.

Limnol. Oceanogr., 56(4), 2011, 1200–1212

doi:10.4319/lo.2011.56.4.1200

Warmer more acidic conditions cause decreased productivity and calcification in subtropical coral reef sediment-dwelling calcifiers

Sutinee Sinutok,[a] Ross Hill,[a,*] Martina A. Doblin,[a] Richard Wuhrer,[b] and Peter J. Ralph[a]

[a] Plant Functional Biology and Climate Change Cluster, School of the Environment, University of Technology, Sydney, Australia
[b] Centre of Expertise Microstructural Analysis, University of Technology, Sydney, Australia

Abstract

The effects of elevated CO_2 and temperature on photosynthesis and calcification in the calcifying algae *Halimeda macroloba* and *Halimeda cylindracea* and the symbiont-bearing benthic foraminifera *Marginopora vertebralis* were investigated through exposure to a combination of four temperatures (28°C, 30°C, 32°C, and 34°C) and four CO_2 levels (39, 61, 101, and 203 Pa; pH 8.1, 7.9, 7.7, and 7.4, respectively). Elevated CO_2 caused a profound decline in photosynthetic efficiency ($F_V : F_M$), calcification, and growth in all species. After five weeks at 34°C under all CO_2 levels, all species died. Chlorophyll (Chl) *a* and *b* concentration in *Halimeda* spp. significantly decreased in 203 Pa, 32°C and 34°C treatments, but Chl *a* and Chl c_2 concentration in *M. vertebralis* was not affected by temperature alone, with significant declines in the 61, 101, and 203 Pa treatments at 28°C. Significant decreases in $F_V : F_M$ in all species were found after 5 weeks of exposure to elevated CO_2 (203 Pa in all temperature treatments) and temperature (32°C and 34°C in all pH treatments). The rate of oxygen production declined at 61, 101, and 203 Pa in all temperature treatments for all species. The elevated CO_2 and temperature treatments greatly reduced calcification (growth and crystal size) in *M. vertebralis* and, to a lesser extent, in *Halimeda* spp. These findings indicate that 32°C and 101 Pa CO_2, are the upper limits for survival of these species on Heron Island reef, and we conclude that these species will be highly vulnerable to the predicted future climate change scenarios of elevated temperature and ocean acidification.

Since the beginning of the industrial revolution, human activities such as the burning of fossil fuels, industrialization, deforestation, and intensive agricultural activities have raised atmospheric CO_2 concentrations (Gattuso and Lavigne 2009). As a consequence, surface seawater temperature has increased by 0.6°C over the last century (Houghton 2009). Moreover, a 35% increase in atmospheric CO_2 concentration (from preindustrial levels of 28.4 Pa to approximately 38.9 Pa today) has led to ocean acidification by elevating the dissolved CO_2 concentration in the surface ocean, which lowers pH (Solomon et al. 2007). The rate of change is 100–1000 times faster than the most rapid changes in temperature and CO_2 in at least the last 420,000 yr (Hoegh-Guldberg et al. 2007). Models parameterized with CO_2-emission trends for 1990–1999 (the so-called "Special Report on Emissions Scenarios"; Solomon et al. 2007) predict that CO_2 concentrations will rise 150–250% (to $\leq$ 101 Pa) by the year 2100 (Friedlingstein et al. 2006). The surface ocean pH is already 0.1 units lower than preindustrial values (Orr et al. 2005), which is equivalent to a 30% increase in H^+ ions (Raven et al. 2005) and is predicted to decrease by a further 0.4 to 0.5 units by 2100 (Raven et al. 2005; Lough 2007).

An increase in sea temperature and atmospheric CO_2 will influence the health and survivorship of marine organisms, especially calcifying species, such as molluscs, crustaceans, echinoderms (Doney et al. 2009), corals (Reynaud et al. 2003; Jokiel et al. 2008), calcareous algae (Jokiel et al. 2008), foraminifera (Hallock 2000), and some phytoplankton (Raven et al. 2005; Iglesias-Rodriguez et al. 2008). Temperature influences physiological processes, including photosynthesis, respiration, and calcification (Howe and Marshall 2002; Necchi 2004). In reef-building (scleractinian) corals, warmer temperatures increase the rate of calcification (Lough and Barnes 2000), although increases beyond a thermal threshold as small as 1–2°C above summer averages can lead to mass coral bleaching events (large areas of coral colonies expelling symbiotic algae) and sometimes death (Hoegh-Guldberg 1999).

Ocean acidification has been suggested to have a positive effect on organisms such as seagrass and noncalcifying macroalgae, which utilize CO_2 as the substrate for carbon fixation in photosynthesis (Gao et al. 1993; Short and Neckles 1999). However, ocean acidification is likely to have a negative effect on calcified organisms by decreasing the availability of carbonate ions (CO_3^{2-}) and hence the organisms' ability to produce their calcium carbonate skeleton (Feely et al. 2004). Acidification has been shown to reduce calcification, recruitment, growth, and productivity in the articulated coralline alga *Corallina pilulifera* Postels and Ruprecht as well as in crustose coralline algae (CCA) when exposed to elevated pCO_2 (partial pressure of CO_2) seawater (Kuffner et al. 2007; Anthony et al. 2008). Reduced abundance of CO_3^{2-} ions could also lead to an increase in calcium carbonate dissolution in the future (Feely et al. 2004).

Synergistic effects of elevated temperature and pCO_2 have had limited examination, but Reynaud et al. (2003) observed 50% lower calcification rates in the scleractinian coral *Stylophora pistillata* Esper compared to either high temperature or low pH conditions in isolation. However, in the corals *Acropora intermedia* Brook and *Porites lobata* Dana, Anthony et al. (2008) found that combined ocean acidification and warming scenarios (rather than ocean

* Corresponding author: ross.hill@uts.edu.au

acidification conditions in isolation) resulted in bleaching, reduced productivity, and calcium carbonate dissolution and erosion in *A. intermedia* and *P. lobata* and in the CCA species *Porolithon onkodes* (Heydrich) Foslie.

Reef-building and sediment-dwelling species, *Halimeda* and symbiont-bearing foraminifera are prominent, co-existing taxa in shallow reef systems and play a vital role in tropical and subtropical ecosystems as producers of sediment in coral reefs (Hallock 1981). However, there is limited evidence of the effects of ocean warming and acidification in these two important carbonate sediment producers. Elevated seawater temperatures of 30°C to 35°C reduced the growth rate in the benthic foraminifera *Rosalina leei* Hedley and Wakefield (Nigam et al. 2008) and induced algal symbiont loss in *Amphistegina gibbosa* d'Orbigny when temperatures reached 32°C (Talge and Hallock 2003). Borowitzka and Larkum (1976) showed an inhibition in calcification in *Halimeda tuna* (Ellis and Solander) Lamouroux when seawater pH was dropped from 8.0 to 7.5. A more recent study found thinner aragonite crystals and higher crystal density in *H. tuna* and *Halimeda opuntia* grown in pH 7.5 as compared to those grown at pH 8.1 (L. L. Robbins unpubl.). Research on symbiotic and nonsymbiotic planktonic foraminifera (*Orbulina universa* d'Orbigny and *Globigerina sacculifers* Brady, respectively) and symbiotic benthic foraminifera (*Marginopora kudakajimensis* Gudmundsson) showed a decrease in shell weight with decreasing availability of the carbonate ion in seawater (Kuroyanagi et al. 2009). These results indicate that a decrease in calcification is likely in these organisms under the acidified conditions that are expected to occur in the future. However, there have been no studies on the combined effect of elevated temperature and CO_2 concentration on the photosynthetic marine calcifiers, *Halimeda* spp. and benthic foraminifera.

Halimeda spp. precipitate calcium carbonate as aragonite, whereas foraminifera precipitate high-magnesium calcite. The current saturation state of aragonite (Ω_a = 3 to 4) is greater than that of the high-Mg calcite mineral (Ω_c = 2 to 3; Kleypas et al. 1999; International Society for Reef Studies 2008), which means that organisms that precipitate high-Mg calcite are expected to have more difficulty in producing their $CaCO_3$ skeleton under elevated pCO_2 conditions compared to organisms that precipitate $CaCO_3$ as aragonite (Kleypas et al. 1999). Thus, the hypothesis tested in this study was that the calcifying macroalga *Halimeda* would perform better than benthic foraminifera under high-CO_2 conditions and that all organisms would show greater effects under the combined effects of elevated CO_2 and temperature.

Methods

Experimental design—Whole specimens of *Halimeda macroloba* Decaisne (thallus size, 13–18 cm long), *Halimeda cylindracea* Decaisne (15–20 cm long), and *Marginopora vertebralis* Quoy and Gaimard (0.3–0.6 cm diameter) were collected by hand from the Heron Island reef flat at low tide at 0.3-m depth in the Southern Great Barrier Reef of Australia (151°55′E, 23°26′S). Symbiont-bearing foraminifera *M. vertebralis* hosts symbiotic alga *Symbiodinium* sp. in interior shell chambers (Pawlowski et al. 2001). The specimens of these species were maintained in a 500-liter aquarium with artificial seawater (pH 8.1, 26°C, salinity 33) under 250 μmol photons m^{-2} s^{-1} (at water surface) on a 12 : 12 light : dark (LD) cycle. Mature segments of *H. macroloba* (0.8–1.1 cm long) and *H. cylindracea* (1.5–2.0 cm long) from the middle part of the thallus and *M. vertebralis* (320 each species) were randomly allocated to one of four temperature treatments (28°C, 30°C, 32°C, and 34°C) in combination with one of four pH treatments (8.1, 7.9, 7.7, and 7.4; the current and the predicted pH values for the years 2065, 2100, and 2200, respectively, and equivalent to pCO_2 38.5, 60.8, 101, and 203 Pa in this experiment; Houghton 2009). Within each tank, samples of each of the three species were placed in separate, open petri dishes, so that there was no direct physical interaction between specimens. Samples were ramped from 26°C and pH 8.1 to their treatment conditions over 1 week and maintained in the 16 treatments for a further 4 weeks (n = 4). The tanks set at an ambient pH of 8.1 and 28°C acted as controls. The water salinity in the 100-liter experimental tanks was maintained at 33, and the light intensity at the sample height was 300 μmol photons m^{-2} s^{-1} on a 12 : 12 LD cycle (on at 06:00 h and off at 18:00 h). The treatment tanks were 0.2 m deep, consistent with sampling depth. The carbonate hardness (concentration of CO_3^{2-} + HCO_3^-), calcium, nitrate, and phosphate concentration were maintained at 2.3, 10, < 0.0016, and < 0.0005 mmol L^{-1}, respectively, and monitored weekly using test kits (Aquasonic Pty). The concentration of CO_2 in both treatments and controls was maintained by CO_2 gas bubbling through the water held in the sump before it was recirculated to the aquaria containing the samples. CO_2 dosing was automated using a pH-controller (Tunze) connected to a solenoid valve on a CO_2 gas line. CO_2 gas was bubbled through the seawater once pH increased beyond the target pH and was maintained at a precision of ± 0.01 pH units. pH electrodes (National Bureau of Standards scale; Tunze), each connected to a pH-controller, were calibrated every week, during which time no detectable drift in pH was found. Water temperature in each treatment was controlled by water heaters and chillers (Hailea) to ± 0.1°C. Water changes (20%) to each treatment were performed every week using seawater media set to the required pH using CO_2 bubbling prior to addition. Salinity was measured daily with a salinity meter (Salt 6, Eutech Instruments), while total alkalinity (TA) was measured weekly by titrating 30 g of seawater with 0.1 mol L^{-1} hydrochloric acid using an autotitrator (Mettler Toledo; Gattuso et al. 1993). From each treatment tank, TA was determined as the average from three independent samples of water. Dissolved inorganic carbon (DIC) concentrations were calculated using the CO2SYS program (version 01.05; Brookhaven National Laboratory; Lewis and Wallace 1998). A summary of the TA, total inorganic carbon (DIC, CO_2, CO_3^{-2}, HCO_3^-), pCO_2, and saturation state of seawater with respect to calcite (Ω_c) and aragonite (Ω_a) from each pH (8.1, 7.9, 7.7, 7.4) and temperature (28°C, 30°C, 32°C, 34°C) treatment are shown in Table 1. There

Table 1. Parameters of the carbonate system; total alkalinity (TA), CO_2 partial pressure (pCO_2), total inorganic carbon (CO_2, CO_3^{-2}, HCO_3^-, DIC), and saturation state of seawater with respect to calcite (Ω_c) and aragonite (Ω_a) from each pH (8.1, 7.9, 7.7, 7.4) and temperature (28°C, 30°C, 32°C, 34°C).

Treatment								
pH	Temp (°C)	TA (mmol kg^{-1})	pCO_2 (Pa)	CO_2 (mmol kg^{-1})	CO_3^{2-} (mmol kg^{-1})	HCO_3^- (mmol kg^{-1})	DIC (mmol kg^{-1})	Ω_c	Ω_a
8.1	28	2.314±0.187	32.2±2.6	0.008±0.001	0.280±0.035	1.635±0.135	1.923±0.160	6.03±0.95	4.04±0.61
8.1	30	2.647±0.190	36.8±2.7	0.008±0.001	0.340±0.030	1.842±0.145	2.190±0.166	7.40±0.55	4.99±0.63
8.1	32	2.695±0.189	36.9±2.6	0.008±0.001	0.365±0.042	1.835±0.138	2.209±0.162	8.02±0.73	5.44±0.60
8.1	34	2.392±0.190	32.2±2.6	0.007±0.001	0.338±0.035	1.579±0.133	1.924±0.160	7.50±0.74	5.13±0.60
7.9	28	2.685±0.169	66.9±4.6	0.016±0.002	0.231±0.004	2.140±0.170	2.387±0.170	3.34±0.10	3.34±0.09
7.9	30	2.624±0.168	65.1±4.5	0.016±0.002	0.240±0.003	2.058±0.173	2.314±0.173	3.52±0.15	3.52±0.10
7.9	32	2.607±0.170	64.6±4.5	0.015±0.002	0.238±0.003	2.044±0.180	2.297±0.182	3.49±0.12	3.49±0.10
7.9	34	2.309±0.170	56.3±4.6	0.012±0.002	0.235±0.004	1.743±0.175	1.990±0.176	3.57±0.14	3.57±0.12
7.7	28	2.532±0.110	108.0±4.7	0.027±0.001	0.148±0.018	2.172±0.080	2.347±0.101	2.14±0.44	2.14±0.33
7.7	30	2.565±0.108	110.0±4.7	0.025±0.001	0.160±0.019	2.185±0.082	2.370±0.099	2.36±0.52	2.36±0.32
7.7	32	2.427±0.110	104.0±4.8	0.024±0.001	0.162±0.018	2.042±0.083	2.228±0.110	2.41±0.49	2.41±0.34
7.7	34	2.691±0.109	115.0±4.8	0.025±0.001	0.191±0.020	2.244±0.080	2.460±0.095	2.90±0.49	2.90±0.33
7.4	28	2.696±0.136	247.0±12.5	0.062±0.004	0.085±0.008	2.495±0.145	2.642±0.133	1.84±0.16	1.23±0.15
7.4	30	2.568±0.129	236.0±12.2	0.056±0.005	0.087±0.007	2.362±0.135	2.505±0.132	1.89±0.15	1.28±0.15
7.4	32	2.827±0.134	262.0±12.7	0.059±0.005	0.102±0.008	2.588±0.130	2.749±0.139	2.26±0.18	1.53±0.17
7.4	34	2.526±0.135	235.0±12.5	0.051±0.005	0.098±0.005	2.295±0.140	2.444±0.135	2.18±0.15	1.49±0.16

was no significant difference in TA among the 16 pH and temperature treatments, and pCO_2, CO_2,CO_3^{-2}, HCO_3^-, DIC, Ω_c, and Ω_a remained consistent within each pH treatment.

Mortality assessment—Mortality in *H. macroloba* and *H. cylindracea* was determined by presence of bleached and disintegrated segments, whereas mortality in *M. vertebralis* was determined by bleached and broken tests. In addition, the lack of variable fluorescence from measures of pulse amplitude modulated (PAM) fluorometry (indicative of photosynthetic activity by algal symbionts) was an indication of mortality.

Photosynthesis—Photosynthetic condition was determined through measures of chlorophyll (Chl) *a* fluorescence, oxygen production, photosynthetic pigment concentration, and, for foraminifera, algal symbiont density. To avoid diel and non–steady state variability, steady state light curves (SSLCs), with one irradiance step (372 μmol photons m^{-2} s^{-1} applied for 300 s) were performed with a 6-mm-diameter fiber-optic on a Diving-PAM fluorometer (Walz) every week at 10:00 h over the duration of the experiment, following 10 min of dark adaptation (Diving-PAM settings: measuring intensity < 0.15 μmol photons m^{-2} s^{-1}, saturating intensity > 4500 μmol photons m^{-2} s^{-1}, saturating width = 0.8 s, gain = 2, damping = 2). Photosystem II (PSII) photosynthetic efficiency was determined through weekly measures of maximum quantum yield, $F_V : F_M$, and effective quantum yield, Y(II). In addition, the capacity for photoprotection (nonphotochemical quenching yield, Y[NPQ]) and level of photoinhibition (nonregulated heat dissipation yield, Y[NO]) were determined through SSLCs (Kramer et al. 2004).

Oxygen production was measured using a needle-type fiber-optic oxygen microsensor PSt1 connected to a Micro TX3 transmitter (Presens). After 10 min of dark adaptation, the samples were placed in 10-mL glass bottles filled to the top with treatment water; then the bottles were sealed and placed in a water bath (Julabo) set to the relevant treatment temperature. The sensor was inserted through a resealable hole in the bottle lid to determine the oxygen production during 5 min under 300 μmol photons m^{-2} s^{-1} of irradiance, and rates were calculated according to Ulstrup et al. (2005).

Photosynthetic pigment concentration (Chl *a* and Chl *b* for *H. macroloba* and *H. cylindracea* and Chl *a* and Chl c_2 for *M. vertebralis*) was determined using the standard spectrophotometric method of Ritchie (2008) at the beginning and end of the 5-week experiment. Chl *a*, Chl *b*, and Chl c_2 were extracted by soaking samples in 3 mL of 90% acetone at 4°C in darkness for 24 h. Samples were centrifuged at 1500 × *g* for 10 min; the supernatant was placed into a quartz cuvette in a spectrophotometer (Varian); and absorbance was measured at 630, 647, and 664 nm. Chlorophyll concentrations were determined using the equations of Ritchie (2008), and the results were expressed in μg mm^{-2}.

Algal symbiont density in the foraminifera was investigated using a confocal microscope (Nikon A1). For each

individual foraminiferan, four randomly selected interrogation areas were chosen from the edge, middle, and center of the test (shell). Algal symbionts in the chambers within each area were counted and expressed in terms of surface area.

Calcification—Calcification was determined using the buoyant weight technique (Jokiel et al. 2008), with comparisons made between measurements at the start and end of the experimental period. The buoyant weight technique is a reliable measure of calcification, inferred from changes in skeletal weight (Langdon et al. 2010). It was determined by weighing each sample in seawater of known density and applying Archimedes' principle to compute the dry weight of the sample in the air (Jokiel et al. 1978; Langdon et al. 2010). Weight was measured using an electronic balance with accuracy to 0.1 mg. The samples were placed on a glass petri dish hung below the balance using nylon thread suspended in seawater. The density of water at salinity 33 and 25°C was 1026.42 kg m^{-3} (Jokiel et al. 1978), and the densities of *H. macroloba*, *H. cylindracea*, and *M. vertebralis* at salinity 33 and 25°C were 2052.37, 5384.9, and 2733.98 kg m^{-3}, respectively (Jokiel et al. 1978).

Images of aragonite and magnesium calcite crystals were examined for size and abundance analysis using a field emission gun scanning electron microscope (Zeiss Supra 55VP). The instrument was operated at 20 kV with 30-μm aperture, ~ 4-mm working distance in Hi-Vac mode and imaged using the secondary In-lens detector. Samples were mounted on aluminum stubs using carbon adhesive tape and then placed in a carbon coating unit (Balzers) operated at 40-mm working distance. An area of 9 μm^2 was selected, and the crystal abundance was determined ($n = 4$ per sample with 10 measurements per replicate) along with crystal width, which was calculated using spatial analysis software (University of Texas Health Science Center, San Antonio, Image Tool version 3; University of Texas).

Statistical analysis—To determine any significant differences among treatments in growth rate, Chl *a*, Chl *b*, and Chl c_2 concentration, chlorophyll fluorescence parameters ($F_V : F_M$, Y[II], Y[NPQ], and Y[NO]), oxygen production, and crystal density and width over time, repeated-measures ANOVA (rmANOVA) tests were performed. One-way ANOVA tests were used to compare treatments at the initial or final time point (Statistical Package for the Social Sciences version 17). All tests were performed with a significance level of 95%, and Tukey's Honestly Significant Difference post hoc tests were used to identify the statistically distinct groups. If data did not meet the assumptions of normality (Kolmogorov-Smirnov test) and equal variance (Levene's test), the data were transformed using $\log_{10}$ or square root. Differences in symbiont density among treatments were tested using the Friedman test at a 95% significance level.

Results

Calcification and mortality—The calcification rates of *H. macroloba*, *H. cylindracea*, and *M. vertebralis* were slightly positive in the control treatment and were highly negative in the other treatments, indicating dissolution of calcium carbonate. Calcification rate was significantly reduced by elevated temperature (34°C) at all pH levels ($p < 0.05$). Calcification rate of *H. macroloba* at pH 7.4 and 34°C (-1.24 ± 0.70 mg $CaCO_3$ d^{-1}) was significantly lower than the control (0.02 ± 0.01 mg $CaCO_3$ d^{-1}; $p < 0.001$; Fig. 1A–D). In *H. cylindracea*, calcification rate significantly declined at pH values 7.7 and 7.4 in 34°C treatments ($p < 0.001$; Fig. 1E–H), whereas in *M. vertebralis* calcification rate significantly decreased at pH values 7.9, 7.7, and 7.4 at 30°C, 32°C, and 34°C ($p < 0.05$; Fig. 1I–L). Foraminiferan mortality was first observed at day 21 of the experiment at pH 7.4, 30°C and 34°C; whereas, in *H. macroloba* and *H. cylindracea*, mortality was found at day 28 at pH values 8.1, 7.9, and 7.4 at 34°C and pH 8.1 at 34°C, respectively. *H. macroloba* and *H. cylindracea* had 100% mortality at the end of the experiment at pH 7.4 and 34°C, whereas 100% mortality of *M. vertebralis* was observed at pH values 7.7 and 7.4 in the 32°C and 34°C treatments. At lower pH treatments (all except control) and higher temperature (32°C and 34°C) treatments, the symbiont density of foraminifera significantly decreased ($p < 0.001$; Fig. 2A–E), and foraminifera bleaching and death was observed.

Pigment content—After 5 weeks, the Chl *a* and Chl *b* concentration in *H. macroloba* significantly declined at pH values 8.1, 7.9, and 7.7 with 34°C and at pH 7.4 with 32°C and 34°C treatments ($p < 0.001$; Fig. 3A–E). However, no significant change was detected in Chl *a* and Chl *b* concentration at pH values 8.1, 7.9, and 7.7 with 28°C, 30°C, and 32°C treatments over the 5-week experiment ($p > 0.05$; Fig. 3A–E). The Chl *a* and Chl *b* concentration in *H. cylindracea* after 5 weeks significantly declined at pH values 8.1 and 7.9 with 34°C and at pH 7.4 with 28°C and 34°C treatments ($p < 0.001$; Fig. 3F–J). In *M. vertebralis*, Chl *a* and Chl c_2 concentration significantly decreased at pH values 7.9, 7.7, and 7.4 at all temperature treatments and at pH 8.1 with 34°C treatment ($p < 0.001$; Fig. 3K–O).

Chl a fluorescence—Maximum quantum yield ($F_V : F_M$) and effective quantum yield (Y[II]; data not shown) in the control treatment was constant in *H. macroloba*, *H. cylindracea*, and in the symbionts of *M. vertebralis* ($p > 0.05$; Fig. 4A,E,I). A significant decrease in $F_V : F_M$ and Y(II) was found in all species when exposed to elevated CO_2 (pH 7.4 in all temperature treatments) and temperature (32°C and 34°C in all pH treatments) over the length of the experiment ($p < 0.001$; Fig. 4A–L). In *H. macroloba*, $F_V : F_M$ declined to zero after being treated at 34°C at all pH levels for 28 d ($p < 0.001$; Fig. 4A–D). $F_V : F_M$ of *H. cylindracea* decreased to zero after 28 d at 34°C, in pH 8.1, 7.9, and 7.7 treatments ($p < 0.001$; Fig. 4E–H). In symbionts of *M. vertebralis*, $F_V : F_M$ significantly decreased at 34°C and in all pH treatments after 14 d of experimentation and also reached zero within 14 d at pH 8.1 and 34°C treatment ($p < 0.001$; Fig. 4I–L). At lower temperatures (28°C and 30°C) with lower pH treatments (pH values 7.7 and 7.4), effective quantum yield (Y[II]; $p <$

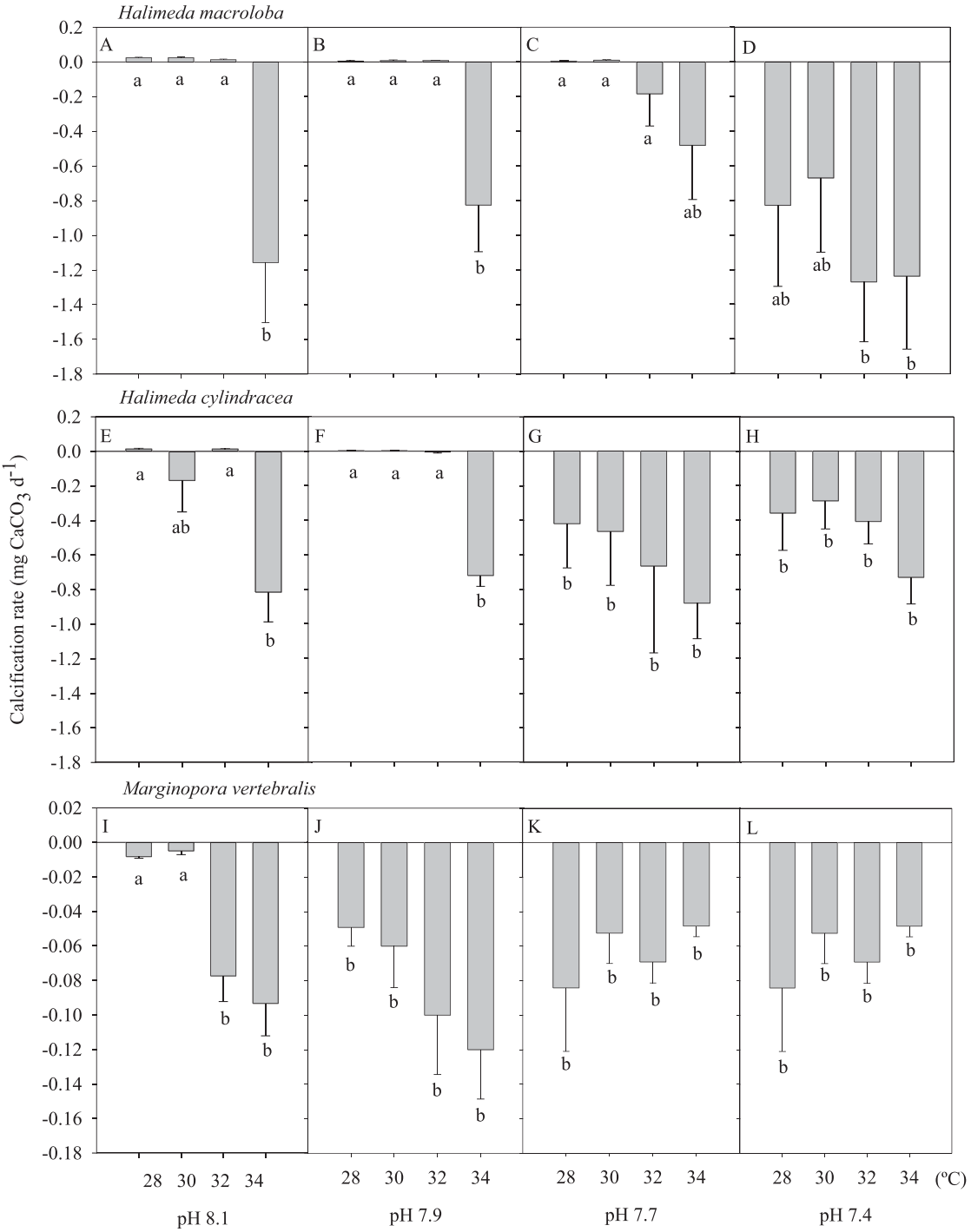

Fig. 1. Calcification rate (mg $CaCO_3$ d^{-1}) over the 5-week period in (A–D) *H. macroloba*, (E–H) *H. cylindracea*, and (I–L) *M. vertebralis* in each pH and temperature treatment. Data represent means ($n = 4$, SEM).

0.001; data not shown) and maximum quantum yield ($F_V : F_M$; $p < 0.001$) of *H. macroloba* (Fig. 4A–D), *H. cylindracea* (Fig. 4E–H) and *M. vertebralis* (Fig. 4I–L) significantly decreased after 5 weeks of experimentation. Moreover, there was a greater decrease in $F_V : F_M$ and Y(II) in all species when exposed to the combined treatment of elevated temperature and CO_2. The capacity for photoprotection, Y(NPQ), and the level of photoinhibition, Y(NO), were similar over time in all pH and temperature treatments prior to mortality ($p > 0.05$; data not shown).

Oxygen production—The rate of oxygen production of *H. macroloba*, *H. cylindracea*, and symbionts of *M. vertebralis* significantly decreased when exposed to elevated

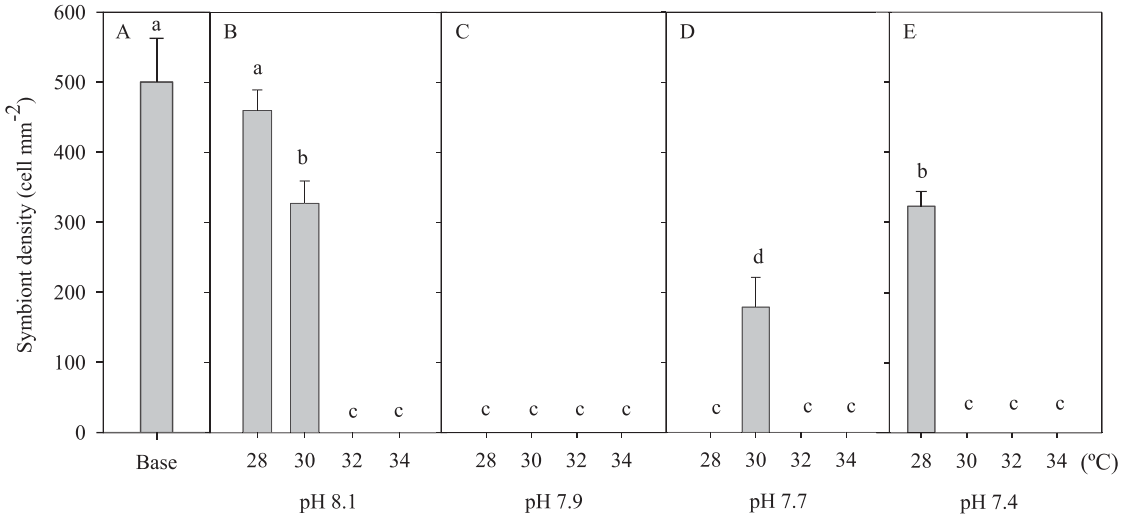

Fig. 2. Symbiont density (cells mm^{-2}) of *M. vertebralis* at (A) time zero (base) and each of the four temperature treatments (28, 30, 32, and 34°C) at pH (B) 8.1, (C) 7.9, (D) 7.7, and (E) 7.4. No bar indicates the absence of symbionts. Data represent means ($n = 4$, SEM).

CO_2 at pH 7.4 for 18 d ($p < 0.001$, Fig. 5A–L). Higher temperature (34°C) significantly lowered the oxygen production rate in *H. macroloba* only when maintained at a pH of 8.1. Greatest oxygen production of *H. macroloba* was found at pH 8.1, 30°C (14.06 ± 1.47 μmol L^{-1}) on day 0, whereas the lowest oxygen production was found at 34°C in all pH treatments on day 35 (0 ± 0 μmol L^{-1}; Fig. 5A–D). Similarly, *H. cylindracea* had its highest and lowest oxygen production on day 0, pH 7.9, 34°C and in pH 8.1, 7.9, and 7.4 treatments (14.85 ± 4.82 and 0.0 ± 0.0 μmol L^{-1}), respectively; whereas, in symbionts of *M. vertebralis*, the highest and lowest oxygen production was found on day 18, pH 7.9, 34°C and on day 27 and day 35, 32°C and 34°C at all pH treatments (11.71 ± 4.17 and 0.0 ± 0.0 μmol L^{-1}; Fig. 5E–L).

Calcification—After 5 weeks, the calcium carbonate crystal width of *H. macroloba*, *H. cylindracea*, and *M. vertebralis* significantly decreased when exposed to elevated CO_2 at pH values 7.7 and 7.4 ($p < 0.05$; Figs. 6, 7). Elevated temperature had no effect on the crystal width in *H. macroloba* ($p = 0.562$) or *H. cylindracea* ($p = 0.926$) but caused a significant decrease in the crystal width of *M. vertebralis* at 32°C and 34°C in all pH treatments ($p < 0.001$; Fig. 6). In contrast, crystal abundance in the foraminiferans increased significantly at high CO_2 at pH values 7.9, 7.7, and 7.4 and high temperature at 32°C and 34°C ($p < 0.001$) from 25.46 ± 0.77 crystals μm^{-2} in the control to 39.93 ± 0.43 crystals μm^{-2} at pH 7.4 and 34°C. However, there was no significant difference in crystal abundance of *H. macroloba* and *H. cylindracea* among pH and temperature treatments ($p > 0.05$).

Discussion

To our knowledge, this is the first investigation on the combined effects of elevated temperature and ocean acidification on photosynthesis and calcification in the photosynthetic marine calcifying algae *H. macroloba* and *H. cylindracea* and the benthic symbiotic foraminifera *M. vertebralis*. As we hypothesized, the calcifying macroalga *Halimeda* performed better than benthic foraminifera under high CO_2 conditions, and the combined factors had a more detrimental (synergistic) effect on growth, photosynthesis, and calcification in all species. Unexpectedly, elevated temperature and lowered pH (34°C and pH 7.4) caused mortality in *H. macroloba* and *H. cylindracea* within 4 weeks and in *M. vertebralis* within 3 weeks. The cause of the mortality of the foraminiferan is likely due to damage to the symbionts, as indicated by changes in photosynthetic pigments, Chl *a* fluorescence ($F_V : F_M$, Y[II]), and oxygen production. There was a decline in Chl *a*, Chl *b*, and Chl c_2 concentrations in lower pH treatments (pH values 7.7 and 7.4) after 5 weeks, indicative of chlorophyll degradation, decreased photosynthetic unit size, and/or a decrease in the number of PSII reaction centers. There was also a significant decline in photosynthetic efficiency and primary production after 28 d of exposure to 32°C and 34°C, and pH 7.4 conditions in all three species (Figs. 4, 5). It is clear that elevated CO_2 and temperature conditions cause a reduction in the photosynthetic efficiency of PSII. Heat stress is likely to damage PSII, possibly by damaging the D1 protein and disrupting the thylakoid membrane stability (Allakhverdiev et al. 2008), whereas pH stress may disrupt the CO_2 accumulation pathway at the site of Rubisco or interfere with electron transport via the thylakoid proton gradients (Anthony et al. 2008).

Lower pH and higher temperature (all treatments except control pH and 28°C, 30°C) significantly triggered the bleaching and death of *M. vertebralis*. Symbiont expulsion is suggested to occur when the symbionts are damaged through photoinhibition (Hallock et al. 2006). Promotion of photooxidative reactions is likely under the stress conditions of pH and temperature applied here, through the degradation of the D1 protein (Talge and Hallock 2003). Alternatively, the symbionts may be digested by the

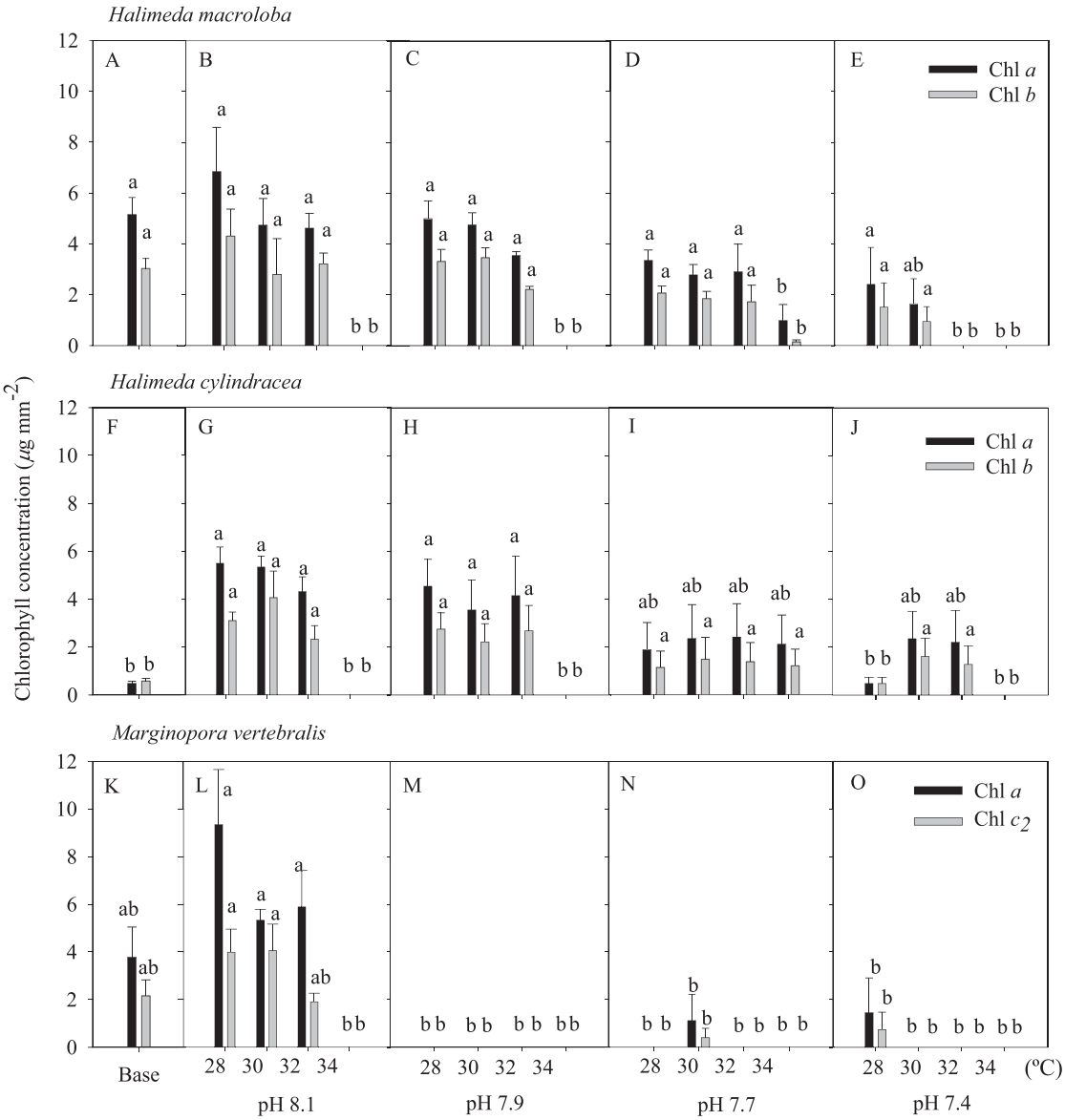

Fig. 3. Chl *a* and Chl *b* concentrations (μg mm^{-2}) in (A–E) *H. macroloba* and (F–J) *H. cylindracea* and Chl *a* and Chl c_2 concentrations (μg mm^{-2}) in (K–O) *M. vertebralis* at time zero (base) and each pH and temperature treatment at week 5. No bar indicates the absence of chlorophyll. Data represent means (n = 4, SEM).

host when they are damaged (Hallock et al. 2006). Our results are consistent with the recent study of Talge and Hallock (2003), which demonstrated that bleaching in the foraminifera *Amphistegina gibbosa* is triggered by thermal stress.

Rising pCO_2 will inhibit calcification in calcifying organisms by decreasing the availability of CO_3^{2-} ions required for the deposition of calcium carbonate skeletons. However, in photosynthetic organisms (e.g., fleshy algae and seagrass), rising pCO_2 is expected to promote photosynthesis and, hence, enhance growth due to the greater abundance of substrate (CO_2) required for carbon fixation (Gao et al. 1993; Short and Neckles 1999). Therefore, the relationship between CO_2 abundance, photosynthesis, and growth is dependent upon whether or not the organism calcifies.

This study demonstrated that increased CO_2 (yielding potentially more substrate available for carbon uptake) did not lead to increased production in any organisms, suggesting that the main effect was one of pH affecting the overall metabolism of the organisms.

There was, however, a dramatic effect on calcification rates. Calcification rate was negative in *H. macroloba*, *H. cylindracea*, and *M. vertebralis* under the highest pCO_2 treatment, with high-Mg calcite species experiencing greater decline than aragonite-forming species. The calcification rate of the control did not change over time. The application of heat caused increasingly negative calcifica-

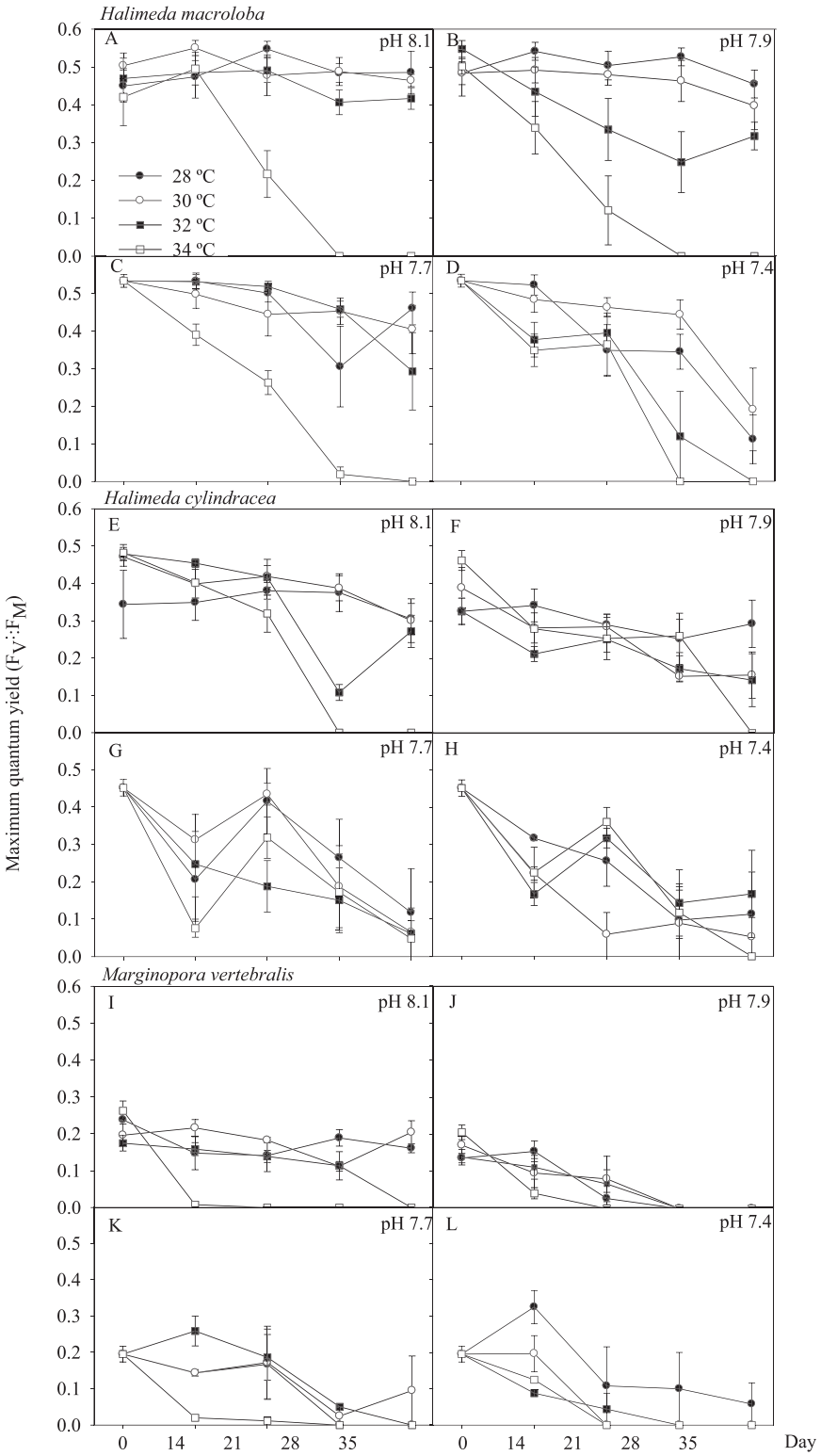

Fig. 4. Maximum quantum yield ($F_V : F_M$) of (A–D) *H. macroloba*, (E–H) *H. cylindracea*, and (I–L) *M. vertebralis* in each pH and temperature treatment over the length of the experimental period. Data represent means ($n = 4$, SEM).

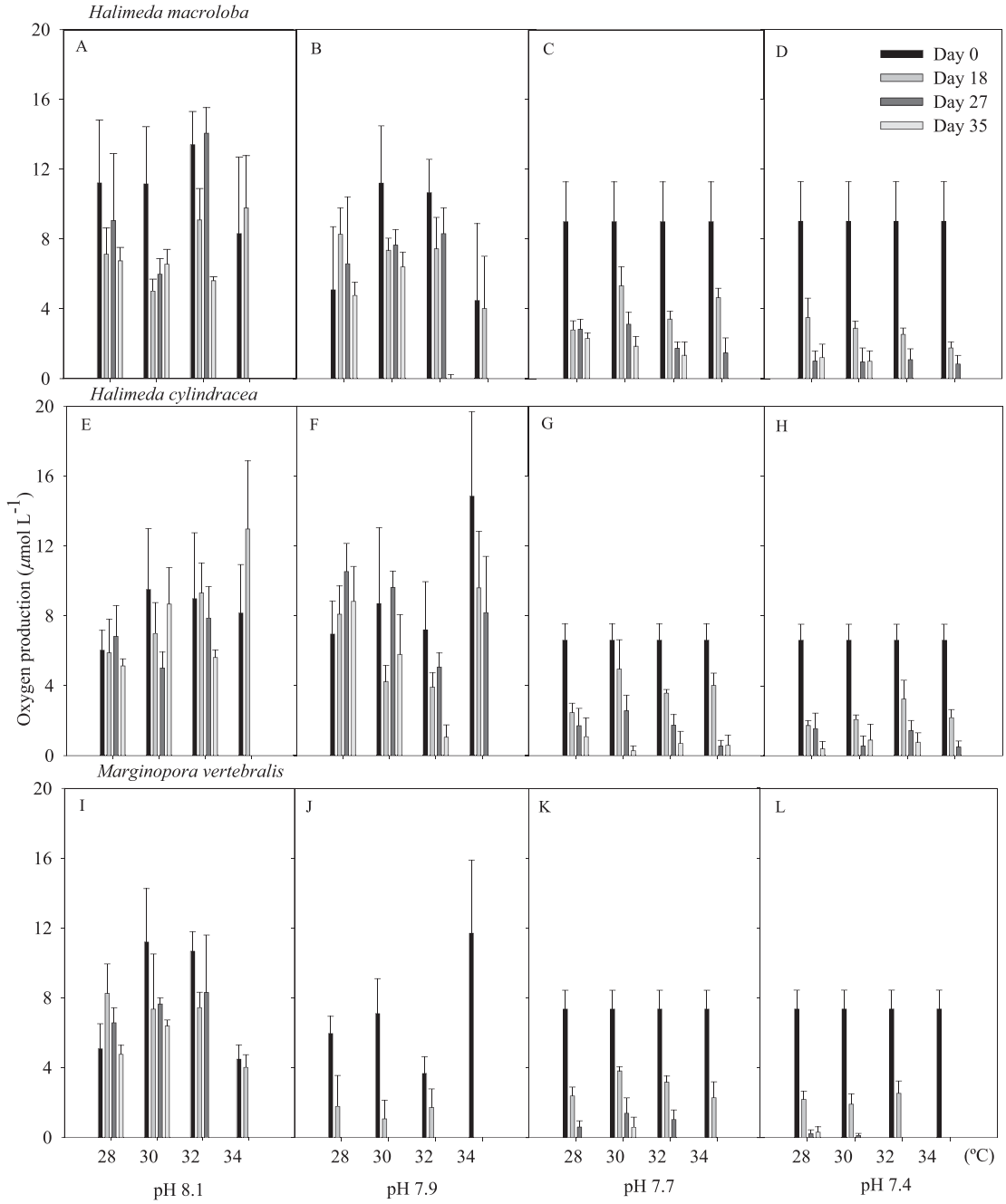

Fig. 5. Oxygen production (μmol O_2 L^{-1}) in (A–D) *H. macroloba*, (E–H) *H. cylindracea*, and (I–L) *M. vertebralis* in each pH and temperature treatment over the length of the experimental period. Data represent means (n = 4, SEM).

tion rates in all species, with *M. vertebralis* being most sensitive under all pCO_2 treatments at the highest temperature (pH values 8.1, 7.9, 7.7, and 7.4, and 34°C; Fig. 1), whereas calcification rate of the control did not change over time. The extreme CO_2 treatment of our experiments created the greatest reduction in CO_3^{2-} saturation state (to 1.23 ± 0.15 for Ω_a and 1.84 ± 0.16 for Ω_c; Table 1), which virtually prevented calcification in all three organisms and increased the potential for dissolution of the calcium carbonate structure. Increased temperature above the optimum temperature for these species will have a negative effect on calcification by decreasing enzyme activity and photosynthetic CO_2 fixation (Borowitzka 1986; Hallock 2000; Gonzalez-Mora et al. 2008). Thinner aragonite and calcite crystals were observed in the two *Halimeda* species when exposed to high pCO_2 (pH values 7.7 and 7.4) and in *M. vertebralis* when exposed to high pCO_2 and elevated temperature conditions (pH values 7.7 and 7.4, and 32°C and 34°C; Figs. 6, 7). Crystal density in *M. vertebralis* increased with higher pCO_2 and

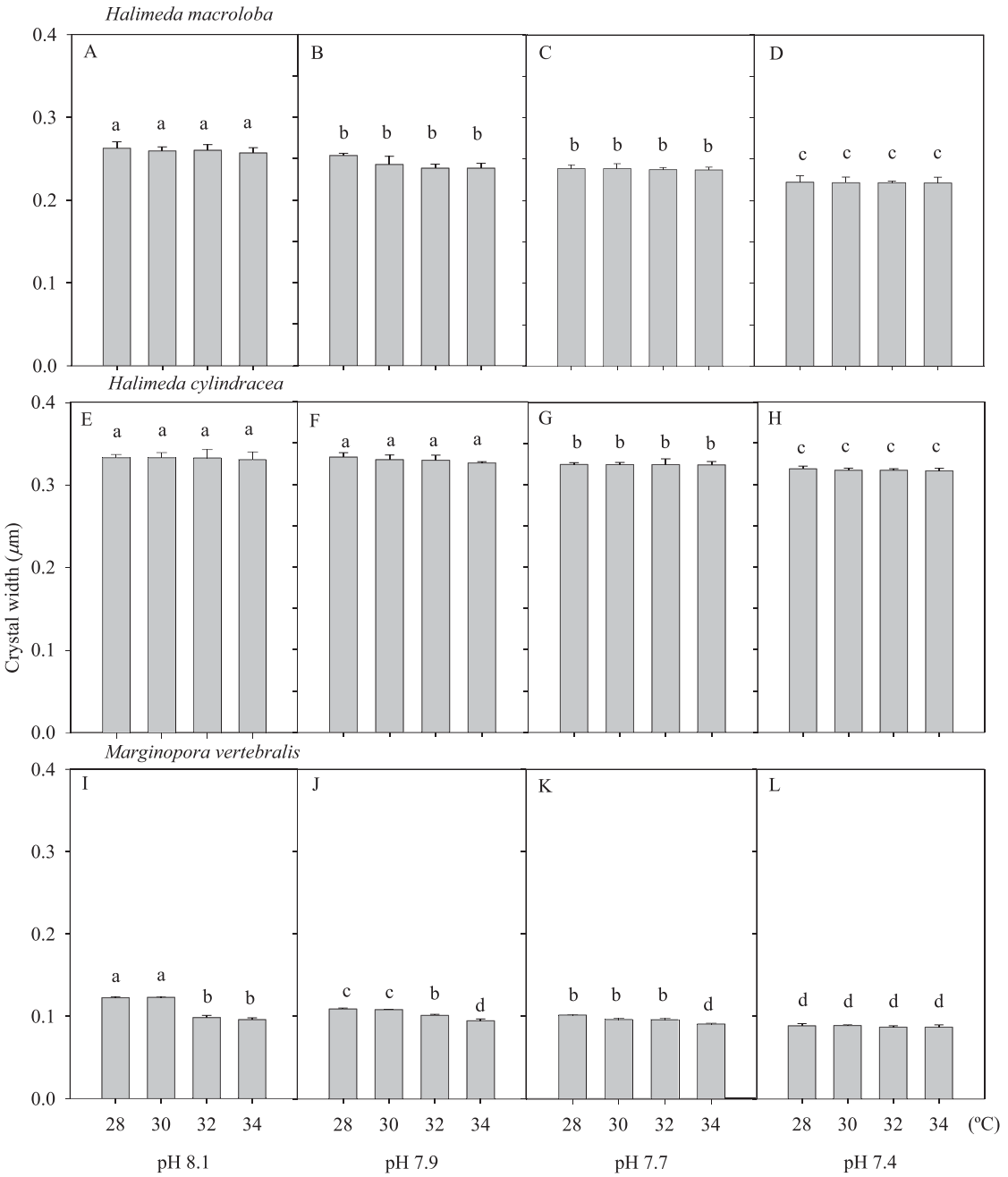

Fig. 6. Crystal width (μm) in (A–D) *H. macroloba*, (E–H) *H. cylindracea*, and (I–L) *M. vertebralis* under pH and temperature conditions at the end of the 5th week. Data represent means (n = 4, SEM).

temperature levels (pH values 7.9, 7.7, and 7.4, and 32°C and 34°C); however, there was no change in calcium carbonate crystal abundance in *H. macroloba* and *H. cylindracea* at elevated pCO_2 and temperature conditions. Previous studies on *H. opuntia* and *H. tuna* that found a reduction in crystal width and an increase in crystal abundance with decreasing pH indicate that the crystallization may be initiated and terminated more frequently with increasing pCO_2 (L. L. Robbins unpubl.). The decrease in crystal width and increase in crystal density in *M. vertebralis* in this study shows that calcification in this high-Mg calcite species (*M. vertebralis*) is more sensitive to lower pH and higher temperature than in the aragonite-forming species of *Halimeda* spp. This finding is consistent with the prediction of Kleypas et al. (1999) based on calcium carbonate saturation state, in which the saturation threshold is lowest in high-Mg calcite–depositing species.

Furthermore, photosynthetic marine calcifiers may experience conditions that reduce calcification rate but enhance photosynthetic rate (e.g., low pH, high CO_2

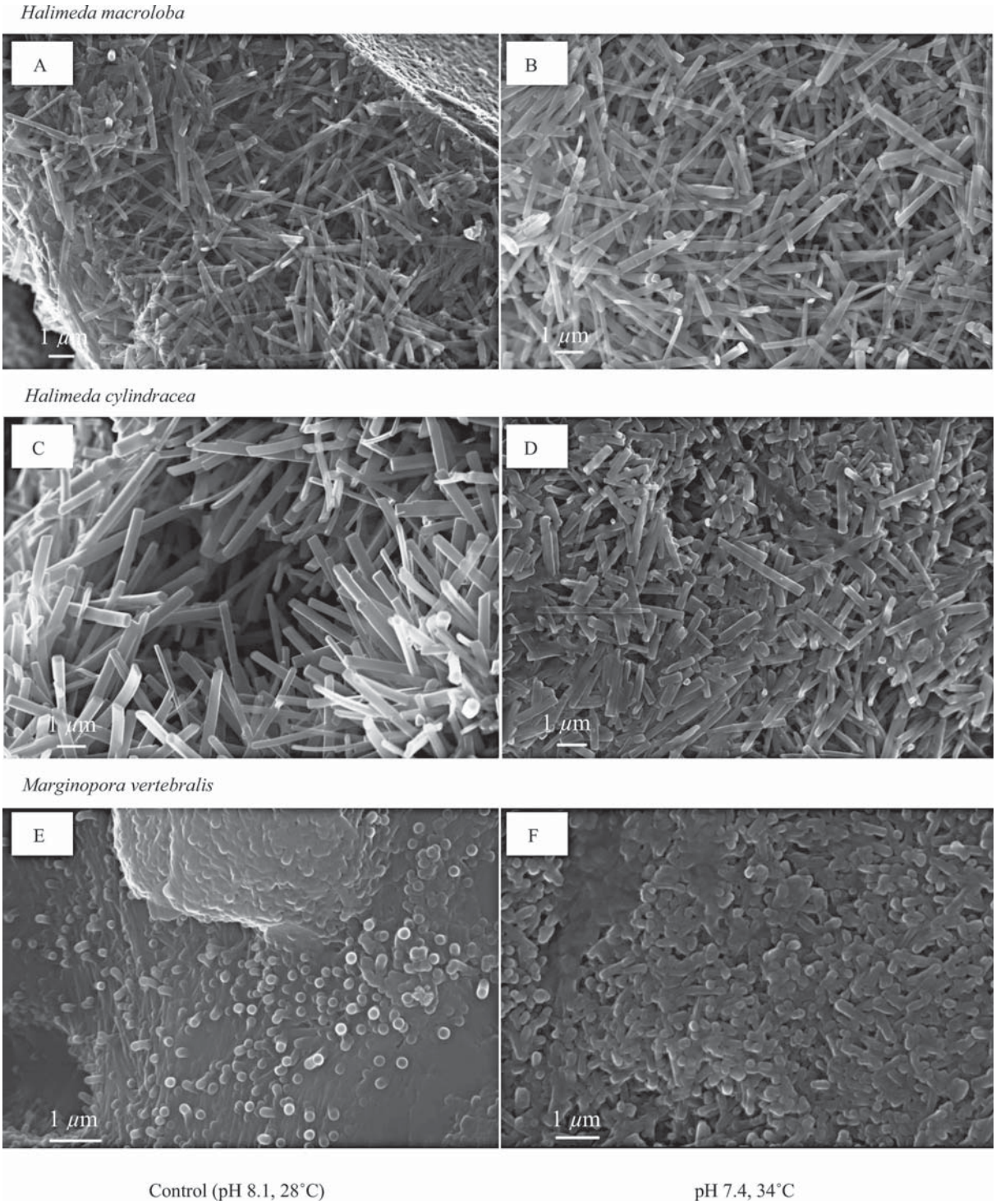

Fig. 7. SEM photographs of crystals in (A–D) *H. macroloba*, (E–H) *H. cylindracea*, and (I–L) *M. vertebralis* in control (pH 8.1, 28°C) and pH 7.4, 34°C treatment at the end of the 5th week.

availability). In this study, although rising pCO_2 resulted in an increase in dissolved CO_2 and HCO_3^{2-} availability (substrates for photosynthesis), the increases in these carbon species might be too small to promote photosynthesis and growth but large enough to reduce calcification (Reynaud et al. 2003).

Exposure to elevated temperature (32°C and 34°C) alone or reduced pH (7.7 and 7.4) alone reduced photosynthesis

and calcification in *H. macroloba, H. cylindracea,* and *M. vertebralis.* However, there was a strong synergistic effect of elevated temperature and reduced pH, with dramatic reductions in photosynthesis and calcification in all three species. It is suggested that rising temperature and pCO_2 exceeds the threshold for survival of these species. Subsequent mortality may be the cause of the reduced calcification and photosynthesis. A simultaneous reduction in pH and higher temperature will result in the greatest effect on these species. It is likely that the elevated temperature of 32°C and the pCO_2 concentration of 101 Pa are the upper limit for survival of these species at our site of collection (Heron Island on the Great Barrier Reef, Australia). However, when taking into account the effects of high solar radiation (including ultraviolet light), this upper limit of survival may be an overestimate (i.e., the upper limit of survival may be below 32°C and 101 Pa pCO_2); Gao and Zheng (2010) showed that photosynthesis and calcification are dramatically reduced under high irradiance in combination with elevated CO_2 concentration.

Under the predicted climate change scenarios of rising ocean temperatures and ocean acidification, the vulnerability of calcifying algae and foraminifera is of great concern. With some predictions estimating that atmospheric CO_2 concentrations will reach 101 Pa by 2100 and 203 Pa by 2200 (Friedlingstein et al. 2006; Houghton 2009) and that the ocean temperature will rise by 2–6°C over the next 100–200 yr (Houghton 2009), the survival of these photosynthetic marine calcifiers is under threat. Furthermore, noncalcifying macroalgae, which may benefit from near-future climate change scenarios (Gao et al. 1993; Hobday et al. 2006), are expected to exhibit a competitive advantage over calcifying species (Fabry et al. 2008; Martin and Gattuso 2009). The loss of these calcifying keystone species will affect many other associated species, such as fish communities, in the future (Kleypas and Yates 2009). Consequent changes in community structure and habitat structure for many marine organisms could very well influence trophic interactions and habitat availability for other coral reef organisms. The loss of these sediment-producing species will also reduce the sediment turnover rate and decrease the amount of carbonate sands in the marine environment.

Acknowledgments

We thank Michael Johnson and the Institute for the Biotechnology of Infectious Diseases, University of Technology, Sydney, for access to the confocal imaging facility and Linda Xiao and the Centre of Expertise Chemical Technologies, University of Technology, Sydney, for autotitrator assistance. We also thank the two anonymous reviewers for improving the quality of this publication. This project was supported by the Plant Functional Biology and Climate Change Cluster, School of the Environment, University of Technology, Sydney, and an Australian Coral Reef Society student research award. This research was performed under Great Barrier Reef Marine Park Authority permit G09/30853.1.

References

Allakhverdiev, S., V. D. Kreslavski, V. V. Klimov, D. A. Los, R. Carpentier, and P. Mohanty. 2008. Heat stress: An overview of molecular responses in photosynthesis. Photosynth. Res. **98:** 541–550, doi:10.1007/s11120-008-9331-0

Anthony, K. R. N., D. I. Kline, G. Diaz-Pulido, S. Dove, and O. Hoegh-Guldberg. 2008. Ocean acidification causes bleaching and productivity loss in coral reef builders. Proc. Natl. Acad. Sci. USA **105:** 17442–17446, doi:10.1073/pnas.0804478105

Borowitzka, M. A. 1986. Physiology and biochemistry of calcification in the Chlorophyceae, p. 107–124. *In* B. Leadbeater and H. Riding [eds.], Biomineralization in the lower plants and animals. Oxford Univ. Press.

———, and A. W. D. Larkum. 1976. Calcification in the green alga *Halimeda* III. The sources of inorganic carbon for photosynthesis and calcification and a model of the mechanism of calcification. J. Exp. Bot. **27:** 879–893, doi:10.1093/jxb/27.5.879

Doney, S. C., V. J. Fabry, R. A. Feely, and J. A. Kleypas. 2009. Ocean acidification: The other CO_2 problem. Annu. Rev. Mar. Sci. **1:** 169–192, doi:10.1146/annurev.marine.010908.163834

Fabry, V. J., B. A. Seibel, R. A. Feely, and J. C. Orr. 2008. Impacts of ocean acidification on marine fauna and ecosystem processes. ICES J. Mar. Sci. **65:** 414–432, doi:10.1093/icesjms/fsn048

Feely, R. A., C. L. Sabine, K. Lee, W. Berelson, J. Kleypas, V. J. Fabry, and F. J. Millero. 2004. Impact of anthropogenic CO_2 on the $CaCO_3$ system in the oceans. Science **305:** 362–366, doi:10.1126/science.1097329

Friedlingstein, P., and others. 2006. Climate-carbon cycle feedback analysis: Results from the C^{4}MIP model intercomparison. J. Clim. **19:** 3337–3353, doi:10.1175/JCLI3800.1

Gao, K., Y. Aruga, K. Asada, T. Ishihara, T. Akano, and M. Kiyohara. 1993. Calcification in the articulated coralline alga *Corallina pilulifera*, with special reference to the effect of elevated CO_2 concentration. Mar. Biol. **117:** 129–132, doi:10.1007/BF00346434

———, and Y. Zheng. 2010. Combined effects of ocean acidification and solar UV radiation on photosynthesis, growth, pigmentation and calcification of the coralline alga *Corallina sessilis* (Rhodophyta). Glob. Change Biol. **16:** 2388–2398, doi:10.1111/j.1365-2486.2009.02113.x

Gattuso, J.-P., and H. Lavigne. 2009. Technical note: Approaches and software tools to investigate the impact of ocean acidification. Biogeosciences **6:** 2121–2133, doi:10.5194/bg-6-2121-2009

———, M. Pichon, B. Dellesalle, and M. Frankignoulle. 1993. Community metabolism and air-sea CO_2 fluxes in a coral reef ecosystem (Moorea, French Polynesia). Mar. Ecol. Prog. Ser. **96:** 259–267, doi:10.3354/meps096259

Gonzalez-Mora, B., F. J. Sierro, and J. A. Flores. 2008. Controls of shell calcification in planktonic foraminifers. Quat. Sci. Rev. **27:** 956–961, doi:10.1016/j.quascirev.2008.01.008

Hallock, P. 1981. Algal symbiosis: A mathematical analysis. Mar. Biol. **62:** 249–255, doi:10.1007/BF00397691

———. 2000. Symbiont-bearing foraminifera: Harbingers of global change? Micropaleontology **46:** 95–104.

———, D. E. Williams, E. M. Fisher, and S. K. Toler. 2006. Bleaching in foraminifera with algal symbionts: Implications for reef monitoring and risk assessment. Anu. Inst. Geociênc. **29:** 108–128.

Hobday, A. J., T. A. Okey, E. S. Poloczanska, T. J. Kunz, and A. J. Richardson. 2006. Impacts of climate change on Australian marine life—Part B: Technical report. CSIRO Marine and Atmospheric Research.

Hoegh-Guldberg, O. 1999. Climate change, coral bleaching and the future of the world's coral reefs. Mar. Freshw. Res. **50:** 839–866, doi:10.1071/MF99078

———, AND OTHERS. 2007. Coral reefs under rapid climate change and ocean acidification. Science **318:** 1738–1742.

HOUGHTON, J. 2009. Global warming: The complete briefing, 4th ed. Cambridge Univ. Press.

HOWE, S. A., AND A. T. MARSHALL. 2002. Temperature effects on calcification rate and skeletal deposition in the temperate coral, *Plesiastrea versipora* (Lamarck). J. Exp. Mar. Biol. Ecol. **275:** 63–81, doi:10.1016/S0022-0981(02)00213-7

IGLESIAS-RODRIGUEZ, M. D., AND OTHERS. 2008. Phytoplankton calcification in a high-CO_2 world. Science **320:** 336–340, doi:10.1126/science.1154122

INTERNATIONAL SOCIETY FOR REEF STUDIES. 2008. Coral reefs and ocean acidification. Briefing paper 5. Available from http://www.coralreefs.org/documents/ISRS%20Briefing%20Paper%205%20-%20Coral%20Reefs%20and%20Ocean%20Acidification.pdf

JOKIEL, P. L., J. E. MARACIOS, AND L. FRANZISKET. 1978. Coral growth: Buoyant weight technique, p. 529–541. *In* D. R. Stoddard and R. E. Juhannes [eds.], Coral reefs: Research methods. UNESCO.

———, K. S. RODGERS, I. B. KUFFNER, A. J. ANDERSSON, E. F. COX, AND F. T. MACKENZIE. 2008. Ocean acidification and calcifying reef organisms: A mesocosm investigation. Coral Reefs **27:** 473–483, doi:10.1007/s00338-008-0380-9

KLEYPAS, J. A., R. W. BUDDEMEIER, D. ARCHER, J. -P. GATTUSO, C. LANGDON, AND B. N. OPDYKE. 1999. Geochemical consequences of increased atmospheric carbon dioxide on coral reefs. Science **284:** 118–120, doi:10.1126/science.284.5411.118

———, AND K. K. YATES. 2009. Coral reefs and ocean acidification. Oceanography **22:** 108–117.

KRAMER, D. M., G. JOHNSON, O. KIIRATS, AND G. E. EDWARDS. 2004. New fluorescence parameters for the determination of QA redox state and excitation energy fluxes. Photosynth. Res. **79:** 209–218, doi:10.1023/B:PRES.0000015391.99477.0d

KUFFNER, I. B., A. J. ANDERSSON, P. L. JOKIEL, K. U. S. RODGERS, AND F. T. MACKENZIE. 2007. Decreased abundance of crustose coralline algae due to ocean acidification. Nat. Geosci. **1:** 114–117, doi:10.1038/ngeo100

KUROYANAGI, A., H. KAWAHATA, A. SUZUKI, K. FUJITA, AND T. IRIE. 2009. Impacts of ocean acidification on large benthic foraminifers: Results from laboratory experiments. Mar. Micropaleontol. **73:** 190–195, doi:10.1016/j.marmicro.2009.09.003

LANGDON, C., J.-P. GATTUSO, AND A. ANDERSSON. 2010. Chapter 13: Measurements of calcification and dissolution of benthic organisms and communities, p. 213–232. *In* U. Riebesell, V. J. Fabry, L. Hansson, and J.-P. Gattuso [eds.], Guide to best practices for ocean acidification research and data reporting. Publication Office of the European Union, Available from http://www.epoca-project.eu/index.php/guide-to-best-practices-for-ocean-acidification-research-and-data-reporting.html

LEWIS, E., AND D. W. R. WALLACE. 1998. Program developed for CO_2 system calculations. Carbon Dioxide Information Analysis Center. Tennessee. Available from http://cdiac.ornl.gov/oceans/co2rprt.html

LOUGH, J. 2007. Climate and climate change on the Great Barrier Reef, p. 15–74. *In* J. E. Johnson and P. A. Marshall [eds.], Climate change and the Great Barrier Reef: A vulnerability assessment. Great Barrier Reef Marine Park Authority and Australian Greenhouse Office.

LOUGH, J. M., AND D. J. BARNES. 2000. Environmental controls on growth of the massive coral *Porites*. J. Exp. Mar. Biol. Ecol. **245:** 225–243, doi:10.1016/S0022-0981(99)00168-9

MARTIN, S., AND J. -P. GATTUSO. 2009. Response of Mediterranean coralline algae to ocean acidification and elevated temperature. Glob. Change Biol. **15:** 2089–2100, doi:10.1111/j.1365-2486.2009.01874.x

NECCHI, O., JR 2004. Photosynthetic responses to temperature in tropical lotic macroalgae. Phycol. Res. **52:** 140–148, doi:10.1111/j.1440-1835.2004.tb00322.x

NIGAM, R., S. R. KURTARKAR, R. SARASWAT, V. N. LINSHY, AND S. S. RANA. 2008. Response of benthic foraminifera *Rosalina leei* to different temperature and salinity, under laboratory culture experiment. J. Mar. Biol. Assoc. U.K. **88:** 699–704, doi:10.1017/S0025315408001197

ORR, J. C., AND OTHERS. 2005. Anthropogenic ocean acidification over the twenty-first century and its impact on calcifying organisms. Nature **437:** 681–686, doi:10.1038/nature04095

PAWLOWSKI, J., M. HOLZMAN, J. FAHRNI, X. POCHON, AND J. J. LEE. 2001. Molecular identification of algal endosymbionts in large miliolid foraminifers; Part 2. Dinoflagellates. J. Eukaryot. Microbiol. **48:** 368–373, doi:10.1111/j.1550-7408.2001.tb00326.x

RAVEN, J., AND OTHERS. 2005. Ocean acidification due to increasing atmospheric carbon dioxide. The Clyvedon Press.

REYNAUD, S., N. LECLERCQ, S. ROMAINE-LIOUD, C. FERRIER-PAGÈS, J. JAIBERT, AND J.-P. GATTUSO. 2003. Interacting effects of CO_2 partial pressure and temperature on photosynthesis and calcification in a scleractinian coral. Glob. Change Biol. **9:** 1660–1668, doi:10.1046/j.1365-2486.2003.00678.x

RITCHIE, R. J. 2008. Universal chlorophyll equations for estimating chlorophylls *a*, *b*, *c*, and *d* and total chlorophylls in natural assemblages of photosynthetic organisms using acetone, methanol, or ethanol solvents. Photosynthetica **46:** 115–126, doi:10.1007/s11099-008-0019-7

SHORT, F. T., AND H. A. NECKLES. 1999. The effects of global climate change on seagrasses. Aquat. Bot. **63:** 169–196, doi:10.1016/S0304-3770(98)00117-X

SOLOMON, S., AND OTHERS. 2007. Climate change 2007: The physical science basis. Contribution of Working Group I to the Fourth Assessment Report of the Intergovernmental Panel on Climate Change. Cambridge Univ. Press.

TALGE, H. K., AND P. HALLOCK. 2003. Ultrastructural responses in field-bleached and experimentally stressed *Amphistegina gibbosa* (Class Foraminifera). J. Eukaryot. Microbiol. **50:** 324–333, doi:10.1111/j.1550-7408.2003.tb00143.x

ULSTRUP, K. E., R. HILL, AND P. J. RALPH. 2005. Photosynthetic impact of hypoxia on *in hospite* zooxanthellae in the scleractinian coral *Pocillopora damicornis*. Mar. Ecol. Prog. Ser. **286:** 125–132, doi:10.3354/meps286125

Associate editor: John Albert Raven

Received: 20 October 2010
Accepted: 22 March 2011
Amended: 31 March 2011

APPENDIX

APPENDIX 2 PUBLICATION ARISING FORM CHAPTER 5:

Sinutok S, Hill R, Doblin MA, Kühl M, Ralph PJ (2012) Microenvironmental changes support evidence of photosynthesis and calcification inhibition in *Halimeda* under ocean acidification and warming. *Coral Reefs* 31:1201-1213.

Coral Reefs (2012) 31:1201–1213
DOI 10.1007/s00338-012-0952-6

REPORT

Microenvironmental changes support evidence of photosynthesis and calcification inhibition in *Halimeda* under ocean acidification and warming

S. Sinutok · R. Hill · M. A. Doblin · M. Kühl · P. J. Ralph

Received: 17 April 2012 / Accepted: 21 August 2012 / Published online: 8 September 2012

Abstract The effects of elevated CO_2 and temperature on photosynthesis and calcification of two important calcifying reef algae (*Halimeda macroloba* and *Halimeda cylindracea*) were investigated with O_2 microsensors and chlorophyll *a* fluorometry through a combination of two pCO_2 (400 and 1,200 μatm) and two temperature treatments (28 and 32 °C) equivalent to the present and predicted conditions during the 2100 austral summer. Combined exposure to pCO_2 and elevated temperature impaired calcification and photosynthesis in the two *Halimeda* species due to changes in the microenvironment around the algal segments and a reduction in physiological performance. There were no significant changes in controls over the 5-week experiment, but there was a 50–70 % decrease in photochemical efficiency (maximum quantum yield), a 70–80 % decrease in O_2 production and a threefold reduction in calcification rate in the elevated CO_2 and high temperature treatment. Calcification in these species is closely coupled with photosynthesis, such that a decrease in photosynthetic efficiency leads to a decrease in calcification. Although pH seems to be the main factor affecting *Halimeda* species, heat stress also has an impact on their photosystem II photochemical efficiency. There was a strong combined effect of elevated CO_2 and temperature in both species, where exposure to elevated CO_2 or temperature alone decreased photosynthesis and calcification, but exposure to both elevated CO_2 and temperature caused a greater decline in photosynthesis and calcification than in each stress individually. Our study shows that ocean acidification and ocean warming are drivers of calcification and photosynthesis inhibition in *Halimeda.* Predicted climate change scenarios for 2100 would therefore severely affect the fitness of *Halimeda*, which can result in a strongly reduced production of carbonate sediments on coral reefs under such changed climate conditions.

Keywords Chlorophyll fluorescence · Climate change · Microsensor · Macroalgae · Coral reefs

Communicated by Biology Editor Dr. Anastazia Banaszak

S. Sinutok · R. Hill (✉) · M. A. Doblin · M. Kühl · P. J. Ralph
Plant Functional Biology and Climate Change Cluster, School of the Environment, University of Technology Sydney, PO Box 123, Broadway, Sydney, NSW 2007, Australia
e-mail: ross.hill@unsw.edu.au

Present Address:
R. Hill
Centre for Marine Bio-Innovation and Sydney Institute of Marine Science, School of Biological, Earth and Environmental Sciences, The University of New South Wales, Sydney, NSW 2052, Australia

M. Kühl
Marine Biology Section, Department of Biology, University of Copenhagen, Strandpromenaden 5, 3000 Helsingør, Denmark

M. Kühl
Singapore Centre on Environmental Life Sciences Engineering, School of Biological Sciences, Nanyang Technological University, Nanyang Avenue, Singapore

Introduction

The anthropogenic use of fossil fuels, industrialization, deforestation and agricultural activities has raised the concentration of carbon dioxide (CO_2) in the atmosphere and increased CO_2 dissolution into the surface ocean (Gattuso and Lavigne 2009). This has stimulated global warming and more acidic conditions, that is, a pH decrease in the ocean's surface layer. The latter affects the inorganic carbon speciation inducing further changes in seawater

chemistry including a reduction in carbonate ion (CO_3^{2-}) abundance and a decreased aragonite saturation state (Feely et al. 2004) leading to a decrease in the capacity for marine calcifiers to produce their $CaCO_3$ skeleton (Diaz-Pulido et al. 2007; Fujita et al. 2011; Sinutok et al. 2011). Under such conditions, non-calcifying macrophytes such as seagrasses and fleshy algae may therefore have benefits over calcifying algae, as evidenced in naturally high CO_2 regions, such as the volcanic vents off Ischia Island, Italy (Hall-Spencer et al. 2008). These studies point towards likely consequences of acidification for marine ecosystems and predict an expected reduction in calcifier diversity and abundance, which will result in significant changes in habitat structure and function (Gao et al. 1993; Hall-Spencer et al. 2008; Kleypas and Yates 2009).

Halimeda is a sediment-dwelling, calcifying siphonalean green macroalga, which is widely distributed in tropical and subtropical marine environments, where it plays a major role as a carbonate sediment producer. In coral reef ecosystems, *Halimeda* is known to produce around 2.2 kg of $CaCO_3$ m^{-2} $year^{-1}$, which is equivalent to the rate of production by scleractinian corals (Smith and Kinsey 1976; Drew 1983). *Halimeda* thus provides essential ecological services as a habitat-forming bioengineer in these marine ecosystems (Drew 1983). The algal thallus consists of articulated, plate-like and calcified segments, which are joined together by small, uncalcified nodes forming branching chains (Blaxter et al. 1980). *Halimeda* precipitates $CaCO_3$ in the form of aragonite into the intercellular (utricular) space of its segments (Borowitzka et al. 1974; Borowitzka and Larkum 1977). New segments can be formed rapidly, involving a complex sequence of local decalcification, filament extension and chloroplast migration from old segments overnight, followed by the onset of calcification (Larkum et al. 2011).

The current saturation state of aragonite, Ω_a, is 3.5–4.0 for the Pacific region and is expected to decline ~30 % by 2,050 under predicted future climate scenarios (Kleypas et al. 1999; Guinotte et al. 2003). Elevated pCO_2 has previously been shown to reduce calcification, growth and productivity in the articulate coralline alga *Corallina pilulifera* and *C. officinalis* and crustose coralline algae (Kuffner et al. 2007; Anthony et al. 2008; Hofmann et al. 2012). Combined effects of elevated temperature and pCO_2 cause bleaching, calcium carbonate dissolution and erosion in the reef-building corals *Acropora intermedia* and *Porites lobata* (Anthony et al. 2008). Recently, Sinutok et al. (2011) showed that pCO_2 levels representative of modelled climate scenarios for the years 2100 and 2200 (Houghton 2009) significantly reduced calcification and photosynthetic efficiency in *Halimeda*. Such impairment was attributed to lower seawater pH and reduced abundance of CO_3^{2-} as already shown by Borowitzka and Larkum (1976b), leading to a decline in calcification rate, calcium carbonate crystal size, photosynthetic pigment content (chlorophyll *a* and *b*) and photosynthetic efficiency. The decline of photosynthesis and calcification was amplified by concurrent exposure to elevated temperatures, that is, 2–6 °C above typical summer average seawater temperature. While bulk seawater characteristics had an obvious impact on photosynthesis and calcification, the microenvironmental conditions and regulatory mechanisms involved in such impairment of photosynthesis and calcification in *Halimeda* under elevated pCO_2 and temperature remain unknown.

Microsensors enable mapping of physicochemical microenvironment of marine calcifying organisms at high spatio-temporal resolution (De Beer and Larkum 2001; Al-Horani 2005; Köhler-Rink and Kühl 2005). Oxygen (O_2), carbon dioxide (CO_2), pH and calcium (Ca^{2+}) microsensors have been used to study the photosynthesis and calcification in *Halimeda discoidea.* De Beer and Larkum (2001) showed that calcium dynamics and calcification in *H. discoidea* are determined by the pH at the segment surface, and they hypothesized that acidification of sea water would decrease the calcification rate. Here, we investigate the effects of ocean acidification and ocean warming on the microenvironment and photosynthesis of *Halimeda* spp. using O_2 microsensors and chlorophyll *a* fluorometry and present the first data on how the microenvironment, photosynthesis and respiration of *Halimeda* are affected by changing pCO_2 and temperature conditions.

Materials and methods

Sample collection and experimental design

Halimeda macroloba and *H. cylindracea* specimens (thallus length of 13–20 cm) were collected by hand from Heron Island reef flat (Southern Great Barrier Reef, Australia; 151°55′E, 23°27′S) at low tide at 0.3 m depth and maintained at the University of Technology, Sydney, for 2 months in a 500-L aquarium with artificial seawater (26 °C, pH 8.1, salinity of 33) under an incident irradiance (PAR, 400–700 nm) of 250 μmol photons m^{-2} s^{-1} over a 12-h/12-h light–dark cycle. Seawater concentrations of carbonate, calcium, nitrate and phosphate were maintained at 2.3, 10, <0.0016 and 0.0005 mM, respectively. Whole specimens of *Halimeda* were randomly allocated to one of four treatments (1 sample per tank, 4 tanks per treatment): (1) control (pH 8.1 and 28 °C; equivalent to current summer temperature average at Heron Island and a pCO_2 of 400 μatm), (2) elevated temperature only (pH 8.1 and 32 °C), (3) reduced pH only (pH 7.7 and 28 °C) and (4) a combination of both low pH and high temperature (pH 7.7 and 32 °C). The elevated temperature and decreased pH

Table 1 Parameters of the carbonate system; total alkalinity (TA), CO_2 partial pressure (pCO_2), dissolved inorganic carbon species (DIC; CO_2, CO_3^{-2}, HCO_3^-), total DIC and saturation state of sea water with respect to aragonite (Ω_a) from each pH (8.1, 7.7) and temperature (28, 32 °C) treatment used in this study

Treatment		TA (mmol kg^{-1})	pCO_2 (µatm)	CO_2 (mmol kg^{-1})	CO_3^{-2} (mmol kg^{-1})	HCO_3^- (mmol kg^{-1})	DIC (mmol kg^{-1})	Ω_a
pH	Temp (°C)							
8.1	28	2.327 ± 0.002	380.8 ± 0.4	0.010 ± 0.001	0.239 ± 0.024	1.745 ± 0.020	1.993 ± 0.020	3.87 ± 0.01
8.1	32	2.326 ± 0.036	444.9 ± 7.4	0.010 ± 0.002	0.239 ± 0.039	1.742 ± 0.030	1.881 ± 0.033	3.97 ± 0.07
7.7	28	2.512 ± 0.030	1208.1 ± 14.6	0.032 ± 0.004	0.122 ± 0.015	2.219 ± 0.027	2.373 ± 0.028	1.97 ± 0.02
7.7	32	2.508 ± 0.015	1394.2 ± 8.6	0.034 ± 0.002	0.123 ± 0.007	2.212 ± 0.014	2.369 ± 0.014	2.05 ± 0.01

Data represent means ($n = 3$, ±SE)

treatments represent conditions predicted by current climate change models for the year 2100, equivalent to a 4 °C temperature rise and a pCO_2 concentration of 1200 µatm (Houghton 2009). Samples were ramped from 26 °C and a pH of 8.1 to their treatment conditions over 1 week and were maintained for another 4 weeks in their treatments. pCO_2 and temperature were controlled using pH controllers (7020/2, Tunze, Germany) connected to CO_2 bubblers, and water thermostats (TC10, Teco, Italy), as described in Sinutok et al. (2011). Salinity was set at 33, and quantum irradiance (PAR) at the sample surface was 300 µmol photons m^{-2} s^{-1} on a 12/12-h light–dark cycle (light on at 0900 h and light off at 2100 h). The water quality was maintained identical to the holding tank with carbonate, calcium, nitrate and phosphate concentrations of 2.3, 10, <0.0016 and 0.0005 mM, respectively. Total alkalinity (TA) was measured weekly by titrating 30 g of sea water with 0.1 M HCl in an autotitrator (DL50, Mettler Toledo). The speciation of dissolved inorganic carbon (DIC) into CO_2, CO_3^{-2} and HCO_3^-, the CO_2 partial pressure (pCO_2) and the saturation state of sea water with respect to aragonite (Ω_a) were determined using CO2SYS (version 01.05; Brookhaven National Laboratory; Lewis and Wallace 1998). A summary of the TA, total inorganic carbon (DIC), DIC speciation, pCO_2 and Ω_a from each temperature (28 °C, 32 °C) and pH (8.1, 7.7) treatment is shown in Table 1.

Calcification

Whole specimen calcification rates were determined using the buoyant weight technique (Jokiel et al. 2008; Sinutok et al. 2011) with weight comparisons made between measurements at the start and end of the experimental period. The buoyant weight technique is a reliable measure of calcification by weighing each sample in sea water of known density and applying Archimedes' principle to compute the dry weight of the sample in the air (Jokiel et al. 1978; Langdon et al. 2010). Samples were placed on a glass Petri dish hung below an electronic balance (AB204-S, Mettler Toledo, USA; accuracy ~0.1 mg) using nylon thread suspended in sea water.

Variable chlorophyll *a* fluorescence

Photosynthetic performance of *Halimeda* was quantified every 10 days over the duration of the experiment by variable chlorophyll fluorescence measurements using a 6-mm-diameter fibre-optic probe connected to a Diving-PAM fluorometer (Walz, Germany). Photosystem II (PSII) photochemical efficiency was measured as the maximum quantum yield of PSII (F_V/F_M) at 0900 h (before lights were turned on) and the effective quantum yield ($\Delta F/F_M'$) at 1300 h, after which the maximum excitation pressure over photosystem II (Q_m) was calculated. The parameter Q_m quantifies non-photochemical quenching and is defined as $Q_m = 1-(\Delta F/F_M')/(F_V/F_M)$ according to Iglesias-Prieto et al. (2004).

Photosynthetic pigment concentration

Concentrations of chlorophyll (Chl) *a* and *b* were determined in extracts of *Halimeda* samples using the spectrophotometric method of Ritchie (2008) at the beginning and end of the 5-week experiment and expressed in µg Chl g^{-1} fresh weight (fw) of *Halimeda*. Chl *a* and *b* were extracted by grinding samples in 4 ml of 90 % acetone at 4 °C followed by extraction in darkness for 24 h. Subsequently, samples were centrifuged at 1,500*g* for 10 min, after which the supernatant was transferred to a quartz cuvette and its absorbance measured at 647 and 664 nm on a spectrophotometer (Cary 50, Varian, Australia).

Oxygen microsensors

Microsensor measurements of O_2 concentration were performed in a 2-L flow chamber as described by Köhler-Rink and Kühl (2000) at the start of the experiment, and after 3 and 5 weeks. Segments of *H. macroloba* (0.8–1.2 cm long)

and *H. cylindracea* (1.5–2.0 cm long) from the treatment tanks were placed on the bottom of the chamber, with a water flow of 2.5 cm s^{-1} maintained by a submersible aquarium pump. The thallus surface O_2 concentration and rate of O_2 production was determined under quantum irradiances of 0, 80, 150, 230, 570 and 900 µmol photons m^{-2} s^{-1}, as controlled by a fibre-optic halogen lamp (KL-2500, Schott, Germany) equipped with a collimating lens and a heat filter. The O_2 microsensor was mounted on a motorized micromanipulator (Oriel Encoder Mike, United States) which, along with data acquisition, was regulated by Profix software (Pyro-Science, Denmark).

Oxygen concentration profiles and the rate of gross photosynthetic O_2 production were measured at the surface (0–300 µm) of *H. macroloba* and *H. cylindracea* using an O_2 microelectrode (OX-100, Unisense, Denmark) connected to a picoammeter (PA2000, Unisense, Denmark) and a strip chart recorder (BD12E, Kipp&Zonen, the Netherlands). The microelectrode had an outer tip diameter of 100 µm, a 90 % response time of <8 s and a stirring sensitivity of <1.5 %. A linear calibration of the microelectrode was performed at chamber temperature in air-saturated sea water and O_2-free sea water (made anoxic by addition of sodium dithionite). A proxy for gross photosynthesis (P_y; nmol O_2 cm^{-3} s^{-1}) at the specimen surface of *Halimeda* spp. was estimated after a short experimental light–dark shift by measuring the rate of O_2 depletion over the first 10 s after darkening (Revsbech et al. 1981; Köhler-Rink and Kühl 2000). According to the limitation of microsensor response time (<8 s), the gross photosynthesis from this measurement is underestimated and represents an integral over a large sample volume; however, it can still be used to compare between treatments.

The local diffusive O_2 flux (J; nmol O_2 cm^{-2} s^{-1}), that is, the O_2 uptake rate in darkness and the net O_2 production rate in light, was calculated from measured steady-state O_2 concentration profiles by Fick's first law (Köhler-Rink and Kühl 2000): $J = -D_0\,(dC/dz)$ where D_0 is the molecular diffusion coefficient in sea water at experimental salinity and temperature, and dC/dz is the linear slope of the O_2 concentration profile in the diffusive boundary layer (DBL) above the *Halimeda* thallus surface. We note that the presence of microsensor above the *Halimeda* thallus can compress the diffusive boundary layer leading to a locally accelerated flow around the microsensor tip (Glud et al. 1995). However, as flow conditions were identical between treatments, diffusive fluxes can still be compared.

Statistical analysis

To identify significant differences ($\alpha = 0.05$) among treatments in calcification, Chl *a* and *b* concentration, a series of one-way and two-way analysis of variance (ANOVA) tests were performed (SPSS v17). To determine significant differences among treatments and over time in chlorophyll fluorescence parameters (F_V/F_M, $\Delta F/F_M'$, Q_m), O_2 concentration at the thallus surface, diffusive O_2 flux and proxy gross photosynthesis, repeated measures analysis of variance (rmANOVA) tests, with pH and temperature as between-subject independent variables and time as a within-subject independent variable (repeated measures factor), were performed. Tukey's honestly significant difference post hoc tests were used to identify statistically distinct groups. If data did not meet the assumptions of normality (Kolmogorov–Smirnov test) and equal variance (Levene's test), the data were transformed using $\log_{10}$ or square root.

Table 2 Calcification rate (% increase day^{-1}) and chlorophyll (Chl) *a* and *b* concentration (µg g^{-1} fw) of *H. macroloba* and *H. cylindracea* after 5 weeks in each pH and temperature treatment

	Calcification rate (% per day)	Chl *a* (µg g^{-1} fw)	Chl *b* (µg g^{-1} fw)
H. macroloba			
Time 0	–	42.1 ± 5.8	24.5 ± 3.0
pH 8.1, 28 °C	0.45 ± 0.07	45.8 ± 5.1	32.5 ± 3.8
pH 8.1, 32 °C	0.26 ± 0.14	39.4 ± 3.6	24.5 ± 2.7
pH 7.7, 28 °C	−0.51 ± 0.16	28.5 ± 2.1	18.2 ± 2.5
pH 7.7, 32 °C	−1.57 ± 0.71	29.7 ± 2.5	20.8 ± 3.6
P value			
pH	0.003*	0.005*	0.012*
Temperature	0.123	0.529	0.412
pH*Temperature	0.269	0.374	0.115
H. cylindracea			
Time 0	–	43.6 ± 3.3	28.9 ± 1.7
pH 8.1, 28 °C	0.38 ± 0.14	43.3 ± 2.5	24.1 ± 2.3
pH 8.1, 32 °C	0.26 ± 0.18	34.5 ± 1.3	21.3 ± 2.1
pH 7.7, 28 °C	−0.29 ± 0.08	29.4 ± 1.2	17.3 ± 2.7
pH 7.7, 32 °C	−0.31 ± 0.04	26.2 ± 0.7	16.0 ± 1.9
P value			
pH	<0.001*	<0.001*	0.014*
Temperature	0.586	0.011*	0.375
pH*Temperature	0.697	0.189	0.732

Data represent means ($n = 4$, mean ± SE)

* Signifies $p < 0.05$

Results

Calcification rate

The calcification rates of *H. macroloba* and *H. cylindracea* were slightly positive in the control (pH 8.1, 28 °C; <0.5 % increase per day; Table 2) and the elevated

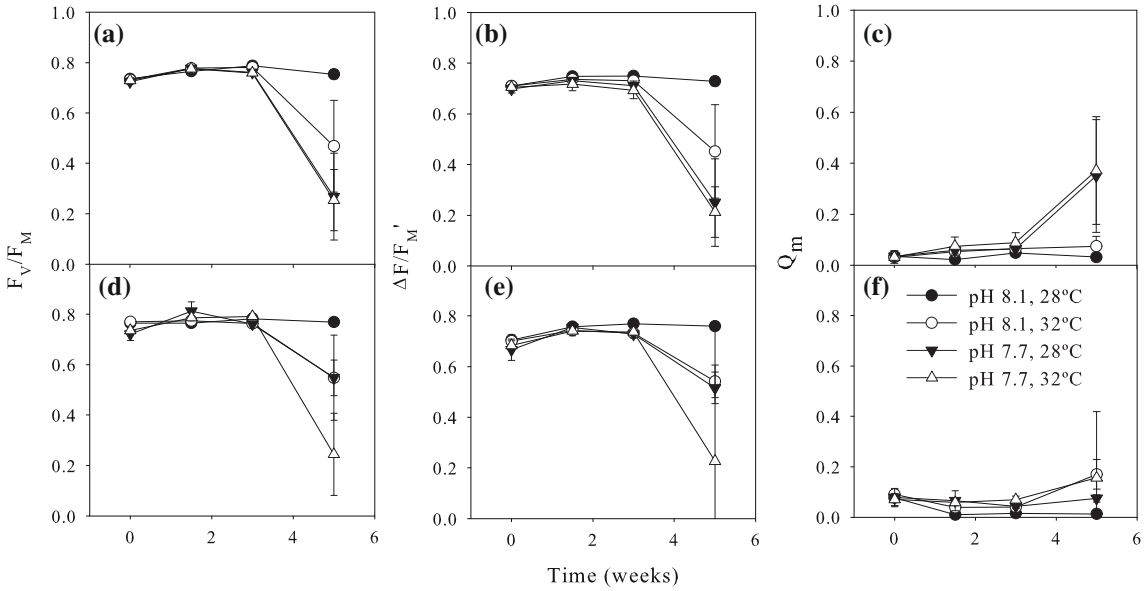

Fig. 1 Maximum quantum yield (F_V/F_M), effective quantum yield ($\Delta F/F_M'$) and maximum excitation pressure over photosystem II (Q_m) of **a–c** *H. macroloba* and **d–f** *H. cylindracea* in each pH and temperature treatment over the length of the experimental period. Data represent means ($n = 4$, ±SE)

temperature treatment (pH 8.1, 32 °C; <0.3 % per day), but were negative in the elevated pCO_2 treatments both at control and elevated temperature (pH 7.7, 28 °C and pH 7.7, 32 °C; −0.2 to −1.6 % per day; Table 2). *H. macroloba* and *H. cylindracea* had significantly lower calcification in the reduced pH treatments at both 28 and 32 °C than in the control treatment ($p = 0.003$ and $p < 0.001$, respectively; Table 2). The calcification rate of *H. macroloba* in the elevated CO_2 and elevated temperature treatment was not significantly different from calcification in *H. cylindracea* in the same treatment ($p > 0.05$).

Photosynthetic pigment concentration

Initial Chl *a* and *b* concentrations were 42.1 ± 5.8 and 24.5 ± 3.0 μg g^{-1} (mean ± SE) in *H. macroloba* and 43.6 ± 3.3 and 28.9 ± 1.7 μg g^{-1} (mean ± SE) in *H. cylindracea*, respectively (Table 2). After 5 weeks, there were no significant changes in Chl *a* and *b* concentration in *H. macroloba* in the control (pH 8.1, 28 °C; $p = 0.651$ for Chl *a*; $p = 0.151$ for Chl *b*) and elevated temperature treatments (pH 8.1, 32 °C; $p = 0.788$ for Chl *a*; $p = 0.997$ for Chl *b*) or in the control treatment for *H. cylindracea* (pH 8.1, 28 °C; $p = 0.946$ for Chl *a*; $p = 0.146$ for Chl *b*). In *H. cylindracea* at pH 8.1, 32 °C, Chl *a* concentration significantly declined to 34.5 ± 1.3 μg g^{-1} (mean ± SE; $p < 0.046$), whereas there were no significant changes in Chl *b* concentration ($p > 0.05$; Table 2). The Chl *a* and *b* concentration in *H. macroloba* and *H. cylindracea* significantly declined at pH 7.7 within the 28 and 32 °C treatment ($p < 0.05$; Table 2).

Variable chlorophyll fluorescence

The maximum quantum yield (F_V/F_M), effective quantum yield ($\Delta F/F_M'$) and maximum excitation pressure on PSII (Q_m) in the control treatment remained constant over the experimental period in both species of *Halimeda*, ranging from 0.73–0.79, 0.70–0.77 and 0.01–0.08, respectively ($p > 0.05$; Fig. 1a, d). There was, however, a significant decrease (50–70 %) in F_V/F_M and $\Delta F/F_M'$ in *H. macroloba* and *H. cylindracea* at week 5 under elevated CO_2 and temperature treatments (pH 8.1, 32 °C, pH 7.7, 28 °C and pH 7.7, 32 °C; $p < 0.001$; Fig. 1a–b, d–e). Both *Halimeda* species under elevated CO_2 and temperature showed very large Q_m values (0.2–0.6) at week 5. At this time, *H. macroloba* exhibited significantly higher Q_m values under elevated CO_2 in both temperature treatments ($p < 0.022$; Fig. 1c), whereas *H. cylindracea* showed significantly higher Q_m values in all treatments except the control ($p < 0.038$; Fig. 1f).

O_2 microenvironment

Oxygen concentration profiles measured towards the thallus surface of *H. macroloba* and *H. cylindracea* were affected by irradiance, pCO_2, temperature and time of exposure to elevated pCO_2 and temperature ($p < 0.05$; Figs. 2, 3, 4). Initially, in all light treatments, the O_2 concentration surpassed the ambient O_2 concentration in the surrounding water (209 μM) at the upper boundary of the diffusive boundary layer ~150 μm above the *H. macroloba* segment surface and reached an O_2 concentration of

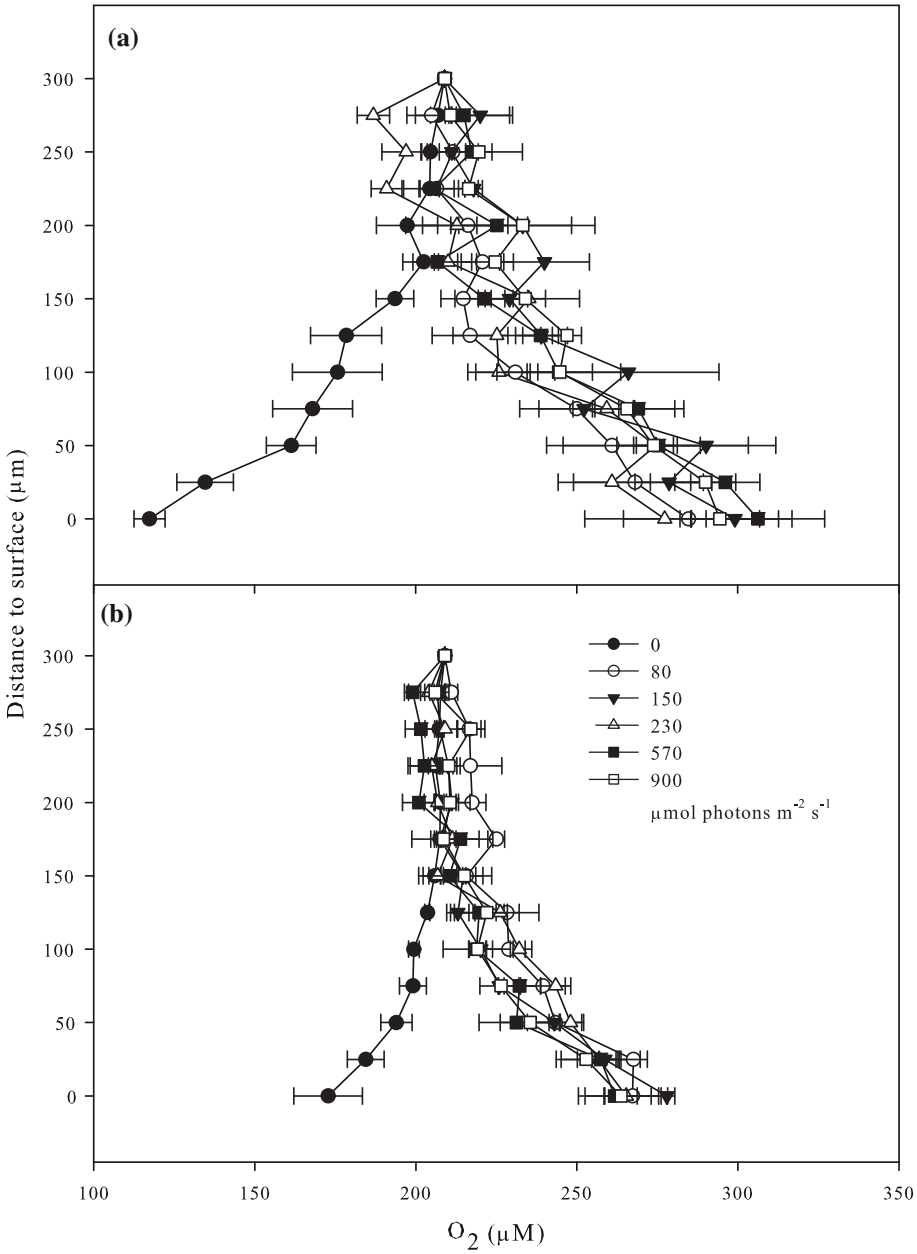

Fig. 2 Oxygen concentration profile towards the thallus surface measured at week 1 from **a** *H. macroloba* and **b** *H. cylindracea* at each experimental irradiance (0, 80, 150, 230, 570 and 900 µmol photons m^{-2} s^{-1}). Data represent means ($n = 4$, ±SE)

277–306 µM at the segment surface (Fig. 2a). In the dark, the ambient O_2 concentration decreased from 209 µM at 150 µm above the *H. macroloba* segment to 117 µM at the segment surface (Fig. 2a). The O_2 concentration at the segment surface in all light treatments was higher compared to when in darkness ($p < 0.001$; Fig. 2a).

After 3 and 5 weeks, the O_2 concentration profiles in *H. macroloba* showed different responses in each pH and temperature treatment (Fig. 3a–h). The O_2 concentration at the shell surface changed over time and between pH and temperature treatments ($p < 0.001$; Figs. 2a, 3a–h). After 3 weeks, the control treatment of *H. macroloba* showed an increasing O_2 concentration at the segment surface reaching ~230–330 µM in all light treatments and a decrease in O_2 concentration to 202 µM under dark conditions (Fig. 3a). Significant increases in segment surface O_2 concentration were found in the pH 8.1, 32 °C treatment reaching 333–461 µM at all irradiance levels ($p < 0.001$), whereas segment surface O_2 concentration significantly decreased to 180 µM in the dark ($p < 0.001$; Fig. 3b). There was a significant decrease in segment surface O_2 concentration in the pH 7.7, 28 °C treatment at 570 and 900 µmol photons m^{-2} s^{-1} ($p < 0.001$; Fig. 3c), whereas it was not observed in *H. cylindracea*. After 5 weeks, the pH 8.1, 32 °C treatment in *H. macroloba* showed no significant changes in O_2 concentration at the segment surface ($p > 0.05$; Fig. 3f). Similar

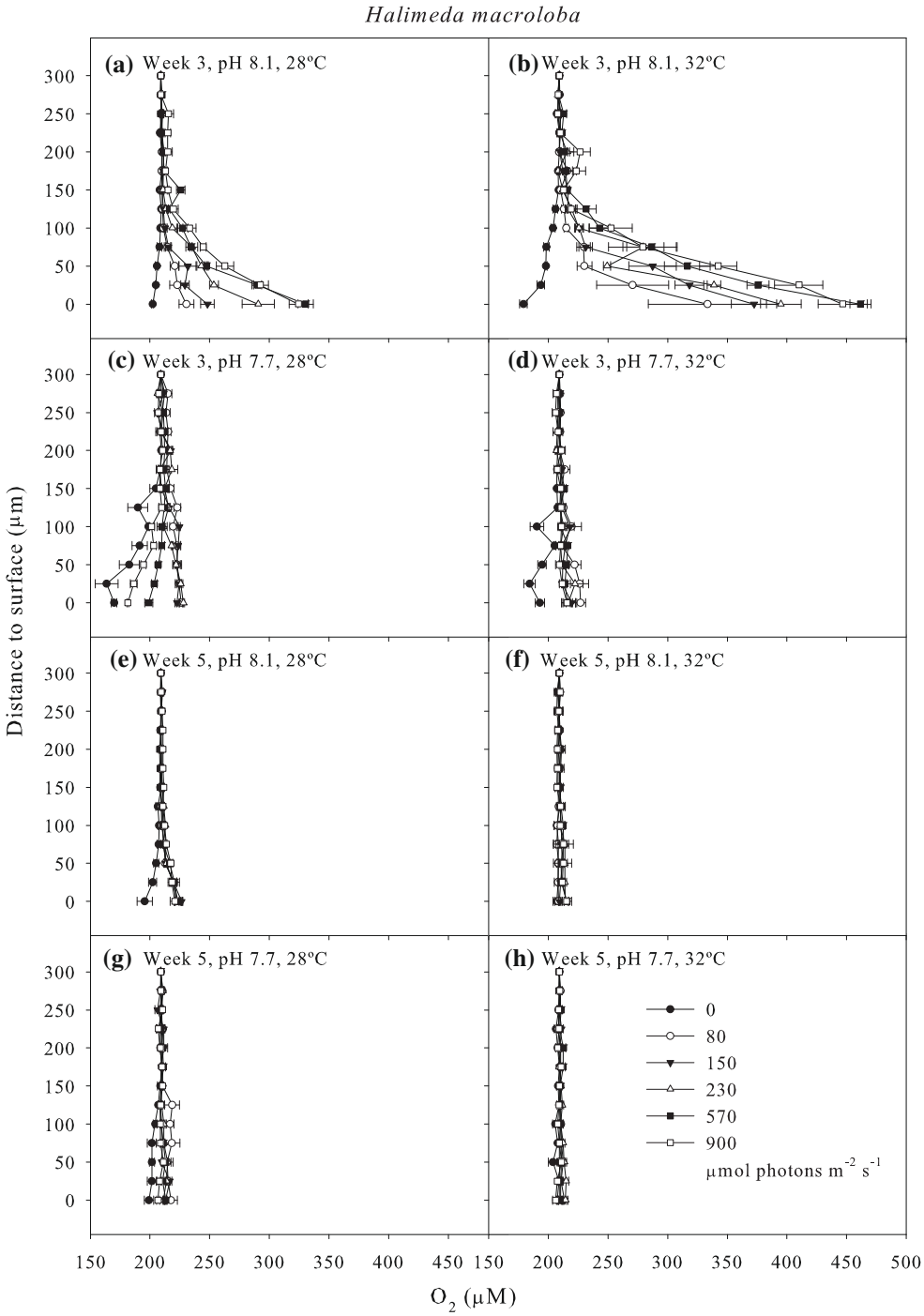

Fig. 3 Oxygen concentration profile towards the thallus surface measured at **a–d** week 3 and **e–h** week 5 from *H. macroloba* at each pH and temperature treatment at each experimental irradiance (0, 80, 150, 230, 570 and 900 µmol photons m^{-2} s^{-1}). Data represent means ($n = 4$, ± SE)

observations were seen at pH 7.7 and both temperature treatments at 3 and 5 weeks in *H. macroloba* (Fig. 3c–d, g–h).

In *H. cylindracea* at the start of the experiment, the ambient O_2 concentration increased from 209 µM at 125 µm above the segment to 260–277 µM at the segment surface when in light. A decrease to 172 µM was found at the tissue surface when in darkness (Fig. 2b). There were significant changes in O_2 concentration at the shell surface over time and between pH and temperature treatments ($p < 0.001$; Figs. 2b, 4a–h). At 3 weeks, *H. cylindracea* in the control treatment and pH 8.1, 32 °C treatment, a significant increase in O_2 concentration was found when reaching the segment surface at about 265–580 and 336–400 µM, respectively, in all light treatments ($p < 0.001$; Fig. 4a, b). In addition, a significant decrease in O_2 concentration was found when reaching the segment surface at about 128 and 184 µM in darkness, respectively ($p < 0.001$; Fig. 4a, b). No significant changes in O_2 concentration at the segment surface were observed at 3 and 5 weeks at pH 7.7 in both temperature treatments and at 5 weeks in the pH 8.1, 32 °C treatment ($p > 0.05$; Fig. 4c–d, f–h).

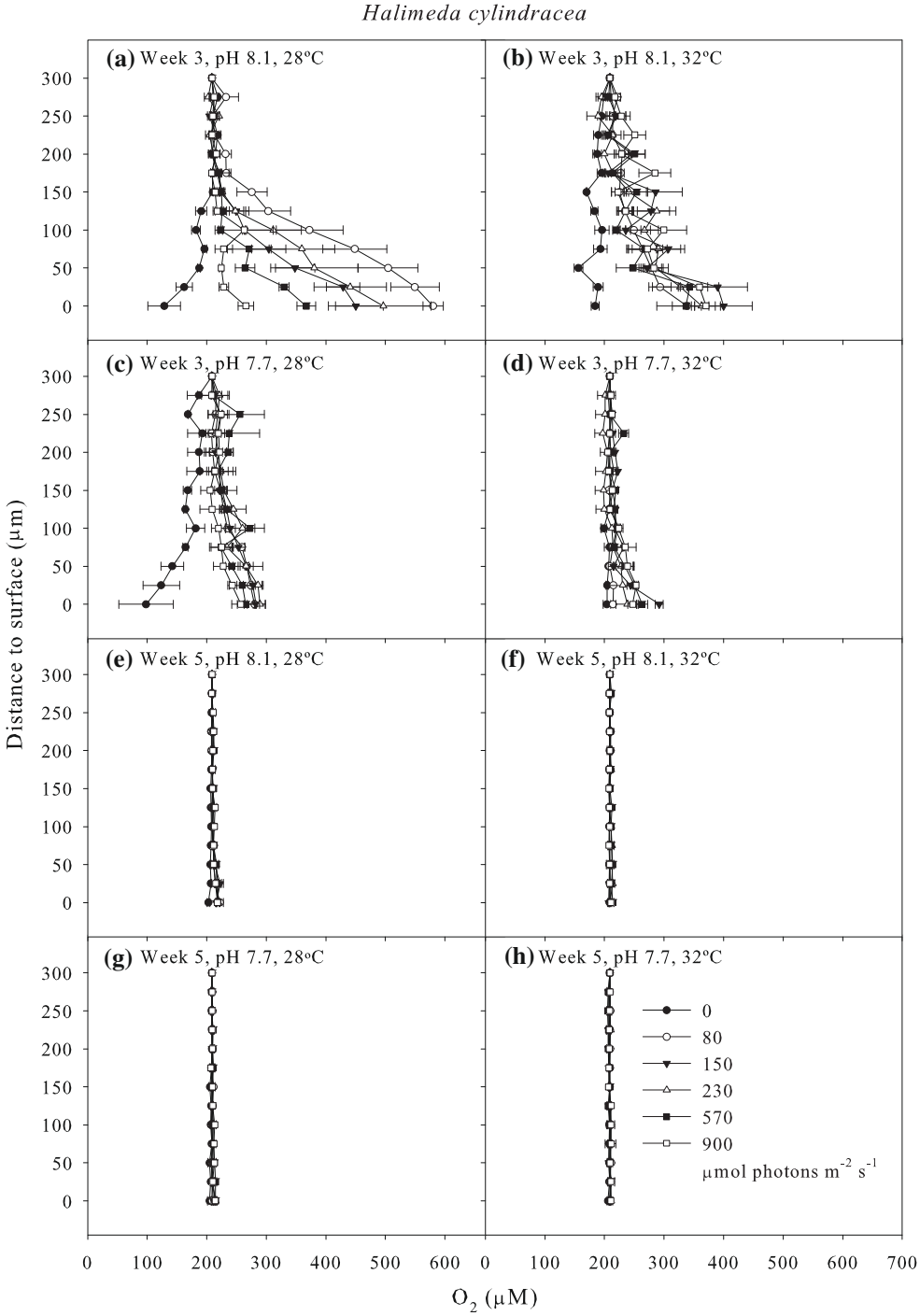

Fig. 4 Oxygen concentration profile towards the thallus surface measured at **a–d** week 3 and **e–h** week 5 from *H. cylindracea* at each experimental pH and temperature treatment at each irradiance (0, 80, 150, 230, 570 and 900 µmol photons m^{-2} s^{-1}). Data represent means ($n = 4$, ±SE)

Gross photosynthesis and O_2 flux

Estimated rates of gross photosynthesis and O_2 flux, that is, net photosynthesis, of both *Halimeda* species were influenced by CO_2 and time of exposure to elevated CO_2 and temperature ($p < 0.001$; Figs. 5, 6). In *H. macroloba*, gross photosynthesis decreased with elevated pCO_2 (pH 7.7 at both temperatures; $p < 0.001$; Fig. 5a) and long-term exposure (5 weeks) to elevated pCO_2 and temperature ($p < 0.001$; Fig. 5b). Gross photosynthesis in *H. cylindracea* also declined at week 5 at pH 7.7 at 28 and 32 °C ($p < 0.001$; Fig. 5d).

After 3 weeks, a significant decrease in the rate of O_2 efflux in light was observed in both species under elevated CO_2 conditions (pH 7.7, at both temperatures; $p < 0.001$; Fig. 6a, c). After 5 weeks, the rate of O_2 efflux in both species decreased under elevated CO_2 treatments (pH 7.7, at both temperatures for 70–80 %) ($p < 0.001$; Fig. 6b, d).

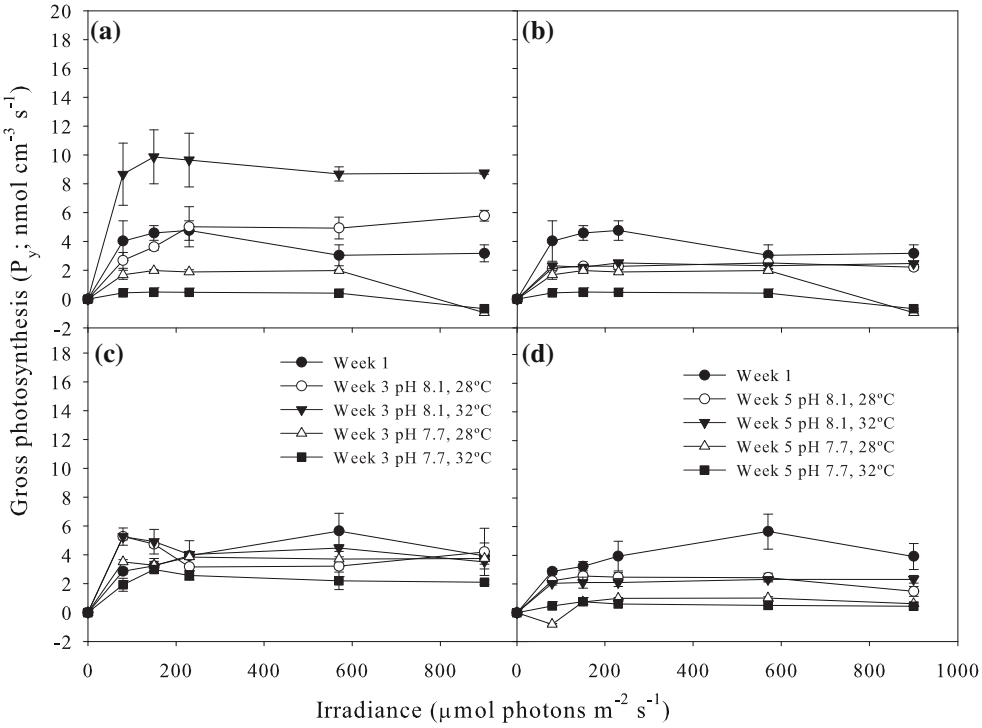

Fig. 5 Gross photosynthesis estimates (P_y; nmol O_2 cm^{-3} s^{-1}) at the thallus surface measured at week 1, 3 and 5 from **a**, **b** *H. macroloba* and **c**, **d** *H. cylindracea* in each pH and temperature treatment. Data represent means ($n = 4$, ±SE)

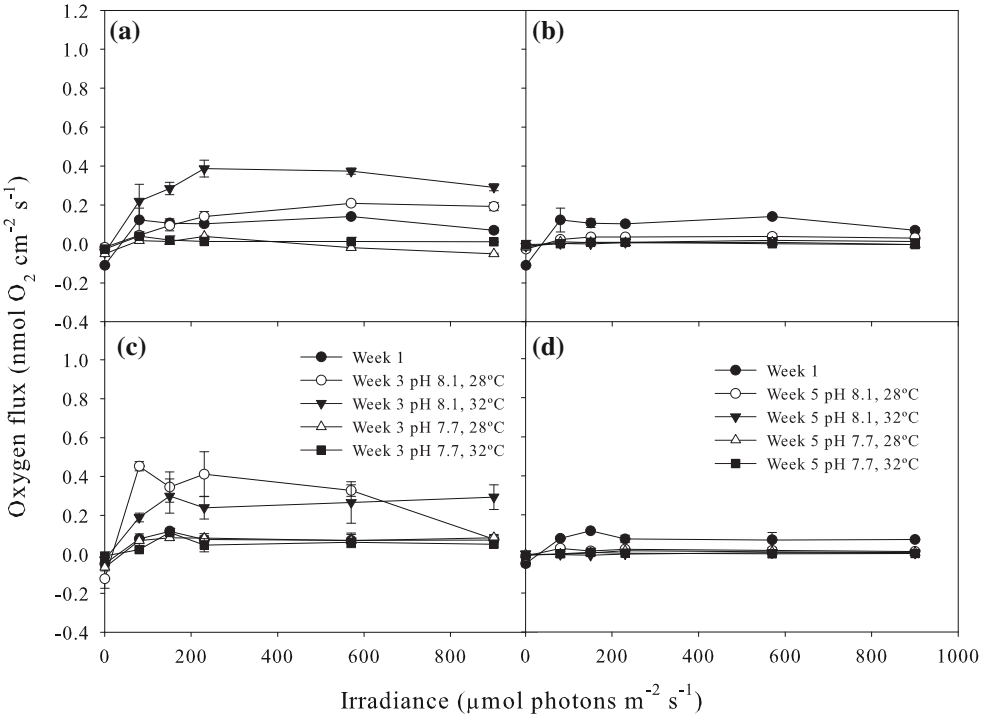

Fig. 6 Diffusive O_2 flux (nmol O_2 cm^{-2} s^{-1}) at the thallus surface measured at week 1, 3 and 5 from **a**, **b** *H. macroloba* and **c**, **d** *H. cylindracea* in each pH and temperature treatment. Data represent means ($n = 4$, ±SE)

Discussion

Previous applications of pH and O_2 microsensors have demonstrated their ability to resolve the dynamic microenvironment of calcifying reef algae, corals and foraminifera at high spatio-temporal resolution (e.g. De Beer and Larkum 2001; Al-Horani 2005; Köhler-Rink and Kühl 2005), but this is the first study to investigate the

combined effects of elevated temperature and pCO_2 on the O_2 microenvironment of *Halimeda.* Our results showed strong effects of elevated temperature and pCO_2 on the microenvironment around the segments of two *Halimeda* species, as well as strong reductions in physiological performance.

Temporal changes in productivity in response to ocean acidification and ocean warming

There was net O_2 production in the light in the control treatment over the 5-week experiment, which was reversed in darkness due to respiration. Short-term exposure (3 weeks) to elevated temperature (32 °C) and current pCO_2 (400 µatm) increased the productivity of both species, with increasing O_2 concentration and O_2 flux at the segment surface and increasing gross photosynthesis, while long-term exposure (5 weeks) to elevated temperature led to a decrease in the productivity of both species. These observations are consistent with a previous study, where high O_2 production was found after short-term (18 days) exposure to elevated temperature, while long-term exposure (35 days) resulted in decreased productivity and metabolism in these species (Sinutok et al. 2011). Although short-term exposure to elevated temperature (32 °C) may lead to increasing productivity and metabolism in this species, 32 °C was found to be an upper limit for survival (Sinutok et al. 2011). Exposure to 32 °C for 5 weeks may damage PSII, possibly by damaging the D1 protein and disrupting the thylakoid membrane stability (Warner et al. 1999; Hill et al. 2004; Allakhverdiev et al. 2008). This suggests that the potential for acclimation to thermal stress is limited. After 3 and 5 weeks under elevated CO_2 and temperature, the rate of O_2 consumption in darkness and net O_2 production in light decreased even further. This suggests that ocean acidification compounds the reduction in photosynthetic activity and elevated photoinhibition under temperature stress.

Net O_2 production and consumption in *H. macroloba* and *H. cylindracea* controls were significantly greater than in other treatments. However, we found a sharp decrease in net O_2 production in both species in controls at week 5 compared to week 1 and week 3, suggesting that the algae were relatively unhealthy. However, the photosynthetic efficiency (F_V/F_M) in the controls at week 5 did not show the same trend. This may be explained due to O_2 production measurements detecting oxygen evolved during photosynthesis which includes respiration. In contrast, F_V/F_M is a measurement of PSII photochemistry and represents the maximum efficiency at which light absorbed by PSII is used for photochemistry and indicates stress or damage in PSII (Maxwell and Johnson 2000; Schreiber 2004; Baker 2008).

Ocean acidification is more influential than ocean warming in reducing *Halimeda* productivity

Although CO_2 uptake during photosynthesis mainly occurs at the cell wall surface facing into the intercellular space (Borowitzka and Larkum 1976b), De Beer and Larkum (2001) observed that photosynthetic CO_2 uptake in *Halimeda* leads to an increase in extracellular pH at the thallus surface, whereas CO_2 and H^+ production from respiration and calcification leads to a decrease in pH. This study showed that elevated CO_2 conditions, and thus increased availability for carbon uptake, did not lead to increased O_2 production in these *Halimeda* species, suggesting that pH may be the main factor inhibiting their metabolism. A reduction in pH may disrupt the CO_2 accumulation pathway at the site of Rubisco or disrupt electron transport via the thylakoid proton gradients (Anthony et al. 2008). A reduction in photosynthesis due to these stressors will consequently have an impact on calcification due to the loss of elevated intracellular pH at the site of calcification.

Calcification is promoted under high pH conditions, as the speciation of dissolved inorganic carbon is favoured towards carbonate (Table 1), which was clearly shown in Borowitzka and Larkum (1976b). Therefore, any alterations of intracellular pH will influence calcification rate. Reduced pH as a direct consequence of ocean acidification as well as through the inhibition of photosynthesis is therefore likely to slow the rate of calcification (Borowitzka and Larkum 1976b; De Beer and Larkum 2001). Rising CO_2 will inhibit calcification by decreasing the availability of CO_3^{2-} ions required for calcium carbonate precipitation (De Beer and Larkum 2001; Feely et al. 2004; Ries 2011). Although elevated temperature leads to an increase in aragonite saturation state (less solubility of $CaCO_3$; Weyl 1959) as shown in Table 1, this increase in saturation state is not large enough to offset the pH effects, so pH seems to be the main factor affecting calcification in *Halimeda*.

Intracellular mechanisms of calcification and the interaction with respiration and production

In this study, we observed that calcification rates declined with decreasing pH, with a concomitant decline in photosynthetic efficiency. This suggests that calcification in these *Halimeda* species is closely coupled to photosynthesis, such that a decrease in photosynthetic efficiency leads to a decrease in calcification. It has been proposed that calcification and photosynthesis are tightly coupled, with calcification promoting photosynthesis by providing a proton source through calcium carbonate deposition, and these protons promote the conversion of HCO_3^- to CO_2, which is used in the dark reactions of photosynthesis

(Borowitzka 1977, 1989; McConnaughey 1989; McConnaughey and Whelan 1997). As a result, the pH in the DBL surrounding *Halimeda* increases due to CO_2 uptake for photosynthesis in the light, whereas pH decreases due to CO_2 and H^+ released from respiration and calcification (Borowitzka 1986; De Beer and Larkum 2001). pH and light also influence Ca^{2+} dynamics. In the light, the Ca^{2+} concentration in sea water decreases due to Ca^{2+} diffusion for calcification (Borowitzka and Larkum 1976a; De Beer and Larkum 2001). Borowitzka and Larkum (1976b) showed that the rate of calcification is proportional to the photosynthetic rate; for every mole of $CaCO_3$ precipitated, 4–8 mol of CO_2 must be fixed in photosynthesis.

Ocean acidification and ocean warming as drivers of calcification and photosynthesis inhibition in *Halimeda*

Negative calcification rates were observed in *H. macroloba* and *H. cylindracea* under high pCO_2 conditions, independent of treatment temperature, suggesting that dissolution of the calcium carbonate structure occurred primarily in response to shifts in carbonate chemistry, rather than increased temperature. The elevated pCO_2 in the treatments changed the carbonate chemistry of sea water by decreasing the availability of CO_3^{2-} ions required for calcification and resulted in a decreased aragonite saturation state (Ω_a) to 1.97 ± 0.02 and 2.05 ± 0.01 (mean ± SE) at pH 7.7, 28 and 32 °C, respectively (Table 1). This finding is consistent with the previous studies that observed negative calcification rates and decreasing aragonite crystal width in *Halimeda* spp. (Sinutok et al. 2011) under ocean acidification and ocean warming conditions.

Increases in pCO_2 are expected to promote photosynthesis and growth in some marine phototrophs such as seagrasses, and non-calcifying macroalgae, due to an increased availability of inorganic carbon sources for photosynthesis (Gao et al. 1993; Short and Neckles 1999; Palacios and Zimmerman 2007). However, we found that 5 weeks at elevated pCO_2 lead to a decline in Chl *a* and *b* concentration in both temperature treatments, indicating decreased chlorophyll production or pigment degradation in *Halimeda*, leading to less capacity for light absorption and photosynthesis. Reductions in PSII photochemical efficiency (F_V/F_M and $\Delta F/F_M'$) were observed at elevated pCO_2 and temperature treatments, similar to the previous findings (Sinutok et al. 2011) indicating a loss of functional PSII reaction centres, downregulation of photochemistry and/or photoinhibition. In addition, increases in the maximum excitation pressure (Q_m), an indicator of non-photochemical quenching, were observed under elevated pCO_2 and temperature stress. Values close to 1 were observed in the high CO_2 and temperature treatment, indicating that most of the PSII reaction centres are closed under maximum irradiance increasing the potential for photoinhibition (Iglesias-Prieto et al. 2004).

Under ocean acidification and ocean warming conditions, the reductions in PSII photochemical efficiency (F_V/F_M and $\Delta F/F_M'$) and increases in the maximum excitation pressure (Q_m) suggested that the level of non-photochemical quenching was elevated via heat dissipation. Both observations indicated a decrease in physiological performance and the onset of a combination of photoprotective processes and photoinhibition in these species under pH and thermal stress (Iglesias-Prieto et al. 2004; Kuguru et al. 2010). Our results from O_2 microprofiles support the photosynthetic pigment and chlorophyll fluorescence data, showing decreasing O_2 production with declining Chl *a* and *b* concentrations and a decreased photosynthetic efficiency under pH and/or heat stress (Table 2; Figs. 1–6).

Ecological implications

A recent study in a naturally high CO_2 region at volcanic vents off Ischia Island, Italy, observed high seagrass production and a lack of calcifying organisms (e.g. *Halimeda* and corals) at pH 7.6 and $\Omega_a < 2.5$ (Hall-Spencer et al. 2008). Our study is consistent with those findings and indicates that rising pCO_2 and temperature will have a negative impact on photosynthesis and calcification in *Halimeda* leading to a reduction in its abundance and primary productivity on coral reefs. We found strong effects of temperature and pCO_2 on the microenvironment of two *Halimeda* species, as well as significant reductions in physiological performance. As an ecosystem engineer and a key sediment producer, the loss or severe decline of *Halimeda* from reef ecosystems will thus have a dramatic impact on carbonate accumulation, sediment turnover, habitat structure as well as trophic food webs associated with these species.

Acknowledgments We thank Louise Evans and Linda Xiao and the School of Chemistry and Forensic Science, University of Technology, Sydney, for assistance with the autotitrator. Anthony Larkum, Daniel Nielsen, Daniel Wangpraseurt and Ponlachart Chotikarn are thanked for their assistance with microsensor experimental set-ups. This project was supported by the Plant Functional Biology and Climate Change Cluster, School of the Environment, University of Technology, Sydney, an Australian Coral Reef Society student research award (SS), and the Phycological Society of America Grant-in-Aid of Research award (SS). Additional support was due to the Danish Natural Science Research Council (MK). The research was performed under Great Barrier Reef Marine Park Authority permit G09/30853.1.

References

Al-Horani FA (2005) Effects of changing seawater temperature on photosynthesis and calcification in the scleractinian coral

Galaxea fascicularis, measured with O_2, Ca^{2+} and pH microsensors. Sci Mar 69:347–354

Allakhverdiev SI, Kreslavski VD, Klimov VV, Los DA, Carpentier R, Mohanty P (2008) Heat stress: an overview of molecular responses in photosynthesis. Photosynth Res 98:541–550

Anthony KRN, Kline DI, Diaz-Pulido G, Dove S, Hoegh-Guldberg O (2008) Ocean acidification causes bleaching and productivity loss in coral reef builders. Proc Natl Acad Sci USA 105:17442–17446

Baker NR (2008) Chlorophyll fluorescence: a probe of photosynthesis in vivo. Annu Rev Plant Physiol 59:89–113

Blaxter JHS, Russel FS, Young M (eds) (1980) Ecology and taxonomy of *Halimeda*: primary producer of coral reefs. Academic Press, New York

Borowitzka MA (1977) Algal calcification. Oceanogr Mar Biol Annu Rev 15:189–223

Borowitzka MA (1986) Physiology and biochemistry of calcification in the Chlorophyceae. In: Leadbeater B, Riding H (eds) Biomineralization in the lower plants and animals. Oxford University Press, Oxford, pp 107–124

Borowitzka MA (1989) Carbonate calcification in algae—initiation and control. In: Mann S, Webb J, Williams RJP (eds) Biomineralization: Chemical and biochemical perspectives. VCH, Weinheim, pp 63–94

Borowitzka MA, Larkum AWD (1976a) Calcification in the green alga *Halimeda* II. The exchange of Ca^{2+} and the occurrence of age gradients in calcification and photosynthesis. J Exp Bot 27:864–878

Borowitzka MA, Larkum AWD (1976b) Calcification in the green alga *Halimeda* III. The sources of inorganic carbon for photosynthesis and calcification and a model of the mechanism of calcification. J Exp Bot 27:879–893

Borowitzka MA, Larkum AWD (1977) Calcification in the green alga *Halimeda*. I. An ultrastructure study on thallus development. J Phycol 13:6–16

Borowitzka MA, Larkum AWD, Nockolds CE (1974) A scanning electron microscope study of the structure and organization of the calcium carbonate deposits of algae. Phycologia 13:195–203

De Beer D, Larkum AWD (2001) Photosynthesis and calcification in the calcifying algae *Halimeda discoidea* studied with microsensors. Plant, Cell Environ 24:1209–1217

Diaz-Pulido G, McCook LJ, Larkum AWD, Lotze HK, Raven JA, Schaffelke B, Smith JE, Steneck RS (2007) Vulnerability of macroalgae of the Great Barrier Reef to climate change. In: Johnson JE, Marshall PA (eds) Climate change and the Great Barrier Reef. Great Barrier Reef Marine Park Authority and Australian Greenhouse Office, Australia, pp 153–192

Drew EA (1983) *Halimeda* biomass, growth rates and sediment generation on reefs in the Central Great Barrier Reef Province. Coral Reefs 2:101–110

Feely RA, Sabine CL, Lee K, Berelson W, Kleypas J, Fabry VJ, Millero FJ (2004) Impact of anthropogenic CO_2 on the $CaCO_3$ system in the oceans. Science 305:362–366

Fujita K, Hikami M, Suzuki A, Kuroyanagi A, Sakai K, Kawahata H, Nojiri Y (2011) Effects of ocean acidification on calcification of symbiont-bearing reef foraminifers. Biogeosciences 8:2089–2098

Gao K, Aruga Y, Asada K, Kiyohara M (1993) Influence of enhanced CO_2 on growth and photosynthesis of the red algae *Gracilaria* sp. and *G. chilensis*. J Appl Phycol 5:563–571

Gattuso J-P, Lavigne H (2009) Technical note: approaches and software tools to investigate the impact of ocean acidification. Biogeosciences 6:2121–2133

Glud RN, Gundersen JK, Revsbech NP, Jørgensen BB (1995) Effects on the benthic diffusive boundary layer imposed by microelectrodes. Limnol Oceanogr 39:462–467

Guinotte JM, Buddemeier RW, Kleypas JA (2003) Future coral reef habitat marginality: temporal and spatial effects of climate change in the Pacific basin. Coral Reefs 22:551–558

Hall-Spencer JM, Rodolfo-Metalpa R, Martin S, Ransome E, Fine M, Turner SM, Rowley SJ, Tedesco D, Buia M-C (2008) Volcanic carbon dioxide vents show ecosystem effects of ocean acidification. Nature 454:96–99

Hill R, Larkum AWD, Frankart C, Kühl M, Ralph PJ (2004) Loss of functional photosystem II reaction centres in zooxanthellae of corals exposed to bleaching conditions: using fluorescence rise kinetics. Photosynth Res 82:59–72

Hofmann LC, Yildiz G, Hanelt D, Bischof K (2012) Physiological responses of the calcifying rhodophyte, *Corallina officinalis* (L.), to future CO_2 levels. Mar Biol 159:783–792

Houghton J (2009) Global warming: the complete briefing. Cambridge University Press, United Kingdom

Iglesias-Prieto R, Beltrán VH, LaJeunesse TC, Reyes-Bonilla H, Thome PE (2004) Different algal symbionts explain the vertical distribution of dominant reef corals in the eastern Pacific. Proc R Soc Biol Sci Ser B 271:1757–1763

Jokiel PL, Maracios JE, Franzisket L (eds) (1978) Coral growth: buoyant weight technique. In: Stoddart DR, Johannes RE (eds) Coral reefs: Research methods, UNESCO, pp 529–541

Jokiel PL, Rodgers KS, Kuffner IB, Andersson AJ, Cox EF, Mackenzie FT (2008) Ocean acidification and calcifying reef organisms: a mesocosm investigation. Coral Reefs 27:473–483

Kleypas JA, Yates KK (2009) Coral reefs and ocean acidification. Oceanography 22:108–117

Kleypas JA, Buddemeier RW, Archer D, Gattuso J-P, Langdon C, Opdyke BN (1999) Geochemical consequences of increased atmospheric carbon dioxide on coral reefs. Science 284:118–120

Köhler-Rink S, Kühl M (2000) Microsensor studies of photosynthesis and respiration in larger symbiotic foraminifera. I The physio-chemical microenvironment of *Marginopora vertebralis*, *Amphistegina lobifera* and *Amphisorus hemprichii*. Mar Biol 137:473–486

Köhler-Rink S, Kühl M (2005) The chemical microenvironment of the symbiotic planktonic foraminifer *Orbulina universa*. Mar Biol Res 1:68–78

Kuffner IB, Andersson AJ, Jokiel PL, Rodgers KS, Mackenzie FT (2007) Decreased abundance of crustose coralline algae due to ocean acidification. Nat Geosci 1:114–117

Kuguru B, Achituv Y, Gruber DF, Tchernov D (2010) Photoacclimation mechanisms of corallimorpharians on coral reefs: photosynthetic parameters of zooxanthellae and host cellular responses to variation in irradiance. J Exp Mar Biol Ecol 394:53–62

Langdon C, Gattuso J-P, Anderson A (2010) Measurements of calcification and dissolution of benthic organisms and communities. In: Riebesell U, Fabry VJ, Hansson L, Gattuso J-P (eds) Guide to best practices for ocean acidification research and data reporting. Publication Office of the European Union, Luxembourg, pp 213–232

Larkum AWD, Salih A, Kühl M (2011) Rapid mass movement of chloroplasts during segment formation of the calcifying siphonalean green alga *Halimeda macroloba*. PLoS One 6. doi: 10.1371/journal.pone.0020841

Lewis E, Wallace DWR (1998) CO2SYS—Program developed for the CO2 system calculations. Carbon Dioxide Information Analysis Center; Report ORNL/CDIAC-105, Oakridge National Laboratory, Oakridge, TN

Maxwell K, Johnson GN (2000) Chlorophyll fluorescence—a practical guide. J Exp Bot 51:659–668

McConnaughey T (1989) Biomineralization mechanisms. In: Crick RE (ed) Origin, evolution, and modern aspects of biomineralization in plants and animals. Plenum Press, New York, pp 57–73

McConnaughey TA, Whelan JF (1997) Calcification generates protons for nutrient and bicarbonate uptake. Earth-Sci Rev 42:95–117

Palacios SL, Zimmerman RC (2007) Response of eelgrass *Zostera marina* to CO_2 enrichment: possible impacts of climate change

and potential for remediation of coastal habitats. Mar Ecol Prog Ser 344:1–13

Revsbech NP, Jorgensen BB, Brix O (1981) Primary production of microalgae in sediments measured by oxygen microprofile, $H^{14}CO_3^-$ fixation, and oxygen exchange methods. Limnol Oceanogr 26:717–730

Ries JB (2011) A physicochemical framework for interpreting the biological calcification response to CO_2-induced ocean acidification. Geochim Cosmochim Acta 75:4053–4064

Ritchie RJ (2008) Universal chlorophyll equations for estimating chlorophylls *a, b, c*, and *d* and total chlorophylls in natural assemblages of photosynthetic organisms using acetone, methanol, or ethanol solvents. Photosynthetica 46:115–126

Schreiber U (2004) Pulse-amplitude-modulation (PAM) fluorometry and saturation pulse method: An overview. In: Papageorgiou GC, Govindjee (eds) Chlorophyll *a* fluorescence: A signature of photosynthesis. Springer, Dordrecht, pp 279–319

Short FT, Neckles HA (1999) The effects of global climate change on seagrasses. Aquat Bot 63:169–196

Sinutok S, Hill R, Doblin MA, Wuhrer R, Ralph PJ (2011) Warmer more acidic conditions cause decreased productivity and calcification in subtropical coral reef sediment-dwelling calcifiers. Limnol Oceanogr 56:1200–1212

Smith SV, Kinsey DW (1976) Calcium carbonate production, coral reef growth, and sea level change. Science 194:937–939

Warner ME, Fitt WK, Schimidt GW (1999) Damage to photosystem II in symbiotic dinoflagellates: a determinant of coral bleaching. Proc Natl Acad Sci USA 96:8007–8012

Weyl PK (1959) The change in solubility of calcium carbonate with temperature and carbon dioxide content. Geochim Cosmochim Acta 17:214–225